

MODELLING OF POLLUTANT DISTRIBUTION IN SURFACE RUNOFF IN
UNGAUGED CATCHMENTS USING
GEOGRAPHICAL INFORMATION SYSTEMS

CARLOS ANDRÉ BULHÕES MENDES

A thesis submitted to the University of Bristol

in accordance with the requirements

for the degree of Doctor of Philosophy

in the Faculty of Science

Department of Geography

Bristol, England

August, 1994

Abstract

In developing countries the scarcity of environmental information poses a difficult problem to the planner who is interested in assessing different control strategies for water quality problems. Although sophisticated models exist, the data available to run such models is usually limited. Furthermore, few of the models are easy to use, can operate over a variety of conditions, and can integrate the wide range of data that planners and managers need to compare water quality control strategies.

The aim of this thesis has been to develop a water quality model, suitable for Brazilian conditions and that is capable of estimating the effects of future land use scenarios on water quality. The model is designed to be consistent with the availability of data in less developed countries and one of its major advantages is that the parameters involved are easily defined in terms of physical characteristics alone.

A methodology is presented which has been designed specifically to support the determination of water quality changes resulting from point and non-point sources in a large river basin with varied land use, taking into account both the magnitude and spatial distribution of the loads produced. The methodology is capable of implementation on land surfaces having heterogeneous distribution of water pollution sources.

The model is based on a cellular configuration where information on land use, topography, soil type and rainfall is manipulated using geographical information systems (GIS). Information on land use in each cell is obtained by classifying remotely sensed satellite data. Topographic parameters for each cell are derived from digital elevation models (DEM). Rainfall values for each cell are obtained from the interpolation of point data derived from meteorological stations. Other more conventional data are acquired by digitising maps.

Using this cellular structure, runoff, and chemical outputs from the individual cell, are routed through the catchment using a physically based mixing model to provide input to the drainage network. The network, derived automatically from a digital elevation model (DEM), defines the river system in the model. The link between the catchment and the river network defines a river 'buffer' zone where point and non-point sources are stored. The model enables spatial relationships between point and non-point sources to be investigated and the consequences to the river system can then be modelled using the river network topology.

The model is demonstrated for the Sinos catchment in southern Brazil. Analysis of the case study results indicate the model is capable of generating reasonable trends in water quality which reflect the impact of management activities. However, only limited water quality data availability precludes exhaustive testing of the system, and further work in this area is needed. The use of the model to investigate future water quality scenarios is also illustrated.

Finally, the propagation of errors (due to spatial variation) associated with input variables is investigated. The problem is examined by first order theory and stochastic modelling, combined with the physical models, to show the possible magnitude of error within the model predictions.

Dedicated to the memory of

..Carmelita Bulhões

Acknowledgments

Anyone who has written a thesis probably appreciates how personal such an achievement can be, but without the support of a great number of people I could not imagine having completing this thesis. I am glad to have this opportunity to thank old and new friends alike.

I sincerely thank my advisory committee members: Dr. Peter Smart, for his stimulating supervision, for providing ideas, constructive criticisms and suggestions. I could always be honest with him and feel free to make my own choices. Dr. Andrew Harrison for his help in my Ph.D. program. I cannot imagine completing this thesis in time without his help and support. Dr. Michael Beaumont for his contributions and ideas. They have given me a lot of sound advice, constructive criticism, and have reviewed the text and corrected my English, particularly towards the end of the thesis, when time was definitely running out (they probably also have a long list of 'what can go wrong when a Brazilian tries to write his thesis in the English language').

The financial support came from the Conselho Nacional de Desenvolvimento Científico e Tecnológico - CNPq (Brazilian agency for scientific and technological development) on Grant 201972/91-3.

The pleasant atmosphere in my research group has been a stimulating factor in my work. This is largely thanks to Dr. Eric Barrett, Dominic Kniveton, David Kilhan and to my room mates Richard Kelly and Andrew Barrett. Without this atmosphere and without all your help I would not have survived. I felt at home when I was in the Remote Sensing Unit and I have enjoyed working in the group very much.

The Institute of Hydraulic Research (Federal University of Rio Grande do Sul - Brazil) are thanked for their hospitality during the field work in November/December 1993. I am indebted to Alvaro Frantz for his help during the collection of the samples. I am very grateful to all persons and institutions that supplied the data, and in particular the COMITESINOS. Without the applications this thesis would not have been complete.

I am deeply grateful to Prof. Dr. Eduardo Lanna who gave me strong support in all aspects, in Brazil.

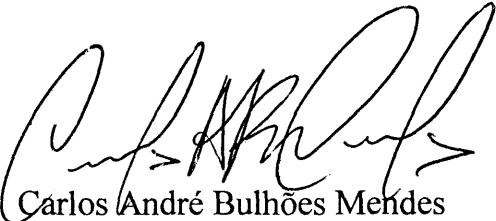
Acknowledgement is also due to Joaquim Eduardo Wiltgen, Maria Teresa and Luis Fernando Franco for taking care of problems during my absence.

I am most grateful to my mother Myriam Bulhões for her continuing support during the years.

Finally, I thank Marta for comforting and supporting me during moments of weakness and despair, for enduring all my restless moments and for patiently listening to my (what must have been boring) scientific monologues.

Declaration

This thesis is the original work of the candidate, except where acknowledgement is given, and has not been submitted for a higher degree in this or any other university.



Carlos André Bulhões Mendes

August 1994

Table of Contents

	<u>Page</u>
Title Page	i
Abstract	ii
Dedication	iii
Acknowledgments	iv
Declaration	v
Table of Contents	vi
List of Illustrations	x
List of Tables	xv
1.INTRODUCTION.....	1
1.1 - MAJOR WATER POLLUTIONS PROBLEMS IN BRAZIL.....	1
1.2 - BACKGROUND TO THE POLLUTION PROBLEM IN AN INDUSTRIALISED CATCHMENT OF SOUTHERN BRAZIL.....	5
1.3 - THE OVERALL PERSPECTIVE OF THE POLLUTION PROBLEM.....	10
1.4 - OBJECTIVES.....	14
1.5 - OVERVIEW OF THE THESIS	16
2.FRAMEWORK FOR ANALYSIS.....	18
2.1 - INTRODUCTION.....	18
2.2 - DEVELOPING A SPATIAL HYDROLOGY MODEL	18
2.2.1 - Hydrologic system	18
2.2.2 - Geographical Information System (GIS)	22
2.2.3 - Integrated use of GIS and hydrologic system.....	25
2.3 - CHARACTERISTICS OF THE RESEARCH CATCHMENT.....	32
2.3.1 - Hydrologic aspects	32
2.3.2 - Water quality aspects.....	36
2.3.3 - Creation of the data set.....	40
2.3.4 - Field data collection.....	42

2.4 - COMPUTING TOOLS	49
2.5 - SUMMARY	51
3.DIGITAL REPRESENTATION OF CATCHMENT BASE SYSTEM.....	55
3.1 - INTRODUCTION.....	55
3.2 - DIGITAL ELEVATION MODELS (DEMs)	55
3.3 - ANALYSIS OF ELEVATION DATA	60
3.4 - APPLICATIONS OF DEM.....	65
3.4.1 - <i>Treatment of depressions</i>	65
3.4.2 - <i>Determination of slope</i>	66
3.4.3 - <i>Determination of flow vectors (aspect)</i>	67
3.5 - HYDROLOGICAL TOPOGRAPHIC ATTRIBUTES	68
3.5.1 - <i>Determination of upstream catchment areas</i>	68
3.5.2 - <i>Determination of catchment boundary</i>	69
3.5.3 - <i>Determination of the drainage network</i>	70
3.5.4 - <i>Evaluation of drainage network composition</i>	72
3.6 - EVALUATION OF SINOS CATCHMENT DIGITAL ELEVATION MODEL (DEM)	75
3.7 - SUMMARY	79
4.GENERATION OF RUNOFF BASED ON DETERMINABLE CHARACTERISTICS	80
4.1 - INTRODUCTION.....	80
4.2 - A GENERAL DISTRIBUTED CATCHMENT MODEL.....	82
4.3 - PREDICTION OF SURFACE RUNOFF IN CATCHMENTS	85
4.3.1 - <i>Theory</i>	85
4.3.2 - <i>Spatial variables</i>	89
4.3.3 - <i>Application and interpretation</i>	94
4.4 - SUMMARY	102
5.CRITICAL AREAS FOR NON-POINT SOURCE POLLUTION.....	103
5.1 - INTRODUCTION.....	103
5.2 - CHARACTERISTICS OF NON-POINT SOURCES	105
5.2.1 - <i>Estimating sediment loss</i>	107

5.2.2 - <i>Nutrient loss from non-point sources</i>	109
5.2.3 - <i>Other losses from non-point sources</i>	111
5.3 - POTENTIAL NON-POINT SOURCE ANALYSIS	111
5.3.1 - <i>Critical area criteria</i>	112
5.3.2 - <i>Critical area selection</i>	114
5.3.3 - <i>Conclusions</i>	124
5.4 - SUMMARY	125
6.AGGREGATING POINT AND NON-POINT SOURCES OF POLLUTANTS	126
6.1 - INTRODUCTION.....	126
6.2 - DISCHARGE OF POLLUTANT SOURCES INTO RIVERS	128
6.2.1 - <i>Load function for point sources</i>	132
6.2.2 - <i>Load function for non-point sources</i>	136
6.3 - EVALUATION IN SINOS CATCHMENT.....	140
6.4 - SUMMARY	143
7.RIVER PROCESSES.....	144
7.1 - INTRODUCTION.....	144
7.2 - CHARACTERISTICS OF RIVER SYSTEMS.....	145
7.3 - DEVELOPMENT OF A SQUARE-GRID TRANSPORT MODEL.....	150
7.3.1 - <i>Mixing cell model</i>	150
7.3.2 - <i>Interface with drainage network topology</i>	153
7.4 - CONCLUSIONS	155
8.CASE STUDY: SINOS CATCHMENT	157
8.1 - INTRODUCTION.....	157
8.2 - EVALUATION OF SYSTEM BEHAVIOUR	158
8.2.1 - <i>General assessment</i>	158
8.2.2 - <i>Specific junction behaviour</i>	162
8.2.3 - <i>Comparing observed and simulated pollutant concentrations</i>	163
8.2.4 - <i>Estimating the effects of spatial changes in land use</i>	167
8.3 - CONCLUSIONS	174

9.ENVIRONMENTAL EVALUATION UNDER UNCERTAINTY.....	177
9.1 - UNCERTAINTIES IN WATER RESOURCES.....	177
9.1.1 - <i>Statistical representation of the real world</i>	178
9.1.2 - <i>Analysis of uncertainties</i>	181
9.1.3 - <i>Discussions</i>	184
9.2 - IMPLEMENTATION OF UNCERTAINTY ANALYSIS FOR ENVIRONMENTAL DISTRIBUTED MODELS.....	185
9.2.1 - <i>DEM evaluation under uncertainty</i>	185
9.2.2 - <i>Uncertainty assessment of runoff production</i>	188
9.2.3 - <i>Critical area uncertainty analysis</i>	197
9.3 - CONCLUSIONS.....	199
10.SUMMARY AND CONCLUSIONS.....	201
10.1 - REVIEW OF MAJOR POINTS.....	201
10.2 - CONCLUDING REMARKS.....	203
10.3 - RESEARCH ISSUES FOR THE NEAR FUTURE.....	205
BIBLIOGRAPHY.....	208
APPENDIX - Computer programs.....	228

List of Illustrations

	<u>Page</u>	
1.1	Same major water quality problems in Brazil	4
1.2	The Sinos catchment in Southern Brazil	5
1.3	Sinos catchment	7
1.4	Administrative division in Sinos catchment	9
1.5	Flow diagram - water quality engineering	11
2.1	Basic representations of: (A) Lumped system and (B) distributed system	19
2.2	A system's classification based on randomness, space and time	20
2.3	Functional organisation of the catchment system	21
2.4	The representation of the real world by a series of map layers	23
2.5	GIS operations	24
2.6	Integration Model/GIS through: (A) common file and (B) common program	27
2.7	Different views about the 'Real World'	28
2.8	Logical and Physical space	29
2.9	Two types of field representation: Lagrange and Euler's views	30
2.10	Distribution of the stream gauges in Sinos catchment	33
2.11	Plots of three time series in Table 2.2	34
2.12	Longitudinal flow variation in Sinos river, from data in Table 2.2	35
2.13	Longitudinal relative variation in Sinos river, from data in Table 2.3	36
2.14	Main point sources of waste disposal in the Sinos river	37
2.15	Distribution of water quality samples in Sinos river	39
2.16	Digital representation of land use data	43
2.17	Digital Elevation Model (DEM) of Sinos catchment	43
2.18	Digital representation of soils data	44
2.19	Areal distribution of rainfall for January (daily average values)	44
2.20	Distribution of water quality samples in Sinos catchment (1993)	46
2.21	Measurements of water quality constituents in Sinos catchment	46
2.22	Sample point 7 in figure 2.20	47
2.23	Sample point 19 in figure 2.20	47
2.24	Near sample point 35 in figure 2.20	48

2.25	Sample point 34 in figure 2.20	48
2.26	University of Bristol's computer network	50
2.27	Group of models integrated with GIS	53
3.1	Flow diagram illustrating a series of programs for the calculation of properties of catchments from DEMs	56
3.2	Digitiser table	57
3.3	Point data sets	58
3.4	Geometrical interpretation of finite differences	61
3.5	Example topographic map	63
3.6	Grey scale surface	63
3.7	Spatial variation of the prediction	64
3.8	True elevation (1) and apparent elevation (2)	66
3.9	Slope of example area	67
3.10	Aspect of example area	68
3.11	General strategy of upstream catchment areas	69
3.12	Example of upstream catchment areas	70
3.13	Example catchment boundary	70
3.14	Drainage network extraction	71
3.15	Example drainage network	71
3.16	Network concepts	72
3.17	Definition of a topologic code	73
3.18	Link number configuration	74
3.19	Observed and simulated drainage network configuration for Sinos catchment	76
3.20	Linear profiles over areas of good simulation (1) and inferior simulation (2) of the drainage network configuration	77
3.21	Linear profiles over DEM: (a) profile 1 and (b) profile 2	78
4.1	Flow diagram showing the calculations of runoff's spatial distribution	80
4.2	Catchment as a distributed system	83
4.3	Vertical flux of water at a point x,y	84
4.4	Distribution of $\xi(x, y)$ for a time t over a catchment	85
4.5	Time variability of precipitation, rainfall excess and storage	92
4.6	Example of a digital representation of soils data	94

4.7	Example of distributed rainfall data	95
4.8	Example of a digital representation of land use	95
4.9	Possibility of runoff's generation based in soil type and land use	96
4.10	Upstream catchment area produced by the eight nearest neighbours' algorithm	97
4.11	Topographic parameter of equation 4.6 ($\ln(A/\tan \beta)$) using the multiple downslope nearest neighbours' algorithm	98
4.12	Full implementation of equation 4.6 using the multiple downslope nearest neighbours' algorithm within the catchment	98
4.13	Potential of runoff generation in Sinos catchment	99
4.14	Predicted and observed runoff indices	100
4.15	Observed, estimated and one standard deviation of January mean flow values in Sinos catchment	101
5.1	Flow diagram showing the calculations of the spatial distribution of critical areas for non-point pollutant production	104
5.2	Analysis of geocoded data	113
5.3	Conceptual illustration of overlay process	114
5.4	Potential to produce sediments	116
5.5	Potential to produce nitrogen	118
5.6	Potential to produce biochemical oxygen demand	119
5.7	Effective depth of interaction as a function of soil type and slope	120
5.8	Potential to produce phosphorus	121
5.9	Nitrogen critical areas for Sinos catchment (Water resource perspective)	121
5.10	Nitrogen critical areas for Sinos catchment (Land resource perspective)	123
6.1	Flow diagram showing the calculations of the loading functions for point and non-point sources	126
6.2	Assumptions for non-point sources: (a) Typical situation and (b) "Mixed" situation	132
6.3	Scheme of a conservative substance	133
6.4	Scheme of a non-conservative substance	135
6.5	Point sources around drainage network	135
6.6	Point sources indicated as lighter grey levels around the drainage network	136
6.7	Loading functions for estimate non-point sources pollution entering in a drainage network	137

6.8	Buffer zones around drainage network	139
6.9	Buffer zone around drainage network	140
6.10	Load of non-point pollutant (nitrogen), using runoff prediction	141
6.11	Load of non-point pollutant (nitrogen), without runoff prediction	142
7.1	Flow diagram illustrating the operations of river processes	144
7.2	Changes in river water quality	146
7.3	Input of non-point pollution as a distributed source	149
7.4	Mass balance components	151
7.5	Mixing cell model	152
7.6	Spatial distribution of pollutant concentration	155
8.1	BOD critical area for Sinos catchment	160
8.2	Load of non-point pollutant (BOD)	160
8.3	Intensities and spatial distribution of BOD concentration considering only non-point loads	161
8.4	Predicted and observed runoff indices	159
8.5	Intensities and spatial distribution of BOD concentration for both types of loads	161
8.6	Water quality behaviour at the junction	163
8.7	Observed and simulated Nitrogen concentration	164
8.8	Observed and simulated Phosphorus concentration	165
8.9	Observed (DO) and simulated (BOD) concentrations for the Sinos catchment	165
8.10	Intensities and spatial distribution of BOD index considering both types of loads and 'without' scenario	169
8.11	Intensities and spatial distribution of BOD index considering both types of loads and 'with' scenario	169
8.12	Percentage of change in Igrejinha valley	170
8.13	Digital representation of land use data with changes proposed by government policies	171
8.14	Nitrogen critical areas for Sinos catchment adopting the agriculture zoning scheme as land use	172
8.15	Intensities and spatial distribution of Nitrogen concentration adopting the agriculture zoning scheme scenario	172
8.16	System framework for evaluating different scenarios	174

9.1	Correlation for spatial attributes	181
9.2	Response surface for output (y) as a function of two inputs (A_1 and A_2)	182
9.3	Slopes of the output y as a measure of models' quality	184
9.4	Spatial autocorrelation	188
9.5	Uncertainties of DEM slope	189
9.6	The discretization scheme	192
9.7	(a) observed data and (b) spatial weight matrix	193
9.8	Intermediate levels for iterative simulation of 100x50 grid	195
9.9	Exampes for different values of the spatial dependence parameter	196
9.10	Examples of generation of attributes ($A(X)$) that satisfies equation 9.7	198
9.11	Uncertainties' results for nitrogen prediction	199

List of Tables

	<u>Page</u>	
1.1	Water availability in some countries of the world	2
1.2	Water quality criteria in river waters used for public supply	2
1.3	Sinos catchment population census	9
2.1	A procedure for a GIS hydrology study	32
2.2	Average flow in Sinos river	33
2.3	Relative variability of stream gauges in Table 2.2	35
2.4	BOD ₅ and discharge from waste disposal in Sinos river	38
2.5	Average water quality samples	39
2.6	Classification accuracy matrix for six classes	41
2.7	Samples in Sinos catchment	46
3.1	Topological table for the drainage network of figure 3.15	74
4.1	Hydrologic soil properties classified by soil texture	91
4.2	SCS hydrologic soil groups	91
4.3	Curve Number (<i>Soil Conservation Service</i>)	92
4.4	Parameter Pa _i	93
4.5	Results of a linear regression between the runoff indices and the flow values	100
5.1	Loading rates and land use	106
5.2	Values for determining critical sources areas for production of nitrogen	118
5.3	Values for determining critical sources areas for biochemical oxygen demand	119
5.4	Values for determining critical sources areas for phosphorus	121
7.1	Sequence of operations applying equations 7.8 and 7.9	154
8.1	Results of a linear regression between the runoff indices and the flow values	159
9.1	Numerical results for a simulation of a 100x50 grid with $\delta=0.001$	194

1.Introduction

1.1 - Major water pollutions problems in Brazil

Over the past decades, the quality of river water has been increasingly affected by human activities. Quality has usually deteriorated gradually over time until degradation has become apparent and measurable. Awareness of a pollution problem has therefore often taken considerable time, and application of the necessary control measures has taken even longer (Helmer, 1987). The appearance of pre-industrial and industrial (types of) water pollution, which occurred over 100 years ago or more in Europe, has occurred within one generation in developing countries with rapidly growing populations such as Brazil, China, India, Indonesia, Mexico and Nigeria, where pollution sources and demands upon water resources are expanding. Only 10 out of the 60 countries in this category have established effective laws, regulations, and an enforcement infrastructure to cope with pollution problems (Helmer, 1987).

In Brazil, which is a huge country (8,512,000 km²) with diverse regions, abundant natural resources, large-scale industry, and strong links with the global economy, there is an increasing growth of urbanisation. In 1990 twelve metropolitan areas had a population of more than one million; moreover, both Rio de Janeiro and São Paulo are now megacities with populations of more than ten million.

Brazil, also has the largest percentage of world river flow (Table 1.1), and needs to be able to monitor and predict the potential impacts of human activities and pollution control programs on the environment. It needs accurate and timely information about the quality of its water resources so that it can make scientifically-based decisions and policy at all governmental levels. During the past two decades Federal, State, and local governments have made significant commitments to the protection and enhancement of water quality. In spite of these investments, information is not available to answer some rather fundamental questions to the satisfaction of the scientific, regulatory, and management communities, and the public. Some example questions include:

- Are national water quality goals being met? How effective have past actions been? Examples of treatment oriented quality criteria for rivers are given in Table 1.2.
- What is the extent of various types of nonpoint-source contamination, and how does nonpoint-source contamination compare to various types of point-source contamination?

- Can regulations be targeted to specific water quality constituents in particularly sensitive hydrologic settings?
- What natural and human-induced constituents in water are most prevalent in the different hydrologic, geologic, climatic, and land-use settings that comprise Brazil?

Country	Area ($km^2 \times 10^3$)	Population ¹ (10^6)	Long-term mean annual riverflow			
			(km^3)	Per unit area ($10^3 m^3 km^{-2}$)	Per Capita ($m^3 \times 10^3$)	Percentage of world riverflow
Brazil	8512	130	9230	1084	71	20.7
China	9561	1024	2550	267	2.5	5.7
Canada	9976	25	2470	248	99	5.6
India	3288	718	1680	511	2.3	3.8
USA	9363	234	1940	207	8.3	4.4
France	544	55	183	336	3.4	0.4

Table 1.1 : Water availability in some countries of the world.

Source: Shiklomanov (1990)

1 - For 1983.

WATER QUALITY VARIABLE	High quality water minimal treatment*				Low quality water advanced treatment**			
	India	Japan	UK	Brazil	India	Japan	UK	Brazil
Dissolved Oxygen, DO ($mg l^{-1}$) (% saturation)	> 6	> 7.5	>80%	> 6	> 4	> 5	>40%	> 4
Biochemical Oxygen Demand, BOD ($mg l^{-1}$)	< 2	< 1	< 3	< 3	< 3	< 3	< 9	< 10
Total coliforms (MPN/100 ml)	50	50	--	1.000	5.000	5.000	--	20.000

Table 1.2 : Water quality criteria in river waters used for public supply.

Source: WHO (1988) and CONAMA (1992).

* - Disinfection and filtration

** - Full treatment and disinfection

River systems are a major source of water for agricultural and urban water needs. Water quality assessments of river systems are becoming critical throughout Brazil and there is a concern about the sustainable supply of quality water and the health of the water bodies. River systems should

be continuously monitored to assess the effects of different land management practices on water quality, but, few of any river system are continuously monitored at present due to high costs. Therefore, there is a need for a complementary tool such as a basin-scale hydrologic/water quality model that is capable of predicting the effects of land management. Consequently, the basic objective of the field of water quality engineering is the determination of the environmental controls that must be instituted to achieve a specific environmental quality objective. Also, nationally consistent and comparable information is needed to make valid regional and national statements about current water-quality conditions and changes in these conditions. Existing programs designed to report on the status of Brazil's water resources have not always proved meaningful. In many instances, there are consistency problems because field and laboratory procedures and methods are not uniform and comparable among Federal, State, and Local agencies and often change through time; sites are selected to investigate a specific water-quality problem that is not representative of the surrounding area; long-term monitoring is lacking and trends are difficult to detect; data are lacking on potentially toxic constituents such as trace elements, pesticides, and other organic constituents of concern; and most studies have not been of an interdisciplinary nature that involve comprehensive use of physical, chemical, and biological data, nor have these studies been integrated to assess the interaction of the various resources on observed or predicted water quality conditions.

Because of the wide range of different government and economic conditions around the world, it is difficult to provide general guidelines regarding the role of government in environmental protection that cover all possible situations. In spite of efforts by Brazilian government at many levels to control the causes of environmental problems, water quality has continued to deteriorate in many streams, lakes, reservoirs and coastal areas in Brazil, produced by a great diversity of pollution types, climatic factors, river flow and pollutant transport capacity, as exemplified in Figure 1.1. Thus, solutions to such problems in industrialised countries are often not directly applicable to developing countries.

Many different surface and subsurface hydrological process may contribute to streamflow generation and quality in catchments, and the relative importance of the processes may vary in space and time. Knowledge of the relative importance of the different processes is central to understanding many of the features of the catchment. This thesis aims to develop a model, appropriate for Brazilian conditions, capable of predicting water quality at the basin scale. The key to this approach is the development of information on physical, chemical, and biological conditions, and responses of individual catchments to both natural and human-induced changes. It

is important that catchment information be comprehensive, include a full description of the hydrologic cycle including the interaction of the quantity and quality of ground water (not included in this thesis), surface water, and atmospheric inputs. In most catchments in Brazil, comprehensive and integrated information of this type is lacking. Where information is available, it has seldom been compiled or analysed with the objective of understanding the interaction of all components of the hydrologic system and using this information to support the development, implementation, and evaluation of water-resource management actions.

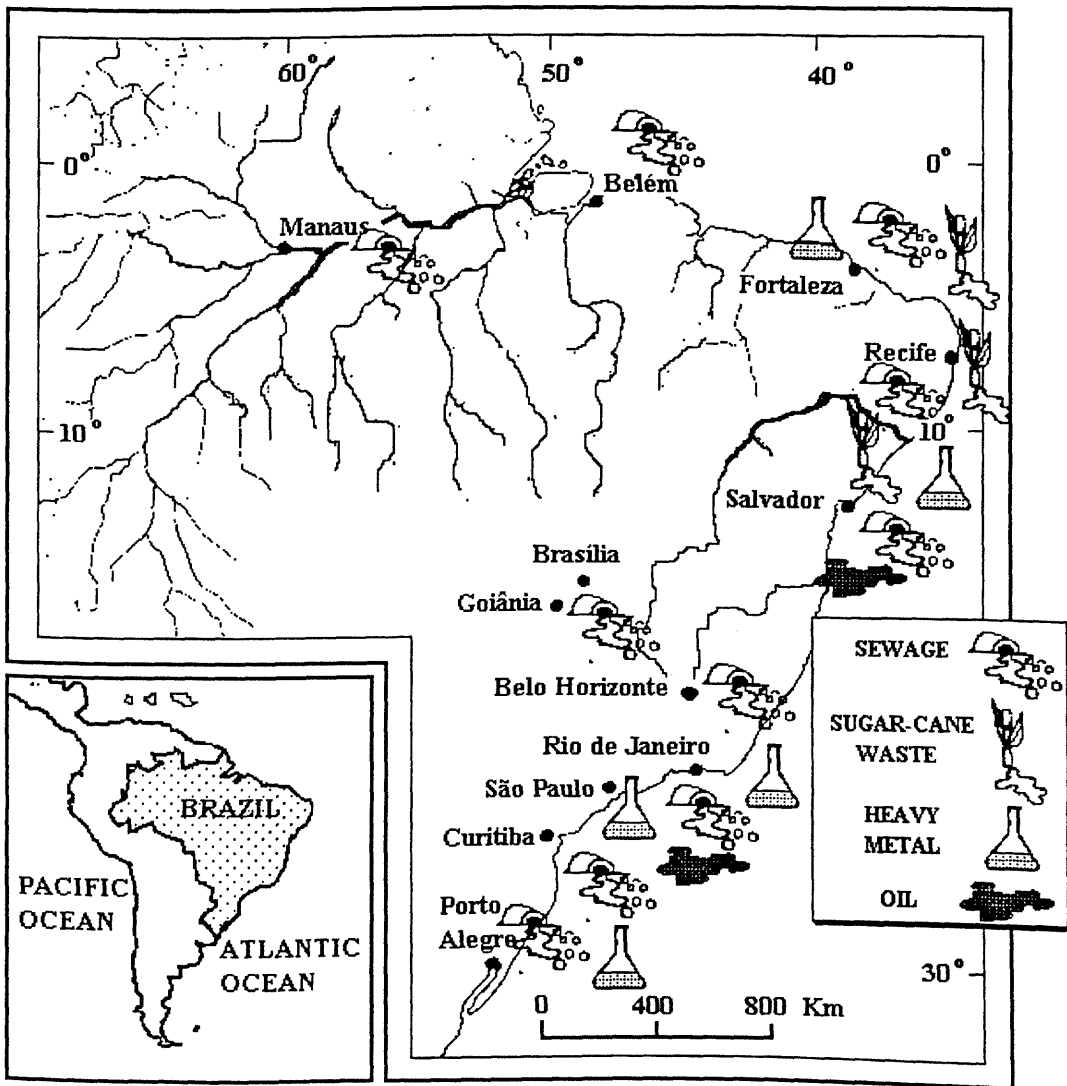


Figure 1.1 : Some major water quality problems in Brazil.

Adapted : Mendes (1990).

1.2 - Background to the pollution problem in an industrialised catchment of southern Brazil

The Sinos river (see Figure 1.2) flows into the Jacuí Delta, a delta located in the south of Brazil in the State of Rio Grande do Sul. The Jacuí Delta is a complex system of branches, confluences and storage basins. Below the downstream section of the delta, there are a series of large lakes that are linked together until they reach the Atlantic Ocean, as shown in Figure 1.2.

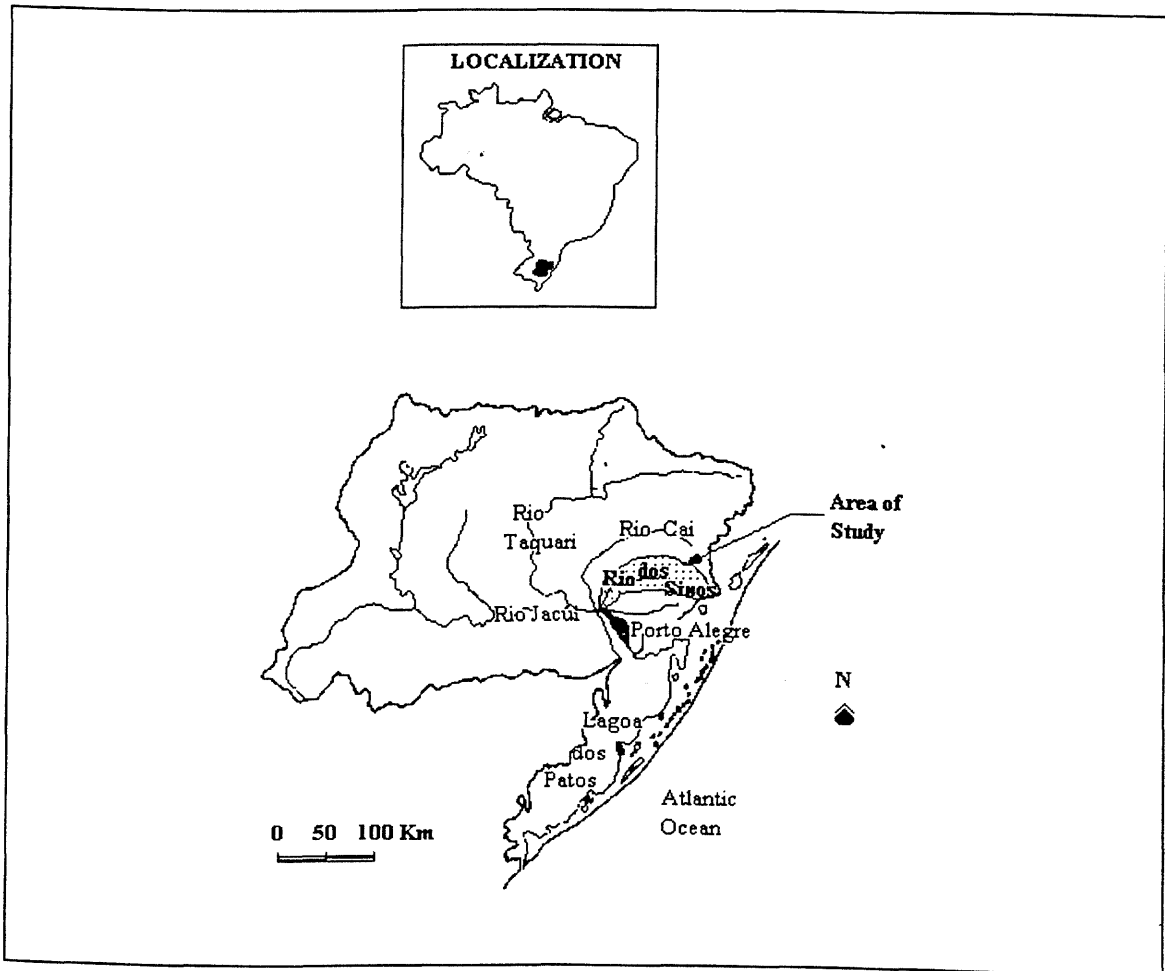


Figure 1.2 : The Sinos catchment in Southern Brazil.

In addition to its high pollution levels, the Sinos river was chosen for this study because of its regional and industrial importance, and associated high population density. It is also the river in the metropolitan area of Porto Alegre, which has the greatest amount of data on water quality and surveys, and basin characteristics (Agrar-und Hydrotechnik, 1969; Viera, 1970; Itaconsult-Latinoconsult Brasileira, 1974; Luna Caicedo et al., 1976; Rezende et al., 1977; Simões Lopes et al., 1978(a); Simões Lopes et al., 1978(b); Moretti, 1979; Moretti, 1980; Silveira, 1980(a);

Silveira, 1980(b); Freitas et al., 1981; DMAE and CESB, 1981; Tucci et al., 1982; DMAE, 1985; Ferreira, 1986; Silveira, 1986; Benetti, 1987; De Luca, 1987;). This river is now of great interest to government agencies such as DMA (Department of the Environment), CORSAN (Rio Grande do Sul Sanitation Company), DMAE (Municipal water and sewage department of Porto Alegre) and METROPLAN (Metropolitan Planning Agency). A basin management organisation was established in 1988, the COMITESINOS-Committee for the conservation, management and research of the Sinos river.

The Sinos river begins in the county of São Francisco de Paula, on the eastern slopes of the catchment, at an altitude of approximately 900 m. The northern part of the basin is a plateau zone, with a mountain area to east and to the south a narrow strip of meridional plateau. These three zones surround a hilly area that descends to the plain of Sinos river mouth, where there is a wetland zone (see Figure 2.17 later in chapter 2).

The natural forest is of sub-tropical humid type in the valleys and araucaria (*Parana pine* or *Araucaria Angustifolia*) forests at higher altitudes. It has been much reduced by settlement and farming development. Forests were reduced, through burning, to remnants close to the rivers, especially on the eastern and northern borders of the basin. The natural forests now cover an area that is only slightly over 10% of the total basin area.

The high temperatures recorded during most months cause high evapotranspiration, and there is a marked water deficit in summer. The water level in the Jacuí delta shows a cyclic variation with an amplitude of about 30 cm within a 24 hour time period caused by a seiche effect in the Lagoa dos Patos. This cyclic variation is sometimes altered by wind effects or floods. In the dry season, when the flow is low, a flow inversion can occur due to seiche effects from the Jacuí delta. The downstream effects on the river are felt up to approximately 40 km upstream.

The catchment is approximately 3700 km² in area, with a length of approximately 190 km as illustrated in Figure 1.3. The area of study is located in a humid climate, between sub-tropical and temperate zones. Mean annual rainfall is 1600 mm throughout the region, ranging from approximately 2300 mm at higher altitudes, to approximately 1400 mm at lower altitudes.

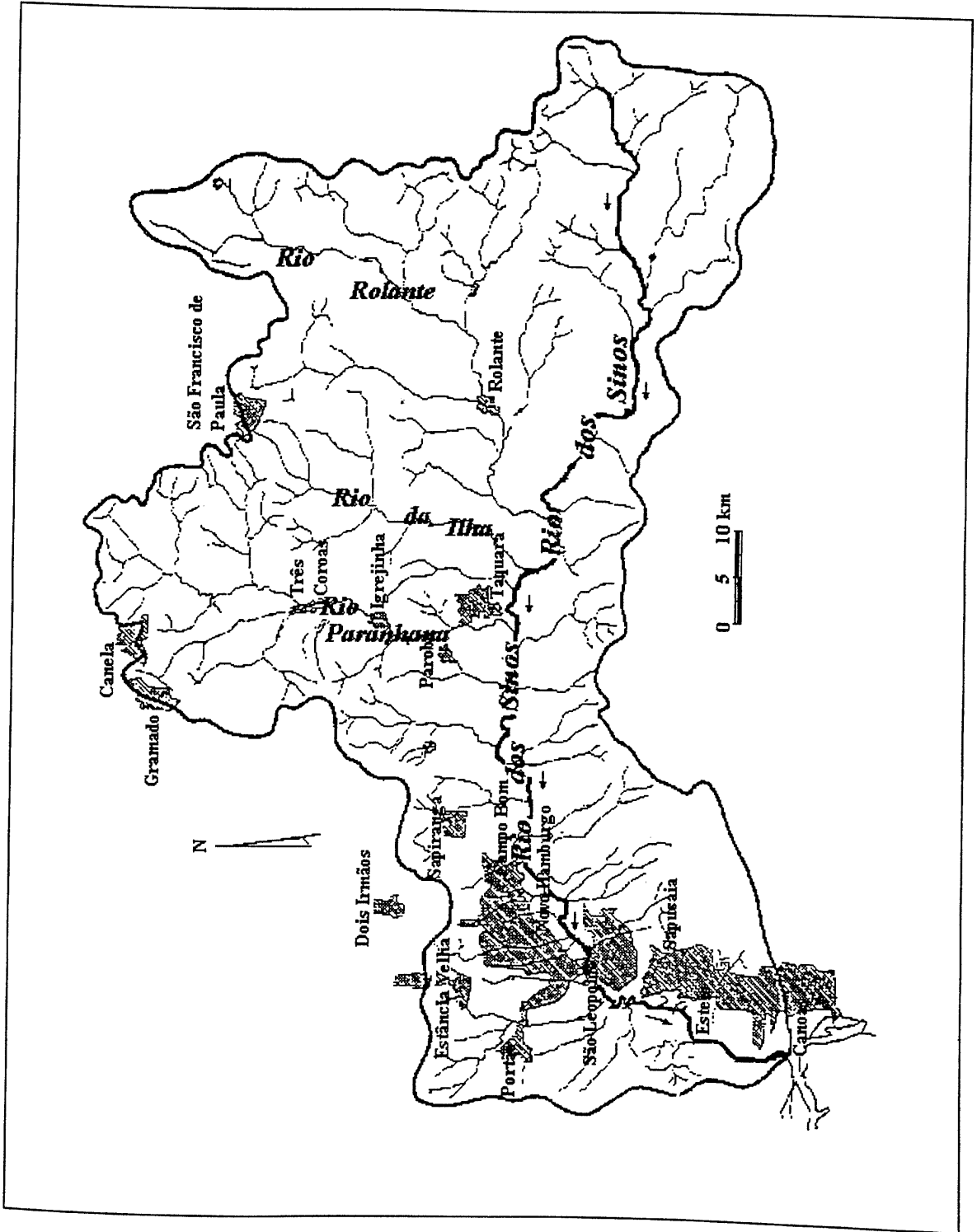


Figure 1.3 : Sinos catchment in Southern Brazil

The mean annual temperature is approximately 18°C; during the hottest month (January) the mean daily temperature is 21°C falling to 12°C in July. Relative humidity for the study area is high with a mean annual value of approximately 80%. The annual average flow is approximately 42 m³s⁻¹, with maximum and minimum flows of 200 m³s⁻¹ and 4 m³s⁻¹ at the basin outlet.

Two main geologic structural settings can be identified in the Sinos catchment: sedimentary basins and igneous rock basins (fractured basalt). The sedimentary-basins setting is typified by a basin partially or entirely surrounded by highlands composed of rocks older than 110 millions years (from the Cretaceous period onwards). Erosion of the highlands adjacent to these basins has resulted in the deposition of relatively large thicknesses of younger basin-fill deposits. Wells in the fractured basalt rock provide high yields (Q ranging from 1.5 to 30.0 m³h⁻¹, according to fracture size), whereas wells in alluvial aquifer system provide low yields (Q ranging from 1.0 to 6.0 m³h⁻¹)

Human influences affecting water quality and quantity in the Sinos catchment include the discharge of domestic and industrial wastewater, development and expansion of urban areas, energy production, livestock production, agriculture, and silviculture. The Sinos river basin has undergone a process of industrialisation, initially linked to the leather and tanning industry, as a natural consequence of the development of cattle farming. This development has been superimposed on the existing industries of timber (Upper catchment), cattle breeding and agriculture (irrigated rice). Through the initial industrialisation and with improvements to the railways and the building of the BR 116 motorway, the population increased rapidly. Growth has been particularly pronounced in the lower basin (counties of Esteio, Canoas, Sapucaia, São Leopoldo, Portão and Novo Hamburgo - see Figure 1.4 and Table 1.3) due to the proximity to Porto Alegre; these counties area growing dormitory district for those people working in the state capital of Rio Grande do Sul. Therefore, in the lower reaches of the Sinos, we find a metropolitan appendage of Porto Alegre, in which the natural-agrarian element re-appears only outside the Campo Bom and Sapiranga counties.

To devise a program of water quality management in the Sinos catchment, it is essential to determine the nature of water resources in the drainage basin as to their magnitude and suitability for different uses. The quantity and quality of river flow are liable to fluctuate from day to day, season to season and year to year. These fluctuations may be very considerable, but water quality

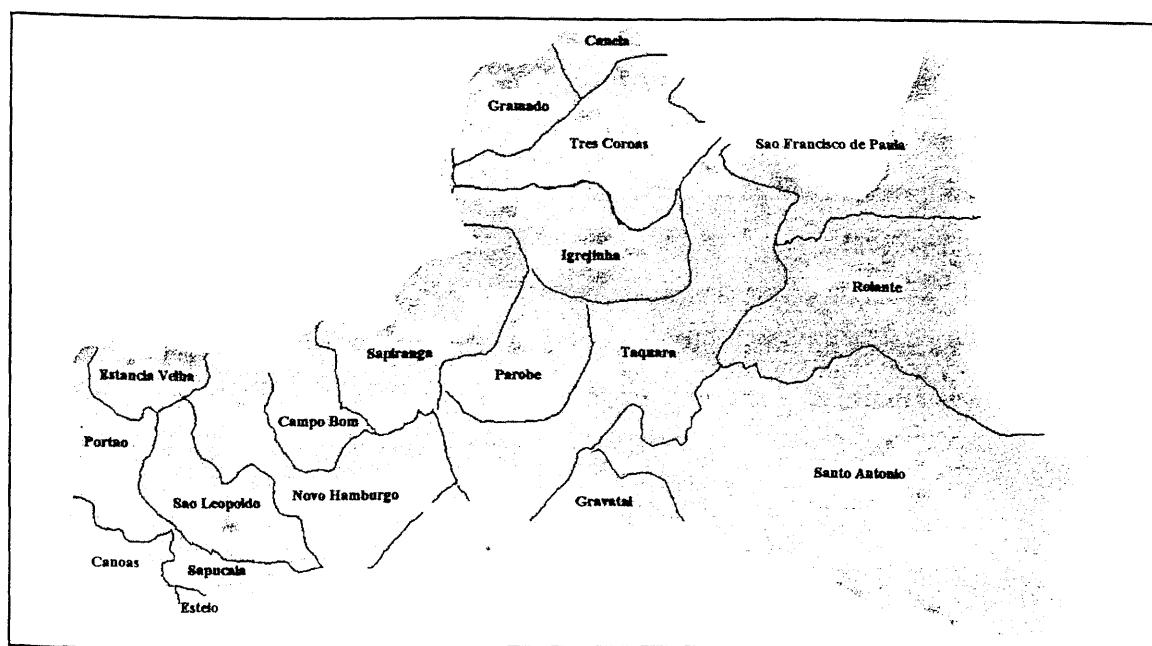


Figure 1.4 : Administrative division in Sinos catchment.

County	Area (ha)	Population 1960	Population 1970	Population 1980	Pop. trend 60-70-80
Campo Bom	5,946	8,511	16,654	34,202	strong increase
Canela	24,149	12,680	14,081	19,484	increase
Canoas	34,269	104,257	154,832	223,333	increase
Estancia Velha	5,185	4,640	9,158	14,467	increase
Esteio	2,863	22,217	35,174	51,874	increase
Gramado	25,271	10,819	12,435	16,541	increase
Gravatai	83,571	34,737	52,733	108,733	strong increase
Igrejinha	15,483	4,864	7,129	12,099	strong increase
Novo Hamburgo	23,223	53,916	85,956	138,400	strong increase
Parobe ¹	10,100	*	*	7,281	*
Portao	17,274	4,634	7,506	10,818	increase
Rolante	63,254	16,381	14,947	11,901	decrease
Santo Antonio	143,960	54,138	53,922	41,787	decrease
Sao Francisco de Paula	462,759	32,388	32,328	23,547	decrease
Sao Leopoldo	11,031	45,617	65,462	104,216	strong increase
Sapiranga	23,760	11,984	16,461	37,517	strong increase
Sapucaia	6,496	18,300	41,965	80,635	strong increase
Taquara	49,202	28,146	31,728	42,296	increase
Tres Coroas	16,756	6,041	6,411	10,514	strong increase

Table 1.3 : Sinos catchment population census.

Source: IBGE - Instituto Brasileiro de Geografia e Estatistica.

¹ - county created in mid 70s.

is generally poorest during periods of low flow. The minimum flow periods are usually the most critical. Restrictive measures are promulgated under extreme drought conditions. The assimilative capacity of a river is related to its low-flow regime. The river and effluent standards are usually geared to low flows. In this research the behaviour of the characteristics of flows in fixed low-flow season are examined. The critical condition, which is a low flow upstream (poor water quality), increases the tidal influence downstream in Sinos catchment. Because the approach used in this thesis does not account for unsteady state behaviour, we have simulated catchment behaviour only upstream of São Leopoldo county (see Figure 1.3). In the following chapter the full features of Sinos catchment are given.

1.3 - The overall perspective of the pollution problem

One of the central problem of waters quality planning and management is the assignment of allowable discharges of pollutants to a river where a designated water use and quality standard have to be met (Figure 1.5). The approach used in this thesis analyses only one component of the problem, the relationship between loads and water quality for actual and projected conditions. Of course, it is not sufficient to make only a scientific analysis of the effect of inputs on water quality. The analysis framework must also include economic impacts and socio-political constraints that are operative in the context of the problem (not included in this thesis). In practice, this link between the physical, economic and socio-political environment can not be undertaken. In fact, it may be extremely difficult to achieve these goals for some time due mainly to the lack of communication between technical staff, economists and planners involved in the process.

In order to be able to address future environmental problems related to water quality it is usual to divide the problem into its principal components. as shown in Figure 1.5. In such an approach there are four basic components:

1. The inputs (point and non point sources of pollutants) discharged into a river, lake, estuary or oceanic region as a result of a natural phenomena or human activity.
2. The river chemical, biological and physical processes (such as bacterial biodegradation, chemical hydrolysis, sedimentation and mass transport), which change the inputs, resulting in different water quality conditions at different locations in the drainage network.
3. The resulting concentration of a pollutant at a particular location in the river.
4. The management alternatives that affect the pollutant concentration.

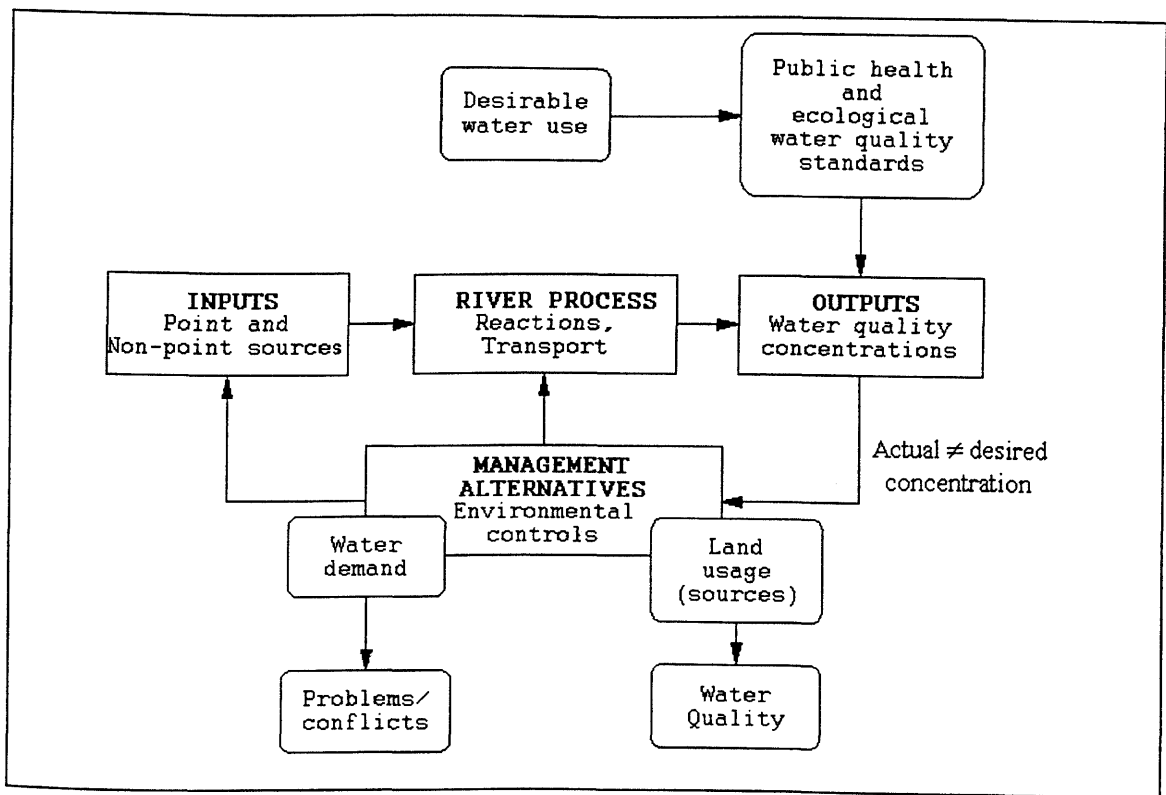


Figure 1.5 : Flow diagram - water quality engineering.

The physical, chemical, and biological quality of the water in any catchment is related to the environmental setting. The resulting water quality is the product of the natural conditions and human factors that make up the environmental setting on the catchment. The following discussion describes the general nature of the implications of environmental setting to water quality. Conceptual models and hypotheses are discussed which relate current water-quality conditions to natural and anthropogenic factors.

Catchments vary in size and shape depending on the kind of topography where they reside. Major factors affecting runoff from catchments include size, shape, orientation, topography, geology, and land use. Most major catchments are composed of smaller units called subcatchments. These consist of the tributaries of the main river drainage for the particular catchment. Land use within each subcatchment, both agricultural and nonagricultural, will determine the overall quality of water within the entire catchment.

Various agricultural activities affect either improvement or degradation of water quality within a given catchment. Management practices such as terraces, conservation tillage, and diversions help to reduce sediment in runoff during heavy rains. Most non-agricultural activities take the

form of some kind of urbanisation, or urban and industrial development. Other land uses may include landfills and mining operations that have an impact upon the subcatchments.

Runoff from cropland can result in the transport of both sediment and agricultural chemicals into surface waters such as streams and lakes, and can also find its way through infiltration into the groundwater. Several factors control the degree of runoff and the potential for contamination of surface water from overland flow. The type of crops planted, soil type, slope, and the type of management practices, if any, that are applied help to determine the degree of overland flow, and potential for contaminant transport that will occur at a given site.

Certain contaminants are of significant concern relative to their biological availability. Phosphorus is one contaminant that is carried by sediment and may be converted to dissolved inorganic phosphorus. Thus, the biological availability of phosphorus is determined by the rate and extent of conversion of particulate phosphorus into dissolved inorganic phosphorus. This process is similar for other contaminants such as nitrogen. Once these contaminants become biologically available, aquatic plant life is able to feed on them, in excess, the result is eutrophication of the water, affecting populations of fish and other organisms within the water body.

Mass loading for waterborne contaminants is usually expressed as $\text{kg}\cdot\text{ha}^{-1}$, in SI units. These units may be applied to either surface, or ground water sources of pollution. Some researchers report mass loads in mass units only for the entire area being studied, such as a sub catchment or a particular farm. If the area of the sub catchment, catchment, or farm is known, then the loading in units of $\text{kg}\cdot\text{ha}^{-1}$, can then be calculated.

The quantity of contaminant load carried by surface and ground water is largely dependent upon land use, and what measures have been taken to reduce potential point and non-point source pollution. Environmental and hydrological modelling is used to simulate the functioning of catchment systems and to understand their behaviour under altered conditions. Such understanding is essential to manage land and water resources effectively, for assessment of environmental risks, and for analysis of impacts of environmental change. At present knowledge about the dynamics of dominant processes in large catchments is still rather limited due to extremely complicated character of these processes and interrelation of many factors of different nature (Beven, 1995). Reliable assessment of point and nonpoint source pollution is one of the

problems involved, especially for larger catchments for both agricultural and non-agricultural land uses.

Some of the available models have been developed to solve a variety of different problems, within a number of different application contexts and, as a consequence, they often require different equations, parameters, and assumptions. Those models that are capable of dealing with this spatial variation do so by using complicated spatial databases [e.g. FESHM (Finite Element Simulation Hydrological Model, Ross et al., 1977); ANSWERS (Areal Nonpoint Source Watershed Environment Response Simulation; Beasley et al., 1980); CREAMS (Chemical Runoff and Erosion from Agricultural Management Systems; Knisel, 1980); HSPF (Hydrological Simulation Program Fortran, Johanson and Kittle, 1983); EPIC (Erosion Productivity Impact Calculator; Williams et al., 1984); SHE (Système Hydrologique Européen; Abbott et al., 1986); AGNPS (AGricultural NonPoint Source; Young et al., 1989); and MEDALUS (MEDiterranean Desertification And Land USE, Kirkby et al., 1992)]. Reviews of existing hydrological, soil erosion and pollution models can be found in Foster (1982), DeCoursey (1985), Marsalek (1989) and Franchini and Pacciani (1991).

It is common, in countries such as Brazil, that only a limited data base is available to support complex modelling activities and extensive analyses. Due to inadequate funds for data acquisition and chemical analysis, one consequence is that we cannot develop a highly detailed physical model, as shown above, to describe the relationships between sources of pollutants, flow characteristics and management alternatives because there are large uncertainties in the input data. The scarcity of data seriously limits the application of complex models in less developed countries. Consequently, the approach to be developed in this thesis must be suitable for application when data are scarce.

In Brazil, there is also a particular concern with environmental problems operating over very wide catchments. The majority of large catchments have both urbanised and agricultural land uses causing both point and non-point sources of pollution. The majority of the above models characterise water quality for both conditions, and while some of them work with either agricultural or urban catchments, they are more limited in their ability to operate within mixed catchments. For example, the application of AGNPS and ANSWERS is limited to catchments of about 200 km².

Another disadvantage of these models is that whilst requiring spatially distributed data, they provide limited facilities for compilation, processing and display of such data. Geographical Information Systems (GISs) and related technologies, such as Remote Sensing, have the potential to meet these needs, and are becoming significant parts of systems for environmental modelling (Kovar and Nachtnebel, 1993).

Despite the proliferation of models and their reported successful application, decision makers in developing countries, such as Brazil, do not have the opportunity to use models directly, because most of them:

1. tend to require a large number of input data, and this can be expensive or impossible to obtain;
2. involve a large number of parameters;
3. are extremely complex and difficult to maintain;
4. tend to produce large quantities of output, much of which can be difficult to summarise and comprehend;
5. need mainframe computers (or workstations) to run, and most of the environmental planning agencies in countries like Brazil only have microcomputers (PCs).

1.4 - Objectives

There are many different aspects of the problem of water quality planning and management, as shown in the preceding section. Therefore, any research that aims at obtaining concrete solutions should necessarily start with selecting a particular segment. In this research, I have solely to restrict myself to analyse the relationship between loads and water quality for actual and projected conditions. In order to investigate this relationship the following steps are required:

1. *Make an inventory of catchment characteristics, including land-use, soils, rainfall and topography information, to predict the generation of runoff for later analysis of the production and transport of pollutants.*
2. *Derive a catchment and river network layout from digital elevation data.*
3. *Separate precipitation into surface runoff, partitioning of chemicals applied to the land use.*
4. *Identify critical source areas in the catchment where potential pollutant loadings are greatest. These areas deserve special attention, since they often exceed surrounding areas in terms of pollutant loading.*
5. *Transport of contaminants through the landscape in water as it flows.*

6. ***Determine critical links in the drainage network. In a link model, a drainage network is divided into a number of links. The sources of pollutants consist of the point and non point inputs to the river link.***
7. ***Determine pollutant dynamics in rivers. This step reflects physical, chemical and biological interactions between the water column in the river and the surrounding drainage basin.***
8. ***Change land use and analyse their effects on water flow, water quality and constituent transport.***

Use of this approach is illustrated for a case study which demonstrates the generation and routing of point and non-point pollutant sources and water quality responses in the Sinos catchment (Southern Brazil).

The system developed in this thesis describes quality of rivers by means of:

- Acquisition and filing of hydrometeorological and environmental data and their introduction into a geographical data bank.
- Manipulation of basic and thematic maps obtained from satellite images using image processing software.
- Determination of parameters from a Digital Elevation Model (DEM) for subsequent use in hydrologic models.
- Creation of a distributed hydrological model with parameters having some physical interpretation.
- Generation of a pollutant propagation models in the surface slopes and drainage network.
- Creation of a pollutant mixing model for the surface drainage network.
- Use of a geographical information system (GIS) for integration of the models and for results display in distributed graphical form.

The above steps should cross-reference with the preceding discussion of the problem (section 1.3). Consequently, the modelling framework proposed will:

1. Be based on generally available data (e.g. topography, land use, rainfall and soil type).
2. Not require extensive calibration procedures.
3. Be simple, robust, rapid and inexpensive in operation.
4. Combine spatially distributed variables using physically based transport/mixing models to generate pollutant loads overland and within the drainage network.
5. Link and propagate the pollution sources through a drainage network via topology.

6. Deal with seasonal fluctuations.
7. Encompass large and diverse land uses, such as agricultural and urban.
8. Combine different sources of pollution (point and non-point sources).
9. Store and manipulate extensive data sets.
10. Test alternative management scenarios.

1.5 - Overview of the thesis

This thesis is organised as follows. Chapter 1 is a brief introduction describing why the problem being investigated is important, how we approached the solution of these problems, and the majority of the system components adopted for these solutions.

Chapter 2 provides an explanation of the fundamental physical concepts along with general GIS ideas and their implications. It also discusses characteristics of the Sinos catchment in southern Brazil.

Chapters 3 to 7 describe the components and formulation of the various model sub-systems. The results presented in these chapters (3 to 7) are derived from a small test data set presented solely to demonstrate the management utility of the approach, and to illustrate the implementation and operation of the algorithms. The development of the problem with respect to the whole catchment is also addressed in each one of these chapters. For example, the Digital Elevation Model theory, which is developed in chapter 3 is carried out for the Sinos catchment within chapter 3.

Chapter 3 presents a set of algorithms that automate the determination of catchment and drainage network parameters, from a Digital Elevation Model (DEM), for later use in hydrologic and water quality models.

Chapter 4 presents a spatially distributed runoff model consisting of a grid of connected cells based on their relative topographic position as defined by a DEM. Each cell receives, as input, the rainfall excess for the area, as well as inflows from upstream cells. Output from the cell is derived from parameters easily defined in terms of topography, land use, soil type and rainfall.

Chapter 5 presents a scheme for pollutant generation within individual cells of the catchment. The geographical information system (GIS) is used to facilitate the identification of critical non-point source areas of pollution.

Chapter 6 aggregates pollution sources from upstream catchment areas on land surfaces having heterogeneous water pollution effects and analyses the spatial relationships between point and non-point sources referenced to a drainage network.

Chapter 7 simulates the distribution of pollutants in the drainage network using a spatial model that exploits the topologic relationships through the drainage network together with a simple mixing model.

Chapter 8 demonstrates a real application of the system to analyse the relationship between loads and water quality for actual and projected conditions in the Sinos catchment (Brazil). The focus of this chapter is solely model validation, having had the development in the preceding chapters. It is shown that the advantage of this system is that it has the capability to analyse an extensive catchment requiring only data obtained from maps (topography, soil, etc.) and remotely sensed data.

Chapter 9 establishes a framework for the identification of uncertainties involved in models of catchment water quality, and defines a methodology for error propagation, which could be incorporated in future developments of the GIS based approach illustrated in Chapter 8.

Finally, in chapter 10, a summary of the main features of the system are given, conclusions relating to its practical uses are presented and suggestions for future research are given.

2. Framework for analysis

2.1 - Introduction

Water resources models provide understanding of water resources problems by representing physical, economic and/or social processes. These processes are then simulated to test alternative scenarios. However, few of these models have the capability to analyse and display spatial information. It would seem, therefore, that water resources models could benefit from the spatial analysis and display capability of Geographical Information Systems (GIS). However, following Parker (1988), GIS offer little modelling capability with most offering only primary modelling tools, such as map overlays and buffering. The conclusion seems to be, therefore, that there are clear benefits to be gained by using both hydrological models and GIS in conjunction.

In this thesis existing GIS capabilities for hydrologic modelling are presented in which two-dimensional spatially distributed hydrologic processes are represented on a grid and one-dimensional flow and transport occurs through an associated network. Once the direction of flow on each grid cell is defined to a single neighbour cell, an implicit flow network is created. Consequently, spatially distributed hydrological formulae for runoff, erosion and generation of pollutants can be used on the grid to determine the rate of supply of pollutants to the river system, and then pollutant routing procedures used on the network to trace the movement of pollutants through a river.

The aim of this chapter is to describe how the fundamental basis of water resources modelling can be reconsidered within a GIS framework allowing the two-dimensional spatially distributed description of climatic conditions, land and water use, geology, physiography, population, surface water and groundwater hydrology, and a description of the water resources issues in Sinos catchment. This description also analyse existing water quality data and a 60 days of field data collection in Brazil.

2.2 - Developing a spatial hydrology model

2.2.1 - Hydrologic system

A system is composed of a number of state variables which are related to one another by operators (i.e. the transfer function - f), and are subjected to inputs (X) to produce outputs (Y)

(Bennett and Chorley, 1978). Therefore, the system can be characterised by:

$$Y = f(X) \tag{2.1}$$

The transfer function has a specific structure composed of a number of parameters or constants that determine the magnitude of the transformation. The location of each system variable (Inputs X and outputs Y) can be lumped or distributed. Lumped systems are derived from a point observation of the system at one location or from an averaging of all spatial input and output effects over an area or region. In distributed systems the variables are considered to be distributed over a spatial domain (Figure 2.1). When time is considered to be constant or time invariant over the period of analysis the system is referred to as steady-state; otherwise the system is unsteady-state.

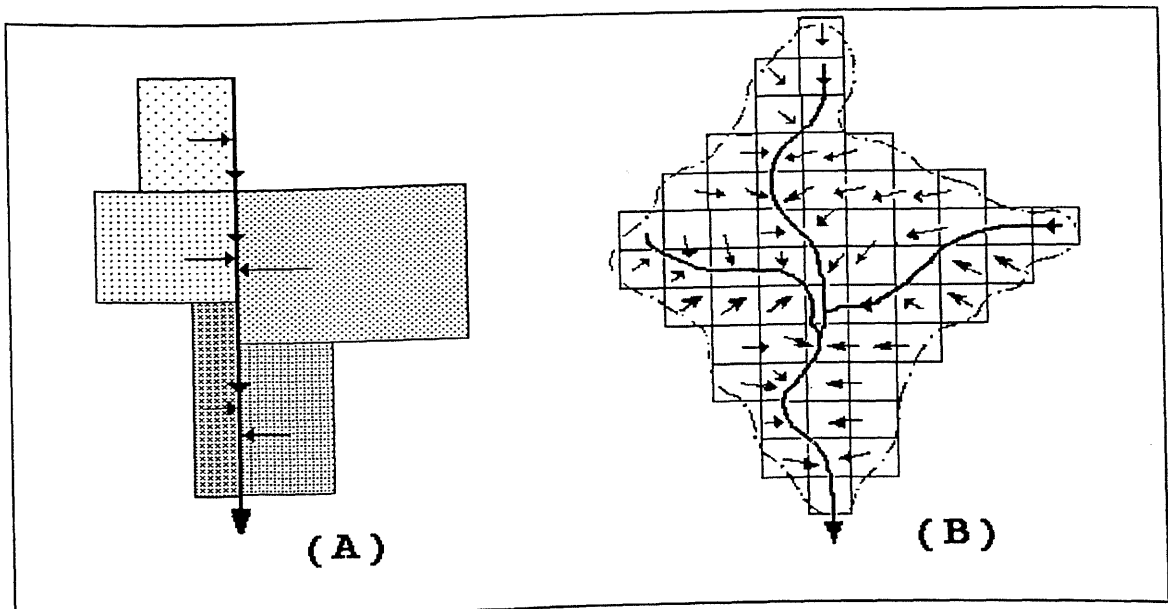


Figure 2.1 : Basic representations of: (A) Lumped system and (B) distributed system.

Systems can be further regarded as either stochastic or deterministic. Stochastic systems are systems in which any of the variables included are considered as random according to some form of probability distribution. If all variables are regarded as free from random variation, the system is deterministic. In practice, randomness or uncertainty has to be considered when many of the properties of the system domain are unknown.

Hydrological models can thus be classified according to the above criteria, i.e. with respect to variations in: time, space and randomness. Figure 2.2 illustrates a classification scheme of systems based on the way they represent randomness, space and time (Chow et al., 1988).

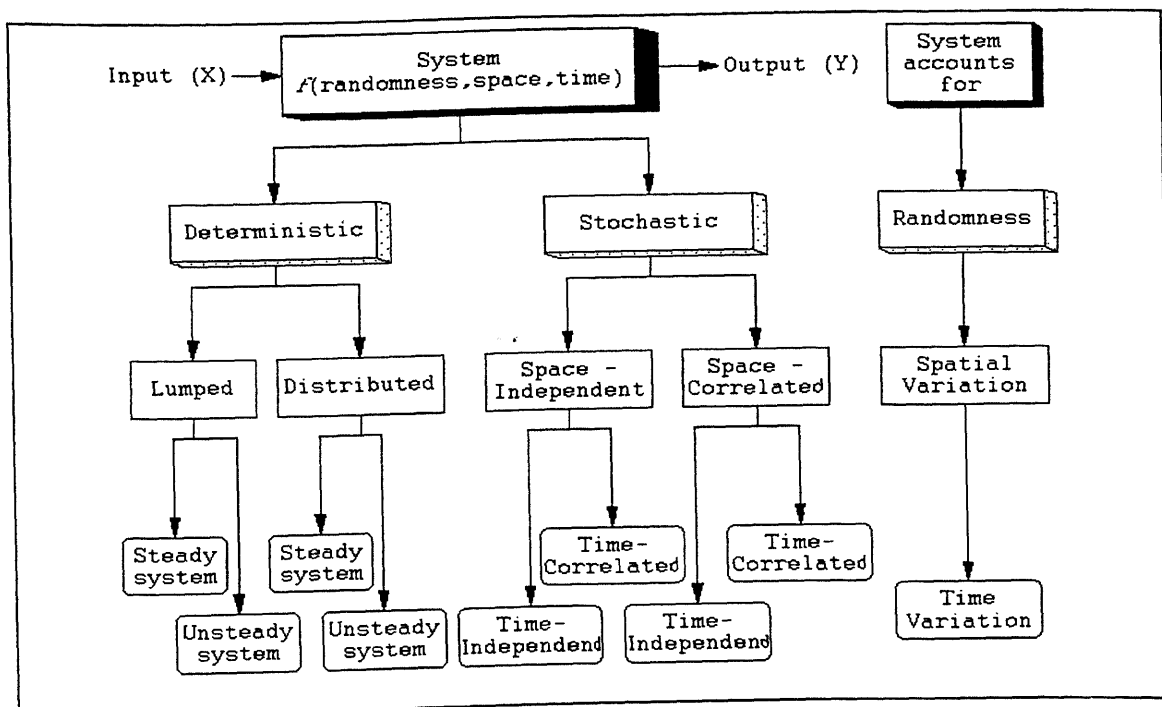


Figure 2.2 : A system's classification based on randomness, space and time.

Adapted : Chow et al. (1988).

A hydrological or catchment system is defined as a set of physical, chemical and/or biological processes acting upon an input variable or variables to convert it (them) into an output variable or variables (Clarke, 1973). The basic functional unit through which the hydrological system operates is the drainage or catchment basin. The major elements in the catchment system are rivers and slopes. These are related in an organisation of slopes converging to rivers that facilitate the function of the system that is to discharge runoff and materials from the catchment (White et al., 1992).

In Figure 2.3 the hydrological system is separated into slope, river and ground water sub-systems. The main input to the slope sub-system is precipitation which also links the hydrological system and atmospheric system. Overland flow, together with pollutants and sediments constitute the bulk of the output from the slope sub-system and represents the major link within the river sub-system.

The main concern in this thesis is the problem of water quality. Examining Figure 2.3 it is possible to see that the delivery of diffuse (non point) pollutants to downstream locations occurs in two phases:

1. Slope-to-river (Slope sub-system) processes where overland and subsurface flow operate, and
2. Within-river (River sub-system) processes where liquid-phase and liquid-solid exchange processes operate.

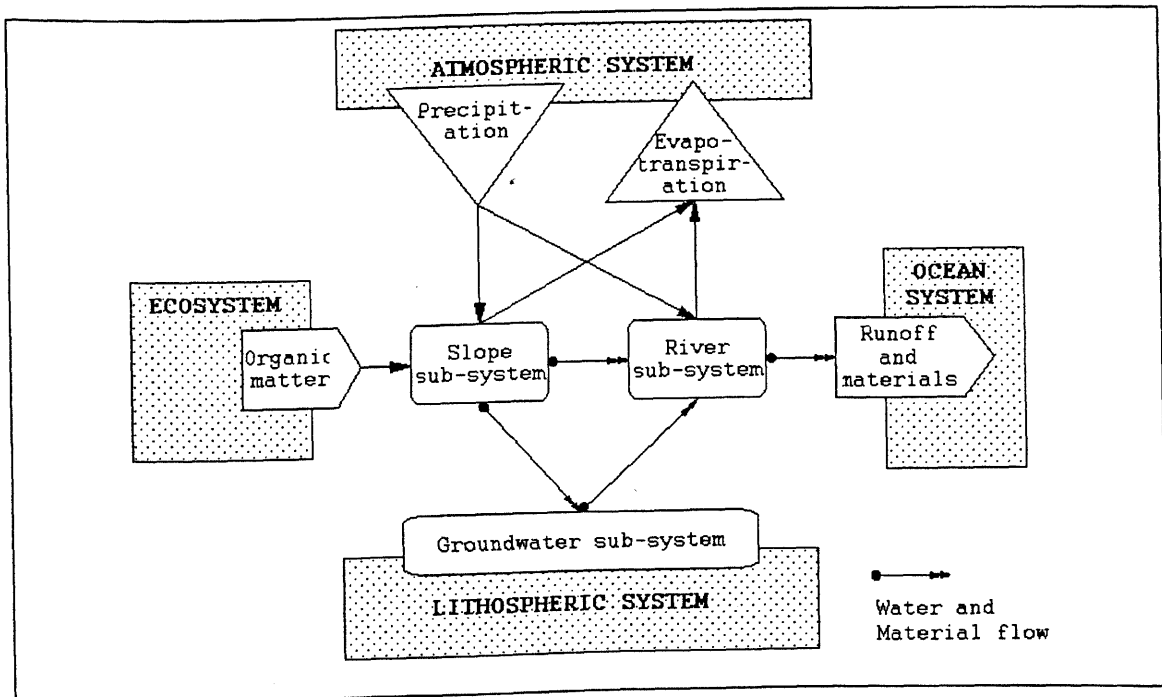


Figure 2.3 : Functional organisation of the catchment system.

Adapted : White et al., (1992).

The slope-to-river process can also be divided into three parts:

- 1.a Production of runoff.
- 1.b Production of pollutants.
- 1.c Transport of pollutants.

Within-river processes are divided into two parts:

- 2.a Aggregation of sources of pollutants (point and non-point sources)
- 2.b The river process (hydraulics, chemical, biological processes, etc.)

This basic division into slope and river sub-systems is used to provide a functional structure to this thesis. Figure 2.27, at the end of this chapter, illustrates the specific structure of the thesis which is embodied in chapters 3-7 and defines the core of the work presented here.

The structure indicated in Figure 2.3 can equally be described in terms of its spatial organisation. Following Wood et al., (1988) a catchment can be treated as being composed of numerous points where precipitation, infiltration, evaporation and runoff form the local water balance fluxes. In order to replace the actual catchment with all its heterogeneity in soils, land use, topography and rainfall inputs with a spatially integrated representative catchment there is a need to describe these elements in terms of their attributes and their spatial relationship. A Geographic Information System (GIS) offers the possibility to handle these spatial elements together with their relationship, in both numerical and descriptive details.

The main focus of this chapter is to present a framework within which GIS and hydrology can be viewed as an integrated subject, and to examine how spatial hydrologic models can be created for natural systems. A further and more complicated question is to ask how hydrologic modelling can be rethought in the spatial context that GIS provides. In other words, instead of attaching existing models to GIS databases, can new hydrologic models be created that take advantage of the spatial data organising capabilities of GIS? This question implies, on my personal approach, a reversal of traditional priorities in hydrologic modelling where the emphasis has always been on the way that physical processes are represented, and the manner in which the parameters are to be obtained for a particular environment plays a relatively minor role. In a spatial hydrology model, the emphasis is first on the digital description of the environment, and then on the formulation of process models which can fit the available data and environmental description

2.2.2 - Geographical Information System (GIS)

The terminology in this area still somewhat complicated due mainly to theoretical discussions about what a GIS can or can not do. We have obtained some responses (compiled from many authors) about 'what is a GIS ?' from Frequently Asked Questions (FAQ) about Geographic Information Systems (GIS), posted into a USENET group comp.infosystems.gis and retrieved via anonymous FTP on abraxas.adelphi.edu (192.100.55.80) in the file /pub/gis/FAQ. These definitions follow.

'An information system that is designed to work with data referenced by spatial and geographic coordinates. In other words, a GIS is both a database system with specific capabilities for spatially referenced data, as well as a set of operations for working [analysis] with the data.'

'A system for capturing, storing, checking, integrating, manipulating, analysing and displaying data which are spatially referenced to the Earth.'

'Automated systems for the capture, storage, retrieval, analysis, and display of spatial data.'

'GIS are simultaneously the telescope, the microscope, the computer, and the Xerox machine of regional analysis and synthesis of spatial data.'

Geographical information systems (GIS) are much more than the above definitions and extend beyond the technical capabilities for coding, storing and retrieving spatial data. In a very real sense the data in a GIS (aspects of the Earth's surface) model the real world (Burrough, 1992), the real world being represented as a series of map layers, in which one aspect of reality is recorded as shown in Figure 2.4.

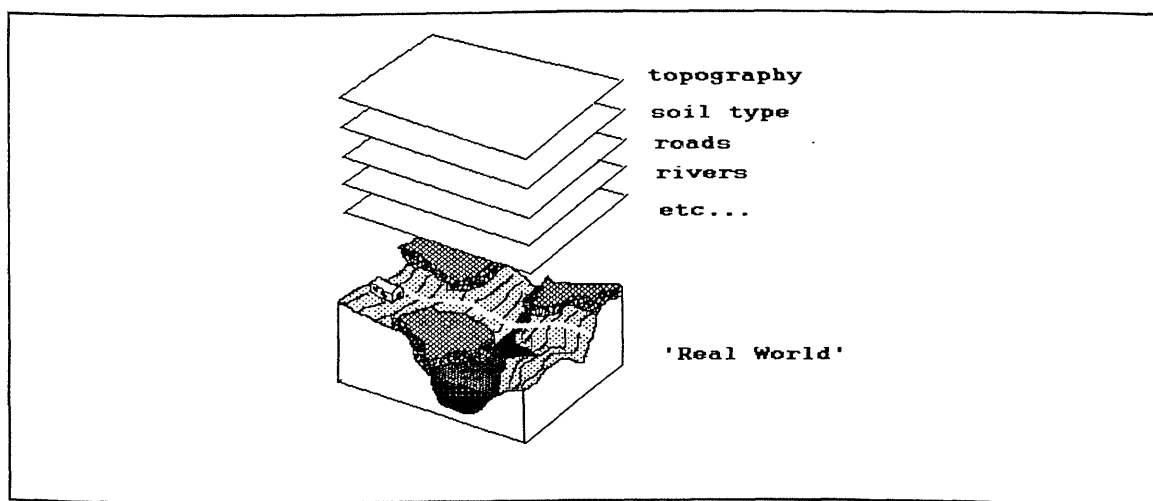


Figure 2.4 : The representation of the real world by a series of map layers.

A map layer is a flat drawing indicating the nature, the form, the relative position, and the size of selected characteristics in a geographic area. Map layers are similar to what are variously called themes, overlays, coverages, maps, layers, data elements, images and variables (Tomlin, 1990).

Once this digital abstraction of the real world has been created as a set of map layers there is a need to analyse the relationships between these spatial variables. Tomlin (1990) describes a spatial modelling language for overlays with three major classes of map operations: functions of individual cells (Figure 2.5a); functions of cells within neighbourhoods (Figure 2.5b); and functions of cells within regions (Figure 2.5c). This classification can be applied to image processing operations as well because image processing systems employ analysis methods that are very similar to some of these GIS operations (Burrough, 1986).

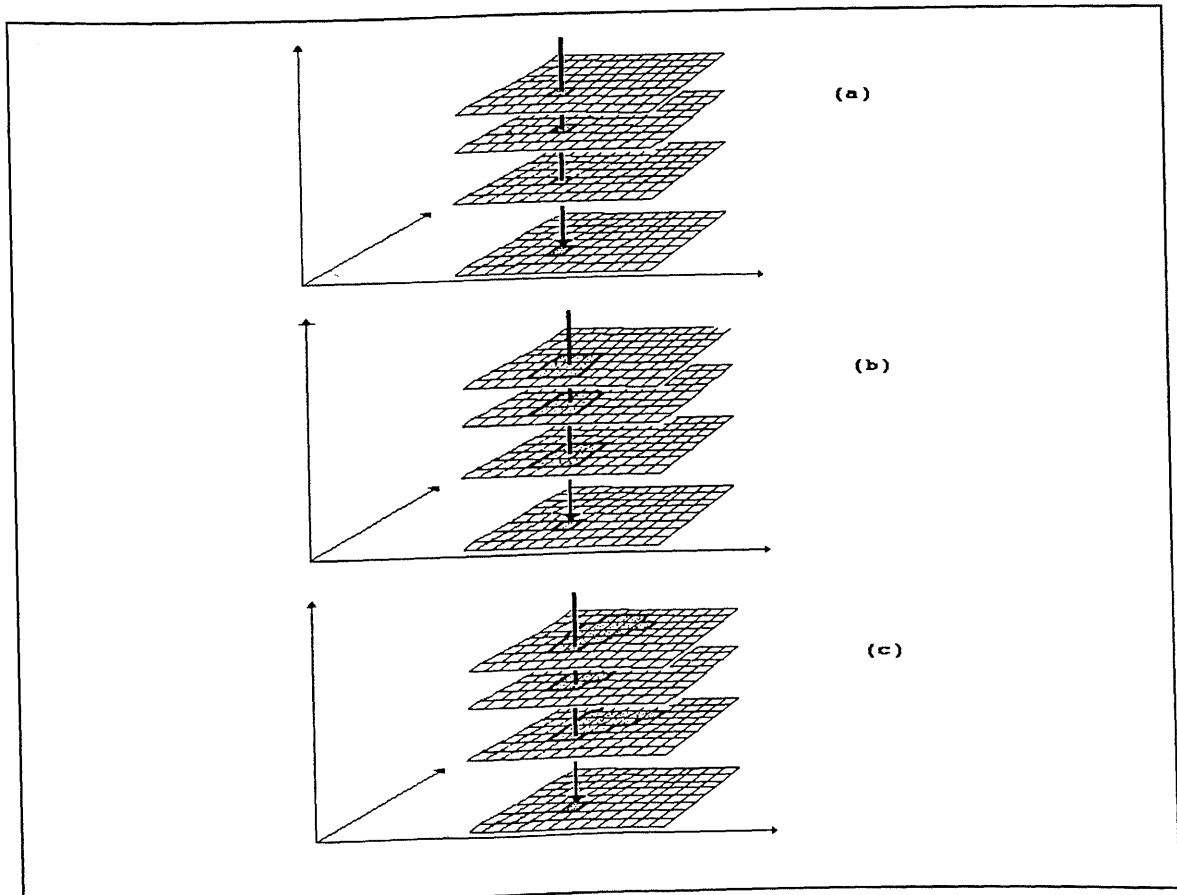


Figure 2.5 : GIS operations: (a) individual locations, (b) locations within neighbourhoods and (c) locations within regions.

Catchment simulation models represent physical and biochemical processes in a dynamic way. Conceptually, such models describe mathematically water fluxes and associated pollutant fluxes from the land surface and soil profile. Source areas can be categorised by a distinct cover and soil type. Dissolved and solid-phase concentrations of chemical compounds can be obtained from lumped modelling of biogeochemical cycling at a source area. These concentrations vary with land cover, soil type, management practices and season of year. Transport (or retention) factors

reflect a complex chain of physical and biochemical processes which can affect pollutant movement from a subbasin to the river outlet and must be taken into account.

The complexity of the specific catchment simulation model depends on the temporal and spatial resolution, and on the extent to which important biochemical processes are considered in the model. While there is a certain progress in water runoff simulation for larger basins, erosion and pollutant transport from larger catchments represent a field, where a compromise solution between very complex models with too many parameters and inadequate simplified models should be found.

Previous efforts in catchment modelling were concentrated mainly on developing either continuous-time spatially lumped models or single event spatially distributed models. Most of the models tended to focus on the patch scale or small homogeneous watersheds, where data availability is certainly better (models CREAMS (Knisel, 1980), EPIC (Williams et al., 1984)). Recent development of deterministic models provides also spatially distributed tools, among them: AGNPS (Young et al., 1989), ANSWERS (Beasley et al., 1980), SWRRB (Arnold et al., 1990). In a sense, all the models made use of previous approaches. In particular, CREAMS and its components were used as a basis for many further tools. For example, SWRRB is a distributed version of CREAMS, which can be applied to a basin with maximum 10 subbasins. However, the general tendency is that the data requirements increase exponentially with the increase in watershed size.

The availability of GIS tools and more powerful computing facilities made it possible to overcome many difficulties and limitations and to develop distributed continuous time models, based on available regional information. While the application of AGNPS and ANSWERS is limited to watersheds of about 200 km², SWRRB was developed with limited distributed parameter capability to be used in agricultural basins as large as 600-800 km². All these models are to a certain extent integrated with GIS tools.

2.2.3 - Integrated use of GIS and hydrologic system

GIS and hydrologic modelling are two separate technologies and are not, therefore, comparable techniques. Their computer programs have very different data structures, functions and methods for inputting and outputting spatial information (Maidment, 1993).

The utilisation of GIS concepts in conjunction with hydrologic models is not, however, a new concept. Solomon et al., (1968) presented the application of a square gridded system to the estimation of the precipitation, temperature and runoff distribution in a large area. Pentland and Cuthbert (1971) generated synthetic streamflow for ungauged catchments using square gridded techniques. Grayman et al., (1975) developed the ADAPT (Areal Design and Planning Tool) system, based on a triangular irregular network, for use in water quality planning considering land-use characteristics of catchments. Walesh et al. (1977) described a digital computer based Land Data Management System (Land DMS) designed to store, retrieve, analyse and display in tabular or graphic form, data used in land and water resources planning. Gupta and Solomon (1977) used a regular gridded system to store land and stream information for use in modelling runoff and sediment. Davis (1978) used a similar system in conjunction with hydrologic models to estimate flood damage. Cluis et al., (1979) presented a transport model related to a nutrient-oriented land use data bank and based on a square gridded system.

Following Ross and Tara (1993) a typical application of a combined GIS-model system consists of five phases:

1. Digital data aggregation performed on map overlays, and spatial analysis to develop input data for the hydrologic models.
2. GIS operations, such as shown in Figure 2.5, providing the linkage mechanism between models with different spatial representations.
3. Model input data processing providing the conversion of overlays with different projections and scale to a common format.
4. Hydrologic simulation representing analytically the flow of water and its constituents in the environment.
5. Output processing providing graphics output display and spatial analysis for evaluation of hydrologic simulation results.

In practice, only phase 4 involves the integration desired, other phases comprising normal GIS operations. Fedra (1993) affirms that the integration of GIS and models can come in two main forms:

- 4.1. Model/GIS data file linkage exchanging information via flat data file transfer, as illustrated in Figure 2.6a. The model reads some of its input data from GIS files, and produces output in a format that can be processed and displayed using a GIS. The file linkage approach is used in this thesis.

4.2. Internal Model/GIS functions built into the GIS as shown in Figure 2.6b. Berry and Sailor (1987) made an attempt to perform runoff modelling within a GIS using a simplified, empirically based model. Most GIS systems do not support the analytical functionality necessary to perform calculations employed in conventional models (Meyer et al., 1993). However, the analytical capabilities of many GIS packages are improving allowing, in the near future, realistic hydrologic model using a GIS framework.

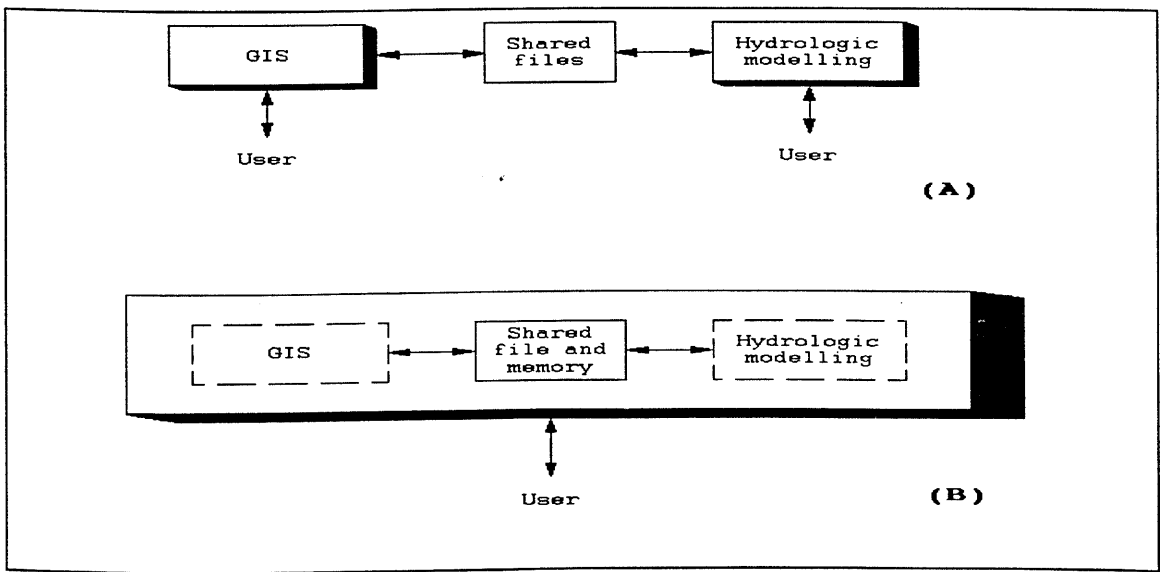


Figure 2.6 : Integration of Model/GIS through : (A) common file and (B) common program.

However apart from the technical linkage of software components shown above, there is a deeper problem of how the fundamental elements of water resources modelling can be reconsidered in GIS terms. This issue is discussed below.

Hydrological models deal with dynamic and continuous phenomena while present GIS manage only static and discrete data. It is fundamental that modellers recognise this essential problem, and understand the assumptions and limitations of discrete representations of continuous reality (handled by GIS) used in models (Kemp, 1993). This section discusses how existing concepts of hydrologic systems can be adapted to conduct hydrological modelling within a GIS framework (see Figure 2.7).

The hydrological model is applied over a domain (catchment), which is a region of space and time where the variables are assumed to be continuous and are simulated. A continuum describes the

behaviour of solids and fluids on the macroscopic scale. It ignores the discrete nature of matter, and treats material as uniformly distributed through regions of space (Spencer, 1980).

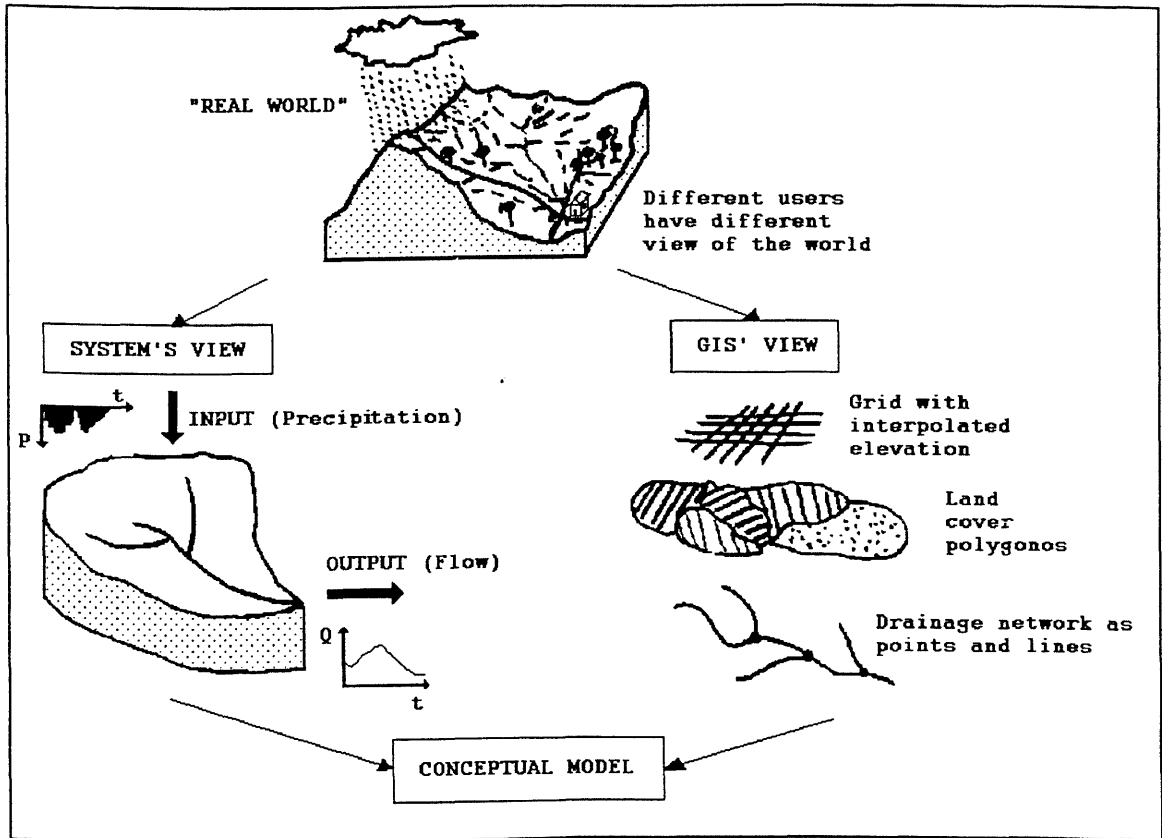


Figure 2.7 : Different views of the 'Real World'.

To use a distributed hydrological model over a catchment (a continuous space), with all its heterogeneity in soils, land use, topography, rainfall inputs, etc., it is necessary to convert the continuum to a finite set of points at which the solution is determined for each spatial element. To discretize a continuous region it is necessary to construct a transformation between this region and another region that will be used as a computational space. The given region is called physical space, while the computational region is called logical space (Castillo, 1991). Figure 2.8 illustrates the physical space using the variables x and y while logical space is described using the variables ξ and η . So, the continuum transformation can be written as (Eiseman, 1985):

$$x = x(\xi, \eta) \qquad y = y(\xi, \eta) \qquad (2.2)$$

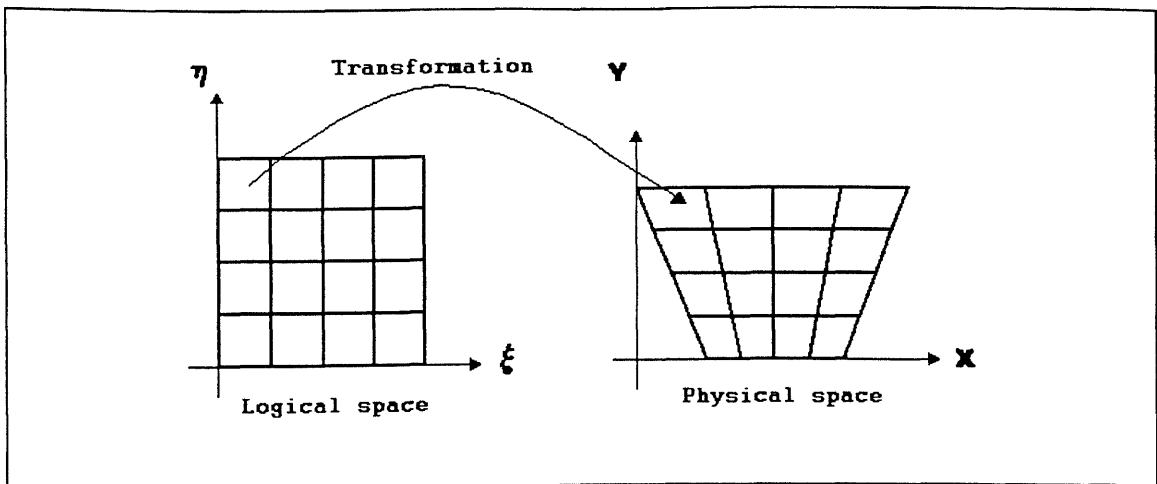


Figure 2.8 : Logical and Physical space.

Some GIS represent the real world (continuum) as exact objects (points, lines and areas) with associated attributes. Others characterise the world as fields, or an array of cells, with associated attributes. Of course, the behaviour of a physical process that can be represented by a field relies on the ability to express what is happening from point to point and from time to time. In summary, the spatial entities, represented by GIS, can be grouped into two views (Goodchild, 1992a): (1) The field view representing continuous surfaces and (2) The object view characterising exact objects as point, line and area. In this thesis I employ the field approach, as a means of linking GIS and hydrologic modelling, and enabling the representation and analysis of spatial variation.

A field is a continuous distribution of a scalar or vector or tensor quantity described by functions of space and time (Spencer, 1980). For example, weather maps illustrating the rainfall variation over the United Kingdom are published daily in newspapers. Since precipitation is a scalar quantity (only the magnitude of the function is needed), such maps are an example of a scalar field. A wind map has to show summary information about magnitude and direction defined as a vector field. There is also a tensor field that shows the stress at a point P in a continuum. This state of stress is known only when the nine components of stress relative to any given set of cartesian axes is known.

In modelling hydrologic processes there are two distinct forms of representation for fields, Lagrange's form and Euler's form. The difference between these approaches lies in the manner in which the position in the fields is identified. In the Lagrangian approach the physical variables are described for a particular element that is moving. The Eulerian approach gives the physical

properties at a given point at a given time. The distinction between the two forms is illustrated in Figure 2.9. A GIS uses the Eulerian approach because it presents fixed frames in space through which the physical property passes (Maidment, 1993).

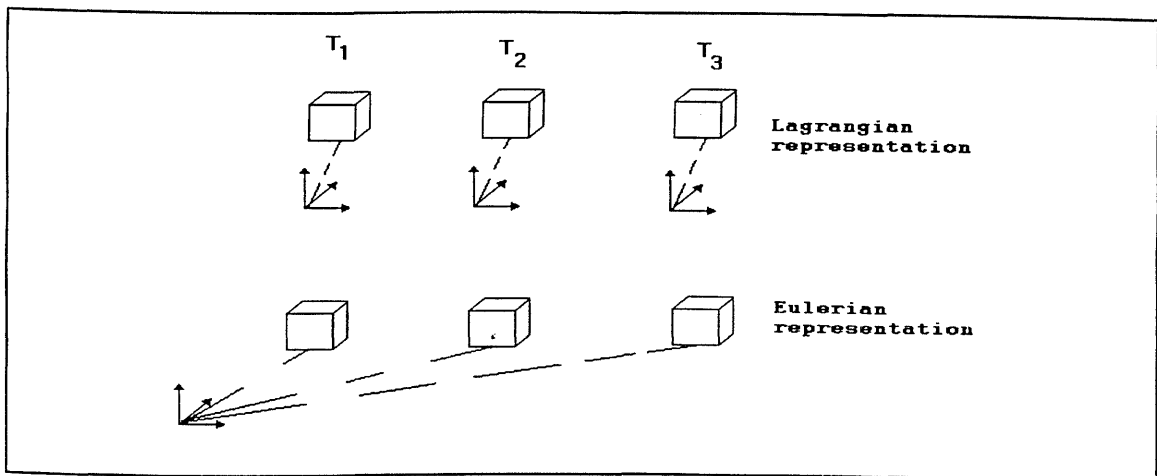


Figure 2.9 : Two types of field representation: Lagrange and Euler's views.

Adopting the Eulerian approach all the physical variables will be a function of (x,y,z,t) . If the physical property at every point in the field is independent of time, the field is termed steady. If the physical property varies with time the field is termed unsteady. There is also a third approach that considers a single time input to a system, called the event model.

Most currently available GIS only handle static (steady) spatial databases and are only useful for handling steady or event cases. To solve an unsteady problem it is necessary to work using a model and use GIS solely as a spatial data source (Kemp, 1993).

The above transformations associate each point in the continuum with an area in logical space over which average values are taken. This area acts as the smallest discernible point that is representative of the continuum. As explained by Cushman (1984), the size of the area, over which averaging takes place, is crucial to the validity of the continuum concept. Following Band (1989) the size of this area should capture the geographic patterns of catchment response by maximising the proportion of surface cover variance that exists between each area and minimising the proportion that exists within an area.

Groundwater hydrologists usually work at the macroscopic level at which scale only averaged phenomena are considered, by-passing the microscopic or pore-scale where the flow patterns are

analysed inside individual pores. This volume, within which the properties are averaged, is defined as a Representative Elementary Volume (REV) (Hazzanizadeh and Gray, 1979; Dagan, 1986). Wood et al., (1988) defines a Representative Elementary Area (REA), applied to catchments, analogous to the concept of Representative Elementary Volume (REV) in porous media.

A fundamental distinction arises in the treatment of spatial units depending upon whether raster or vector data structures are used. In a raster data structure, a fine mesh of cells is laid over the landscape and all calculations are done for each cell. This approach, based on using digital elevation model (DEM) cells as the spatial units, is very useful for certain kinds of hydrologic analysis. But the number of DEM cells within typical analysis regions is usually very large, typically 10,000 to 1 million, so the number of time periods that can be analysed is usually relatively small. Indeed, one may eliminate time as a dimension of the problem by working with mean event values of all the variables, and the subject of raster based mean event flow and transport models is presented at greater length later in this thesis.

Once the catchment has been discretized properly, it must be handled properly. The discretization process of the catchment deal with defining the framework of the model in space, and time, and in preparing the environmental description, which may include representation of the land surface terrain, soils and land cover, subsurface hydrogeology, and hydrologic data such as precipitation, streamflow and constituent concentrations. The second step deal with simulating the water balance of spatial units, the flow of water and transport of constituents between units, the effect of water utilisation structures such as dams and pumping systems, and finally, with the presentation of the study results. In Table 2.1 is presented a sequence by which preparing a GIS hydrology model can be broken down into component parts.

These fundamental steps are an abstraction of reality, and present a very general description of the behaviour of a catchment. In fact it is too general to be of much use in any particular situation. A more useful formulation is presented in the following chapters, based mainly on the above steps.

<i>Environmental description of the catchment</i>	
1.Study design:	Objectives and scope of study; spatial and time domain; process models needed, variables to be computed
2.Terrain analysis	Deriving a catchment and stream network layout from digital elevation data and mapped streams
3.Land surface	Describing soils, land cover, land use, cities, and roads.
4.Subsurface	Hydrogeological description of aquifers
5.Hydrologic data	Locating point gauges, attaching time series and their average values, interpolating point climatic data onto grids
<i>Hydrological spatial simulation</i>	
6.Soil water balance	Partitioning precipitation into evaporation, groundwater recharge and surface runoff; partitioning of chemicals applied to the land surface
7.Water flow	Movement of water through the landscape in streams and aquifers. Computing streamflow and groundwater flow rates
8.Constituent transport	Transport of sediment and contaminants in water as it flows. Computing concentrations and loadings
9.Impact of water utilisation	Locating reservoirs, water withdrawals and discharges in rivers, and aquifer pumping. Their effects on water flow and constituent transport
10.Presentation of results	Developing visual and tabular presentation of the study results. Use of Internet and CD-ROM to transmit results

Table 2.1 : A procedure for a GIS hydrology study.

2.3 - Characteristics of the research catchment

2.3.1 - Hydrologic aspects

Monthly flow variation was tabulated from 10 stream gauges all over the catchment (Table 2.2), from the National Department of Water and Electric Energy (Brazilian Government), as show in Figure 2.10.

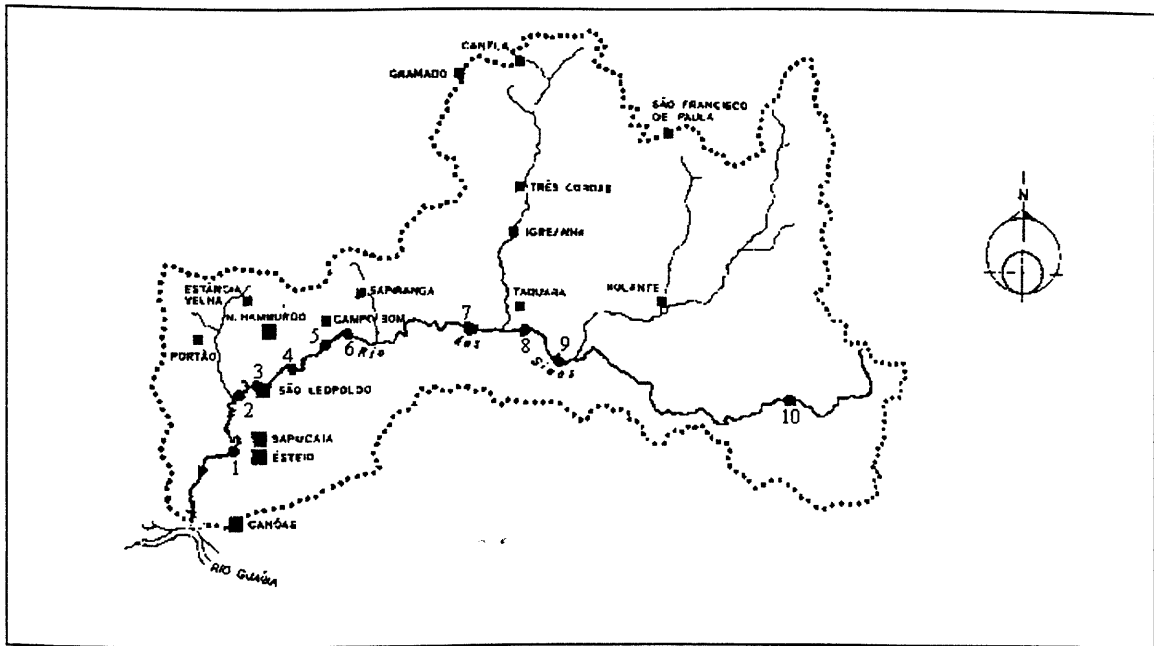


Figure 2.10 : Distribution of the stream gauges in Sinos catchment.

	# 1	# 2	# 3	# 4	# 5	# 6	# 7	# 8	# 9	# 10
JAN	44.8	39.8	39.1	37.3	35.9	35.5	29.8	22.2	18.3	2.5
FEB	61.0	54.1	53.2	50.7	48.8	48.3	40.5	30.2	24.9	3.4
MAR	59.0	52.4	51.4	49.1	47.2	46.7	39.2	29.2	24.1	3.3
APR	63.6	56.5	55.5	52.9	50.9	50.4	42.2	31.5	25.9	3.5
MAY	65.3	58.0	57.0	53.4	52.3	51.8	43.4	32.4	26.6	3.6
JUN	100.8	89.5	87.9	83.9	80.7	79.9	66.9	50.0	41.1	5.6
JUL	110.5	98.1	96.3	91.9	88.4	87.5	73.4	54.8	45.1	6.2
AUG	118.7	105.4	103.5	98.8	95.0	94.0	78.8	58.9	48.4	6.6
SEP	124.8	110.8	108.9	103.9	99.9	98.9	82.9	61.9	50.9	7.0
OCT	89.6	79.5	78.1	74.5	71.7	71.0	59.5	44.4	36.5	5.0
NOV	66.3	58.9	57.8	55.2	53.1	52.5	44.1	32.9	27.1	3.7
DEC	59.5	52.8	51.8	49.5	47.6	47.1	39.5	29.5	24.3	3.3

Table 2.2 : Average flow in Sinos river ($m^3 s^{-1}$) (From 1939 to 1989) with stream gauges # indicated in Figure 2.10.

The hydrological characteristics of the Sinos river (Table 2.2) show marked temporal and spatial variability. Figure 2.11 plots three time series developed from the monthly flow data of Table 2.2.

This Figure shows seasonality, with high flow season (JUN-NOV) and low flow season (DEC-MAY). The water quality is generally poor during periods of low flow. Consequently, this thesis considers only the characteristics related with low flow season, in other words, the period of time used during the simulation will be between DEC until MAY. Figure 2.12 plots the spatial variability from the data of Table 2.2. This Figure plots a rapid increase in flow between gauges # 6 to # 10 due to contributions of the northern rivers of the catchment (see Figure 2.10). In Figure 2.12, also, can be seen a small increase in flow, from gauges # 1 to # 5, due to the absence of large river tributaries to Sinos river.

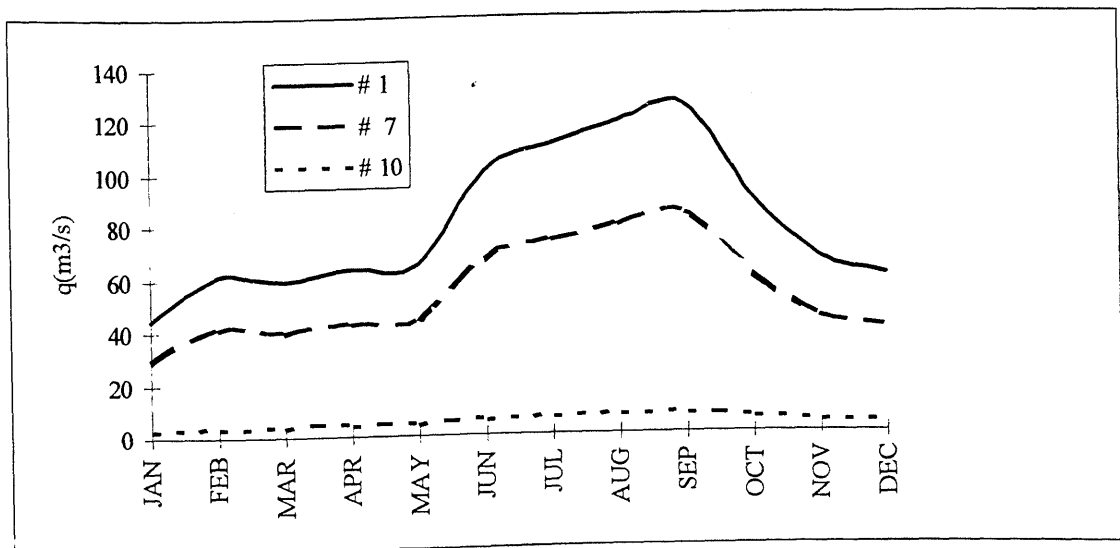


Figure 2.11 : Plots of three time series in Table 2.2.

Table 2.3 expresses the flow movements between gauges in Table 2.2. This relative variability of the downstream gauges relative to the upstream gauges characterise the main river tributaries to Sinos river. The contribution of the northern rivers of the catchment (see Figure 2.10) can be distinguished in Figure 2.13 where huge increases in relative flow are identified among gauges 9-10 (Rolante river), gauges 8-9 (Ilha river - see Figure 1.3) and gauges 7-8 (Paranhana river). The relative increase between gauges 6-7 is due mainly to a high number of contributions of small rivers on both sides of the Sinos river. It is also noted, in Figure 2.13, the seiche backwater effect from Jacuí river due in gauges 1-2.

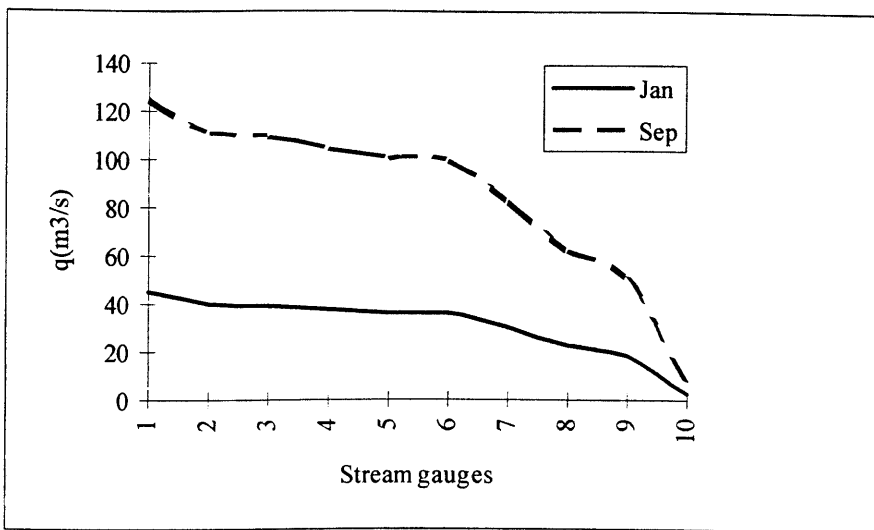


Figure 2.12 : Longitudinal flow variation in Sinos river, from data in Table 2.2.

On the basis of the above data , the hydrological response of Sinos catchment can be summarised as:

- Downstream of gauge 1 (see Figure 2.10): flow dominated by seiche backwater effect from Jacuí river and upstream contributions.
- Downstream of gauge 7 until gauge 1: flow regime explained by upstream and lateral flow contributions.
- Between gauges 7 and 8: contribution of Paranhana river to Sinos’.
- Between gauges 8 and 9: contribution of Ilha river to Sinos’.
- Adjacent to gauge 9: contribution of Rolante river to Sinos’.
- Upstream gauge 9 (After confluence with Rolante river): the beginning of Sinos river.
- Northern area of the catchment (Paranhana, Ilha and Rolante rivers): no flow measurements.

	1-2	2-3	3-4	4-5	5-6	6-7	7-8	8-9	9-10
JAN	5.0	0.7	1.8	1.4	0.4	5.7	7.6	3.9	15.8
FEB	6.9	0.9	2.5	1.9	0.5	7.8	10.3	5.3	21.5
MAR	6.6	1.0	2.3	1.9	0.5	7.5	10.0	5.1	20.8
APR	7.1	1.0	2.6	2.0	0.5	8.2	10.7	5.6	22.4
MAY	7.3	1.0	3.6	1.1	0.5	8.4	11.0	5.8	23.0
JUN	11.3	1.6	4.0	3.2	0.8	13.0	16.9	8.9	35.5
JUL	12.4	1.8	4.4	3.5	0.9	14.1	18.6	9.7	38.9
AUG	13.3	1.9	4.7	3.8	1.0	15.2	19.9	10.5	41.8
SEP	14.0	1.9	5.0	4.0	1.0	16.0	21.1	11.0	43.9
OCT	10.1	1.4	3.6	3.4	0.7	11.5	15.1	7.9	31.5
NOV	7.4	1.1	2.6	2.1	0.6	8.4	11.2	5.8	23.4
DEC	6.7	1.0	2.3	1.9	0.5	7.6	10.0	5.2	21.0

Table 2.3 : Relative variability of stream gauges in Table 2.2.

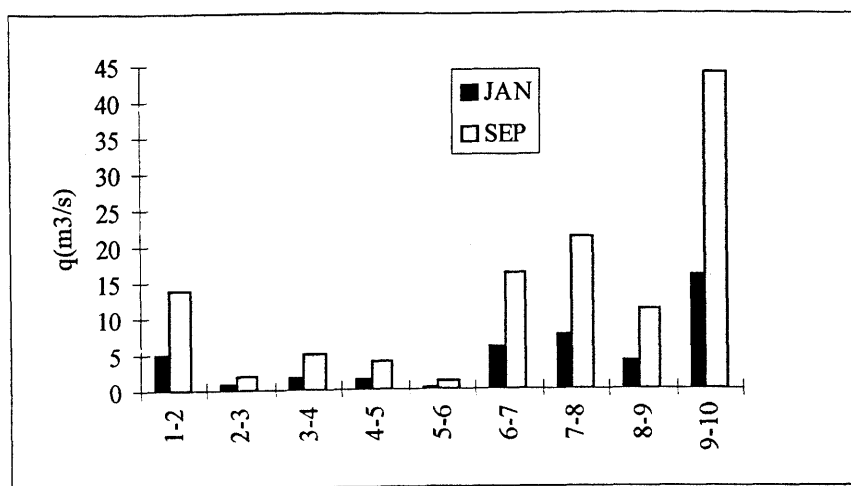


Figure 2.13 : Longitudinal relative variation in Sinos river, from data in Table 2.3.

Although the monthly flows presented in Tables 2.2 and 2.3 are part of the overall hydrologic cycle, the mechanisms producing them and their characteristics are very different. A flow time series extending over long periods of time, as shown in Table 2.2 (50 years), contains information relating to at least five time scales. These are:

1. Variation in evapotranspiration that is semi-diurnal.
2. Thunderstorms in summer low-flow periods that may give rise to daily variation. They are significant in this area of the world, due to cold fronts and convective effects.
3. Interchange with groundwater storage that exhibits long term variation.
4. Antecedent conditions in the previous wet season which shows annual variation.
5. The integrated effect of changes in basin characteristics that is long term.

In addition, there are extraction points for water supply, industrial use and irrigation at several locations in the Sinos catchment (principally in those counties with major increases in population-Table 1.3). These factors frequently give rise to wide fluctuations in the daily flow that is not represented in Table 2.2. Because we do not have availability of daily flow data, this diurnal variation (and all associated data) is considered too restrictive as a measure of the flow characteristics for water quality management. Consequently, only the characteristics related with low flow season are examined here.

2.3.2 - Water quality aspects

The major water quality problems have been perceived by population and subsequently confirmed through water quality sampling and analyses, in lower reaches of Sinos catchment (from the outlet of the catchment until gauge 6 in Figure 2.10). This is linked with the process of

industrialisation and urbanisation that took place in this area of the catchment. The principal uses of water in this area are (Until Campo Bom county - see Figure 1.3):

- Water supply - municipal and industrial.
- Dilution of sewage - municipal and industrial.
- Recreational - swimming, boating, and aesthetics.
- Sport fisheries.
- Navigation.
- Irrigation.

In the lower reaches of Sinos catchment, especially, domestic and industrial effluents are dumped directly into the river without treatment (Figure 2.14). During summer, when low flows occur, water quality problems are most serious. This is due to the lack of dilution of the highly concentrated pollutants from industrial and urban sources. The Biochemical Oxygen Demand - BOD and the discharge of large amounts of effluents have been recorded for this area and are presented in Table 2.4.

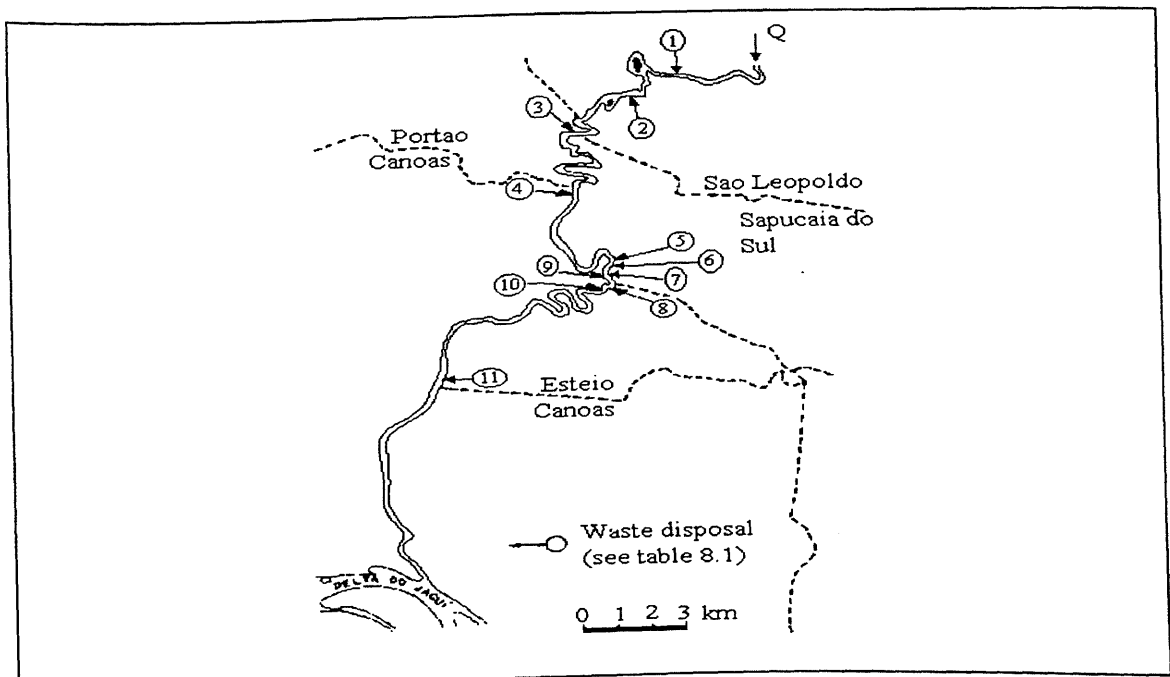


Figure 2.14 : Main point sources of waste disposal in the Sinos river.

Source: Tucci and Moretti (1982).

# in Figure 2.14	Identification	Discharge (l/s)	BOD ₅ (ppm)
1	Paper Mill (I)	51	395
2	J. Correa creek (urban waste)	95	170
3	Portao creek (urban waste)	161	291
4	J. Joaquim creek (urban waste)	15	55
5	Riograndense Steel Mill	275	18
6	Pirelli factory (tyres)	22	4
7	Vachi tannery	29	421
8	Lansul factory (cotton mill)	14	160
9	Paper Mill (II)	22	81
10	SAMRIG factory (food processing)	141	408
11	Petrobras refinery	156	14

Table 2.4 : BOD₅ and discharge from waste disposal in Sinos river.

Source: Tucci and Moretti (1982).

In addition to river pollution caused by industrial discharges (tanneries, wool mills, steel mills, paper and vegetable oils), creeks are used as sewage systems for wastewater, due to the lack of a complete sewage system for urban areas. Part of the discharges infiltrate into the ground, while the remainder ends up in creeks which are tributaries of the Sinos river. These creeks have low gradients, and have low discharges, and thus create conditions for partial deposition of the pollutant load, particularly where the residence time to the Sinos river is long, allowing the depuration (usually anaerobic) of pollutant load in the creek itself. The environmental consequences of this process are shown in the creeks Luiz Rau, J. Joaquim, João Correia, Portão, and others, which drain from the towns of Novo Hamburgo, São Leopoldo e Portão; they are really open sewers.

The results of some technical reports produced by Rio Grande do Sul Government agencies concerning environmental problems in the Sinos catchment are illustrated in Figure 2.15 and Table 2.5.

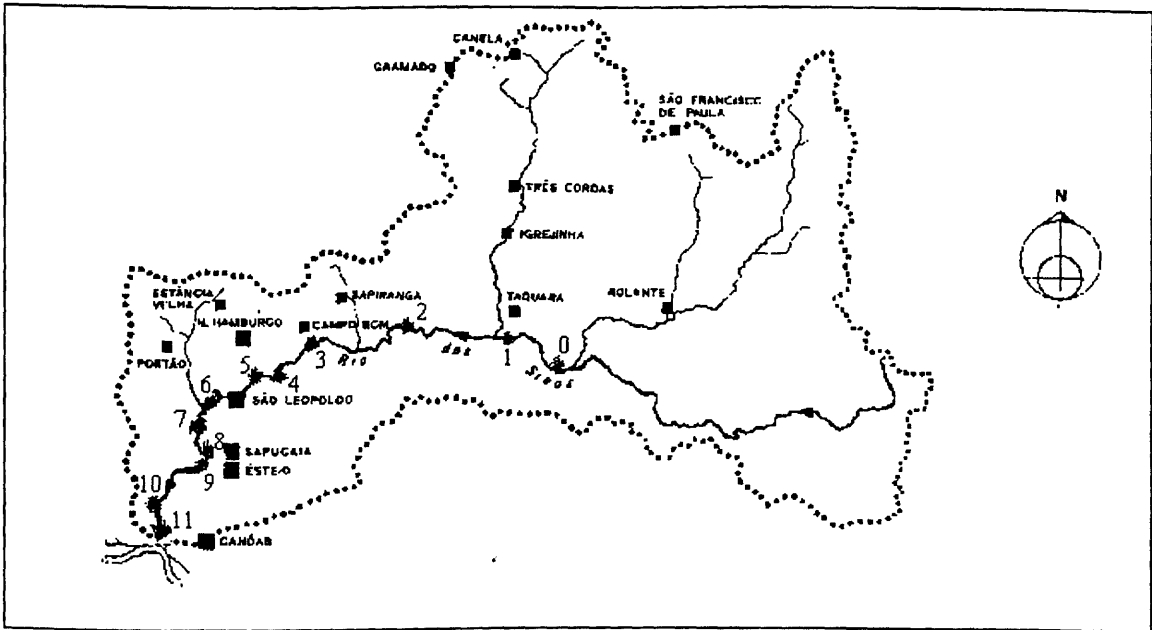


Figure 2.15 : Distribution of water quality samples in Sinos catchment.

Source : Itaconsult-LatinoConsult Brasileira (1974).

#	DO	PO ₄	NO ₃
0	5.67	0.0	0.0
1	5.93	0.0	0.0
2	5.87	0.42	0.1
3	5.87	0.35	0.03
4	5.73	0.35	0.03
5	5.53	0.0	0.0
6	5.2	0.6	0.3
7	5.2	0.5	0.05
8	4.6	0.0	0.0
9	5.5	0.5	0.06
10	5.6	0.5	0.03
11	6.2	*	0.03

Table 2.5 : Average water quality samples (mg/l) (January 1973).

Source : Itaconsult-LatinoConsult Brasileira (1974).

On the basis of the above data, the water quality response of Sinos catchment can be summarised as:

- Upstream of point 1 (Figure 2.15): good water quality due to low agricultural uses, forest areas and counties with decrease in local population (Table 2.5).
- Downstream of point 1 until point 3: contributions from the northern part of the catchment (areas with increased agricultural and urban land uses) reduce the quality of water (especially nutrients).
- Downstream of point 3: increased urban land use and industrial activities (but no agricultural use) reduce the water quality to a poor level.
- Downstream of point 6: eventually water quality improves due to tidal effects upstream of the river mouth (point 11), in which water is less polluted, and with greater discharge than in the Sinos river.
- Northern area of the catchment (Paranhana, Ilha and Rolante rivers): no water quality measurements.

2.3.3 - Creation of the data set

The essential feature of the approach used in this thesis is that the principal input parameters of the system are derived from remotely sensed data, topographic maps, soil maps and rain gauge data, and that the system interfaces with a GIS, which provides data management and analysis capabilities. In order to obtain the best possible relationship between topographic data (the basis of the routing algorithm) and all the other data sets the system should use the smallest grid cell size possible given data source and data quality constraints. Here, the system is based on a square grid of 100x100 m (626x1038 cells), within which it is assumed that every cell is homogeneous in terms of their physical properties. All these data were geometrically rectified to conform to the Universal Transverse Mercator Projection, enabling the corner of each grid cell to be defined by its Brazilian national grid reference.

The land use classification uses as a primary source of information two LANDSAT Thematic Mapper images: (a) LANDSAT-TM 221.81-B (South of the catchment) on 24 January 1986, and (b) LANDSAT-TM 221.80-D (north of the catchment) on 30 April 1986. These were the best quality, satellite images for the area acquired during the summer season. Each image consists of a set of digital radiance values, measured at visible and infra-red wavelengths, for each 30x30m grid cell that makes up the image array.

Because the Sinos catchment is spread over two images it was necessary to combine these images into a single large file (mosaicing). During this process, the cells of the images are transformed to

fit the map projection (rectified) and resampled to a 100x100 m grid size. The images were classified before the rectification process to avoid any spectral distortion of the original data introduced by resampling.

The classification procedure was carried out using the ERDAS software system. A supervised classification procedure was used in which the spectral data for each cell in the image was compared with spectral data for cells with known land use (training data). Cells were assigned to a particular class on the basis of the minimum distance decision rule (Richards, 1986). The land use categories used for the classification are those justified in chapter 4. It should be noted that the technique is capable of achieving a greater level of detail, in terms of land use categories, if required, although classification accuracy will depend on the distinctiveness of the spectral data defining each class.

An estimation of classification accuracy is shown in Table 2.6. The element i of row i (i_{th} diagonal element) of this matrix contains the number of cells identified as belonging to class i that have been correctly labelled. The other cells of row i give the incorrectly labelled cells. The overall classification accuracy is quantified as the average of the individual class accuracy, yielding an overall accuracy = 81.8 %.

	Water	Urban	Grassland	Forest	Soil	Agriculture
Water	96.2			3.8		
Urban		70.8	2.6		26.6	
Grassland			87.4			12.6
Forest	3.9	0.3	17.1	78.2		0.5
Soil		14.1			85.9	
Agriculture		8.9		18.7		72.4

Table 2.6 : Classification accuracy matrix for six classes (per cent).

The process of assigning map coordinates to each cell in the classified image and resampling to a 100x100 m grid size was carried out using a bilinear interpolation technique (Richards, 1986), with a root mean square (RMS) error tolerance within 3 grid cells, i.e., the location of a cell is accurate to within 300 m.

This resulting image contains areas much larger than the Sinos catchment. In order to reduce the size of the image file to include only the area of study, I overlaid a digitised catchment boundary

to extract only the Sinos catchment. The final result of these operations (classification, rectification, mosaicing and extraction) is shown in Figure 2.16.

The topographic data used in the system were extracted from two maps : (a) GRAVATAI (SH.22-X-C and D) and CAXIAS DO SUL (SH.22-V-D), both at a scale of 1:250,000. The contours were digitised from these maps resulting a series of irregularly spaced terrain data points. An elevation value for each grid cell was then interpolated from these terrain height points using the ERDAS interpolation functions (1-distance)² - (distance function 5). This produces the simplest form of terrain model in which the elevation value for each point on a 100x100 m square grid is computed. Values of topographic parameters, such as slope and aspect, can be calculated from these data. The overlaying procedure (catchment boundary) was also applied to this data set. Figure 2.17 shows the topographic data set.

The soil data was prepared from a state-wide soil map (DNPA, 1973) at scale of 1:750,000 by digitising soil types as a series of polygons, and then converting these digitised polygons into a gridded data set (100x100 m). Finally each soil type was grouped into hydrologic soil classes using the procedure described in Chapter 4 (Table 4.1). This procedure resulted in three hydrologic classes representing soils in the catchment (Figure 2.18).

The distribution of rainfall was determined from rain gauge data (30 gauges) using ordinary block kriging (Webster and Oliver, 1990), with a kriging block equal to the grid cell size (100 m). The experimental variogram was computed using block kriging and variogram model fitted by weighted least-squares. Block kriging was carried out using GSLIB program (Deutsch and Journel, 1992). The results are shown in Figure 2.19.

2.3.4 - Field data collection

The available data are very limited. There is a need to undertake additional sampling to give spatially distributed test set and to provide data relating to land use (Satellite images) and the sources of pollution; in order to provide a database for verification of the models used. To achieve this during November and December - 1993, I spent almost 30 days in the Sinos river basin collecting field data. Field data collection used a sampling design based on accessibility and position relative to major land uses areas.

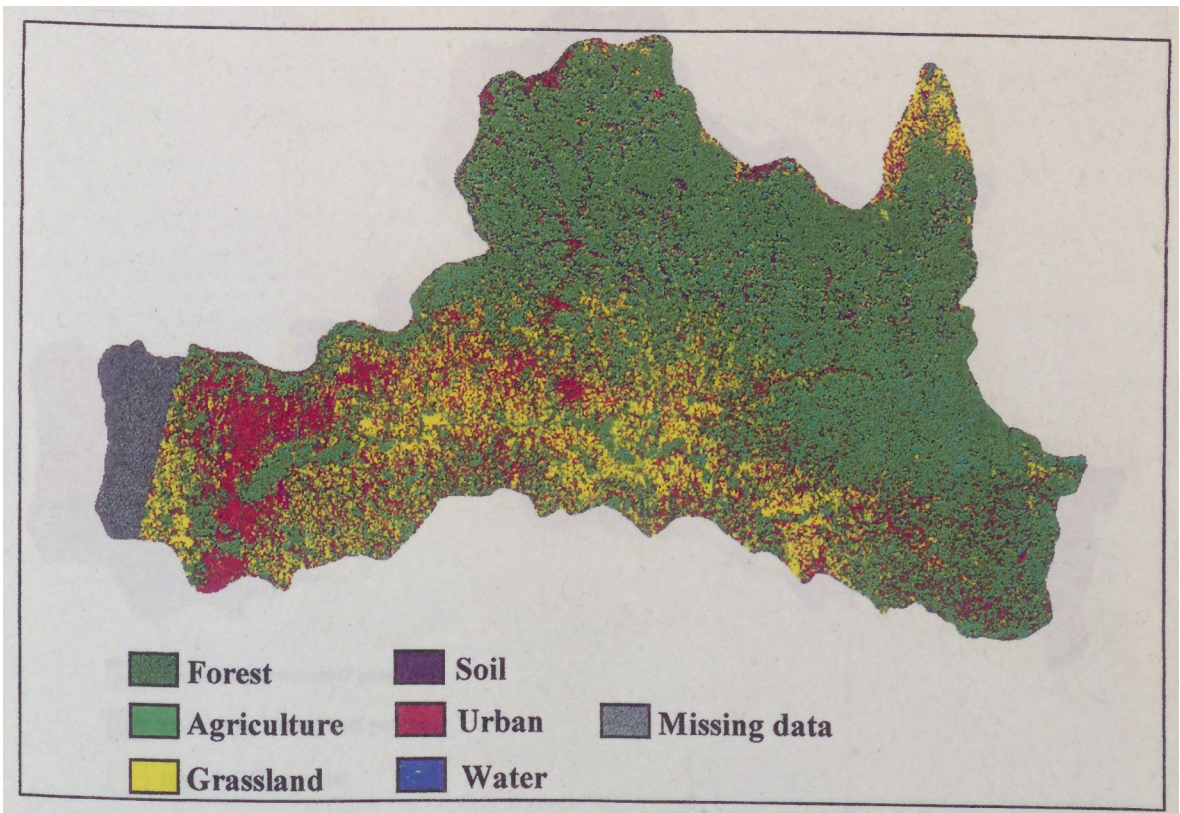


Figure 2.16 : Digital representation of land use data.

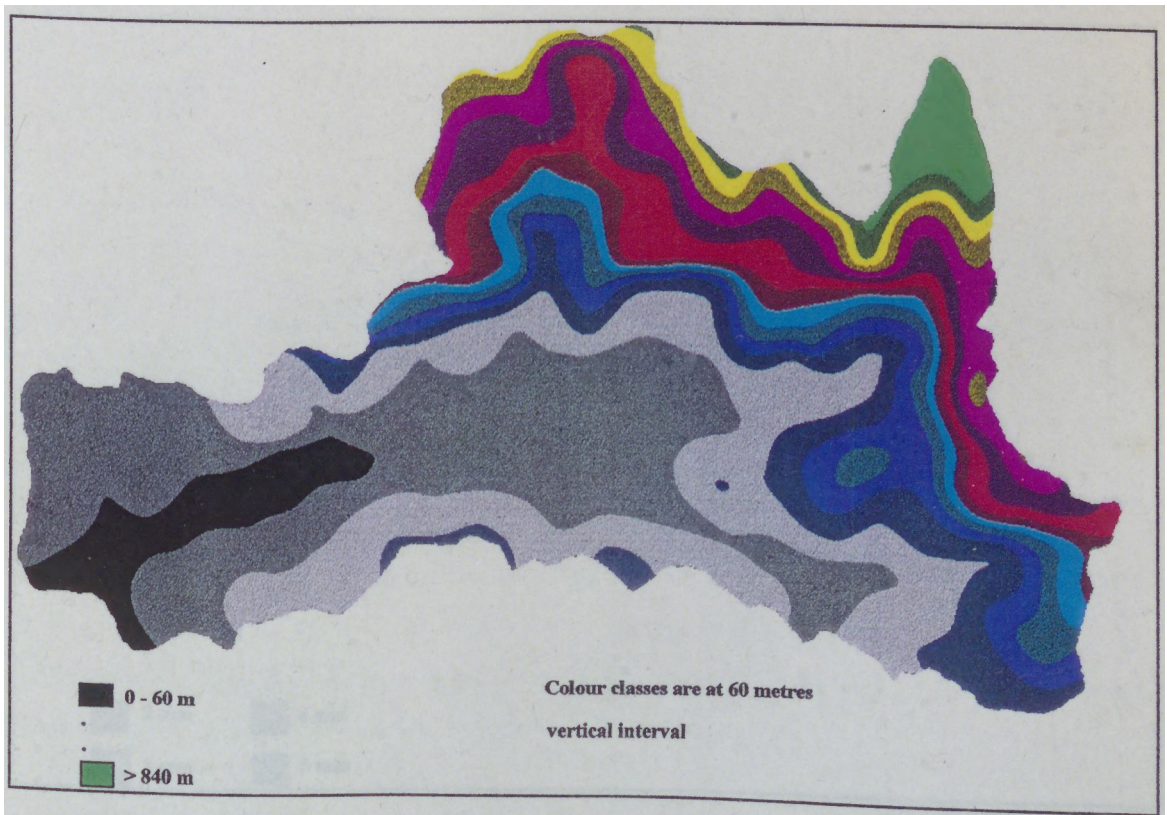


Figure 2.17 : Digital Elevation Model (DEM) of Sinos catchment.

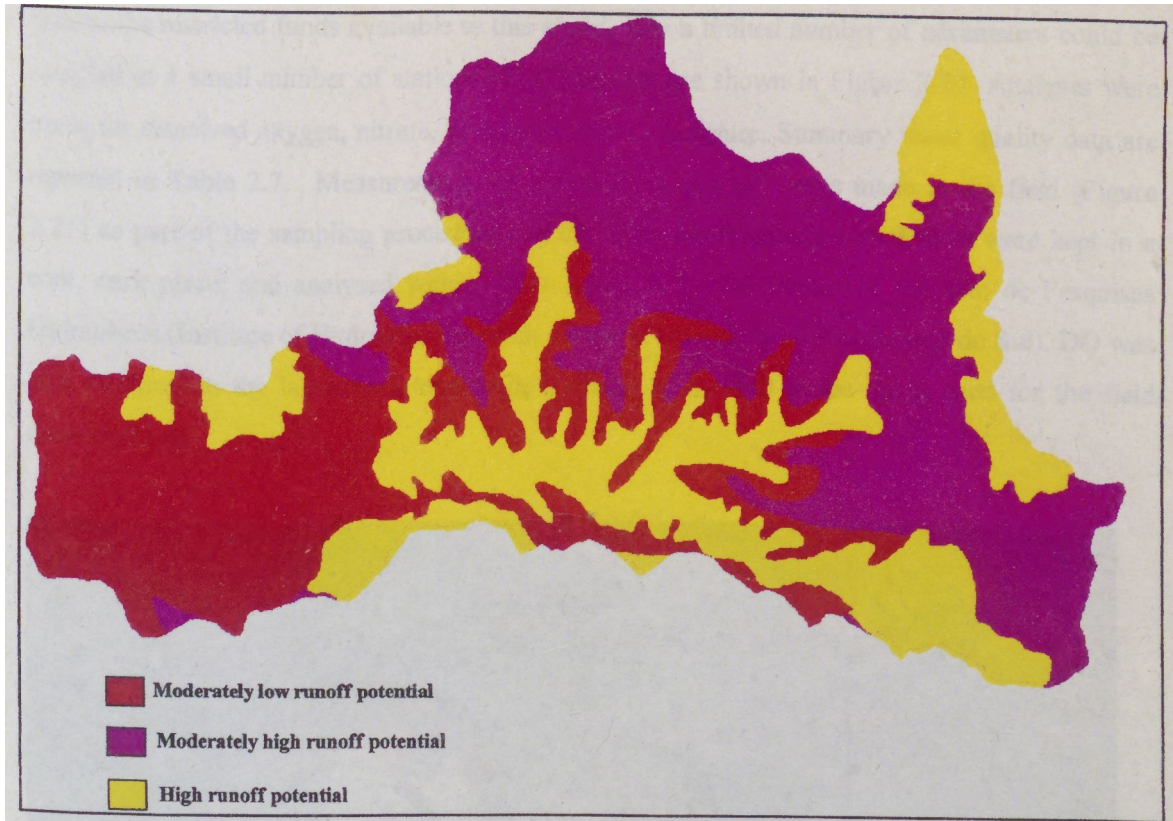


Figure 2.18 : Digital representation of soils data.

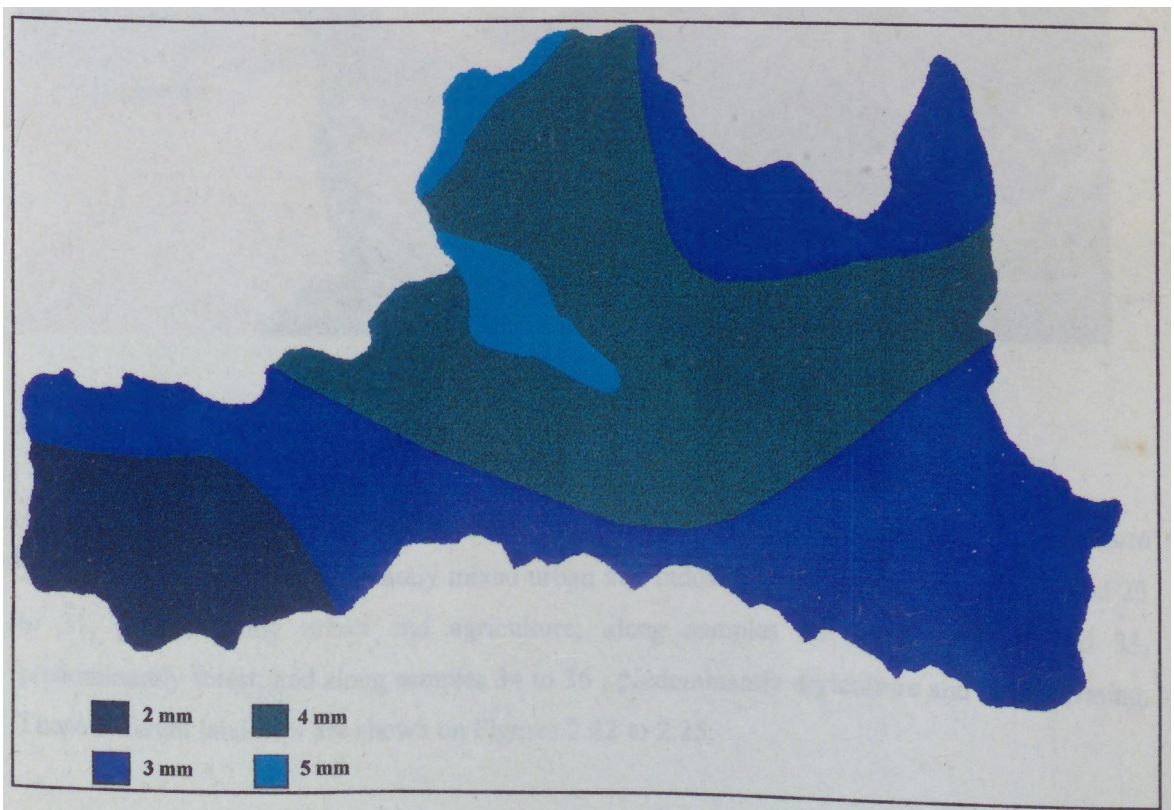


Figure 2.19 : Areal distribution of rainfall for January (daily average values).

Due to the restricted funds available to this study, only a limited number of parameters could be sampled at a small number of stations. The locations are shown in Figure 2.20. Analyses were made for dissolved oxygen, nitrate, phosphate and temperature. Summary water quality data are reported in Table 2.7. Measurements of temperature and DO were made in the field (Figure 2.21) as part of the sampling procedure and the other water quality constituents were kept in a cool, dark place; and analysed within a few hours in the laboratory of Instituto de Pesquisas Hidraulicas (Institute of Hydraulic Research - Federal University of Rio Grande do Sul). DO was also analysed in the laboratory to provide a check of the DO probe being used for the field measurements.



Figure 2.21 : Measurements of water quality constituents in Sinos catchment.

Along the lower course of the river, i.e., that portion of the river between samples 1 to 10 (Figure 2.20), the land use is predominantly mixed urban and industrial; along samples 11 to 17 and 23 to 31, predominantly urban and agriculture; along samples 18 to 22 and 32 and 33, predominantly forest, and along samples 34 to 36 , predominantly agriculture and cattle farming. These different land uses are shown on Figures 2.22 to 2.25.

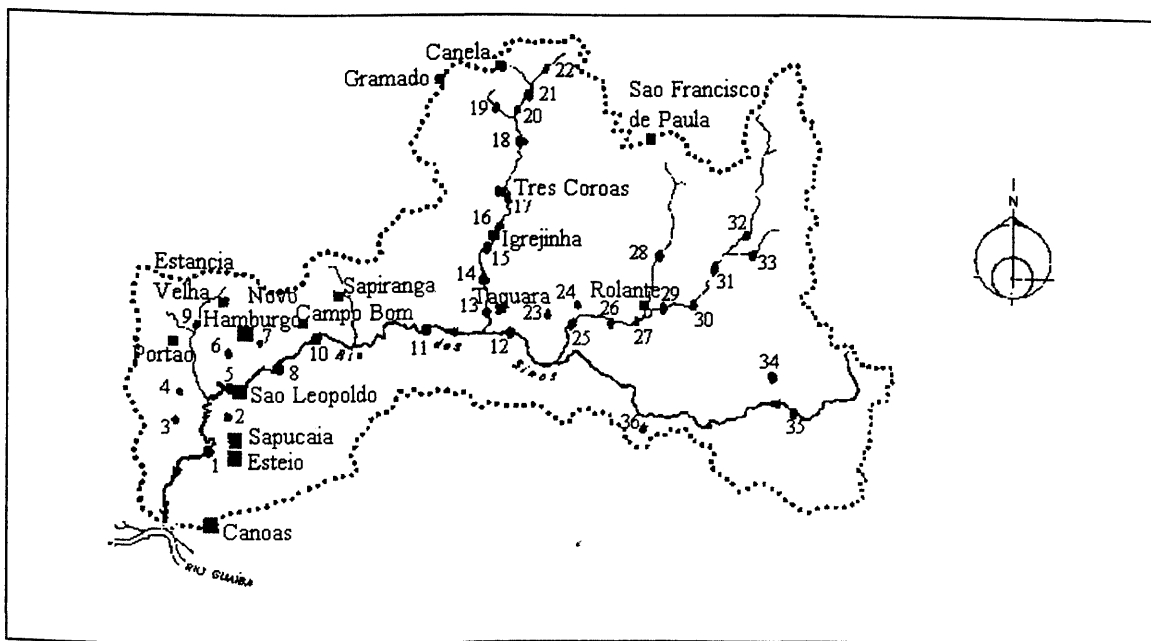


Figure 2.20 : Distribution of the samples in Sinos catchment (1993).

#	DO	PO ₄	NO ₃
1	0.5	0.35	0.0
2	2.9	0.60	0.7
3	3.9	0.20	0.6
4	4.6	0.20	0.7
5	1.4	0.35	0.4
6	0.2	0.70	0.8
7	0.3	0.40	0.5
8	3.7	0.28	0.0
9	0.3	0.80	0.5
10	2.3	0.40	0.6
11	2.5	0.50	0.7
12	4.5	0.10	0.2
13	3.8	0.15	0.0
14	4.4	0.10	0.1
15	4.6	0.19	0.2
16	4.8	0.05	0.2
17	5.0	0.10	0.2
18	4.9	0.05	0.0

#	DO	PO ₄	NO ₃
19	8.4	0.11	0.4
20	4.9	0.12	0.0
21	4.9	0.19	0.20
22	8.6	0.04	0.0
23	6.4	0.05	0.0
24	3.7	0.05	0.0
25	2.7	0.55	0.7
26	3.8	0.60	0.7
27	4.3	0.20	0.2
28	4.5	0.50	0.5
29	4.5	0.20	0.1
30	5.2	0.34	0.4
31	7.0	0.21	0.3
32	7.6	0.15	0.1
33	7.9	0.30	0.1
34	3.6	0.45	0.0
35	4.4	0.22	0.3
36	3.7	0.21	0.0

Table 2.7 : Samples in Sinos catchment.
(values in mg.l⁻¹).

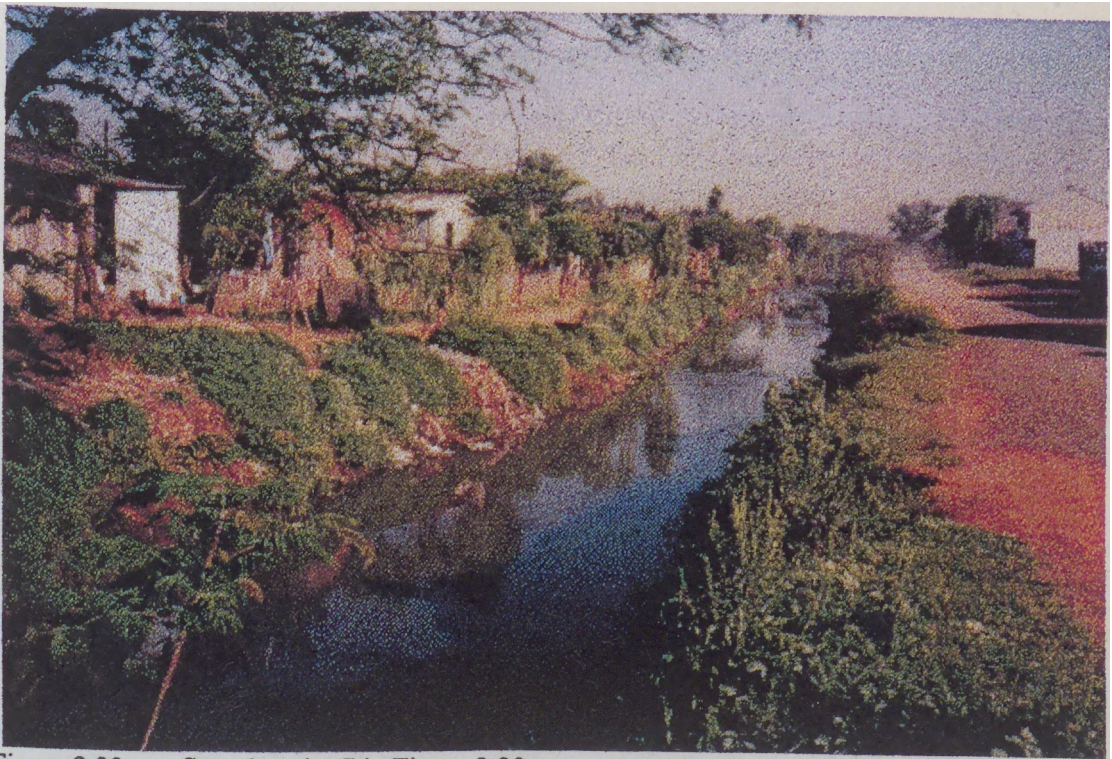


Figure 2.22 : Sample point 7 in Figure 2.20.



Figure 2.23 : Sample point 19 in Figure 2.20.

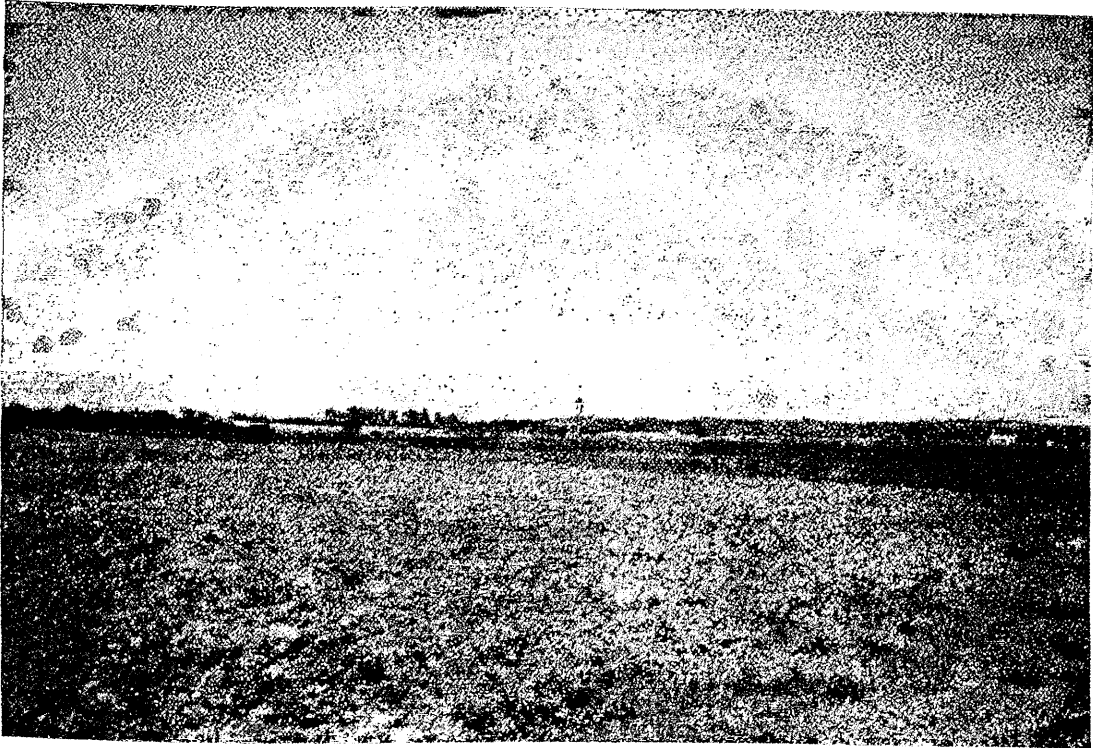


Figure 2.24 : Near sample point 35 in Figure 2.20.

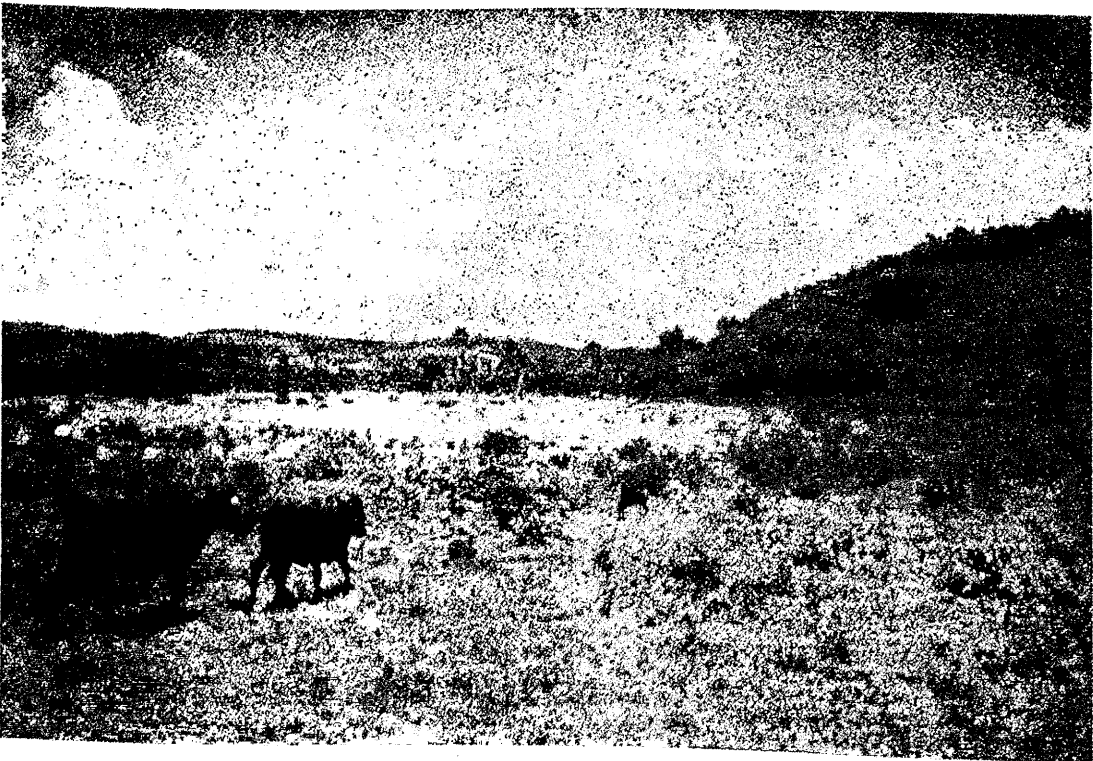


Figure 2.25 : Sample point 34 in Figure 2.20.

2.4 - Computing tools

Most of the computing was carried out on my own 486 PC and using the computing facilities of the Remote Sensing Unit (RSU) within the University of Bristol. My PC is configured with 8 Megabytes of memory, 340 Megabytes of hard disk and a modem/fax card. In addition, I created a partition on the hard disk (220 Megabytes) to run Linux. Linux is a freely distributable UNIX clone that implements a subset of System V and POSIX functionality and supports a large amount of software together with X-Windows and the TCP/IP protocol. It was also used to support a communication channel over a modem connection allowing me to connect the University of Bristol's network using the Internet protocol. As a result of this set-up all the developed programs can run on PCs and workstations and can be processed much faster. Linux (all the software, binaries, sources, releases, etc.), was retrieved via anonymous FTP from src.doc.ic.ac.uk (146.169.2.10).

The computing hardware in the RSU has been up-graded several times since 1983, and now includes:

- One 24 bit Silicon Graphics computer.
- One 24 bit Sun SPARC 330 computer.
- Two 8 bit Sun SPARC 1+ workstations.
- One 8 bit Sun 3/80 workstation.
- One 8 bit Sun ELC workstation.
- A Primary Data Users Station (PDUS) for Meteosat (2 PCs 386, Receiver and Satellite dish).
- One IBM PS/2 with magneto-optical drive.
- Digitising table, size A0 with 286 PC host.
- Half-inch tape-drive, 800, 1600 and 6250 bpi.
- HP paintjet XL printer.
- Postscript laser printer.
- General text printer.

The total amount of disk space on the RSU computers is around 10 Gigabytes. All the hardware is connected via Ethernet link into a local area network. Through this, all the machines are connected to the University of Bristol's network and Internet for United Kingdom and international communications and facilities as shown in Figure 2.26.

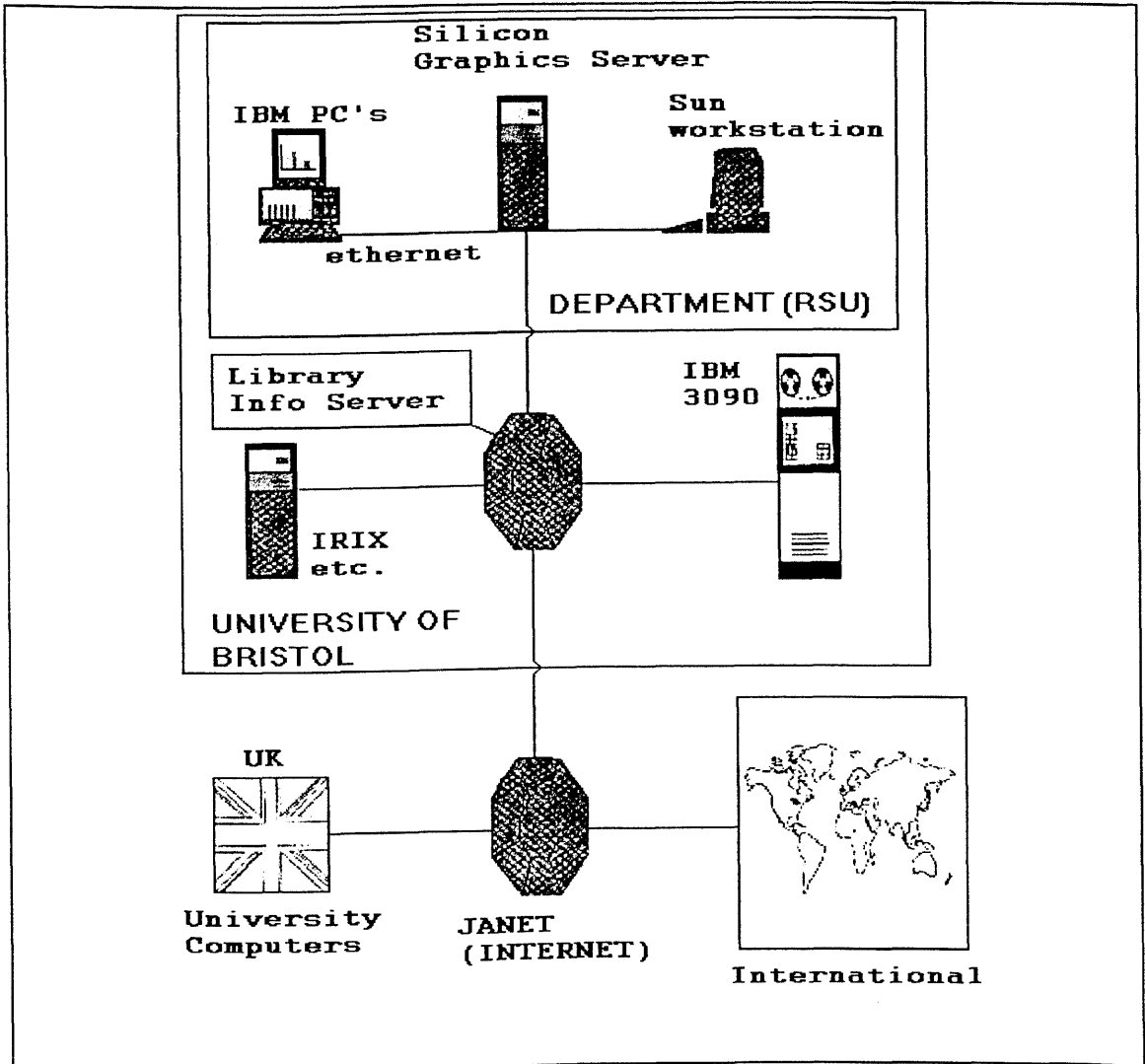


Figure 2.26 : University of Bristol's computer network.

In addition to the above equipment, a wide variety of software was used, including word processing, spreadsheets, charts and graphics, statistics packages, network software, compilers, etc. The system proposed here has general validity and is not constrained to any particular GIS implementation. In practice, IDRISI, ERDAS and GRASS have been used as GIS packages.

IDRISI is a grid-based Geographic Information System and image processing system developed by the Graduate School of Geography at Clark University. IDRISI runs under MSDOS and contains a collection of over 100 program modules that may be linked by a unified menu system.

ERDAS (Earth Resources Data Analysis System) is a GIS software system developed and marketed by ERDAS Inc. of Atlanta, Georgia, U.S.A. The ERDAS system incorporates the functions of both image processing and raster GIS. These functions includes about 100 programs, such as collecting, viewing, altering and analysing raster data sets. The ERDAS system software is available on several platforms, including IBM-PC, SUN, HP, etc, running MSDOS, UNIX and VMS.

GRASS, more formally known as the Geographical Resources Analysis Support System, is fundamentally Geographical Information System (GIS) software. Basically, GRASS is a public domain raster GIS, vector GIS, image processing system, and graphics production system produced by the U.S. Army Corps of Engineers's Construction Engineering Research Laboratory. It encompasses some 300 user programs, is written mostly in C for UNIX machines. I have run this package on a Sun workstation, and ported GRASS 4.0 to run on the UNIX partition in my own PC. GRASS (all the software, binaries, sources, releases, etc.) was retrieved via anonymous FTP from max.cecer.army.mil (129.229.20.254).

In addition, the system also comprises the software created by myself. Most of this software is explained in the thesis, and the source code is given in the appendix.

2.5 - Summary

Other advantages offered by the integration between GIS and models are the use of physically based mathematical relationships, the incorporation of information about the spatial variability of land characteristics, and the detailed spatially displayed output of the system, useful for planners.

In this thesis a methodology is presented which has been designed specifically to support the determination of water quality changes resulting from point and non point sources in a large river basin with diverse land uses, taking in account both the intensity and spatial distribution of the produced loads. The methodology is capable of implementation on land surfaces having heterogeneous water pollution effects.

The system is based on a cellular configuration where information on land use, topography, soil type and rainfall is manipulated using models and geographical information systems (GIS). Information on land use in each cell is obtained by classifying remotely sensed satellite data. Topographic parameters for each cell are derived from digital elevation models (DEM). Rainfall

values for each cell are obtained from the interpolation of point data derived from meteorological stations. Other more conventional data are acquired by digitising maps.

Using this cellular structure, runoff, and chemical outputs from the individual cell, are routed through the catchment using a physically based mixing model to provide input to the drainage network. The network, derived automatically from a digital elevation model (DEM), defines the river system in the model. The link between the catchment and the river network defines a river 'fringe' zone where point and non point sources are stored. The system enables spatial relationships between point and non point sources to be investigated and consequences to the river system can then be explored via the topology of the river network.

In general, the mechanics of the proposed approach consist of seven steps:

1. Parameterization of the catchment and drainage network properties from a Digital Elevation Model (DEM) for further use in hydrological and water quality models.
2. Determination of the flow field over the catchment.
3. Generation of critical areas (in general, flow field and land use).
4. Use of the flow vector field to trace the non point sources of pollution until a river 'fringe' zone.
5. Aggregate the sources of pollutants (point and non point).
6. Calculate the dispersed pollutant concentrations over the drainage network.

The water resources models used in this thesis implements the above steps. They are illustrated in Figure 2.27 and are described in detail in the following chapters. Throughout these chapters (i.e. 3-7) the models are demonstrated using a test data set that was chosen arbitrarily in order to illustrate.

A complete evaluation of a complex model is a time-consuming process, and only certain elements are implemented in this thesis. The evaluation strategy used here considers the following questions:

1. Whether the computer program actually carries out the logical processes expected of it (i.e. does the computer implementation operate as the mathematical model has defined?).
2. Whether the program is consistent with the functionality of the mathematical model?
3. Whether the physical processes (hydrological and transport) act rationally?

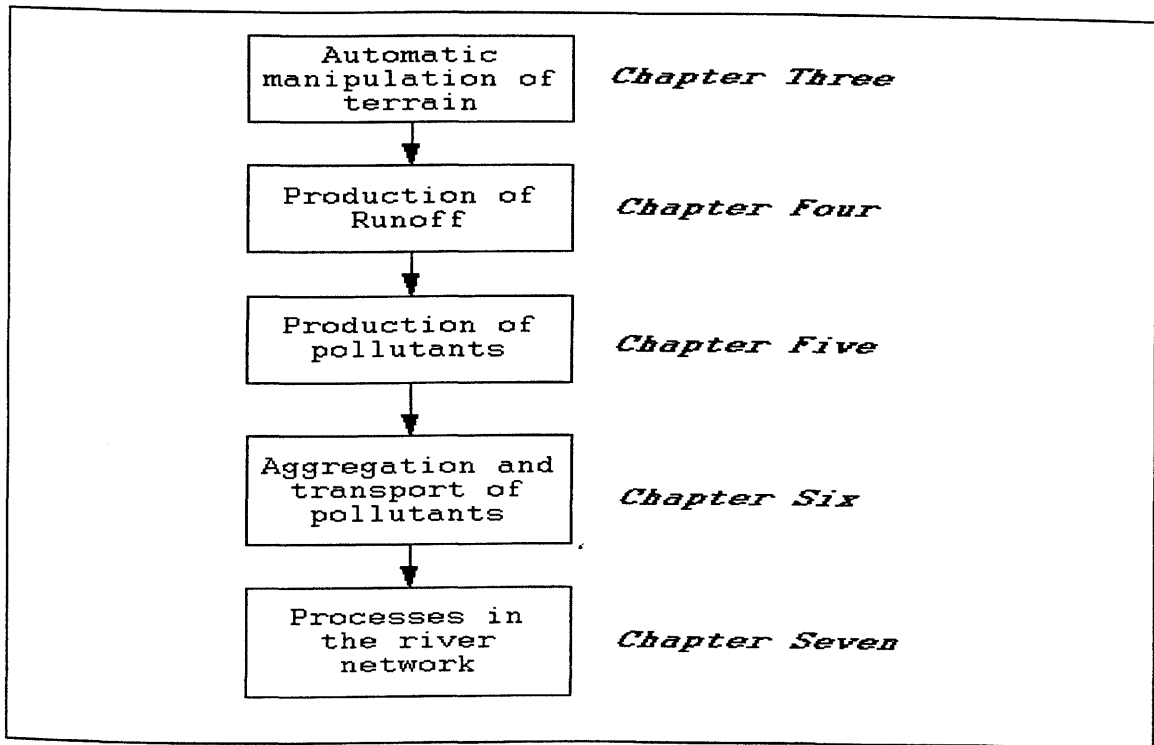


Figure 2.27 : Group of models integrated with GIS.

The majority of software errors, items 1 and 2 above, are known to occur during the translation of the mathematical concepts into computer code. Obviously, in the process of coding and software testing most errors are eliminated. However, although the models have been run many times, and numerous checks been made, it is possible that some errors remain to be discovered and remedied.

Some more specific aspects of item 3 above have also been checked, and are presented in the remainder of this thesis. These questions are:

1. Do the extracted terrain features provide sensible output for the flow routing algorithms?
2. How does the system perform if a central assumption, such as the transport of pollutants by flow, is not met?
3. Are the point source impacts really important to characterise water quality conditions?
4. Does the model provide a sensible output at river confluences?
5. How well does the overall system predict the various outcomes of the modelled processes?

A further set of criteria on which the models can be judged concerns the range of conditions over which they can be applied, and their utility and efficiency. To be efficient, a model must be a satisfactory compromise between simplicity and accuracy. Some of the above questions (1-4) are

addressed in the following chapters (3-7). The overall system behaviour (Question 5) will be analysed in chapter 8.

The focus of these chapters (3-7) is on the explanation of the algorithms and demonstration of their use based in a small illustrative examples and on the development of the problem with respect to the whole catchment.

The cumulative effect of several pollutant sources may be simulated by applying this approach. It is argued that this approach offers the decision-maker a greater degree of flexibility in determining the form and the domain in which water quality processes are represented. It also allows the water quality models to utilise directly the spatial data structures and analysis functions provided by the GIS.

Maps of critical areas, and the spatial distribution of pollutant concentration based on the scenarios can be displayed. These maps indicate where hypothetical scenarios would have the greatest positive or negative consequences. Planners can then decide whether to combine the positive elements from several scenarios or to leave out the negative elements and develop new scenarios. The advantage of using this approach is that this operation can be done very quickly by simply combining available information (generally maps). The database can easily be updated with new data (such as field and laboratory measurements), followed by new interpolations to produce maps or new satellite images.

Chapters 3 to 7 shows the various components, shown diagrammatically in Figure 2.27, of a water quality planning based on the GIS/modelling framework presented above. Chapter 8 focus solely on the overall model validation, using a real example in the South of Brazil. Chapter 9 presents an approach to handling error within the system. Chapter 10 presents the general conclusions of the use of such a system. In the following chapters it will become clear that knowledge of the theoretical framework presented here is imperative in order to adequately support water quality decision analysis based on multiple attributes.

3. Digital representation of catchment base system

3.1 - Introduction

Surface runoff, overland flow and the consequent effects of erosion, sedimentation, chemical and nutrient transport, are affected by the spatial variability of soils, topography, land use and land cover, climate, and management practices. All these processes are driven by flow characteristics, such as flow depth, flow velocity and flow pathways. Consequently, many hydrological processes are sensitive to topographic position.

Eagleson (1970) defined catchment systems as open physical systems where there is import and export of matter across their closed bounding surfaces. For surface runoff, all precipitation (import) and flow, sediments and pollutants (export) occur across the land surface (boundary). The potential energy of runoff enables the transport of pollutants and sediments, and forms a drainage network (Yang, 1971). Thus, topography exerts an important control on the movement of water and pollutants.

The main purpose of this chapter is to describe an algorithmic approach for the rapid parameterization of catchment and drainage network properties from available Digital Elevation Models (DEMs) for use in hydrologic and water quality models. This is achieved by a set of computer programs that calculate properties of catchments from a Digital Elevation Model (DEM), as illustrated in Figure 3.1.

The parameters described in Figure 3.1 have been measured manually for decades (Horton, 1945; Smart, 1968; Gregory and Walling, 1968; Shreve, 1974; Jarvis, 1977). The development of computer power to derive these parameters automatically has resulted from the analysis of larger catchments. Such catchments usually drain areas from hundreds of square kilometres. At this scale, manual determination of catchment parameters is time consuming and tedious, and in many cases impractical.

3.2 - Digital Elevation Models (DEMs)

Water is one of the main erosive agents and transporting mechanisms for land surface processes. Topography is a major determinant of these erosion and transport processes. Surface processes

models usually require topographic-based data defining catchment boundaries, drainage areas, land slopes, channel slopes, aspects, channel networks and land unit connectivities that define how water moves through a landscape.

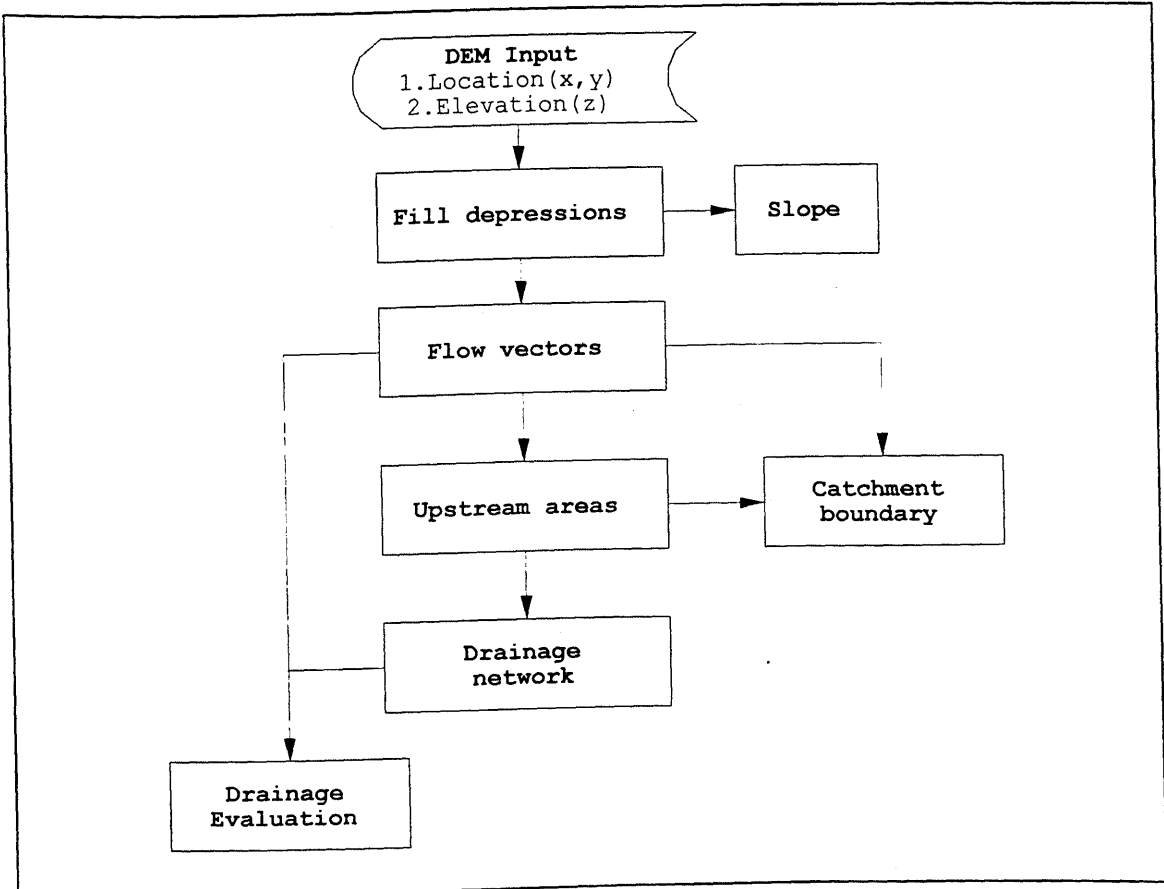


Figure 3.1 : Flow diagram illustrating a series of programs for the calculation of properties of catchments from DEMs.

These topographic-based data can be divided into primary and secondary attributes. Primary attributes are immediately calculated from elevation data (e.g. elevation, slope and aspect). Secondary attributes involve combinations of the primary topographic attributes and are physically based or empirically derived indices that characterise the spatial variability of specific processes occurring in the landscape.

These topographic attributes can be derived from a digital elevation model (DEM) using a variety of terrain analysis techniques. A series of topographic attributes used to characterise the spatial distribution of selected hydrological processes is discussed in more detail later in this chapter.

A Digital Elevation Model (DEM) is an ordered array of numbers that represents the spatial distribution of elevations above some arbitrary datum in a landscape (Moore et al., 1991). It may consist of elevations sampled at discrete points or the average elevation over a specified piece of landscape. Many DEMs are derived from topographic maps. Contour lines can be digitised automatically using the processes of raster scanning and vectorization (Leberl and Olson, 1982) or by manually using a digitiser table. Direct photogrammetric techniques are also available to produce DEMs, from stereophoto pairs. The Gestalt Photomapping system uses photo coordinates of ground control points and their location and elevation as input, to produce a DEM (Kelly et al., 1977).

Digital elevation data are now becoming available for a number of areas in the world (e.g. in the US. (U.S.Geological Survey, 1987) and in the UK (Ordnance Survey, 1994)). However, if digital data for a particular area, like Brazil, are not available they can be derived by digitising existing topographic maps or by photogrammetric methods. A manual digitising approach using an existing map was adopted here.

The process of digitising a map proceeds as follows. The map is fixed to the table and control points, associated with the map co-ordinate system, selected (Figure 3.2). This is a very important step, since an error at this stage would lead to systematic error in every co-ordinate. Digitising then proceeds with the selection of points. Points are entered one at a time, with a pause after each to enter attributes such as precipitation or elevation. Lines are entered as strings of points to form a chain. Polygons are digitised as closed chains.

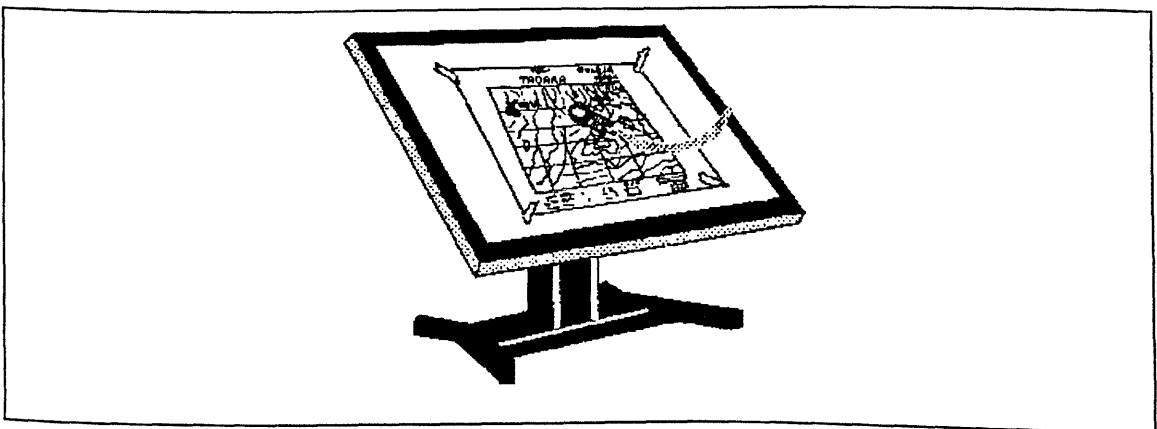


Figure 3.2 : Digitiser table.

Figure 3.3 shows a map where contours have been digitised from topographic maps. The data for these points are stored in a file Example.ASC, shown as an example bellow Figure 3.3.

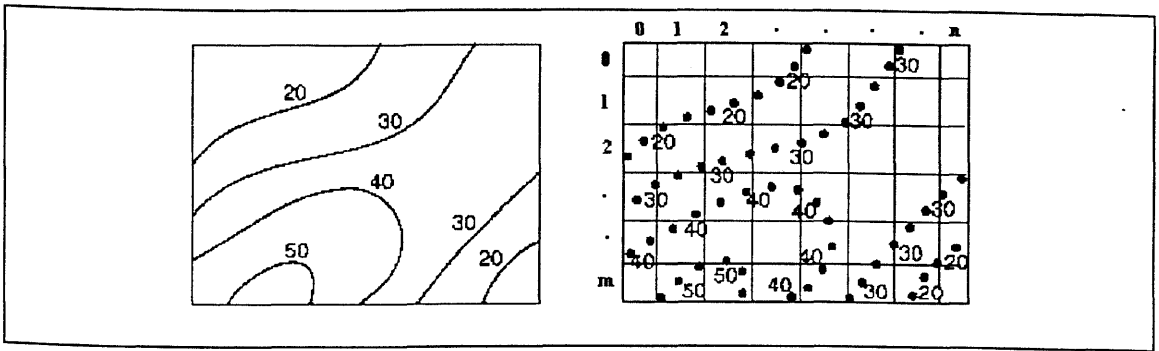


Figure 3.3 : Point data sets.

File: Example.ASC

2	0	20
1	1	20
0	5	20
5	0	30
2	1	30
2	4	30
.	.	.
.	.	.
.	.	.

Figure 3.3 shows a series of observations on a topographic map where each point is characterised by its X, Y co-ordinates and the value of its attribute (Z). To make these data usable, they must be represented as a surface with the elevations values. It is possible to compute this surface by either fitting a surface defined by some function $F(x,y,z)$ to the DEM and using elementary geometry to derive the attributes or by using finite difference techniques directly with the DEM. Methods that fit a surface sequentially to local regions of the DEM are called local interpolation methods, while those that fit a surface to the entire DEM are called global methods.

There are a wide variety of methods for fitting surfaces to point data. They include trend analysis (Equation 3.1) and moving average methods (Equation 3.5), procedures such as kriging (Webster

and Oliver, 1990), and spline interpolation (Dubrule, 1984). Hutchinson (1989) developed a finite difference method that has the efficiency of a local method without sacrificing the advantages of the global methods. This method uses a nested grid strategy that calculates grids at successively finer resolutions.

The ideal structure for a DEM depends on the intended use of the data and how it might relate to the structure of a model. There are three principal ways of structuring a network of elevation data:

1. Regular Grid Network may use a regularly spaced triangular, square, or rectangular mesh or a regular angular grid to store elevation data.
2. Triangulated Irregular Networks (TIN) usually a sample surface at peaks, ridges, and breaks in slope, and forming an irregular network of points stored as a set of x , y , z co-ordinates together with pointers to their neighbours in the net (Mark, 1975).
3. Contour based network methods consist of digitised contour lines stored in the form of x , y co-ordinate pairs along each contour line of specified elevation (Moore, 1988).

Topographic attributes can be derived from all three types of DEM. Jenson and Domingues (1988) presented a detailed description of procedures to be applied to Regular Grid Networks. Depression detection and filling, flow direction computations, and flow accumulation values are conditioning procedures used to create data sets for further analysis. Using these data sets, operations such as catchment delineation, automatic subcatchment delineation, and determination of drainage networks are performed. Mark (1984) presented similar procedures for basin detection and flow network delineation. Quinn et al. (1991) developed a procedure to assign multiple flow paths exiting from a cell rather than a single value.

For DEMs represented by triangulated irregular networks, Gandoy-Bernasconi and Palacios-Velez (1990) present methods for automatic numbering of unit elements while Jones et al. (1991) present procedures for TIN-based catchment delineation. Djokic and Maidment (1991) developed hydrologic models that use parameters derived from a TIN structure.

Hydrologic models simulate the flow of water across a surface so the elemental areas of the DEMs should reflect this requirement. Contour based methods have important advantages in this regard (Moore, 1988; Moore and Grayson, 1989, 1991) because the structure of their elemental areas is based on the way in which water flows on the land surface. Orthogonal to the contours are flowlines so the equations describing the flow of water can be reduced to a series of coupled one-dimensional equations.

The use of Regular Grid Networks for hydrologic analysis is often recommended because they are computationally efficient and simple (Collins and Moon, 1981) and are compatible with remotely sensed data and many geographic information systems. Nonetheless, there are some disadvantages, such as: (1) they cannot easily handle abrupt changes in elevation; (2) the size of grid mesh affects the results obtained; (3) the flow paths tend to zigzag and therefore are somewhat unrealistic and (4) precision is lacking because regular grids are only an approximation to the roughest terrain (Moore et al., 1991). In spite of these problems I have chosen to use a regular grid mainly because it is very easy to implement by computer.

3.3 - Analysis of elevation data

If a surface, defined by a function $F(x,y)$, is fitted to a grid, then a number of hydrological topographic attributes can be derived from this function at the point (x_o, y_o) . As an example, I demonstrate in this section how primary attributes (elevation, slope and aspect), can be determined for a grid based DEM from a function $F(x,y)$ using elementary geometry .

A simple method to predict the value of a surface is to obtain a fit to the data by least squares using a function of the form (Ripley, 1981):

$$F(x, y) = \sum_{r+s \leq p} a_{rs} x^r y^s \tag{3.1}$$

where the integer p is the order of the surface and a are coefficients. The first few functions are:

a	flat
$a + bx + cy$	linear
$a + bx + cy + dx^2 + exy + fy^2$	quadratic (Evans, 1980)
$a + bx + cy + dx^2 + exy + fy^2 + gxy^2 + hx^2y$	cubic (Press et al., 1992)
$a + bx + cy + dx^2 + exy + fy^2 + gxy^2 + hx^2y + ix^2y^2$	quartic (Zevenbergen and Thorne, 1987)

In Figure 3.4, the geometrical interpretation of the finite differences technique is illustrated for the one-dimensional case.

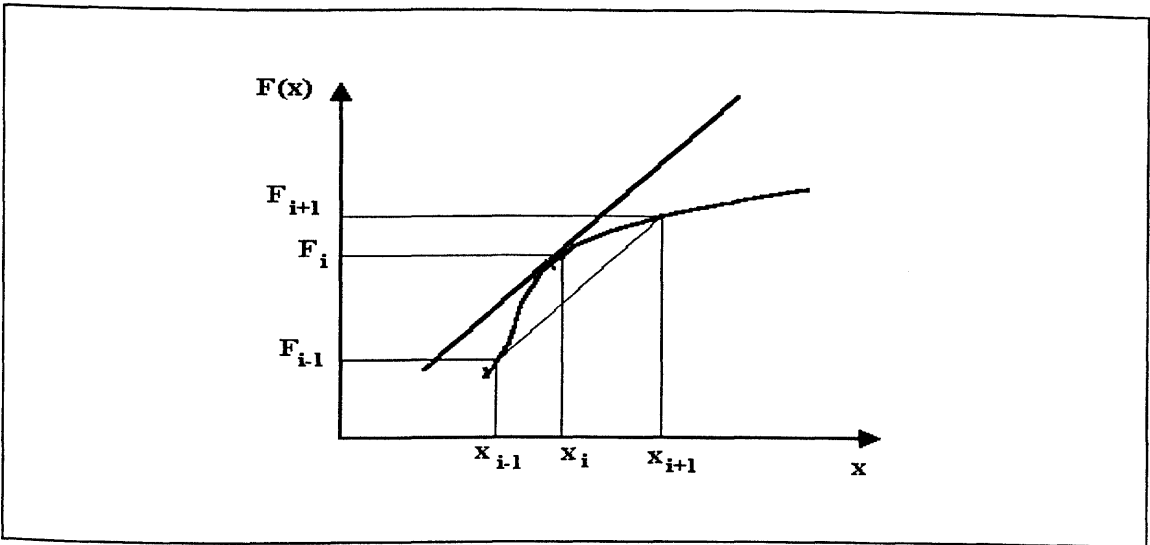


Figure 3.4 : Geometrical interpretation of finite differences.

The error associated with the adjustment of $F(x)$ depends on the shape of the curve $Z(x)$ at the point (x_i, F_i) . To reduce this error the coefficients of equation 3.2 are normally chosen to minimise:

$$\min \sum_{i=1}^{i=n} [Z(x_i) - F(x_i)]^2 \tag{3.2}$$

This is simplified if equation 3.1 is re-expressed to make equation 3.2 a standard multiple regression problem. If I label $1, x, y, x^2, xy, y^2, \dots$ as $f_1(x), \dots, f_p(x)$ and the coefficients β_1, \dots, β_p , this defines a multiple regression of $Z(x_i)$ on $(f_1(x_i), \dots, f_p(x_i))$, giving the result:

$$Z(x) = f(x)^T \beta + \varepsilon(x) \tag{3.3}$$

The above method is the simplest way to describe gradual variations along surfaces and is known as trend surface analysis. However, a disadvantage of this model is that local features are not well accommodated resulting in a smoothed $F(x,y)$.

Another simple method to predict the value of a surface is by a weighted average of the values at the data points. The method works by moving from grid cell to grid cell, each time computing an interpolated value for that grid cell. Mathematically, the most common used formula is (Ripley, 1981):

$$\hat{F}_{i,j} = \frac{\sum_{p=1}^{p=R} F_p d_p^n}{\sum_{p=1}^{p=R} d_p^n} \quad (3.4)$$

where F_p is the attribute at point p in the neighbourhood R , d is a distance from the point being interpolated $F_{i,j}$ to point p . Values of n for natural terrain have varied from 1.0 to 6.0. Perhaps the most commonly used value is 2, in which case the technique is called inverse-squared distance. In general terms the equation 3.4 can be rewritten (Ripley, 1981) to:

$$\hat{F}(x) = \sum_i^N \lambda_i F(x_i) \quad \sum \lambda_i = 1 \quad (3.5)$$

where the weights λ_i are given by a function of the distance between points $\Phi(d(x, x_i))$. A criterion to choose the weights are that $\Phi(\cdot) \rightarrow \infty$ as $d \rightarrow 0$. Another common requirement is that $\Phi(\cdot)$ is chosen to be zero beyond some arbitrarily chosen radius (the neighbourhood radius R from equation 3.4). The above algorithm (Equation 3.5) is controlled by two user-specified variables: (1) the neighbourhood radius R , and (2) the weighting function λ_i . The neighbourhood radius R specifies the distance around each cell in which the algorithm searches for data points. The weighting function λ_i determines how the surface values will be interpolated from the original data points.

Numerous commercial packages are available to perform such techniques. For example, topographic data derived from the area shown in Figure 3.5 was used to create a surface using ERDAS software (available in the department) with a weight function (Equation 3.5) equal to $(1-d)^2$. The resulting surface is illustrated in Figure 3.6.

All the above methods generate smooth surfaces. Because of this, the 'true' value of the attribute (elevation) is unknown. A simple way to cope with this uncertainty is to use an operation like SPAN (Burrough, 1986 - page. 90). This operation calculates the distance of each cell to the nearest of a set of target cells, i.e., point data sets as presented in Figure 3.3. The uncertainties of the prediction are smaller nearer to known values according to the assumptions of equation 3.5. I used the IDRISI package to calculate this surface using digitised elevation points from the

nearest of a set of target cells, i.e., point data sets as presented in Figure 3.3. The uncertainties of the prediction are smaller nearer to known values according to the assumptions of equation 3.5. I used the IDRISI package to calculate this surface using digitised elevation points from the example topographic map in Figure 3.5. This operation calculated a distance surface based on the location of known elevation points used to interpolate the DEM. The results are shown below in Figure 3.7.

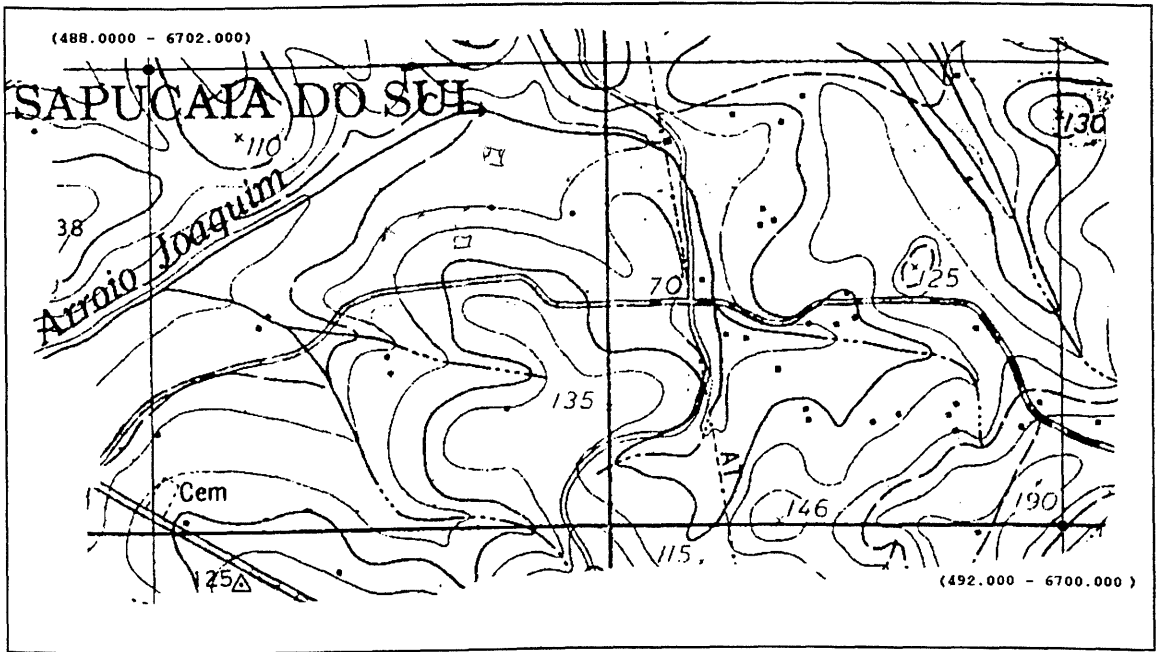


Figure 3.5 : Example topographic map.

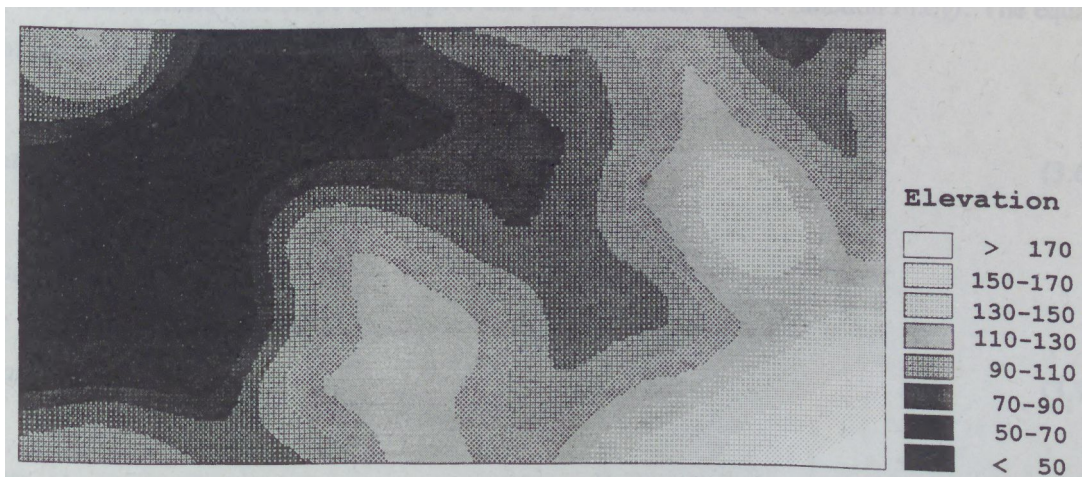


Figure 3.6 : Gray scale surface.

Figure 3.7 shows the spatial variations in the generated surface shown in Figure 3.6. Because we interpolated the topographic surface (Figure 3.6) from a finite sample (Figure 3.5, similarly to Figure 3.3), we do not know the true values of these topographic data at the locations not examined in the sample process. This uncertainty in the topographic surface (Figure 3.7) will undoubtedly be larger at points that are far away from any of the sample points than at points close to the sample points. Figure 3.7 identified the amount of error following these criteria. It is important to distinguish that this surface only refers to the spatial variability of the process. The total uncertainty of the elevation is affected by the amount of spatial variability present, but also by the method of data capture.



Figure 3.7 : Spatial variation of the prediction.

I now demonstrate how slope and aspect can be determined from a function $F(x,y)$. The equation of the surface tangent to the point (x_0, y_0) is:

$$a(x - x_0) + b(y - y_0) = 0 \quad (3.6)$$

or

$$ax + by + c = 0 \quad (3.7)$$

or

$$y = -\frac{a}{b}x - \frac{c}{b} \tag{3.8}$$

where: $c = -ax_0 - by_0 = \text{constant}$.

$$a = \left. \frac{\partial F}{\partial x} \right|_{x=x_0}$$

$$b = \left. \frac{\partial F}{\partial y} \right|_{y=y_0}$$

(3.8) is the equation of a line with slope $-a/b$, and aspect $-b/a$ (orthogonal of slope). The negative sign indicates that the direction is down slope and is, by convention, ignored. Because I use a square grid the partial derivatives a and b can be estimated as finite differences (Rosenberg, 1975). The computations are made within a 3x3 moving window (below) that is centred on every grid location in the DEM.

$F_{i-1,j-1}$	$F_{i-1,j}$	$F_{i-1,j+1}$
$F_{i,j-1}$	$F_{i,j}$	$F_{i,j+1}$
$F_{i+1,j-1}$	$F_{i+1,j}$	$F_{i+1,j+1}$

The simplest finite difference estimate of slope and aspect for the function $F(x,y)$ at cell i,j assuming $a = \frac{\partial F}{\partial x} = \frac{F_{i,j+1} - F_{i,j-1}}{2\delta x}$ and $b = \frac{\partial F}{\partial y} = \frac{F_{i+1,j} - F_{i-1,j}}{2\delta y}$, where δx and δy are the distances between cell centres in the x and y directions and $\delta x = \delta y$, is:

$$\text{SLOPE}_{ij} = \frac{a}{b} = \frac{F_{i,j+1} - F_{i,j-1}}{F_{i+1,j} - F_{i-1,j}} \tag{3.9}$$

$$\text{ASPECT}_{ij} = \frac{b}{a} = \frac{F_{i+1,j} - F_{i-1,j}}{F_{i,j+1} - F_{i,j-1}} \tag{3.10}$$

Algorithms for determining slope and aspect are presented in more detail later in this chapter.

3.4 - Applications of DEM

3.4.1 - Treatment of depressions

One problem with the analysis of DEMs for hydrologic applications is the definition of flow paths when the DEM contains depressions (Figure 3.8). Some depressions are data errors while others are natural features of the terrain. A simple way to produce a depressionless DEM is to modify it by raising the elevation within each closed depression to the elevation of its local outlet (Jenson and Domingues, 1988) as illustrated in Figure 3.8. The program used to produce a depressionless DEM is given in the Appendix . For the purposes of this thesis, it is assumed, in all the following applications, that the Digital Elevation Model has been pre-processed to remove depressions.

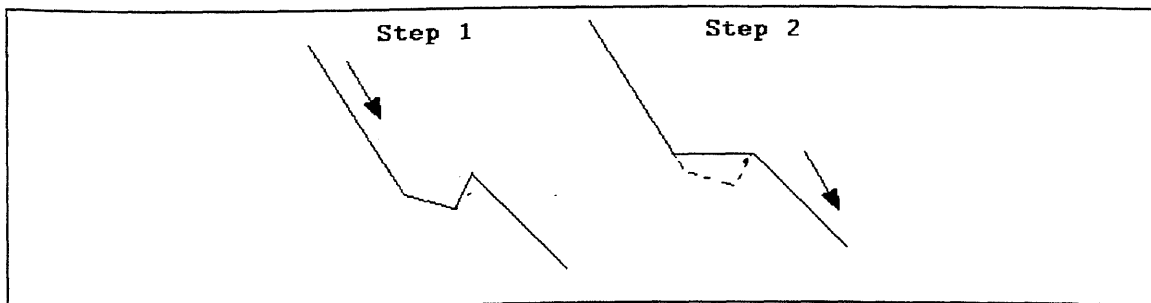


Figure 3.8 : True elevation (1) and apparent elevation (2).

3.4.2 - Determination of slope

This algorithm scans each cell of the depressionless DEM and determines the steepest downward slope to an adjacent cell. I used the GRASS software to obtain this surface. The formulae used are based on a 3x3 matrix of elevations around the cell $Z_{i,j}$ as illustrated below. In this method, the relative slope to each adjacent cell is calculated with allowance for the greater distance to diagonal cells and indicates that the steepest slope is assigned to the cell $Z_{i,j}$ in a new slope grid.

$Z_{i-1,j-1}$	$Z_{i-1,j}$	$Z_{i-1,j+1}$
$Z_{i,j-1}$	$Z_{i,j}$	$Z_{i,j+1}$
$Z_{i+1,j-1}$	$Z_{i+1,j}$	$Z_{i+1,j+1}$

where $Z_{i-1,j-1}, \dots, Z_{i+1,j+1}$ are elevations. First the average x and y changes are computed :

$$\Delta x_1 = Z_{i-1,j+1} - Z_{i-1,j-1}$$

$$\Delta y_1 = Z_{i-1,j-1} - Z_{i+1,j-1}$$

$$\Delta x_2 = Z_{i,j+1} - Z_{i,j-1}$$

$$\Delta y_2 = Z_{i-1,j} - Z_{i+1,j}$$

$$\Delta x_3 = Z_{i+1,j+1} - Z_{i+1,j-1}$$

$$\Delta y_3 = Z_{i-1,j+1} - Z_{i+1,j+1}$$

$$\Delta x = (\Delta x_1 + \Delta x_2 + \Delta x_3) / 3\delta$$

$$\Delta y = (\Delta y_1 + \Delta y_2 + \Delta y_3) / 3\delta$$

$$\Delta h = \sqrt{(\Delta x)^2 + (\Delta y)^2}$$

where δ is the grid spacing. The basic formula is then (Skidmore, 1989):

$$\tan(SLOPE) = \Delta h \tag{3.11}$$

Figure 3.9 shows the slope calculated for the area in Figure 3.5.



Figure 3.9 : Slope of example area.

3.4.3 - Determination of flow vectors (aspect)

Flow vectors are assigned on the basis of the steepest slope direction from the current cell $Z_{i,j}$ calculated by (Skidmore, 1989):

$$\tan(ASPECT) = \frac{\Delta x}{\Delta y} \tag{3.12}$$

and are specified using the numbering convention of Greenlee (1987) shown below. The numerical codes are based on powers of two so that the position of each adjacent cell remains uniquely defined throughout analysis. Those cells forming the border of the data set are assigned direction values pointing away from the interior allowing runoff to flow off the grid at the edges (Jenson and Domingues, 1988). Figure 3.10 presents the aspect, calculated using the GRASS software, for the area given in Figure 3.5. The final result of the flow vector algorithm is a new array containing the aspects for all grid cells


64	128	1
32		2
16	8	4



Figure 3.10 : Aspect of example area.

3.5 - Hydrological topographic attributes

Topographic attributes are calculated from elevation data and are indices that describe the spatial variability of hydrological processes occurring in the landscape (Moore et al., 1991). In this section I describe some topographic attributes and the hydrological processes they attempt to characterise.

3.5.1 - Determination of upstream catchment areas

This algorithmic approach is based on a paper by Jenson and Domingues (1988). Beginning at each cell with a defined elevation and using the flow direction previously calculated, the path downstream is followed until the limit of the DEM is reached. At each cell along this path, the value of this cell is incremented by one. Once the flow path from each cell in the DEM has been evaluated, a new grid is generated containing the number of upslope cells for each grid cell. This new grid represents the distribution of energy along the catchment. Figure 3.13 illustrates the general strategy of the algorithm. Numbers on Figure 3.11a give elevation values and arrows show flowlines. The numbers on Figure 3.11b give upslope values for each grid. Figure 3.12 shows the accumulated values for Figure 3.5. The upstream program is given in the Appendix.

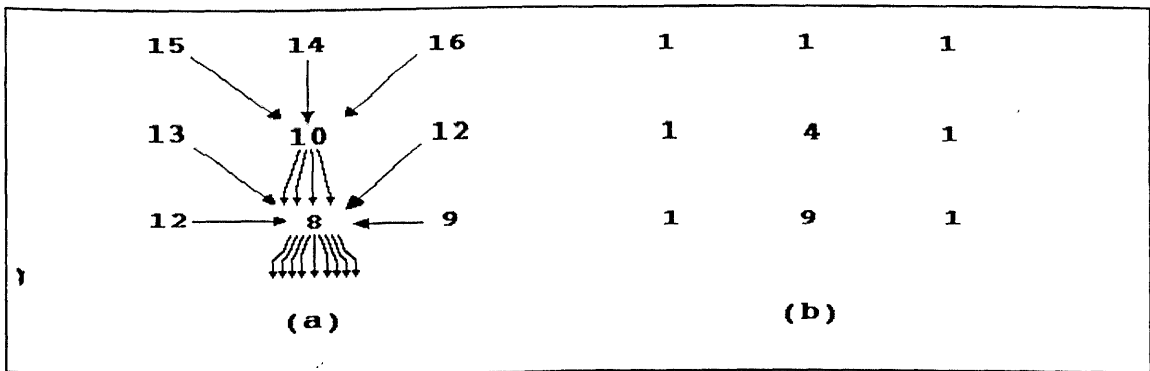


Figure 3.11 : General strategy of upstream catchment areas. (a) Elevation values and (b) Accumulated values.

3.5.2 - Determination of catchment boundary

Jenson and Domingues (1988) developed a technique to delineate catchments using both a flow vector grid and a 'starter' data set. The algorithm determines the boundary of the catchment where all hydrologic and water quality processes are analysed. The row and column of the grid cell ("starter" data) close to the catchment outlet are based on the co-ordinates of the largest upstream catchment area cell position calculated as shown above. The algorithm scans the flow vector, and the cell flow direction, previously defined, marking these cells as being inside the catchment and all other cells as being outside. The scan is repeated to all cells of the grid. The final product of this algorithm is a binary grid defining the cells inside and outside the catchment. Figure 3.13 shows the boundary of the larger catchment of Figure 3.5.

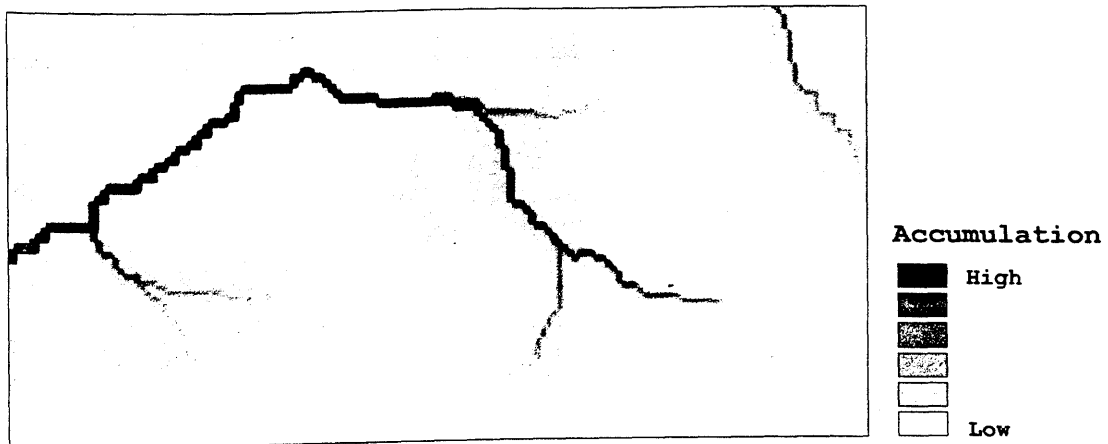


Figure 3.12 : Example of upstream catchment areas.

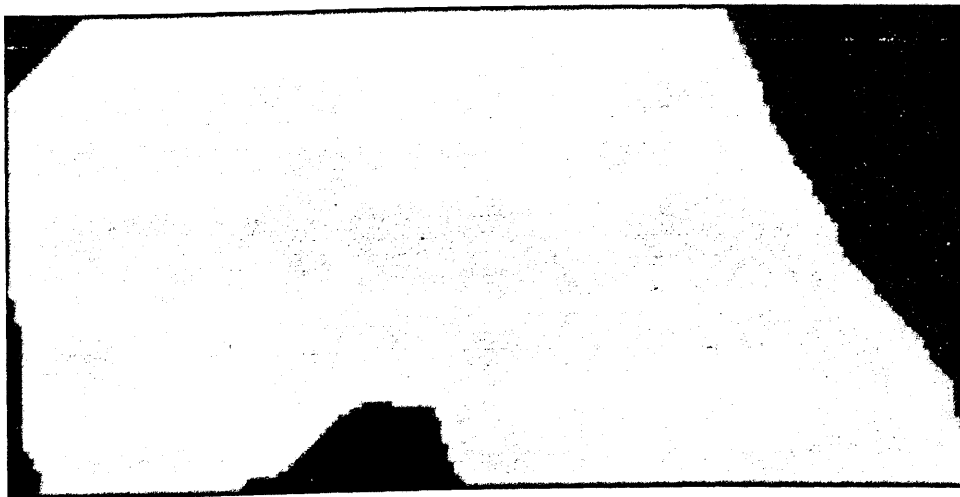


Figure 3.13 : Example catchment boundary.

3.5.3 - Determination of the drainage network

This algorithmic approach to extract drainage network is based on a paper by Band (1986). An upstream catchment area data set is used to produce a drainage network grid. A minimum upstream drainage area is required to initiate a channel (threshold value). Physically it means that any area smaller than the threshold value (given by the user) does not produce enough runoff to form and maintain a channel. This threshold value depends on slope characteristics, surface cover, climatic conditions and soil properties, amongst other things.

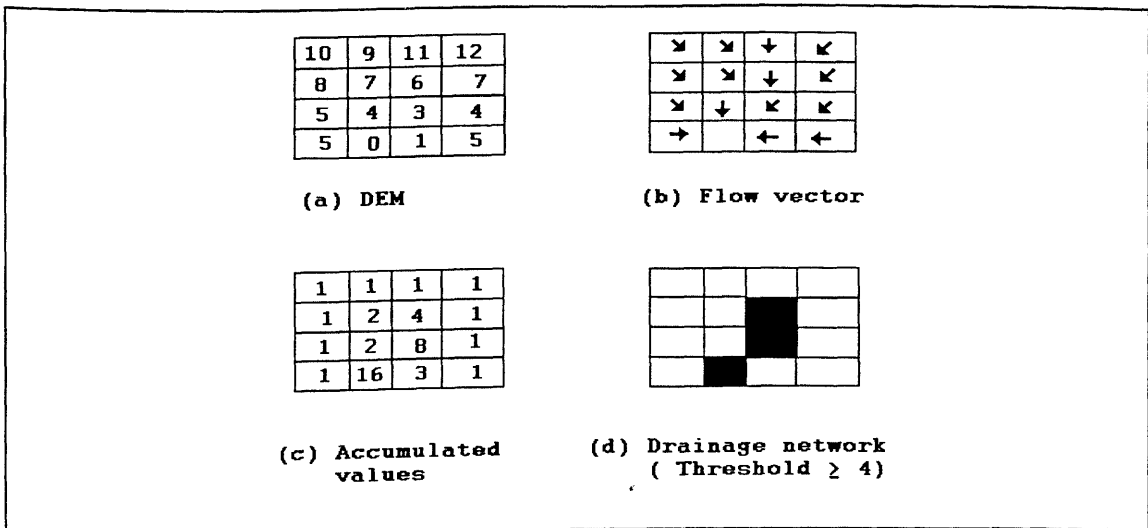


Figure 3.14 : Drainage network extraction.

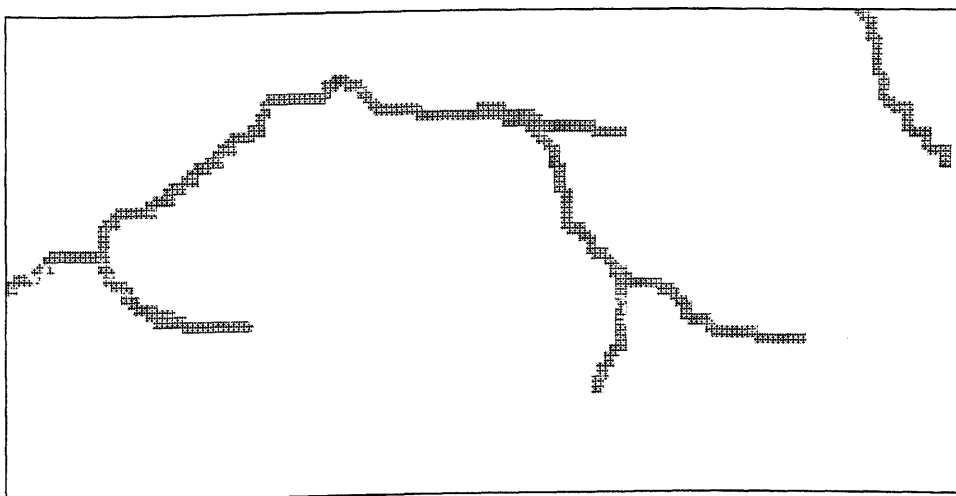


Figure 3.15 : Example drainage network.

3.5.4 - Evaluation of drainage network composition

Distributed parameter hydrologic models are well suited for investigating the effects of land-use changes on runoff hydrographs, tracing the paths of pollutant movement through a catchment (Young et al., 1989), and modelling sediment transport (Gupta and Solomon, 1977). The purpose of this algorithm is to build a database describing the topology of the drainage network. This drainage network database can then be used to drive the models of runoff and water quality (see chapter 7).

Before explaining this algorithm, it is appropriate to define some fundamental concepts. The channels within a catchment are directed according to flow direction and can be represented as a set of edges, named links. Shreve (1966) defines a channel link as an unbranched portion of stream channel. Following Jarvis (1977) a vertex (point) can be defined at the upstream end, normally the source (i.e. a point with no links) or at a junction (i.e. a point with two or more upstream links). The links can then be characterised by the type of point (vertex) at its upstream end. Links beginning at a source are termed exterior links and those starting with junctions at upstream ends are called interior links (Shreve, 1966). Figure 3.16 shows these concepts.

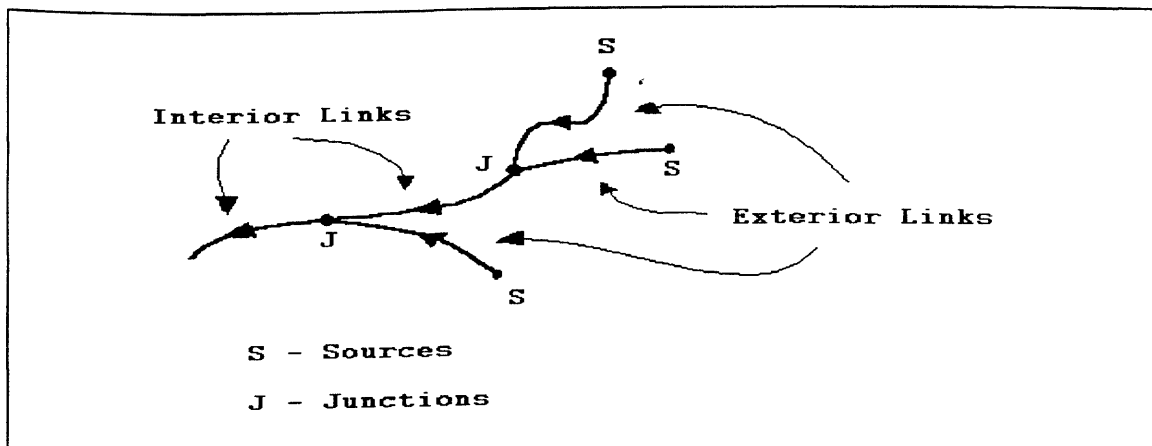


Figure 3.16 : Network concepts.

The idea behind this approach is based mainly on a paper by Smart (1970). The method proposed arranges the network as a binary string of zeros and ones. The string is generated by starting at the catchment outlet, turning left at each junction and turning back at each source. The number '1' is recorded for an exterior link, and '0' for an interior link.

The algorithm starts with the network grid (Figure 3.15) being scanned together with the flow vector grid (Figure 3.10), where network cells that do not receive inflow from any other network cell are identified as a source being recorded as '0' (i.e. there are no contributing cells). The flow vector and network grids are then scanned again moving downslope from the 'source' cells, previously identified, to create the exterior links.

Once all exterior links have been identified, interior links are evaluated. When a cell defined as a junction is encountered, its adjacent cells are examined to determine how many cells flow into the current cell. The network junction code is recorded as the number of upstream links, and a

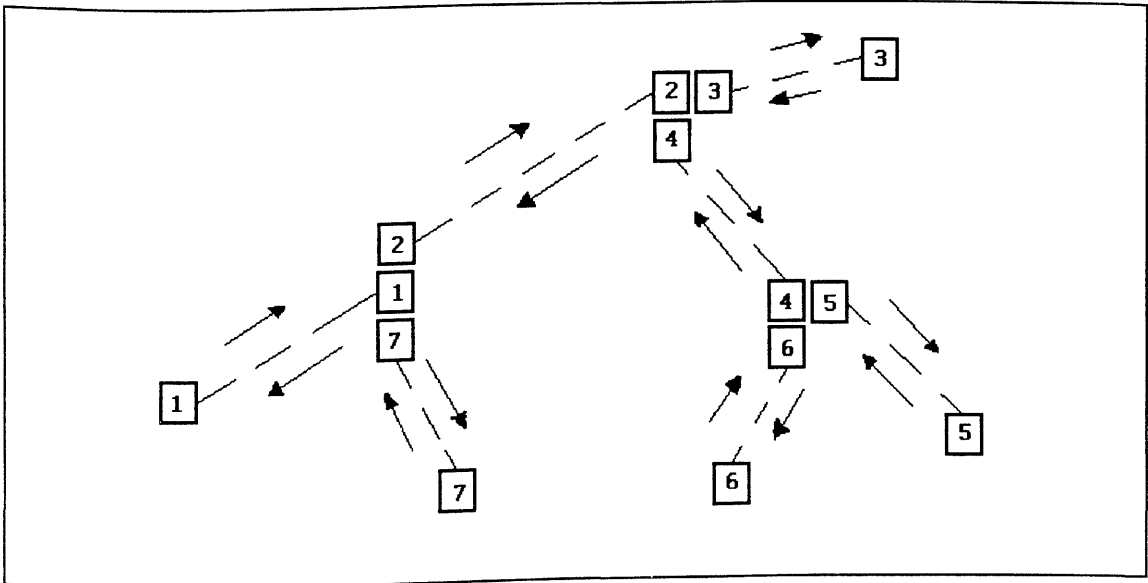


Figure 3.18 : Link number configuration.

Link #	Topological code	Upstream		Downstream	
		x	y	x	y
1	2	40	17	46	1
2	2	18	79	39	17
3	0	20	98	17	80
4	2	43	102	18	80
5	0	55	133	44	103
6	0	63	99	44	102
7	0	53	28	41	17

Table 3.1 : Topological table for the drainage network of Figure 3.15.

3.6 - Evaluation of Sinos catchment Digital Elevation Model (DEM)

This section examines the impact of the construction and resolution of the Digital Elevation Model (DEM) on extracted drainage network properties. This particular aspect of the system was selected because it has a major influence on the output of the flow routing algorithm which is used in all the other components of the modelling system.

The process of flow routing consists of following overland flow paths from each start cell to the catchment outlet. In doing so, the algorithm makes many passes through the catchment, tracing overland paths from start cells to the outlet. Values are assigned to each junction cell depending on the number of times the algorithm has traced an overland path through it. A data preparation algorithm scans the DEM and resolves indeterminate flow paths in depressions of the landscape. The resulting simulated drainage network is based on a single parameter that controls the configuration of the extracted network. This parameter is the minimum source area, that is the upstream drainage area below which a source channel is initiated.

Figure 3.19 shows the drainage network configuration for the Sinos catchment. The simulated network is based on a 100x100 m grid and minimum source area of 300 ha. The minimum source area is the upstream drainage area below which a source channel is initiated. The observed network represents the blue-line drainage network digitised from the 1:250,000 topographic maps. It can be seen that the process defines a fully connected drainage network. In general, the trend of the extracted drainage network seems to converge to the blue-line configuration, although there are a number of instances where the convergence is less than ideal.

The observed divergence between the simulated and observed drainage network configuration takes a number of different forms:

1. Instances of multiple parallel river segments in the simulated network.
2. Differences in channel sinuosity between observed and simulated networks, probably related to the size of the grid (100 m) constraining representation of the simulated network.
3. Large differences between the spatial configuration of first order streams in the observed and simulated networks.

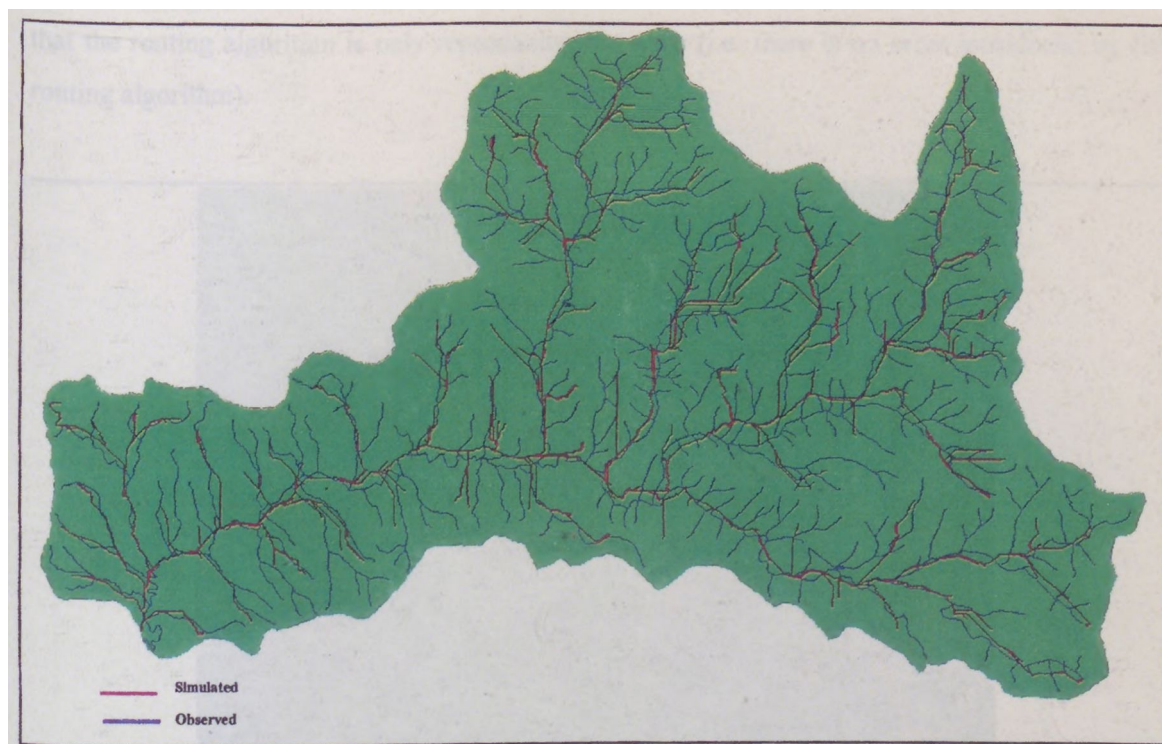


Figure 3.19 : Observed and simulated drainage network configuration for Sinos catchment.

When investigating the occurrence of parallel lines in the simulated channel network the first thought was that it might be due to deficiencies in the interpolation algorithms that produced the DEM, or possibly that some errors still remained in the computer routing programs. In order to examine the problem a series of linear profiles in areas of the DEM with good agreement of observed and simulated network and areas with parallel lines were extracted. The results are shown for two areas within the catchment for 100 m, 200 m and 400m DEM cell resolution. Figures 3.20 and 3.21 show these results.

Close inspection of the terrain profiles for the area generating parallel drainage lines in the simulated network (Figure 3.21b) revealed a series of discontinuities or 'stepped' areas within the profile. This prompted a closer look at the original digitised contour data from which the DEM was generated. This showed that the problem did indeed originate with the digitised data itself due to problems of edge matching within blocks of digitised contours. These edge matching problems stem from the approach taken to digitise the topographic maps, where the map was sub-divided into a series of non-overlapping 10x10 Km tiles, which introduced edge effects when the blocks of data were reconstituted into a single digital data set for interpolation of the DEM. It was concluded that, the occurrence of parallel lines in Figure 3.19 is mainly due to digitising error and

that the routing algorithm is only reproducing the error (i.e. there is no error introduced by the routing algorithm).

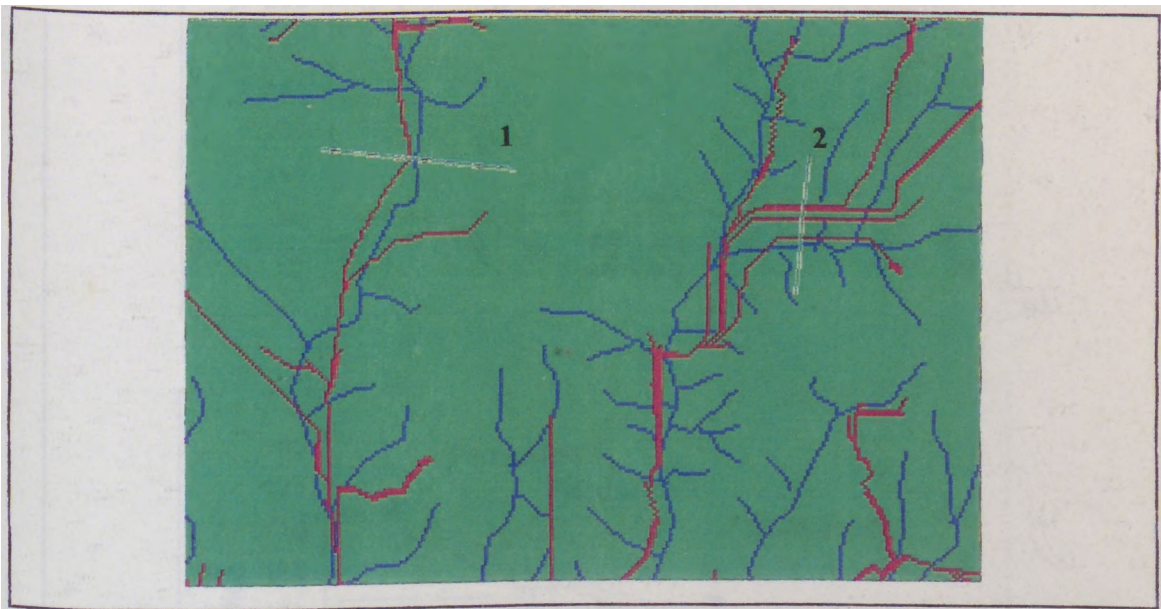


Figure 3.20 : Linear profiles over areas of good simulation (1) and inferior simulation (2) of the drainage network configuration.

The remaining aspects of the drainage network pattern were examined by (i) changing the minimum source area parameter to obtain several drainage network configurations (minimum source areas of 100, 200, 300 and 400 ha) and (ii) changing the grid cell size of the DEM by interpolation to 100, 200 and 400 m grids. The investigation was largely conducted by visual analysis of colour plots similar to Figure 3.19. Results from the comparisons between the twelve drainage network configurations, based on differing DEM grid cell sizes and minimum source area parameter thresholds, demonstrated that:

- The number of channel links decreases with increasing grid size, keeping the minimum source area constant.
- The minimum source area has no trend, but a high variability with increasing grid size.
- The inability of a coarse grid to reproduce channel sinuosity results because the amplitude of this sinuosity is directly related to grid size, as there is a channel capturing effect introduced as the digital representation of the terrain become coarser.

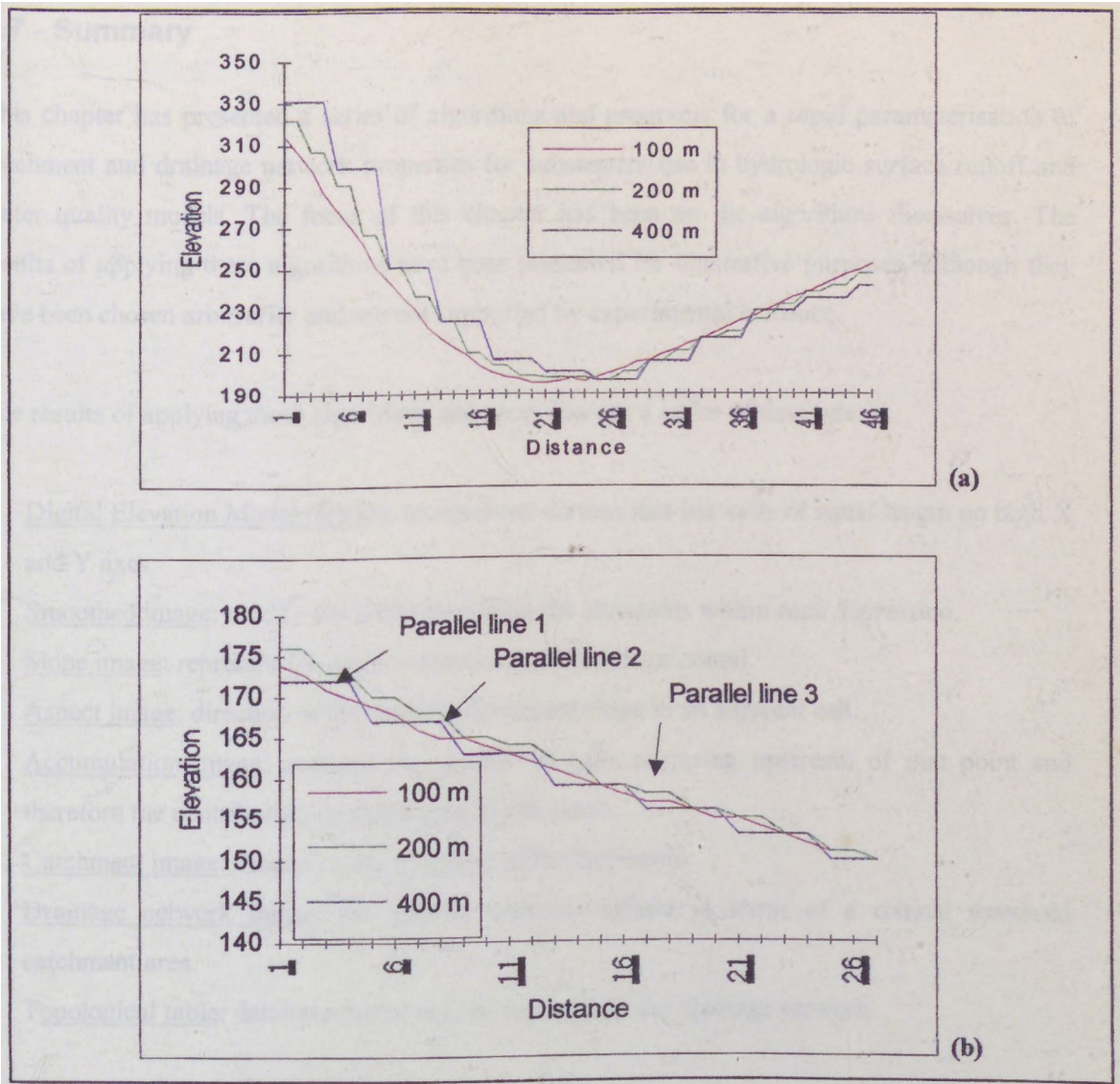


Figure 3.21 : Linear profiles over DEM : (a) profile 1 and (b) profile 2.

In general, grid size dependency results from the inability of the DEM to accurately reproduce drainage features that are at the same scale as the spatial resolution of the DEM. For sinuous channels, this results in a linear channel, and for a network with high drainage densities, it leads to a drainage area capturing effect. For this particular DEM, and DEMs in general, it would be virtually impossible to recapture how the various sources of error, i.e. the errors in the topographic map itself, the digitising error and the interpolation error, combine to yield an overall single estimation of accuracy (similar to the land use classification accuracy).

3.7 - Summary

This chapter has presented a series of algorithms and programs for a rapid parameterisation of catchment and drainage network properties for subsequent use in hydrologic surface runoff and water quality models. The focus of this chapter has been on the algorithms themselves. The results of applying these algorithms have been presented for illustrative purposes, although they have been chosen arbitrarily and are not supported by experimental evidence.

The results of applying these algorithms and programs are a series of data sets:

1. Digital Elevation Model (DEM): interpolated surface that has cells of equal length on both X and Y axes.
2. Smoothed image: modify the DEM by raising the elevations within each depression.
3. Slope image: represent the angle measured down from horizontal.
4. Aspect image: direction of the steepest downward slope to an adjacent cell.
5. Accumulation image: contains the number of cells occurring upstream of that point and therefore the contributing drainage area to that point.
6. Catchment image: determine the boundary of the catchment.
7. Drainage network image: the channel network defined in terms of a critical threshold catchment area.
8. Topological table: database describing the topology of the drainage network.

In the following chapters, these datasets are registered with additional data layers using a GIS or other programs for evaluating the spatial distribution of the production of runoff and pollutants.

4.Generation of runoff based on determinable characteristics

4.1 - Introduction

A fundamental factor in generating and maintaining the transport of pollutants in the environment is the flow of water. Catchment runoff is a function of rainfall intensity and duration, the infiltration capacity of the soil, the cover of the soil, type of vegetation, overland flow characteristics, drainage network topology, catchment geometry, shape and area, river system hydraulics, and various other factors.

The purpose of this chapter is to examine how some of the above factors may be used in predicting the generation of runoff for later analysis of the production and transport of pollutants (Figure 4.1). The proposed approach keeps a balance between simplicity, availability of data and physically based criteria to estimate the spatial distribution of runoff over a catchment.

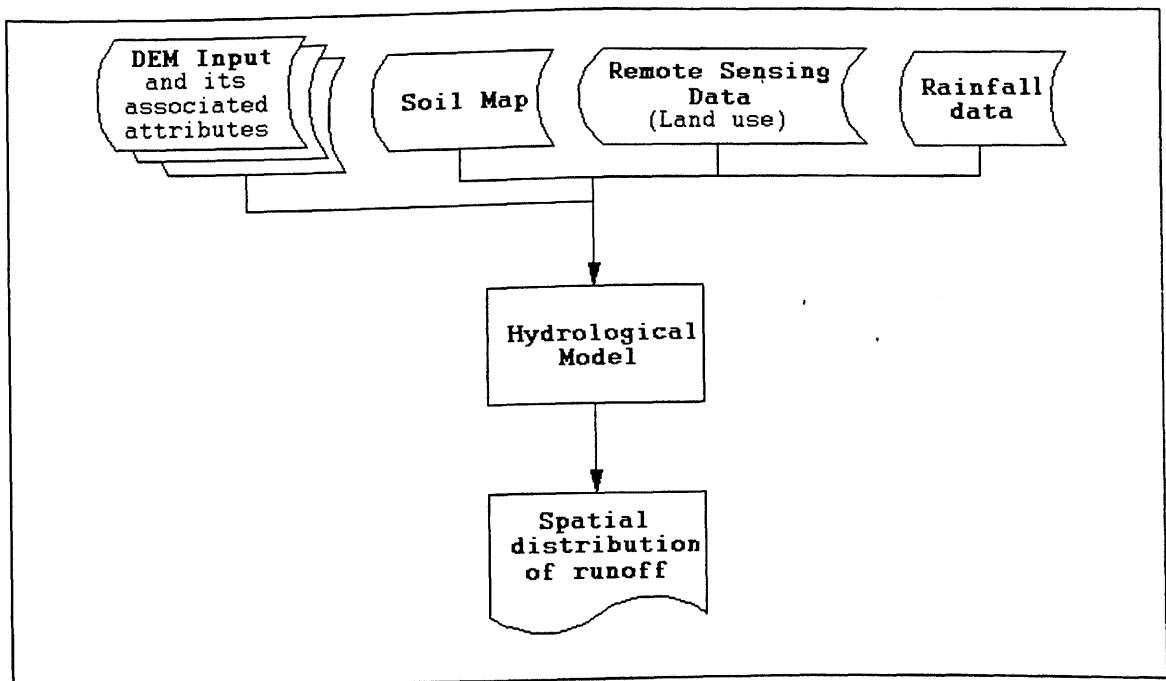


Figure 4.1 : Flow diagram showing the calculation of spatial distribution of runoff.

Hornberger et al., (1985) trying to define the modelling processes using available field data found that '*hydrological quantities measured in the field tend to be either integral variables (that is, river discharge, which reflects an integrated catchment response) or point estimates of variables (such as precipitation, soil hydraulic conductivity, etc.)*'. It was further noted that success in

hydrologic modelling *'has proved elusive because of the complexity of the processes, the difficulty of performing controlled experiments, and the spatial and temporal variability of catchment characteristics.'* They conclude that *'even the most physically based models cannot reflect the true complexity and heterogeneity of the processes occurring in the field'*.

Schilling and Fuchs (1986) note that errors in hydrologic modelling occur for several reasons, including:

1. The input data vary throughout the catchment and cannot be precisely measured.
2. The physical laws are simplified.
3. Model parameter estimates may be in error.

Using a distributed model over a catchment Schilling and Fuchs (1986) concluded that *'it is inappropriate to use a sophisticated runoff model to achieve a desired level of modelling accuracy if the spatial resolution of inputs is low.'* Similarly, Beard and Chang (1979) in their study of 14 urban catchments using complex models (typically having 20 to 40 parameters and functions that must be derived from recorded rainfall-runoff data) concluded that *'changes in the model that would result from urbanisation could not be reliably determined.'*

In a study by Loague and Freeze (1985), three event-based hydrologic models (a regression model, a unit hydrograph model and a kinematic wave quasi-physically based model) were used on three data sets of 269 storm events from three small upland catchments. The three catchments were extensively monitored with rain gauge, stream gauge, neutron probe and soil parameter site testing. In comparative tests between the three modelling approaches to measured rainfall-runoff data it was concluded that all models performed poorly and that the quasi-physically based model performance was only slightly improved by calibration of its most sensitive parameter, hydraulic conductivity. They wrote that the *'conclusion one is forced to draw is that the quasi-physically based model does not represent reality very well; in other words, there is considerable model error present.'* Additionally, *'the fact that simpler, less data intensive models provided as good or better prediction than a quasi-physically based model is food for thought.'*

A major difficulty in the use, calibration and development of hydrologic models therefore appears to be the lack of precise input data and high model sensitivity to data uncertainty. Nash and Sutcliffe (1970) wrote that *'as there is little point in applying exact laws to approximate boundary conditions, this, and the limited ranges of variables encountered, suggest the use of simplified empirical relations.'*

In the absence of more promising results in the use of complex hydrologic models this thesis uses simple models for estimation of runoff quantities over the catchment. A second criterion to be evaluated is that model variables must be correlated to catchment characteristics (physically based). Finally, due to all simplifications adopted to build the model, an uncertainty assessment is carried out in chapter 9. The next sections show how these criteria (simplicity and physical basis) can be met to estimate the spatial distribution of runoff over the catchment.

4.2 - A general distributed catchment model

Hydrology is concerned with study of the earth's waters through the land phase of hydrologic cycle, and the transport of constituents such as sediment and pollutants in the water as it flows. GIS is focused on representing the landscape by means of locationally referenced data describing the character and shape of geographic features. A spatial hydrological model is one which simulates the water flow and transport on a specified region of the earth using GIS data structures. Suppose the boundary of this region is represented by a polygon, such as a river basin boundary or an aquifer boundary. Because both vertical and horizontal water flow can be taking place within the region, hydrologic processes need to be defined over a volume of space rather than an area. Such a volume can be constructed by projecting vertically the lines making up the polygon boundary into the atmosphere and into the earth, and closing the top and bottom of the volume by horizontal planes (Figure 4.2). Such a volume is called a control volume in fluid mechanics and the surface which surrounds it is called the control surface.

Figure 4.2 shows the hydrologic cycle with its principal components: This open system is bounded by impervious rock at the bottom, by the imaginary surface S on the sides and by the imaginary surface A on the top.

Building a hydrologic model involves writing equations that relate the rates of change of water properties within the control volume to flow of those properties across the control surface. For example, a simple soil water balance model for a control volume drawn around a block of soil is:

$$S(t+1) = S(t) + P(t) - E(t) - Q(t) \quad (4.1)$$

Where: $S = \int_V \theta(x, y, z, t). dV = \text{total storage [L}^3\text{]}.$

$P = \int_A \xi^+(x, y, t). dA = \text{precipitation rate [L}^3\text{/T]}.$

$E = \left| \int_A \xi^-(x, y, t). dA \right| = \text{evapotranspiration rate [L}^3\text{/T]}.$

$Q = \int_S \eta(x, y, z, t). ds = \text{net subsurface outflow rate [L}^3\text{/T]}.$

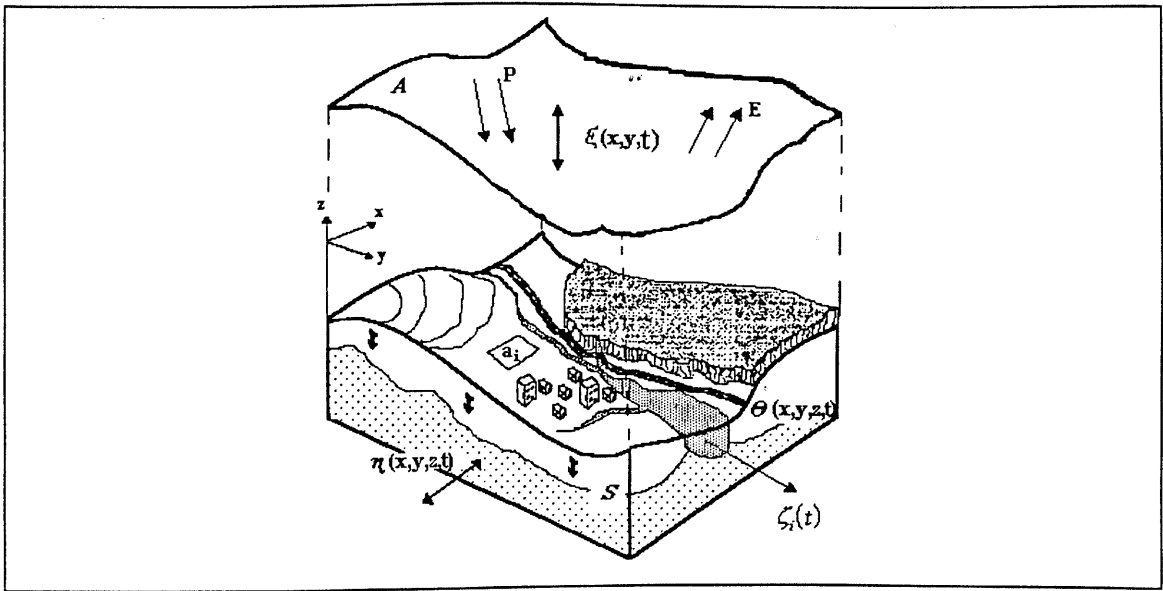


Figure 4.2 : Catchment as a distributed system.

Where : P - Precipitation.

E - Evapotranspiration.

Solving equation 4.1 requires dealing with time series of the four variables: S , P , E , Q , and possibly of other variables related to them. It is implicit in constructing a spatial hydrologic model that the properties of the system will be spatially variable, so a time series for each of the variables just described must be generated for each soil unit in the domain of analysis. Suppose that there are L spatial units, and that analysis on a single unit requires the definition of M variables for each of N time periods. The number of values to be determined is given by the product LMN , a number that can easily explode beyond the capabilities of available computer memory and reasonable computation times. Indeed, it appears that if the product LMN exceeds a limit of approximately 1 million, solution of the model will be computationally difficult. It

follows that in constructing a GIS hydrology model the first task is to determine what variables will be calculated on how many spatial units for a defined number of time periods. Construction of complex models must proceed by partitioning the total problem into a series of submodels that interact with a common database. It is the capacity of GIS for rigorously defining this database which makes possible complex models connecting various parts of the hydrologic cycle within a particular region. One begins with a GIS description of the region and then by modelling adds additional detail to the regional description concerning water flow and constituent transport.

The vertical flux of water through the surface A (Figure 4.2) consists of precipitation (positive) and evapotranspiration (negative) and is named as $\xi(x, y, t)$. Sample functions of this process at time t and point (x, y) are shown in Figures 4.3 and 4.4.

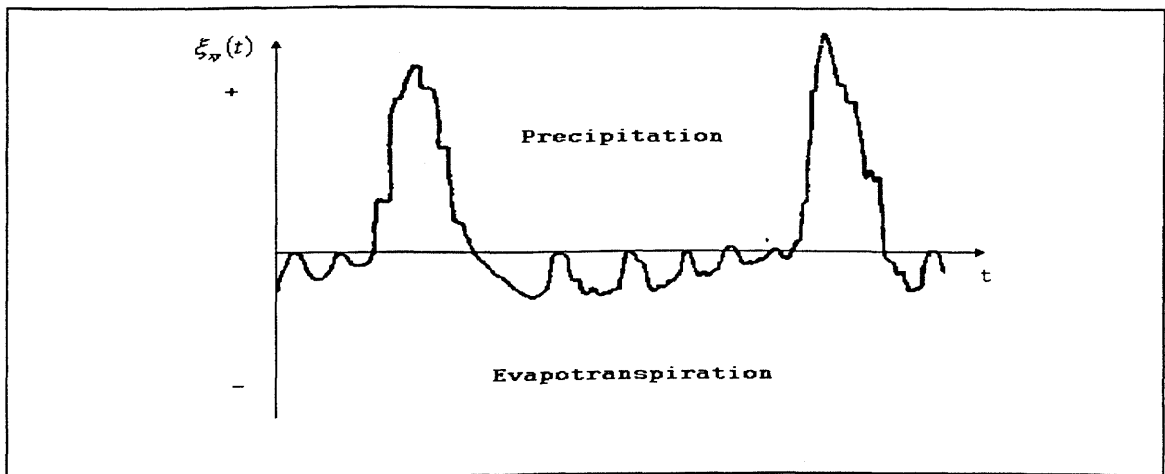


Figure 4.3 : Vertical flux of water at a point x, y .

The flux of water in a direction normal to the surface S is determined as $\eta(x, y, z, t)$. This function includes both ground water (saturated) flow and unsaturated.

The river flow includes both surface runoff and contributions from the saturated zone, and is designated as $\zeta_1(x, y, t)$. Also considered is the mass rate of sediment transports as $\zeta_2(x, y, t)$.

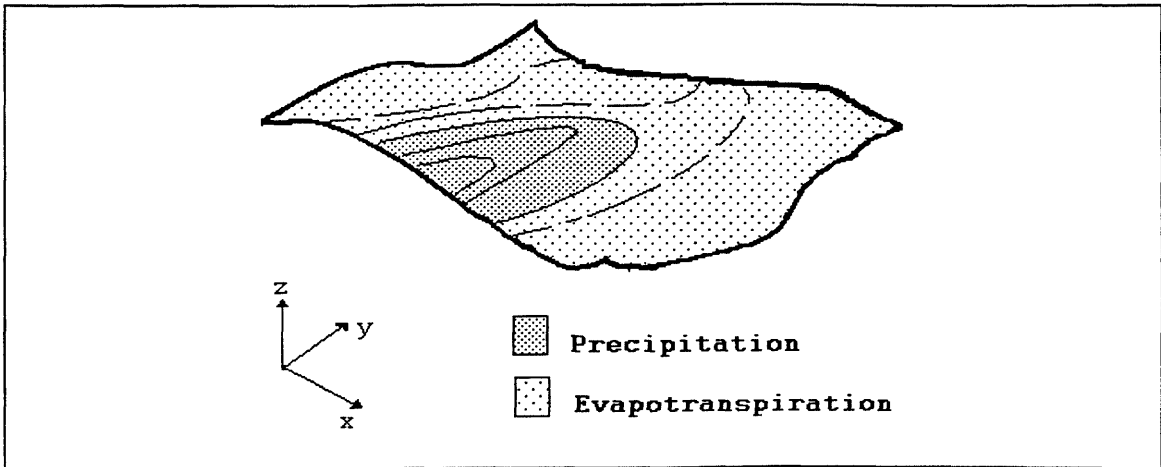


Figure 4.4 : Distribution of $\xi(x, y)$ for a time t over a catchment.

In the next section we present a theory to estimate the spatial distribution of runoff based on simple concepts and where all parameters involved have some physical meaning.

4.3 - Prediction of surface runoff in catchments

4.3.1 - Theory

Hydrological prediction is intimately dependent on the ability to characterise the spatial variability of soil water content. Soil water content and related soil properties exhibit extreme variability under distances of 100 m (Loague and Freeze, 1985). Several factors affect soil water content, including:

1. Soil characteristics: saturated hydraulic conductivity, porosity, and the occurrence of deep percolation and preferential flow.
2. Topography: local slope (measure of hydraulic gradients), specific catchment area (measure of the potential maximum water flux) and aspect (flow paths).
3. Land use: variation in surface cover and water use characteristics.
4. Weather: net rainfall.

In general, the dynamics of soil moisture patterns reflects the overall water balance and can be considered one of the most important variable defining freshwater availability. In order to define production areas we estimated the long-term average seasonal soil moisture dynamics as component of the water balance, based on long-term average climatic data, topography, land use and soil.

Topography-based models like TOPMODEL (Beven and Kirkby, 1979), TOPOG (O'Loughlin, 1981) and WET (Moore et al., 1993) provide a simple way to introduce lateral flow components into regional ecosystem models. TOPMODEL and WET are based on the assumption that local soil moisture dynamics strongly depends on the size of the upslope area (a) drained through a catchment point observed, the local surface topographic slope ($\tan \beta$) representing the hydraulic gradient for saturated water flow, and the downslope soil transmissivity (T).

The hydrological model used in this thesis is derived from that used in a study by Beven and Kirkby (1979). This model (TOPMODEL) can predict the soil water spatial variability on the basis of catchment topography and soil characteristics, using the variable source area concept of streamflow generation. This concept states that overland flow is produced only over a small fraction of the total catchment area. The land surface areas that produce overland flow are those that become saturated during precipitation events; they occur where the water table rises to land surface. Overland flow is produced when precipitation falls on a saturated land surface area or when subsurface flow returns to the land surface and flows overland (Dunne et al., 1975). The saturated land surface areas (called source or contributing areas) are variable in that they contract and expand over parts of the catchment. The dynamics of the saturated land surface area are controlled by catchment topographic and subsurface hydraulic characteristics and the state of wetness of the catchment. The state of wetness of the catchment changes over time as a function of the relative balance between input and output (see, for example, Figure 4.4)

We therefore need a simple physically based hydrological model which allows the prediction of the spatial pattern of runoff taking account of the effect of spatial heterogeneities of topography, soil type, land-use and rainfall.

Following Beven and Kirkby (1979) it is assumed that flow Q at any point i is controlled by a reservoir as:

$$Q_i = K_i \tan \beta e^{-S_i/m} \quad (4.2)$$

where : $\tan \beta$ is the local slope angle.

K_i is a soil transmissivity parameter.

m is a parameter dependent on the rate of change of conductivity with depth in the profile.

S_i is a soil storage deficit.

So, for a steady rainfall r , the flow at any point i is:

$$Q_i = Ar \quad (4.3)$$

where A is the area draining through point i per unit contour length. Combining equations 4.2 and 4.3, gives:

$$S_i = -m \ln \left(\frac{Ar}{K_i \tan \beta} \right) \quad (4.4)$$

or

$$\underbrace{-\frac{1}{m} S_i}_A = \underbrace{\ln \left(\frac{A}{\tan \beta} \right)}_B + \underbrace{[\ln(r) - \ln(K_i)]}_C \quad (4.5)$$

Equation 4.4 and 4.5 determines soil storage deficit (the amount of water that must be added to the soil to bring the water table to the surface), allowing prediction of saturated contributing areas for which $S_i \leq 0$, or areas where there is production of runoff. Where $S_i > 0$ the soil is partially unsaturated. Equation 4.5 consists of three parts: (1) a soil-water distribution function A , (2) a topographic distribution function B , and a soil-rain distribution function C .

The fraction of the land surface area that is saturated is multiplied by precipitation intensity (an observed input) to compute the amount of overland flow. High values of $\ln(A/\tan \beta)$ occur at locations where large upslopes areas are drained (high values of A) and where the local gravitational gradient is low (low value of $\tan \beta$).

The above model is primarily based on three assumptions:

1. Surface runoff is generated when precipitation falls on a saturated portion of the catchment ($S_i \leq 0$).

2. Subsurface flow at a given location in the catchment depends upon the hydraulic conductivity, soil depth, surface slope, and saturation deficit (the amount of water that must be added to the soil to bring the water table to the surface) at that point.
3. Saturated conductivity (K_s) decreases with depth in the upper soil layers, according to an exponential decay primarily due to greater abundance of macropores in the upper soil horizons.

These assumptions lead to the result that saturation deficit at a point depends, in part on the value of $\ln\left(\frac{Ar}{K_s \tan \beta}\right)$ (Equation 4.4) at that point. Because our interest is to capture an approximate spatial pattern of runoff production, parameter m , which is very difficult to obtain, is not considered, and K_s is substituted by parameter P (explained next section) that reflects interrelated factors (soil classification and land use) that influence infiltration volumes. The resulting equation, for position i,j is:

$$Q_{i,j} \cong \ln\left(\frac{Ar}{P \tan \beta}\right)_{i,j} \quad (4.6)$$

By combining the assigned soil hydraulic values for P with the derived topographic values of a and $\tan \beta$ together with precipitation values r we obtained the spatial distribution of equation 4.6. High values of the combined topography/soils/land use/precipitation index indicate the areas within a catchment most likely to saturate and produce surface runoff. These are topographically convergent, low-transmissivity areas; that is, they drain a significant upslope area of the catchment and have limited capacity to conduct water from the drained area in a downslope direction.

If we are considering computational questions, a fundamental distinction arises in the treatment of spatial units depending upon whether raster or vector data structures are used. In a raster data structure, a fine mesh of cells is laid over the landscape and all calculations are done for each cell. This approach, based on using digital elevation model cells as the spatial units, is very useful for certain kinds of hydrologic analysis. But the number of DEM cells within typical analysis regions is usually very large, typically 10,000 to 1 million, so the number of time periods that can be analysed is usually relatively small. Indeed, one may eliminate time as a dimension of the problem by working with seasonal average values of all the variables.

If time dynamics are to be considered, it is usually necessary to employ a vector data structure based on related points, lines and polygons. To describe the values on L spatial units of M computed variables in N time periods requires in concept a 3-D data structure but this can be reduced to a set of 2-D data structures in the following manner. The feature attribute table of the GIS coverage defines the geographic properties of the L spatial units and gives each a unique identifying number. This table has geographic attributes as its columns or fields for which the values in each spatial unit are displayed in rows. The values of a particular computed variable, such as soil moisture storage, S , can be defined by means of a related time table.

This arrangement of time vertically and space horizontally makes it easy to see by reading down a column the temporal sequence of values of a variable in a particular spatial unit. The key point in this description is that using object oriented data structures, a value in one table (the feature identification number) can be related to a field in another table instead of to a single value or a set of such values. For hydrologic modelling, the smooth treatment of time variation within GIS is a critical problem that has strongly limited what could be done in the past.

4.3.2 - Spatial variables

A simple approach to deal with the simplified theory presented above requires to eliminate time as a dimension by restricting the computation to mean flows. This implies that the time step of the soil moisture should be long enough for the effects of upslope inputs to be transmitted to the river. The analysis can then be constructed by using the cells of a DEM grid (see chapter 3) as the computational units. The evolution of more physically realistic models of hydrological processes has been largely based on experiments carried out under laboratory conditions or small uniform fields plot. Application of the principles learned under these conditions to larger catchments necessitates a simplification of the model process description and some method of dealing with land surface heterogeneity.

Basically equation 4.6 accounts for a water balance and flux for different points in a catchment. These points differ from each other in their values of P (land use and soil type), $A/\tan\beta$ (topography) and r (precipitation). So, using equation 4.6 calculations can be made for a number of points of different parameter values, accounting for the spatial variability of topography, land use, soil type and precipitation (Figure 4.1). This section describes the data sources for this approach and how they are produced

The parameter P of equation 4.6 uses the concept of curve number from the U.S. Soil Conservation Service (1986) to define the soil retention capacity of the unsaturated zone. Following Rawls et al., (1982) infiltration rates, shown in Table 4.1, are related to texture class, water capacity, and the Soil Conservation Service (SCS) hydrologic soil grouping (Table 4.2).

There are many interrelated factors that influence infiltration volumes and runoff. One empirical description for infiltration and runoff is the curve number method (US. Soil Conservation Service, 1986). At the start of precipitation P , the intensity of rainfall is usually less than the rate at which water is stored. As the soil and vegetation cover become saturated (storage S becomes filled), rainfall excess R increases. As rains continues to fall, the storage approaches a potential saturation value S' and the infiltration rate approaches zero. A possible relation over time is shown in Figure 4.5 and rainfall excess R is expressed as:

$$R = P - S \quad (4.7)$$

As shown in Figure 4.5, at saturation, the rate of rainfall excess is equal to the intensity of precipitation. So, a proportional relationship can be developed as:

$$\frac{S}{S'} = \frac{R}{P} \quad (4.8)$$

Using more than 3000 soil types divided into four hydrologic groups (Table 4.2) the SCS developed runoff curve number to estimate S' in the above equation. Runoff curve numbers can be estimated if the soil classification and the land use are known. Ragan and Jackson (1980) show an approach to estimate the land cover distribution needed in the curve number procedures utilising remotely sensed estimates of land use.

Texture class	Effective water Capacity (in./in)	Minimum infiltration rate (in./hr)	SCS hydrologic soil grouping
Sand	0.35	8.27	A
Loamy sandy	0.31	2.41	A
Sandy loam	0.25	1.02	B
Loam	0.19	0.52	B
Silt loam	0.17	0.27	C
Sand clay loam	0.14	0.17	C
Clay loam	0.14	0.09	D
Silty clay loam	0.11	0.06	D
Sandy clay	0.09	0.05	D
Silty clay	0.09	0.04	D
Clay	0.08	0.02	D

Table 4.1 : Hydrologic soil properties classified by soil texture.

Source : Rawls et al., (1982).

Soil Group	Description
A	Lowest runoff potential
B	Moderately low runoff potential
C	Moderately high runoff potential
D	Highest runoff potential

Table 4.2 : SCS Hydrologic soil groups.

Source : U.S. Soil Conservation Service (1986).

Remotely sensed data obtained from Landsat images cannot be used to classify the land use with a refined set of classes. Generally, a coarser set of categories must be used. Ragan and Jackson (1980) tested the use of this approximation by comparing it (5 classes of land use) to conventional estimates and found that for their catchment, it did not have a significant effect.

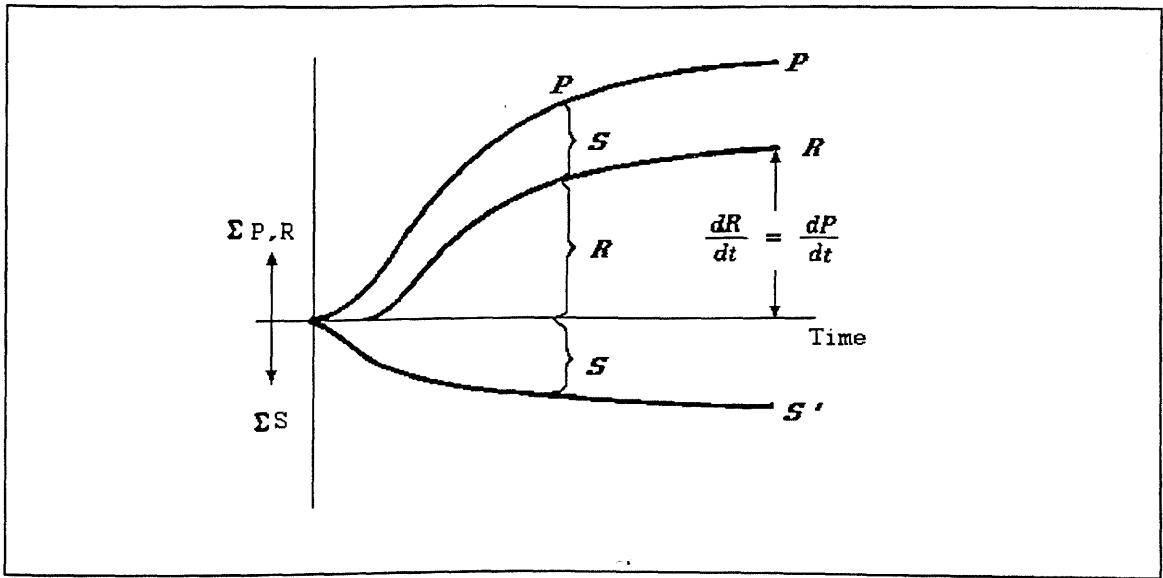


Figure 4.5 : Time variability of Precipitation, Rainfall excess and Storage.

In Table 4.3 runoff curve number is show in terms of soil type (Tables 4.1 and 4.2) and land use (similar to Ragan and Jackson (1980)). The parameter P (equation 4.6) is represented by:

$$P = \left(\frac{1}{CN} \right) * 100 \tag{4.9}$$

where CN is the curve number obtained from Table 4.3. Table 4.4 shows the corresponding values of parameter P using the above approach.

Curve Number (Soil Conservation Service)				
Land Use	Soil type			
	A	B	C	D
Forest land	25	55	70	77
Cultivated land	62	75	83	87
Pasture	36	60	73	78
Bare ground	72	82	88	90
Urban land	82	89	92	93

Table 4.3 : Curve Number (Soil Conservation Service).

Parameter P				
Land Use	Soil type			
	1-A	2-B	3-C	4-D
1- <i>Forest land</i>	4	1.8	1.4	1.2
2- <i>Cultivated land</i>	1.6	1.3	1.2	1.1
3- <i>Pasture</i>	2.7	1.6	1.3	1.2
4- <i>Bare ground</i>	1.3	1.2	1.1	1.1
5- <i>Urban land</i>	1.2	1.1	1.0	1.0

Table 4.4 : Parameter P_{ij}

The values of this parameter simply isolate the effect of a combination of land use/soil type that will be used to compute the possibility of runoff production using equation 4.6. This is easily done, by any GIS, using the cells of a DEM grid for each cover type/soil combination

The areal distribution of rainfall r in equation 4.6 is determined from rain gauge data using interpolation procedures.

Finally, the terms of the topographic based parameter $A/\tan\beta$ from equation 4.6 are obtained using the procedures presented in Chapter 3. This topographic index reflects the disposition of water to accumulate at any point in the catchment (parameter A) and the tendency for gravitational forces to move that water downstream (parameter $\tan\beta$). The computed values of the above topographic parameters depend upon the flow vectors (aspects) of DEM data and the grid resolution used. Usually flow vector analysis is carried out using a single flow direction (using eight possible directions as presented in Chapter 3) based on the local direction of the greatest slope (Band, 1986; Jenson and Domingues, 1988).

Following Quinn et al., (1991), with a grid size of 50 m or coarser, the single flow direction approach may give rise to local inaccuracies with flow in parallel lines rather than the more natural dendritic pattern seen in nature (Figure 4.10). In this thesis an algorithm (equation 4.6) is employed, which allows flow to be distributed to multiple nearest neighbour cells, as grid size is relatively coarse (100m in case study), using methods similar to those proposed by Quinn et al., (1991) and Freeman (1991). The runoff produced in each cell (equation 4.6) is drained to each downslope cell in proportion to the gradient of each downslope flow vector, so the proportion of

runoff to be assigned to multiple downslope nearest neighbours is determined on a slope weighted basis. The results of this approach are shown in Figure 4.12, where a more natural routing pattern is generated. These concepts are implemented by a program in the Appendix.

4.3.3 - Application and interpretation

In this section I show some results for illustrative purposes, where all the examples are chosen arbitrarily and not supported by experimental evidence (similar to Chapter 3) and the spatial pattern of potential runoff generation produced by Equation 4.6 and using the multiple flow direction algorithm in Sinos catchment.

An important feature of the approach described above is that the input parameters are derived from available information; land use (remotely sensed data), soil type (soil map), topography (topography maps) and rainfall (rain gauge data).

The soil type data may be prepared from a state-wide soils map at a scale 1:250,000 by grouping soil types according to hydrologic classes shown in Table 4.1. The polygons of the resulting hydrologic soil types are digitised and converted into gridded form. This procedure results in four hydrologic soil classes as represented in Figure 4.6.



Figure 4.6 : Example of a digital representation of soils data.

The areal distribution of rainfall can be determined from rain gauges (point data), within the catchment, using any interpolation technique to estimate the values of rainfall on a grid. Figure 4.7 shows the rainfall data distributed in a gridded form.

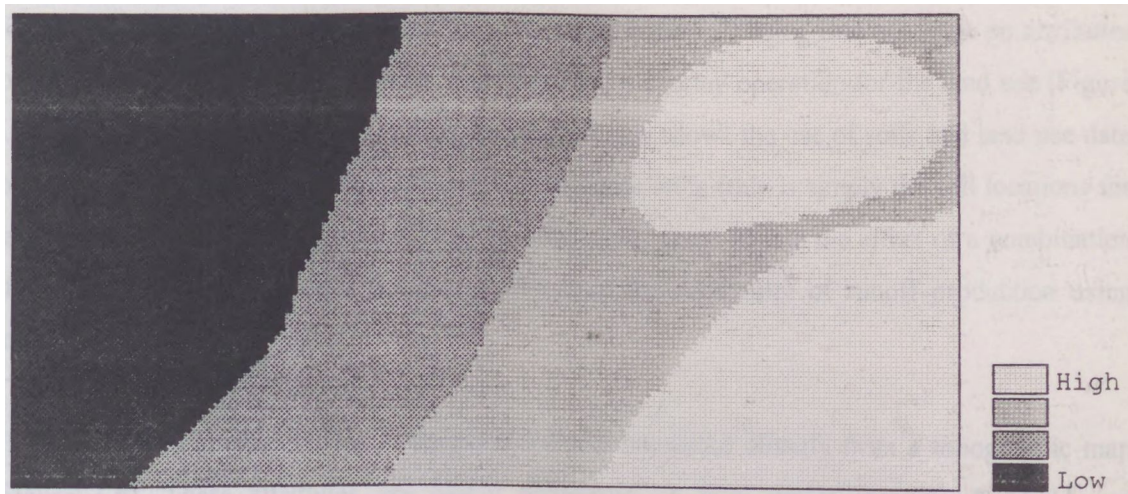


Figure 4.7 : Example of distributed rainfall data.

The land use data is also distributed in the same gridded form as the soils and rainfall data sets. This data set is derived from multispectral scanned data from LANDSAT TM satellite for estimating the land use distributions needed for applying the land classes in Table 4.4. Computer programs are widely available in image processing systems and most grid based GIS (see ERDAS, GRASS, etc.) for analysing these data. Image processing techniques (Richards, 1986) are used to transform the satellite digital data into a digital representation of land classes (Figure 4.8).

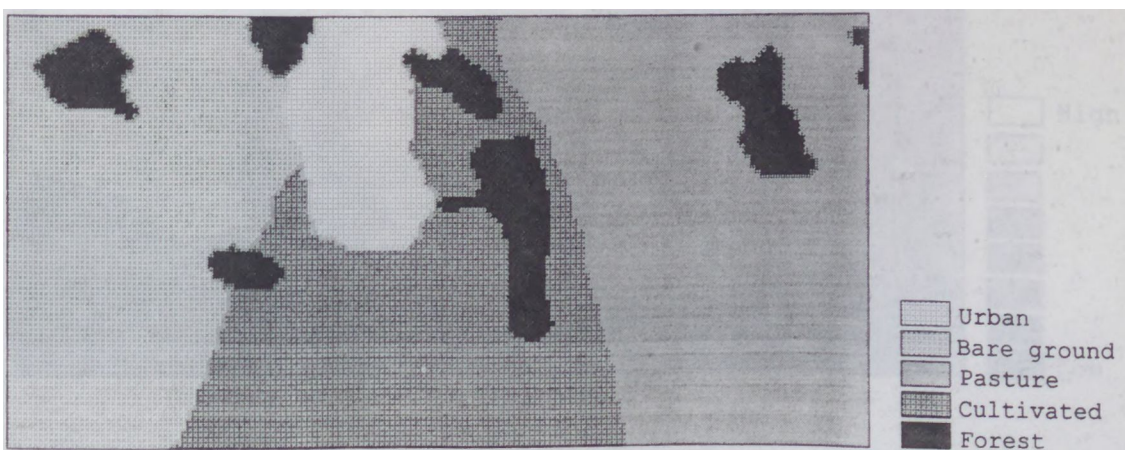


Figure 4.8: Example of a digital representation of land use data.

Two layers of data sets (land use and soil type) were input into the curve number procedure (Table 4.4) to determine the possibility of generating direct runoff on a grid element-by-element basis. This operation is done using an overlay operation in the GIS. This operation combine two discrete maps (land use and soil type) into a third (parameter P) using Boolean logic on attributes to yield a new map. Figure 4.9 shows the results of an overlay operation for the land use (Figure 4.8) and soil type data sets (Figure 4.6). Figure 4.9 also shows the use of soils and land use data to sub-divide the catchment into homogeneous response units (this is simply the cell locations for each cover type/soil combination). These 'homogeneous' areas isolate the effect of a combination of land use/soil type that will be used to compute the possibility of runoff production using equation 4.6.

The topographic attributes used in equation 4.6 are calculated directly from a topographic map (Figure 3.6). These attributes are highly dependent on flow vector (aspect). Fairfield and Leymarie (1991) observed that using the algorithm that allows water flow from a cell to only one of eight nearest neighbours, based on the direction of steepest slope, tends to produce flow in parallel lines along preferred directions. Figure 4.10 show the upstream catchment areas obtained by the use of the eight nearest neighbours' algorithm; the erroneous parallel flow lines pattern can also be seen . Figure 4.11 shows the topographic parameter of equation 4.6 ($\ln(A/\tan \beta)$) using the multiple downslope nearest neighbour algorithm (Quinn et al., 1991) where the flow lines more accurately reflect the true slope and aspect.

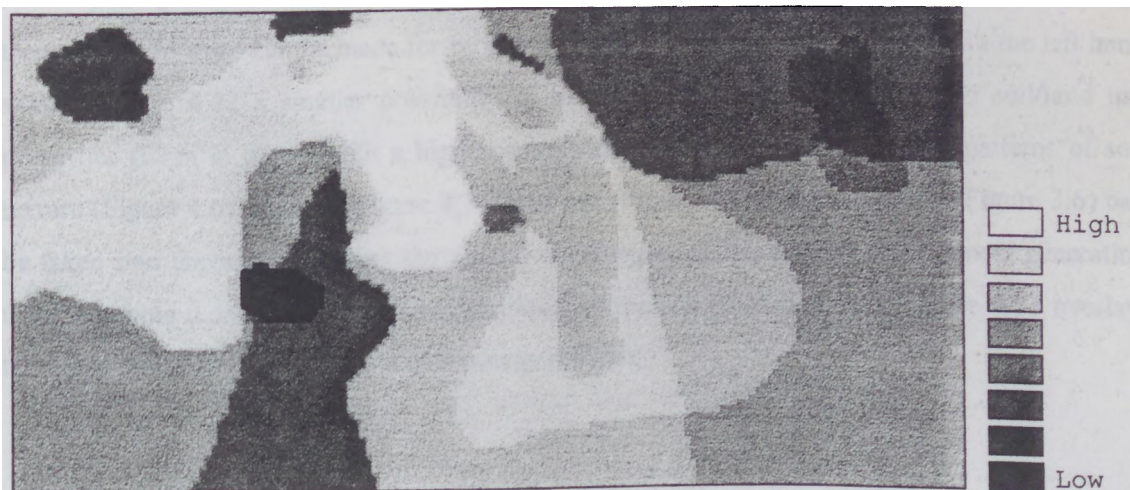


Figure 4.9 : Possibility of runoff generation based on soil type and land use.

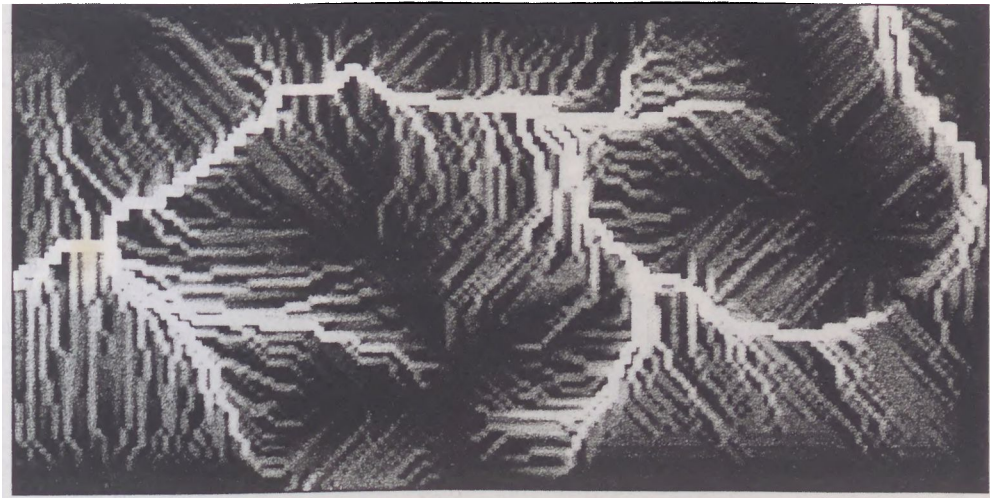


Figure 4.10 : Upstream catchment area produced by the eight nearest neighbours' algorithm. (Brighter grey levels - larger tendency of water to accumulate).

Figure 4.12 shows the full implementation of equation 4.6 where the use of soil, land use, topography and rainfall data is used to subdivide the catchment into homogeneous response units of runoff production. This concept provides a mechanism for routing flow contributions from upslope cells and predicting re-infiltration as flow moves across subsequent elements. This implies that flux and water balance calculations are made for all cells in the catchment.

Once the disposition of water to accumulate at any point in the catchment (parameter A) and the tendency for gravitational forces to move that water downstream (parameter $\tan\beta$) is calculated then a water balance can be made for rainfall and soil type/land use combination. In the left hand side of Figure 4.12 a smaller possibility of runoff production is visible due to soil/land use properties (Even in places with a high accumulation of water). Clearly, actual patterns of soil texture (Figure 4.6), rainfall (Figure 4.7), land use (Figure 4.8) and topography (Figure 3.6) can be taken into account to predict the spatial distribution of the possibility of runoff generation using a simple (conceptually and computationally) method (Equation 4.6). Figure 4.12 overlay, two more maps: catchment area and drainage network.



Figure 4.11 : Topographic parameter of equation 4.6 ($\ln(A/\tan \beta)$) using the multiple downslope nearest neighbours' algorithm.
(Brighter grey levels = higher surface runoff; and white = flat areas).

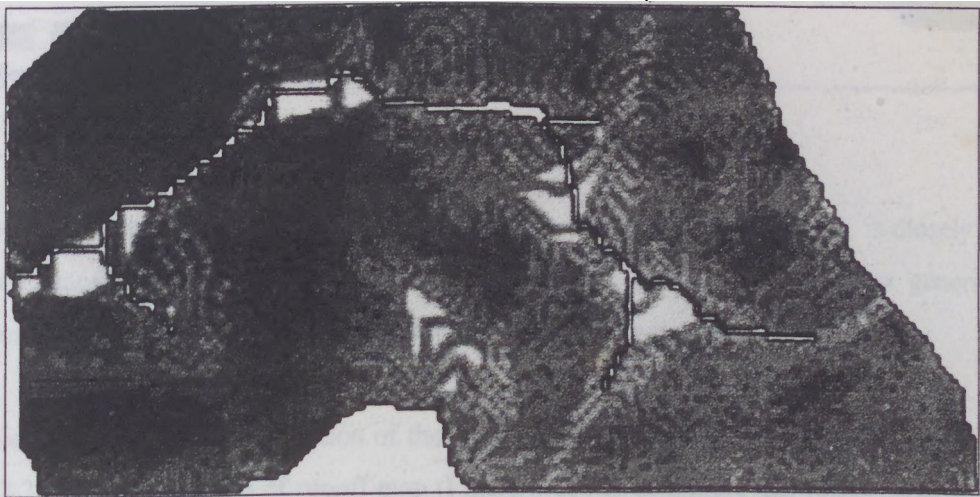


Figure 4.12 : Full implementation of equation 4.6 using the multiple downslope nearest neighbours' algorithm within the catchment.
(Brighter grey levels = higher surface runoff).

Figure 4.13 shows the pattern of potential runoff generation in Sinos catchment produced by Equation 4.6 and using the multiple flow direction algorithm. The runoff effect gives a realistic pattern of accumulating area (see Chapter 3) on the hillslope portion of the catchment but once in

gullies, minor tributaries and valley bottoms, there is a tendency for the cumulative area to spread, giving the impression that these channels have large floodplains.

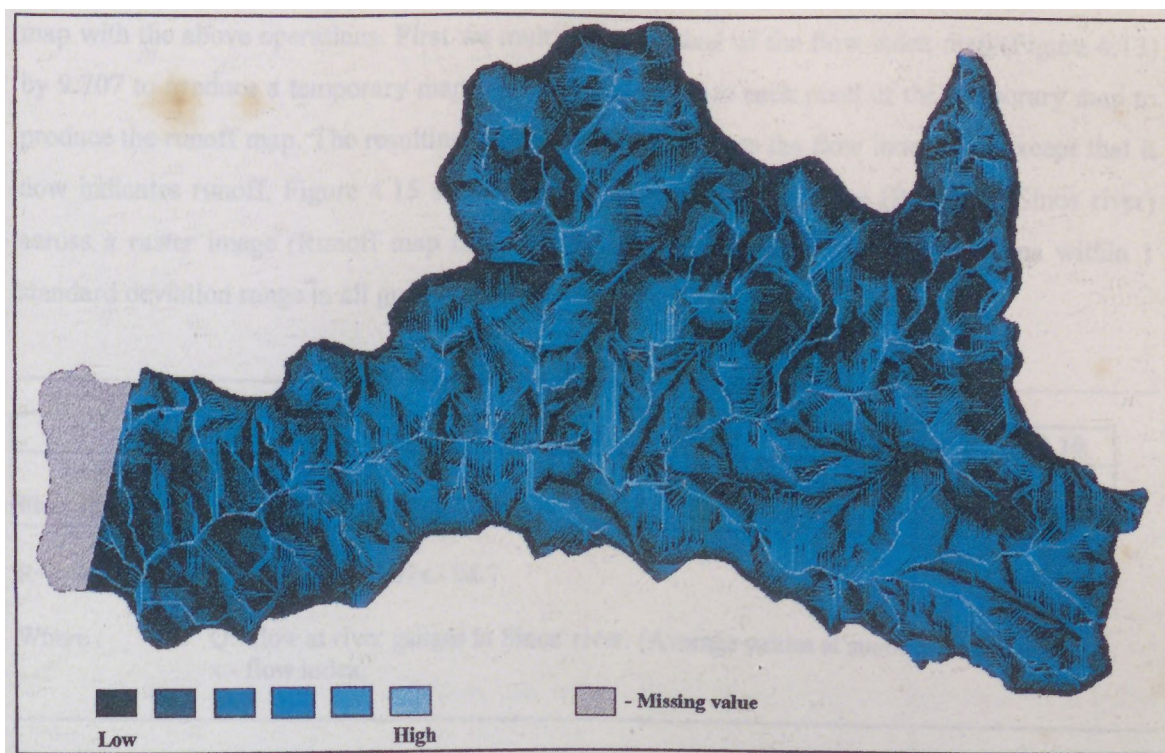


Figure 4.13 : Potential of runoff generation in Sinos catchment.

The potential of runoff generation in Sinos catchment, as shown in Figure 4.13, is closely related to actual runoff. As a first approximation, the runoff can be related to the index generated by Equation 4.6 via an empirical equation as a linear regression equation.

Therefore we can use the distribution of the stream gauges in Sinos catchment (Figure 2.11 and Table 2.2) and our potential of runoff map (Figure 4.13) to determine this relationship (i.e., as a regression model) and then create a runoff map. The first step is to determine the relationship between stream gauges data and potential of runoff. We have data from 10 stream gauges within Sinos catchment, as shown in Table 4.5. To find the values of flow index (with Figure 4.13 on the computer screen) we have to move a mouse to the same position of the stream gauges (Figure 2.11) and read the data value. Once we finished creating the pair of values file we can make the regression analysis. The graph of the relationship and it's equation are shown in Figure 4.14 and Table 4.5.

The equation of Table 4.5 is saying that we can predict the runoff (Q), for this time of the year, at any location within Sinos catchment if we take the flow index data (Figure 4.13), multiply it by 9.707, and add -94.7 to the result. In order to have the runoff map, we need to create a second map with the above operations. First we multiply each pixel of the flow index map (Figure 4.13) by 9.707 to produce a temporary map. Now we add -94.7 to each pixel of the temporary map to produce the runoff map. The resulting map look very similar to the flow index map except that it now indicates runoff. Figure 4.15 shows the runoff values along a line (Profile of Sinos river) across a raster image (Runoff map of Sinos catchment) The actual estimate remains within 1 standard deviation range in all guages in Sinos catchment.

	# 1	# 2	# 3	# 4	# 5	# 6	# 7	# 8	# 9	# 10
JAN	44.8	39.8	39.1	37.3	35.9	35.5	29.8	22.2	18.3	2.5
Flow index	14	14	13	13	14	13	13	13	12	10

$R^2 = 0.828253$ $Q = 9.707x - 94.7$

Where : Q - flow at river gauges in Sinos' river. (Average values at summer season).
 x - flow index.

Table 4.5 : Results of a linear regression between the runoff indices and flow values.

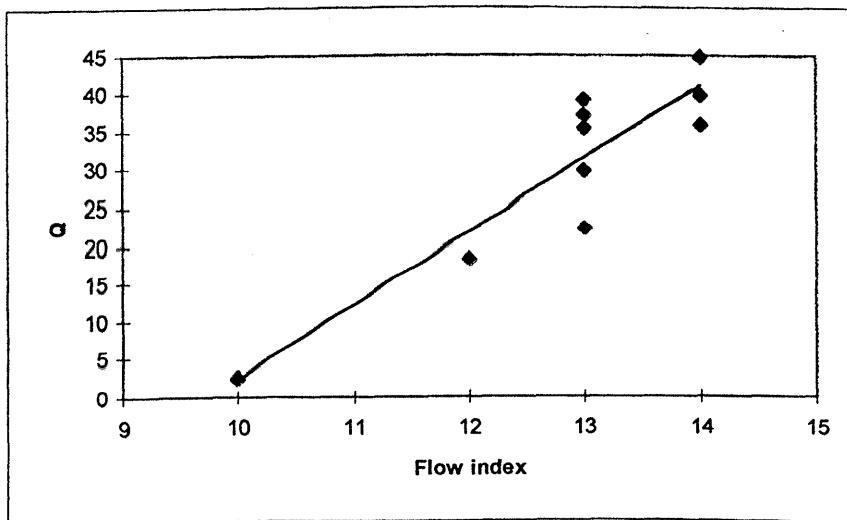


Figure 4.14 : Predicted and observed runoff indices ($Q = 9.707 \times \text{Flow index} - 94.7$).

Despite good results presented in Table 4.5 and Figures 4.14 and 4.15, care must be exercised in applying static indices like those described in this chapter (in particular Equation 4.6) to predict the distribution of a dynamic process like soil water content, especially when changes occur in the

areas of saturation (source or contributing areas). Because of fluctuating rainfall intensities and the short duration of rainfall events compared to the travel time of subsurface throughflow, the subsurface flow regime in a catchment, like Sinos, rarely reaches steady state.

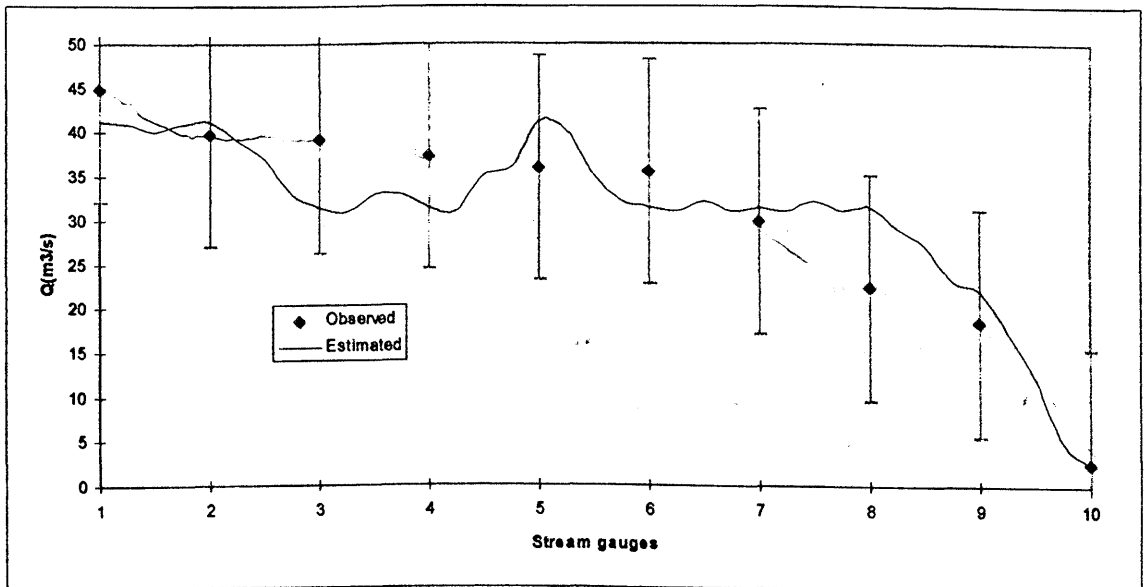


Figure 4.15 : Observed, estimated and one standard deviation of January mean flow values in Sinos Catchment.

Because of the difficulties associated with direct measurement or estimation of the spatial variability of soil properties (K_i in Equations 4.4 and 4.5) we have substituted K_i by parameter P_i (Equation 4.6) that reflects interrelated factors (soil classification and land use) influencing infiltration volumes. We found that this parameter together with topographic attributes and rainfall (Equation 4.6) can characterise the water distribution in Sinos catchment. Nevertheless, this approach must still be validated.

There is a need to include a measure of uncertainty in predicting surface runoff quantities due mainly to the uncertainty of the various above factors and the various mathematical definitions (simplifications) used in hydrological models. An iterative technique is proposed for the simulation of this uncertainty in Chapter 9.

4.4 - Summary

A standard method is not available to model the runoff process, although similar equations are used in some models. When modellers assemble equations to form a model, they must clearly understand the purpose and eventual use of the model so the greatest benefit can be obtained from the model's results. Using equations that are the best available at the time of model development for the particular purpose of the models is essential if the model is to be used as a management tool by eventual users.

A simple physically-based hydrological model is derived here using the concepts of TOPMODEL and curve-number (S.C.S.) by putting together the information from these models into one convenient format (equation 4.6). This procedure was designed to isolate areas with homogeneity such as soil type, land use, topography and rainfall data to form hydrologic response cells distributed over the catchment. A GIS was used to partition the Sinos catchment into areas with such homogeneity.

A geographic information system (GIS) provided information for a regression analysis that was used to identify areas of potential of runoff generation in Sinos catchment. The physical characteristics of the catchment were used to produce the flow index (potential of runoff) and then used as independent variable in the regression analysis.

While the approach does not yield estimates of discharges as accurate as those obtained by direct measurement, the use of GIS-generated information for a regression model provides a method that generally defines areas that might constitute sources of runoff in rivers.

The purpose of this technique is to provide a means to simulate the spatial distribution of surface runoff, for a given rainfall, in an ungauged catchment on the basis of soils, land use and topographic features. Discharge data were not available for all cells, therefore direct experimental verification of the technique was not possible. Comparison between the simulated values in some sections of the drainage network and recorded flow were made in this Chapter.

5.Critical areas for non-point source pollution

5.1 - Introduction

Historically, water pollution policies have focused on control of municipal and industrial sources. Usually certain potential pollution sources have been considered as natural and generally uncontrollable (Browne and Grizzard, 1979). Sources of this type include precipitation, drainage from urban areas, runoff from forests and pasture lands, return irrigation flows, decaying vegetation, and waste from animals (Wanielista et al., 1977). For example, the quality of surface water that flows off an agricultural catchment is affected by chemicals added to the soil as well the cropping practices. In this case, the challenge is to organise management programs that reduce the potential for pollution while achieving optimum yields for farmers.

To identify pollution problem areas within a catchment, planners must define the location of critical areas. The strategy applied here combines land use and runoff (topography, soils, land use and rainfall) factors. Once these areas are identified specific actions to improve water quality can be developed for each targeted area.

The purpose of this chapter is to summarise available information on the characteristics and relative magnitude of certain non-point sources entering surface runoff and to facilitate the identification of these non-point sources within a catchment. Such identification is based on surface runoff (see Chapter 4), soils and land use, as shown in Figure 5.1. Once these critical areas have been identified they can be targeted, and specific actions developed to improve water quality.

Figure 4.2 (see Chapter 4) also represents an idealised hydrological routing of pollutants through the environment showing transport of pollutants in four distinctive categories:

- Atmospheric transport from air movement, wind erosion, rain and snow precipitation;
- Overland flow transport resulting from rain and surface runoff, erosion and sediment transport;
- Infiltration and contamination of ground water, adsorption and transformation of pollutants in soil; and
- Channel flow that represents the longest route of pollutant movement from its entry to a stream through its passage to a lake or ocean boundary.

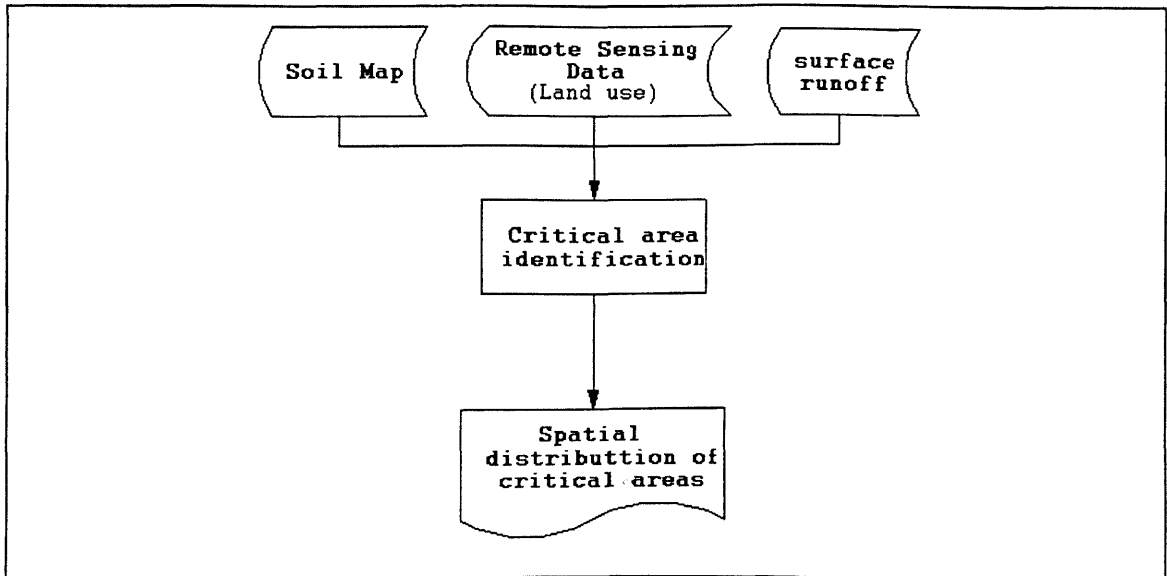


Figure 5.1 : Flow diagram showing the calculations of the spatial distribution of critical areas for non-point pollutant production.

The specific point at which a pollutant enters the hydrological cycle depends: (a) on the type of source and its location; and (b) on the form in which the pollutant occurs (Haith, 1976). According to Harms et al., (1974) some pollutants are highly soluble (like nitrate), whereas others (like phosphorus) are readily adsorbed by soil particles and relatively immobile. Since surface runoff can move and carry soil particles, it can transport non-soluble matter in large concentrations. For this reason, transport by surface runoff (soluble pollutant) and sediments (sediment-attached pollutant) are often at the core of non-point source pollution concerns.

Analysing an area a_i in Figure 4.2, it could be considered that a substance i is added at some rate per unit area (agricultural operations as an example). After some time, the substance added could be transported to the drainage network and could appear in river flow at a concentration $c_i(t)$. The mass rate of transport of substances ζ_i out of the catchment is:

$$\zeta_i = \rho \cdot c_i(x, y, t) \cdot \zeta_1(x, y, t) + \psi[\zeta_2(x, y, t)] \quad (5.1)$$

Where : ρ is density of water.

$\psi[\zeta_2(x, y, t)]$ represents the amount of substance carried by sediment.

$\zeta_1(x, y, t)$ characterises the rate of transport of water out of the catchment.

$\zeta_2(x, y, t)$ identifies the rate of transport of sediment out of the catchment.

For an idealised model, it can be assumed that pollutants enter the drainage network directly from point sources or indirectly by overland or ground water flow discharges (non-point sources). During dry weather periods, these non-point sources arise from ground water discharges, and during storm events, runoff is the single largest contributor of non-point source pollution (Meadows et al., 1978).

5.2 - Characteristics of non-point sources

Water quality is usually expressed in terms of the concentrations of particular constituents. Water pollution occurs when the concentration of a particular substance in water is sufficient to produce harmful effects for the intended use of that water (Browne and Grizzard, 1979).

The principal sources of pollutants can be divided into two categories : (a) point sources and (b) non-point sources. The point sources are those that are considered to have a well-defined point of discharge (which is usually continuous). The two principal point source groupings are : (a) municipal point sources that result in discharges of treated and partially treated sewage and (b) industrial discharges. Non-point source effects on water quality begin with precipitation, which itself is impure and may vary in quality from one area to the next (Browne and Grizzard, 1979). However, land use has a much greater effect on water quality and non-point sources can generally be classified as rural and urban.

Rural non-point sources can contribute major quantities of water pollutants. Agricultural pollutants have their origins in fertilisers, pesticides and animal wastes but several other factors also affect the water quality such as soil type, climate, land use, management practices, topography of the area, animal feed lots, cultivated areas and pasture lands. Generally, the greater the extent of human utilisation and/or animal density, the greater the amounts of pollutants introduced.

Urban non-point sources may contain many pollutant materials including heavy metals, nutrients, pesticides and bacteria. The sources of these pollutants are also widely varied, ranging from birds such as pigeons and solid waste such as litter to vehicle pollutants and sediment derived from

construction activities (Loehr, 1974). All these are widely varied in both quantity and aerial distribution (Loehr, 1974).

Wanielista et al., (1977) using several references, described the magnitude of urban and rural non-point sources (Table 5.1). Table 5.1 also illustrates the extreme variability (large range) in the reported data and indicates that the variability of such information precludes site-specific studies to identify loading rates. However, the extent of field work depends on the site conditions. In addition, the receiving surface waters have varying degrees of pollutant assimilative capacities. Therefore, water quality responses to the loading rates (Table 5.1) will most likely differ with the location. Consequently, instrumentation to collect water quality samples and the loading rates during conditions such before, during, and after precipitation would be valuable but is not available for this research.

Land Use		BOD ₅	Suspended Sediments	Phosphorus	Nitrogen
Urban	R	53-82	728-4794	3.2-18	1.0-5.0
	A	75	1700	8.5	2.0
Pasture	R	6-17	11.8-840	2.5-8.5	0.24-0.66
	A	11	840	5.3	0.30
Cultivated	R	4-31	286-4200	15.0-37.0	0.18-1.62
	A	18	4200	26.0	1.05
Woodland	R	4-7	45-132	2.4-5.1	0.01-0.86
	A	5	98	3.1	0.10

Table 5.1 : Loading rates (Kg.ha⁻¹.y⁻¹) and land use.

Source : Wanielista et al., (1977).

Where: **R** - Range.

A - Average.

The data presented in Table 5.1, aid in understanding the variability of pollutants in rural and urban land areas and it is used in this thesis with this objective. The time of year also plays a role in the amount of surface pollutants (Duda, 1982). The control of non-point sources is usually based on the relative importance of specific sources (Table 5.1) in specific locations, and the extent to which such sources are technically controllable (Loehr, 1974).

5.2.1 - Estimating sediment loss

A major problem facing many developing countries is clearing of forests to increase the availability of agricultural land to provide food for a continually increasing population. If land use changes over an area, the rates of soil loss change as well. While erosion of soil from land and its transportation by water and subsequent deposition elsewhere is a normal process that occurs naturally without any human activities, crop management practices (especially improper ones) accelerate this process. Sediment from soil erosion is often considered the greatest single pollutant of surface waters (Zeid and Biswas, 1990). Sediment is also a carrier of many chemical pollutants. Several mathematical models have been developed to simulate erosion processes. Some models are based on hydraulic and sediment transport theory, while other models are empirically developed. Several assumptions and limitations are inherent in most of these models.

The best known empirical sediment transport model is the Universal Soil Loss Equation (USLE) developed by Wischmeier and Smith (1958). The USLE combines major erosion factors in a predictive relationship:

$$A = 2.24.R.K.LS.C.P \quad (5.2)$$

Where: A = average annual soil loss ($\text{t}\cdot\text{ha}^{-1}$).

R = rainfall and runoff erosivity index (dependent on mean annual and monthly rainfall data). It varies from 20 to 50 in the western US to more than 300 in the south-eastern US.

K = soil erodibility factor (determined from field samples and/or published pedological information). It can vary from 0.0 to 0.70 depending upon soil properties.

LS = topographic factor for length and slope (derived from measurements of slope length and angle from topographic maps). Dimensionless factor.

C = crop cover and management factor (determined from information on vegetation type and cover). C values range from 0.001 for well managed woodland to 1.0 for tilled and continuous fallow cropland.

P = soil conservation factor determined for the conservation practices of contouring, contour strip-cropping and terracing, and contour listing or ridge planting. Dimensionless factor

The constant 2.24 converts A to *SI* units of $\text{t}\cdot\text{ha}^{-1}$.

The USLE was designed to predict long-term average soil losses. Specific-year losses may be lower or greater than the long-term annual averages because of variability in the number, magnitude and frequency of the factors involved. Therefore, soil losses computed by USLE must be accepted as estimates rather than as absolute values (Wischmeier and Smith, 1978). Williams and Berndt (1977) recognised that erosion from large catchments is usually more related to the transportation processes than to soil detachment. They proposed a modification to the USLE (Modified Universal Soil Loss Equation - MUSLE) in which the rainfall factor *R* was eliminated and replaced by a factor composed of the runoff volume and the peak runoff rate, as follows:

$$Y = 6.95(Q \cdot q_p)^{0.56} (K \cdot LS \cdot P \cdot C) \quad (5.3)$$

Where: *Y* = Sediment yield from an individual storm (ton).

Q = Storm runoff volume (m^3).

q_p = Peak runoff rate (m^3s^{-1}).

Stocking (1981) developed the Soil Loss Estimation Model for Southern Africa (SLEMSA) as an alternative for the USLE in this region. The topography sub-model of the equation is an adaptation of the slope factor expression of the USLE, using slope gradient and slope length. SLEMSA also uses seasonal rainfall energy, a soil erodibility factor and the percentage rainfall energy intercepted by crop. The limitation of SLEMSA is that the equation was developed using only data from Zimbabwe. Also, soil erodibility and crop data are given for soils and crops from this region only.

Flacke et al., (1990) proposed the Differentiated Universal Soil Loss Equation (DUSLE), as a version of the USLE modified for mid-European conditions, combined with a digital elevation model, which has the structure of a triangulated irregular network (TIN). The slope length/slope gradient factor *LS* is differentiated for an application on complex slope geometries, with specific consideration given to catchment convergence and divergence.

Many of the parameters required to run USLE or its derived equations are geographic in character and are obtained from geographic sources such as soils maps, topographic maps, and land use maps derived from remotely sensed data. Modellers frequently extract these spatially

organised data, only to input them to a non-spatially organised model (USLE and MUSLE as an example). In the process of translating information about slope, slope length, soil types, land use, basin characteristics, and meteorological characteristics from spatial sources to a model, the geographic character is removed from these primary data.

In contrast, a Geographic Information System (GIS) can manipulate primary data in a spatially structured environment. In this thesis I use a GIS to predict sediment pollution potential which maintains the spatial structure of the original data. This procedure will be explained in later section of this chapter.

5.2.2 - Nutrient loss from non-point sources

The use of chemical fertilisers is necessary in most soils to optimise crop yields and enhance vegetative growth. An overview of fertiliser uses and water quality problems has been published by Zeid and Biswas (1990).

Nitrogen and phosphorus are the nutrients of most concern with respect to water pollution (Harms et al., 1974). Other nutrients and impurities in commercial fertilisers are not currently regarded as potential pollution problems (Loehr, 1974).

Transport of nutrients to the stream is a complex, dynamic process. Fertiliser nitrogen can be applied in one of several chemical forms, which may in turn be altered by soil micro-organisms. Nitrate fertiliser is water soluble and is readily leached or transported in surface runoff. Ammonium nitrogen is adsorbed to soil particles and is not readily transported by surface runoff. Urea is highly water soluble and readily susceptible to runoff (Sievers et al., 1970).

Phosphorus likewise is generally available in highly insoluble form being moved primarily on soil particles. The P concentration is higher in sediment than in the original soil because phosphorus is associated with finer soil particles (Sievers et al., 1970). Nitrogen and phosphorus can be leached from leaves and dead vegetation. While some of these leached nutrients can be transported to rivers, much is returned to the soil (Rouquette et al., 1973).

According to McElroy et al., (1976) the principal method for estimating nutrient and organic matter loads consists of:

- Calculating sediment yields

- Multiplying sediment yields by factors denoting nutrient concentrations in the soil and selective enrichment in the erosion process.
- Estimating nutrients carried in runoff.

So, available nutrient yield is the sum of runoff carried nutrients and the nutrient attached to sediment. For instance the total nitrogen yield N_T ($\text{kg}\cdot\text{ha}^{-1}$) can be calculated as follows (McElroy et al., 1976):

$$N_T = N_E + N_{Pr} \quad (5.4)$$

Where: N_E = total available nitrogen from erosion (solid-phase losses of pollutant in $\text{kg}\cdot\text{ha}^{-1}$).

N_{Pr} = nitrogen from rainfall-runoff process (dissolved losses of pollutant in $\text{kg}\cdot\text{ha}^{-1}$).

The available nitrogen from erosion N_E can be computed from:

$$N_E = a \cdot f_N \cdot S \cdot C_N \cdot r_n \quad (5.5)$$

Where: a = a dimensionless constant.

f_N = decimal fraction of nitrogen that is available.

S = soil loss or sediment yield ($\text{tons}\cdot\text{ha}^{-1}$).

C_N = concentration of nitrogen in soil ($\text{mg}\cdot\text{kg}^{-1}$).

r_n = nitrogen enrichment factor in sediment.

The nitrogen from runoff N_{Pr} is calculated by:

$$N_{Pr} = A \cdot \frac{R}{P} \cdot K_N \cdot b \quad (5.6)$$

Where: A = surface area of source (ha).

R = runoff (mm).

P = precipitation (mm).

K_N = rate of deposition of atmospheric nitrogen in precipitation.

b = attenuation factor.

Suggested values for the factors and constants needed to calculate total nitrogen yield using equations 5.4, 5.5 and 5.6 were published by McElroy et al. (1976), for the conditions in the U.S.A.

Analogous loading functions can also be written for phosphorus and other pollutants; however since phosphorus is carried almost entirely on sediment, the runoff component is negligible so that a single expression, analogous to Equation 5.5 is sufficient. The loading function for available phosphorus from sediment P_E is:

$$P_E = a \cdot f_p \cdot S \cdot C_p \cdot r_p \quad (5.7)$$

5.2.3 - Other losses from non-point sources

Whipple et al., (1978) detected significant amounts of heavy metals in the urban runoff collected from street surfaces. When the metals found in urban runoff were compared with the metals content of sanitary sewage, loadings of 10 to 100 times the concentration of sanitary sewage metals were observed.

Total coliforms were found in urban runoff (Whipple et al., 1978). They were found to be higher in industrial areas than commercial areas. Residential areas had lower total coliform loadings.

Manure has major pollution potential giving significant amounts of oxygen-demanding organic matter, plant nutrients and infectious agents. Representative values of biochemical oxygen demand (BOD₅), chemical oxygen demand (COD), nutrient content and other parameters of non-point sources have been published (Loehr, 1974; Harms et al., 1974). However, all the above parameters only have water quality significance where discharge to a river occurs.

5.3 - Potential non-point source analysis

The management of non-point sources of water pollution requires the isolation of the most probable sources (land use and/or activity) and the application of a programme designed to reduce the magnitude of the impact caused by these sources. Non-point inputs from urban and industrial areas, forests, agricultural areas, and mining activities contain different types of pollutants and represent different transport patterns and conversions in the environment.

Identification of non-point sources and estimation of their relative magnitudes are necessary in order to define critical areas in a catchment. Mass et al., (1985) defined critical source areas as areas where the potential contribution of pollutants to the receiving water is higher than other areas. This concept of targeting critical areas has been recognised by a number of researchers in the non-point source field (Megahan and King, 1985; Mass et al., 1985; Walsh, 1985; Sivertun et al., 1988; Walker et al., 1989; Cook, 1991). Many pollutant delivery models have been developed to assist in obtaining this type of information for various land-use types, such as ANSWERS, CREAMS and AGNPS. Also the USLE and several modified versions have been applied for the purpose of estimating erosion and solids transport.

Although several sophisticated non-point pollution models exist, few are available that are easy to use, cover a variety of conditions, and integrate a wide range of information to allow managers and planners to assess different control strategies. Here a geographical information systems (GIS) is used to identify critical non-point source areas of pollution within a catchment.

An extension of the seasonal flow estimate just derived in Chapter 4 can be used to estimate non-point sources of pollution loading to rivers. Such sources include pollutants from agricultural areas and from urban runoff from areas such as roads and parking lots. Point pollutant sources are those associated with a particular outlet location, such as the outlet of a wastewater treatment plant. A standard assumption in treating non-point source pollution, in this thesis, is to relate the expected concentration of pollutants in runoff to the land use in the drainage basin. By taking a land use map of the area (see Chapter 2), and using a look-up table to connect land use to expected pollutant concentration (Table 5.1), a map of expected concentration, C , can be determined and the expected pollutant concentration in runoff from each DEM cell calculated. By taking the product of the concentration and the flow rate per unit area, a pollutant loading rate per unit area, L , can be calculated for each cell using the relationship:

$$L = C \times Q \quad (5.8)$$

5.3.1 - Critical area criteria

To identify pollution problems within a catchment, planners must define the critical areas. Following Mass et al., (1985) two perspectives can be employed:

1. The land resource perspective.
2. The water resource perspective.

Critical areas, from the land resource perspective, are those lands on which soil loss exceeds the rate at which soil can be replaced by natural processes. From the water resource perspective, critical areas are those areas where the potential contribution of pollutants to the receiving water is higher than other areas (Mass et al., 1985). Once these critical areas have been identified, land use modification strategies can be developed to reduce potential soil erosion or potential contribution of pollutants within a catchment. In this thesis the identification of critical areas uses the water resource perspective in which the main output is the creation of a pollutant "risk" map for the study area. This "risk" map can be used for water quality management, land use planning or zoning, soil conservation and environmental protection.

Because most catchments are non homogeneous in topography, soils, vegetation, and other characteristics, it is necessary to segment the catchment into units that can be treated as homogeneous. Usually the catchment is subdivided into square grids of selected size. The size of these cells is chosen to conform with the catchment geometry and represent the accuracy of the input data and required output.

The ability to convert analogue information, such as soil and topographic maps, into digital data and then edit, manipulate, store and display these data as colour images enables the use of GIS for evaluating these data spatially in order to determine the potential for production of pollutants within an area (Figure 5.2). Walsh (1985) reported the value of using GIS for problems of data integration and synthesising information for spatial examination of pollution from non-point sources. He helped to develop a GIS to delineate areas with high potential for soil erosion using overlays of soils, land cover and topography (slope) and data on precipitation. Evans and Myers (1990) created groundwater pollution risk and hazard assessment maps based on depth to groundwater, hydraulic conductivity, slope and soil permeability.

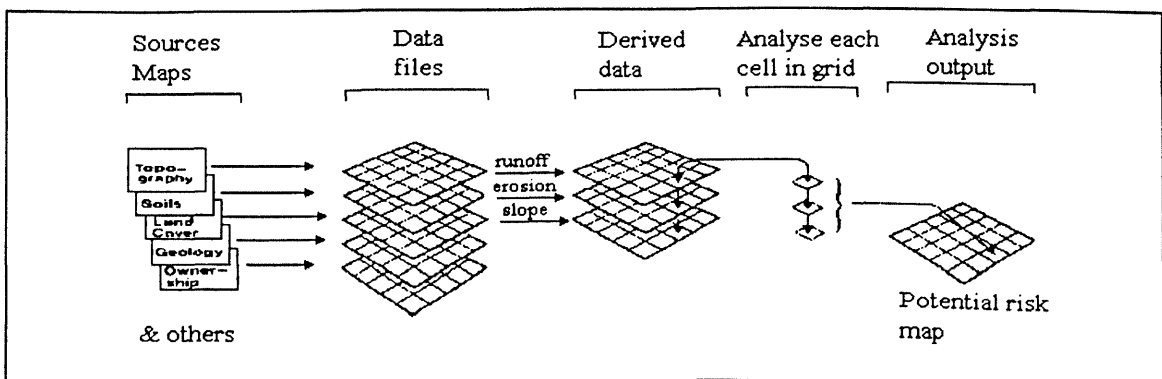


Figure 5.2 : Analysis of geocoded data.

5.3.2 - Critical area selection

Critical area identification, in the context of this thesis, involves manipulating appropriate data in various ways to provide qualitative assessments of the potential for negative pollutant impacts for any given parcel of land, or cell, in the catchment. For any given cell, this assessment takes the form of a numeric value derived by evaluating the cell's respective value for selected data layers and integrating all of the values in a single index value that denotes the water resource pollution potential for that particular location.

For example, parcels of land that exhibit such characteristics as highly permeable soil, a shallow depth to groundwater, and high septic system density would be indicated as highly susceptible to groundwater contamination. On the other hand, a forest parcel of land situated in highly impermeable soil would be designated as much less susceptible to groundwater contamination.

There are a large number of possible operations to combine data overlays (see Chapter 2). For example, the value of a particular cell is multiplied by a coefficient to produce a composite score. This operation is performed for every other cell in the grid and for each grid in the data overlay, and is then summed to produce a "sensitivity" grid (Figure 5.3). The coefficient can be understood as a weight for each grid in terms of its importance of affecting the "sensitivity" grid.

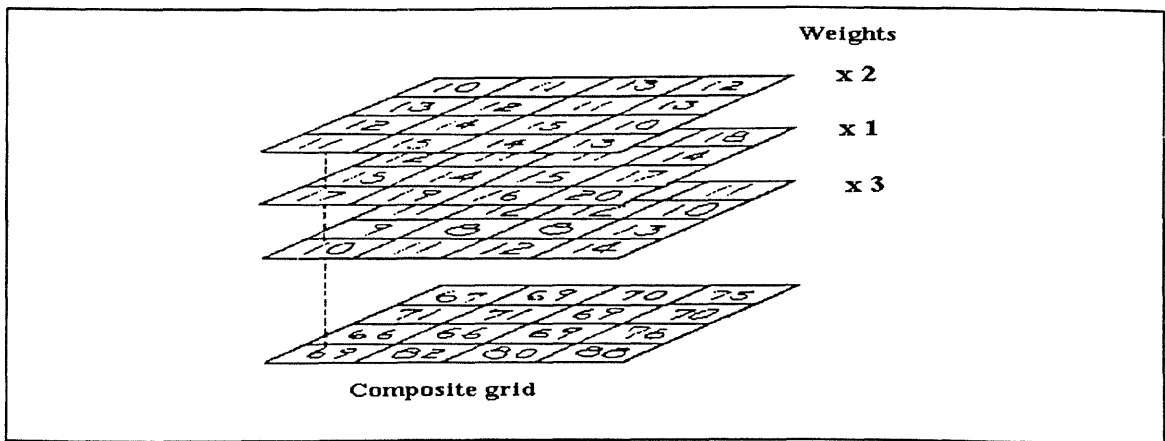


Figure 5.3 : Conceptual illustration of overlay process.

Beyond arithmetical operations such as sum, difference, product or quotient; overlay operations can also be handled by conditional (Boolean) commands. Such commands may take the form "if cell *a* in grid *x* has a value of *n*, change that cell value to *m* in grid *y*". With this combination of

operations (arithmetical and logical) it is possible to change the values of actual cells to meet the requirements of most types of analysis.

Inherent in each parameter studied are the physical characteristics that affect each pollution potential. In the development of a system like this, there are a wide range of technical considerations regarding the relative importance of many physical characteristics that affect pollution potential and how they should be combined as overlays within a GIS. In the approach adopted here, a numerical ranking scheme is used to assess non-point pollution potential in varying hydrologic conditions.

As a result of the above approach I consider the following factors that control non-point pollution potential : (a) sediments, (b) nitrogen-total, (c) phosphorus-total and (d) biochemical oxygen demand (BOD₅). They are explained below.

To select critical areas for production of sediments I use a modified version of USLE (McElroy et al., 1976) in a similar approach to that proposed by Sivertun et al., (1988). To identify potential critical areas for sediment production , two choices have to be made:

1. Assign numerical values to the data classification.
2. Select a method for combining these data.

According to the procedure proposed by McElroy et al., (1976) there are four maps for the identification of potential critical areas for sediment production (P):

1. soil map (*K*).
2. slope map (*S*).
3. land use map (*L*).
4. distance to river map (*D*).

The combination of the data is achieved by the use of the following equation (McElroy et al., 1976):

$$P = K.S.L.D \quad (5.9)$$

Classifications were made for the four maps. These maps were overlaid (map overlay operation in a GIS) to identify potential areas for sediment production (*P*). The values of these maps are intended for use in equations such as USLE or modified soil loss equations. The values for soil

and slope maps were obtained from nomographs of soil erodibility and slope gradient respectively (Wischmeier and Smith, 1978). The land use values were determined using tables based on the relative protection against erosion from various land uses (McElroy et al., 1976). The *distance to the river* map reflect the relative amounts of eroded soil projected to reach the drainage network at the given distances.

In previous chapters I show an example to illustrate the above expression. The soil map was obtained as described in Chapter 4. The explanation for construction of the slope map is in Chapter 3 and land use is in Chapter 2. The distance-to-river map is calculated using a function like SCAN (Burrough, 1986 ; page 90) where the value of each cell is computed according to the distance from that cell to the drainage network. This function is available in most of the GIS (IDRISI, ERDAS, GRASS, etc.).

Figure 5.4a-e shows the data used in Equation 5.9. The result (Figure 5.4e) indicates the potential to produce sediment.

Although the information necessary to run the above criteria is generally available without visiting the site, in practice, a site evaluation of a catchment can provide additional information on pollutant input potential. This site evaluation may reveal that areas designated as critical initially on the basis of erosion rate, distances to river, or other factors actually are not contributing to the water quality problem for one reason or another.

Because most of the nitrogen is water soluble and is readily leached or transported in surface runoff we assume that the choice of critical area for production of nitrogen-total (P_N) is given by:

$$P_N = Q \cdot L_N \quad (5.10)$$

Where: Q = Runoff calculated by Equation 4.5.

L_N = sources of nitrogen considering only land-use, derived from a land use map and Table 5.1 data.

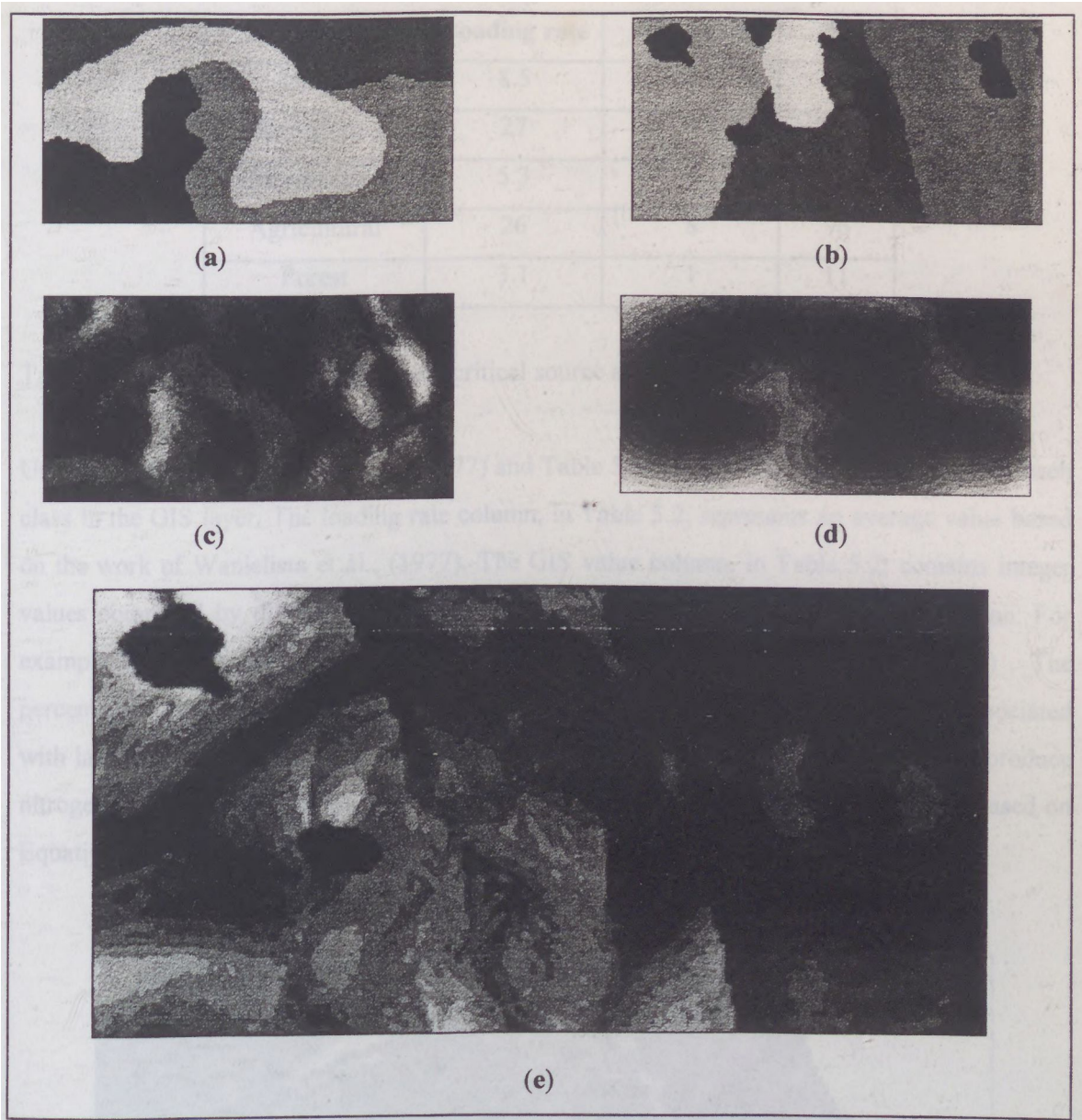


Figure 5.4 : Potential to produce sediments: (a) soil, (b) land use, (c) slope, (d) distance to river and (e) critical areas for production of sediments. The upper grids are categorical data and the classes are explained in Chapters 3 and 4. The middle and bottom grids are continuous data, and lighter tones indicate greater values.

The classes of land use applied to the above equation are the same as those already explained in Chapter 4. We show now how to assign numerical values for these classes representing the ability of a specific land use to produce nitrogen. These numerical values are shown in Table 5.2.

Land use	Loading rate	GIS value	%
Urban	8.5	3	31
Bare ground	27	9	100
Grassed space	5.3	2	20
Agricultural	26	8	96
Forest	3.1	1	11

Table 5.2 : Values for determining critical source areas for production of nitrogen.

Using the paper of Wanielista et al., (1977) and Table 5.1 it is possible to assign a value for each class in the GIS layer. The loading rate column, in Table 5.2, represents an average value based on the work of Wanielista et al., (1977). The GIS value column, in Table 5.2, contains integer values computed by dividing one value by the smallest value of the loading rate column. For example the value, 9, for bare ground, in Table 5.2, is the integer result of $(27/3.1)$. The percentage column, in Table 5.2, reflects the relative amount of nitrogen production associated with land use. For example, the value for urban land use indicates that the potential to produce nitrogen is only 31 per cent of that from bare ground. Figure 5.5 illustrates the results based on Equation 5.10 and Table 5.2.



Figure 5.5 : Potential to produce nitrogen (lighter tones indicate greater values).

We implemented the above approach using a very simple set of hypotheses concerning the origin of non-point sources (intensity and spatial distribution of hydrology and land uses) and their consequences (potential to generate pollutants to surface waters). The model proposed is a developing tool and does not substitute field sampling. Possible sources of error include errors in the spatial distribution of pollutant sources, in the runoff generation, in the analysis procedure, in individual pollutant sources (association of land use and loading rates) and about a seasonal variation. However, despite these weaknesses, the approach seems well adapted to management problems, because the origin of pollutant load and the relative importance of each type of contribution can be assessed very easily, and the impact on water quality due to changes in land use can be predicted. The same procedure was used to calculate the potential for production of biochemical oxygen demand (BOD_5) as shown in Figure 5.6 and Table 5.3.

Land use	Loading rate	GIS value	%
Urban	75	15	100
Bare ground	20	4	27
Grassed space	11	2	15
Agricultural	18	4	24
Forest	5	1	7

Table 5.3 : Values for determining critical sources areas for biochemical oxygen demand



Figure 5.6 : Potential to produce biochemical oxygen demand (lighter tones indicate greater values) using $P_{BOD} = Q \cdot L_{BOD}$.

Phosphorus is released from a thin layer of surface soil that interacts with rainfall and runoff (Sharpley, 1985). Ahuja et al., (1981) proposed an effective depth of interaction (EDI), defined as the thickness of surface soil in which the degree of interaction is equal to that at soil surface. Ahuja et al., (1982) present a conceptual model for EDI based on rainfall energy, soil slope, slope length and runoff rate. Because rainfall-runoff is already explained in the potential pollutant equation (Equation 5.10 - Q) we assume that the EDI mechanism is explained only by slope and soil characteristics (Figure 5.7) such that:

$$P_p = Q \cdot L_p \cdot (EDI) \quad (5.11)$$

Where: P_p = critical area for production of phosphorus-total.

Q = Runoff calculated by Equation 4.5.

L_p = sources of phosphorus considering only land-use.

EDI = effective depth of interaction.

Figure 5.7 shows that the effect of slope on EDI is also a function of soil type. We explore this simple relationship to produce a qualitative EDI evaluation through an overlay operation in a GIS with the two grids (soil and slope).

This procedure (Equation 5.11) was used to calculate the potential for production of phosphorus as shown in Figure 5.8 and Table 5.4.

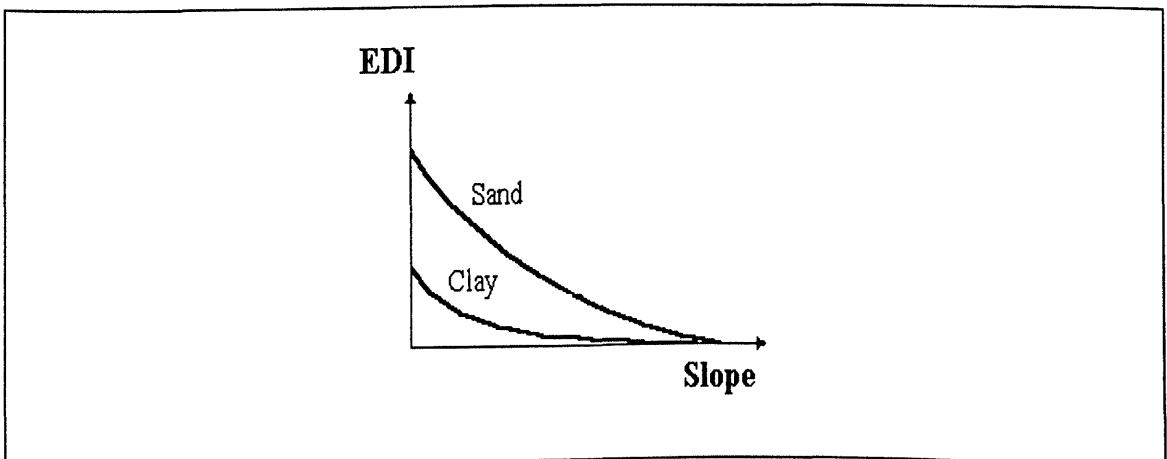


Figure 5.7 : Effective depth of interaction (EDI) as a function of soil type and slope.

Land use	Loading rate	GIS value	%
Urban	2.0	20	100
Bare ground	1.1	11	55
Grassed space	0.3	3	15
Agricultural	1.05	11	53
Forest	0.1	1	5

Table 5.4 : Values for determining critical source areas for phosphorus.

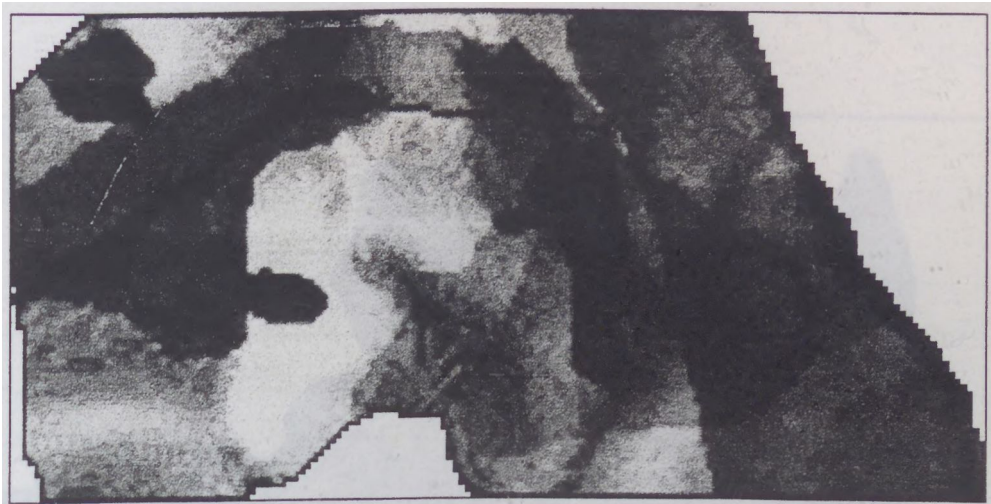


Figure 5.8 : Potential to produce phosphorus (lighter tones indicate greater values) using Equation 5.11.

Seasonal per hectare pollution loads from existing land use were computed for Sinos catchment. Figure 5.9 shows critical areas for nitrogen produced according to the methodology presented in this Chapter in Sinos catchment. By viewing such output grids, users can “*perceive*” areas that contribute the highest non-point source pollution loads within Sinos catchment. Problem areas include the heavily urbanised cities in the west side and along Sinos valley in the south, which supports intensive agriculture.

To investigate the effect of runoff on the identification of critical areas, the overland flow values are set to 1 within each cell of the studied area. The nitrogen critical areas are identified as shown in Figure 5.10 and are simply the land use classification weighted to the production of pollutant.

Figures 5.9 and 5.10 also represent two distinct critical area perspectives:

- The water resource perspective (Figure 5.9) for those areas where an improvement in management practices may result in greater progress towards improving water quality in a catchment.
- The land use perspective (Figure 5.10) for those lands on which the retention of nutrients is higher.

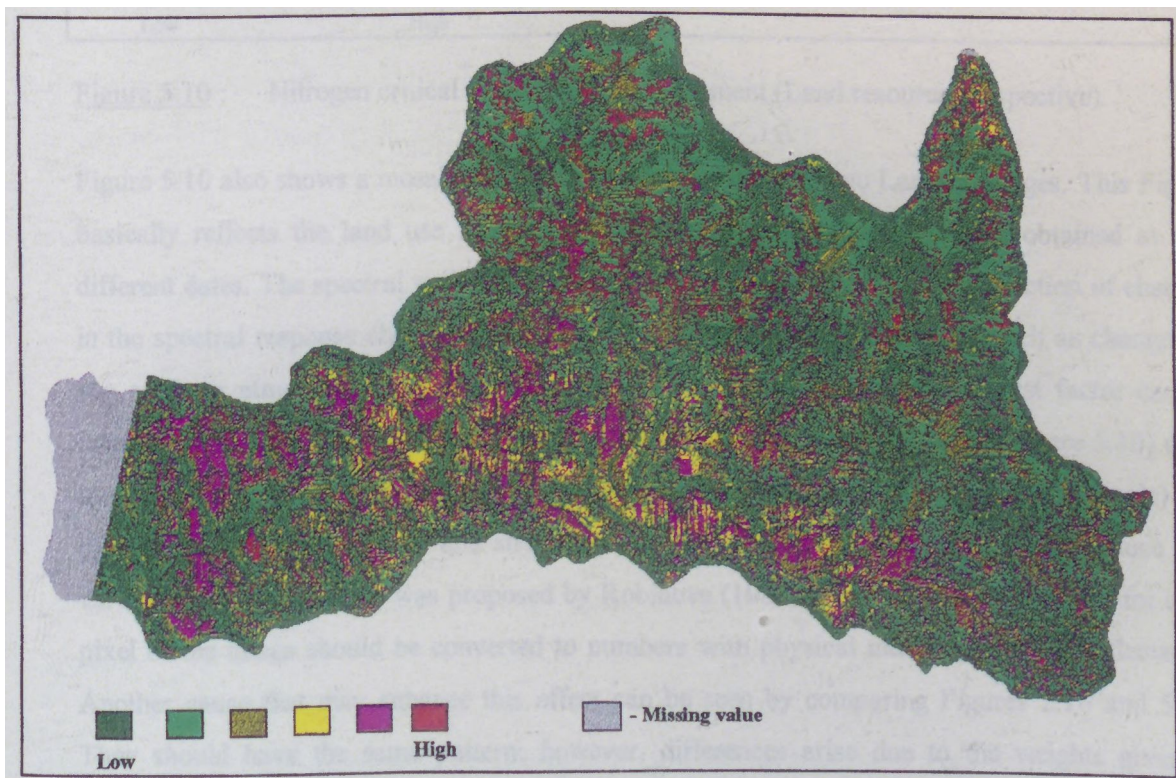


Figure 5.9 : Nitrogen critical areas for Sinos catchment (Water resource perspective).

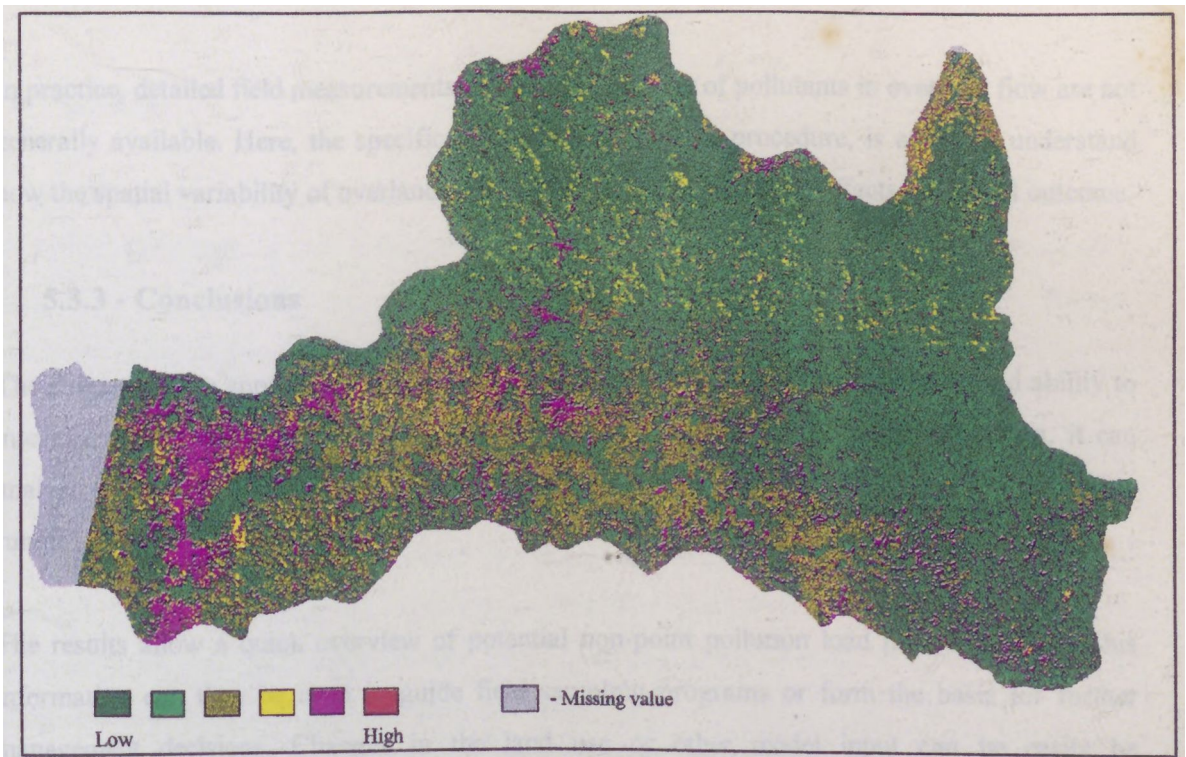


Figure 5.10 : Nitrogen critical areas for Sinos catchment (Land resource perspective).

Figure 5.10 also shows a mosaicing effect problem between the two Landsat images. This Figure basically reflects the land use features obtained from two classified images obtained at two different dates. The spectral variability of a land cover feature over time is a function of changes in the spectral response characteristics of the target and viewing conditions (such as changes in sun angle or atmospheric conditions). In terms of land use assessment, the first factor can be considered useful information, the second, noise. Because the mosaiced scene (Figure 5.10) used multitemporal images (two different dates) the illumination effects (changes in sun angle) are clearly visible in Figure 5.10 and should be removed or corrected. A procedure to reduce this variability between scenes was proposed by Robinove (1982) where the digital numbers for each pixel of the image should be converted to numbers with physical meaning, such as reflectance. Another cause that may enhance this effect can be seen by comparing Figures 2.16 and 5.10. They should have the same pattern; however, differences arise due to the weights given to different land use classes.

According to the requirements of a specific project, both criteria (Figures 5.9 and 5.10) may be useful. For example, from a water quality perspective, the contribution of nitrogen or phosphorus from land may have an environmental cost, justifying control measures; on the other hand, farmers have an interest in retaining nutrients on cropland for uptake by plants.

In practice, detailed field measurements of the concentration of pollutants in overland flow are not generally available. Here, the specific objective of the above procedure, is solely to understand how the spatial variability of overland flow, which is a key parameter, affects the model outcome.

5.3.3 - Conclusions

The strength of the approach presented here is its simplicity, ease of use, flexibility and ability to integrate data from various sources. Using a relatively simple computational algorithm, it can analyse vast areas of land with respect of potential pollution load problems caused by stormwater runoff.

The results allow a quick overview of potential non-point pollution load problems areas. This information can then be used to guide field sampling programs or form the basis for further management decisions. Changes in the land use or other model input can be easily be implemented making the comparison of various management scenarios possible (see this example in Chapter 8). In its existing form, it is a useful management tool.

The objectives of this chapter were:

- To determine whether a non-point pollution problem may exists.
- To reveal changes, if any, over space and time.

Each objective can be implemented at a rapid and inexpensive level. After a preliminary information base is developed, the user has the option of reiterating through the model at a more detailed level. The regional perspective and data resolution employed in the analysis appear to be compatible with information requirements of various planning activities conducted by government agencies.

Basically, the critical area approach utilises the pollutant concentration that is multiplied by runoff to compute the areas over the terrain with a high potential to produce pollutants that reach surface waters in the drainage network. Pollutant concentration should be estimated directly from water sampling (preferentially), or by extrapolation from experimental field studies.

5.4 - Summary

Many models have been developed for evaluating non-point source pollution and implementing management practices to limit pollution to an acceptable level. However, because of the spatial variation of climate, soils, and agricultural practices, no single group of models or control measures can be used in every region all over the world.

The main objective of this chapter was to introduce a methodology to identify critical areas of pollution in the catchment where potential pollutant loadings for water resources are greatest. This objective was achieved by the use of two sets of information: (a) hydrology and (b) land use (also (c) EDI for phosphorus). Hydrologic processes can cause erosion, causes chemical transport which is an uncontrolled natural input. Land use affects the dynamic spatial patterns of runoff, infiltration and potential non-point pollution.

The basic objective of the approach described here is to identify critical areas using a minimum of field data. Where possible, these areas should be locally examined to confirm their validity. However, when local data are not available, the above approach offers an opportunity to judge the relative potential of different portions of the catchment to generate non-point source pollutants. In my opinion, due to the responsibilities of land use planners, engineers, and agriculturists, making this relative judgement is more important than obtaining a precise estimate of magnitudes, as it allows the implementation of best management practices in the critical areas.

The advantages of developing the above approach and archiving the data in a geographical information system include ease of retrieval, variety of output products to fit many needs, and the ability to discover and display information gained by interactions of these data.

6. Aggregating point and non-point sources of pollutants

6.1 - Introduction

This chapter presents a loading function methodology for analysing both point and non-point sources of pollution in large catchments. This is shown diagrammatically in Figure 6.1. The point sources are addressed by municipal and industrial discharges and non-point sources relate to land use characteristics. After these steps, a framework that combines point and non-point sources is proposed.

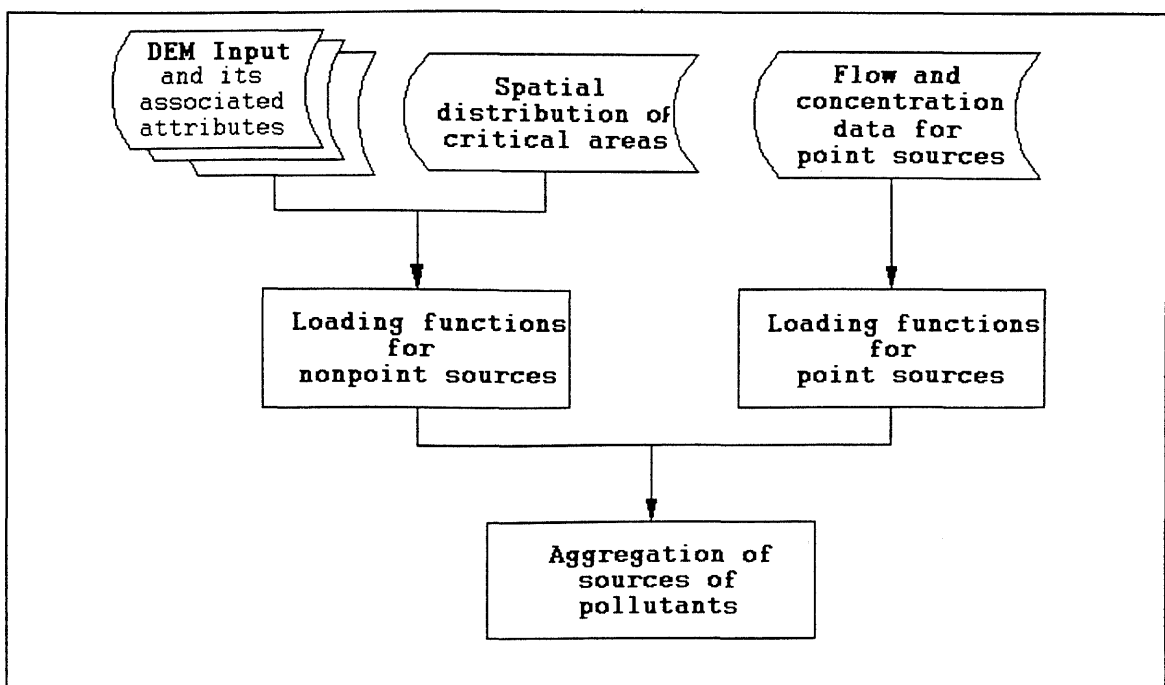


Figure 6.1 : Flow diagram illustrating the calculations of loading functions for point and non-point sources.

Most river water quality models require as basic input data approximate river loadings for point and non-point sources. These models are then used to predict the downstream river water quality using simple relationships to represent the very complex processes taking place in the rivers. Past efforts have been based on deterministic water quality models focused on small drainage areas or on segments of rivers (Meadows et al., 1978). Because of the growing concern with large-scale environmental problems, such as non-point source pollution, acid rain and climate change, there is a need to develop more objective and consistent methods to assess environmental impacts for

large areas. For example, Johnston et al., (1988) attempt to detect and alleviate the effects of large scale environmental problems by relating wetland position in the drainage basin to water quality.

Recently developed deterministic models are spatially distributed using grid cells to discretise the domain (Young et al., 1989; Beasley et al., 1980). However, none of these models encompass large and diverse land use, and combine point and non-point sources of pollution. Consequently, more work is needed to characterise water quality conditions for large catchments that aggregate point and non-point source pollutants originating from both urbanised and agricultural land uses.

A major problem in assessing the impacts on regional surface water quality has been the difficulty in obtaining reliable information on cause and effect relationships for a representative sample of stream segments in a region (Cohen et al., 1988).

Grayman et al., (1975) propose a method to assess regional water quality. They developed the ADAPT (Areal Design and Planning Tool) system for use in water quality planning. In this system the land use/development, waste generation transport-treatment, and the water environment were considered for assessing the water quality management plan over a large area. In their paper they present a case study for an area of 6,000 sq. miles. A major drawback of the system is that it is formulated using a large number of mathematical models and requires extensive parameterisation and data inputs.

Another method is the use of statistical analyses of land use and water quality data for selected catchments. Haith (1976) applied stepwise regression methods to water quality and land use data for 20 catchments putting emphasis on those water quality constituents considered to be associated with non-point sources (i.e. nitrogen, phosphorus and sediments) and major land uses (agriculture, forest, residential and industrial). In Haith's work, catchments were treated as independent in the sense that none were downstream of another and had different sizes. The results indicate that relationships do exist between land use and water quality parameters, however, a mechanism for transportation of pollutants was not taken into account.

Haith and Tubbs (1981) proposed a methodology for analysing agricultural non-point source pollution involving three steps: (1) prediction of soil loss and runoff from the various crop/soil combinations in a catchment; (2) determination of dissolved pollutant concentrations in runoff

and solid-phase concentrations in eroded soil; and (3) estimation of pollutant delivery to surface waters. They do not account for point sources.

Jager et al., (1990) used cokriging to assess regional stream water quality. For these techniques to be applied on a regional scale, data should exhibit spatial autocorrelation in multiple dimensions, however, most influences on regional water quality do not operate in the full two-dimensional landscape. Basically, water quality only displays a spatial autocorrelation along preferred flow paths.

In summary, a regional water quality model must account for: (a) the linkage of pollution sources (point and non-point sources) and (b) large and diverse land uses. This is one of the objectives of this thesis. Here I assume that the environment for water quality management can be considered as a large scale interaction in which the drainage network reflects the loads applied by:

1. Point sources (municipal sewage outfalls and industrial effluents) which are linked directly to a drainage network.
2. Non-point sources (agricultural runoff, natural loads, etc.) which are distributed on a square grid proportionally to the surface areas of the catchments and transported over the terrain until they reach a buffer zone adjacent to a drainage network.

To formulate the loadings for both point and non-point pollutants there is a need to assume that:

1. All contributions are additive.
2. The contribution of a non-point source reaches the surface waters within its original drainage area.
3. On the seasonal time scale, the pollutant transfer is considered to be in a steady-state condition.
4. Lacking detailed environmental data, the catchment is considered to be geomorphologically homogeneous, so the transport coefficients are kept constant for the entire catchment.

6.2 - Discharge of pollutant sources into rivers

Chapter 1 presents the main models used to explain runoff, erosion and pollution processes that occur within catchments. These models are best implemented by trained professionals and must be calibrated using flow and water quality data from the catchments that they are used to study.

Given the difficulty of obtaining such data in Brazil, it is not surprising that such models have seen only limited application in actual water quality management applications.

The purpose of this section is to examine the processes wherein pollutants are discharged into rivers. The principal sources can be divided into two categories : (a) point sources and (b) non-point sources.

The point sources are those that are considered to have a well-defined point of discharge and which is usually continuous. The two principal point source groupings are : (a) municipal point sources that result in discharges of treated and partially treated sewage and (b) industrial discharges.

The principal non-point sources are: (a) agriculture, (b) silviculture, (c) atmospheric, and (d) urban runoff. In each case, the distinguishing feature of the non-point source is that the origin of the discharge is diffuse; in other words, it is not possible to relate the discharge to a specific well-defined location. In addition, non-point sources also tend to be transient in time.

One important aspect of environmental planning is the determination of the input mass loading, that is, the total mass of material discharged per unit time into a specific drainage network.

For sources with continuous flow, the input load is given by:

$$W(t) = Q(t) \times c(t) \quad (6.1)$$

Where: $c(t)$ is the concentration of the input [M/L^3],

$Q(t)$ is the input flow [L^3/T],

$W(t)$ is the mass rate input [M/T], all quantities occurring simultaneously at a given t .

For some sources, the flow is continuously measured (as for example in the tributary to a large river), but estimates of the concentration of the water quality parameter are only available at certain intervals. If Equation 6.1 is applied only when both flow and concentration data are available, the actual loading from the source may be significantly underestimated. If, for example, the concentration is not measured during times of peak runoff, a major component of the load may be missed.

Dolan et al., (1981) applied several estimation procedures to a detailed sampling set of phosphorus and flow. One of the methods was to plot the available concentration data as a function of the river flow, both as logarithms, and estimate the relationship between concentration and flow, giving:

$$c = a.Q^b \tag{6.2}$$

Another method that has been used (Dolan et al., 1981) uses the "unbiased stratified ratio estimator". Here flow record is divided into various periods, for example, seasonal, annual, or high and low flow periods. The mean load is:

$$\overline{W}_p = \overline{Q}_p \times \frac{\overline{W}_c}{\overline{Q}_c} \left[\frac{1 + (1/n)(S_{QW_i} \overline{Q}_c \overline{W}_c)}{1 + (1/n)(S_{Q_i}^2 \overline{Q}_c^2)} \right] \tag{6.3}$$

Where: \overline{W}_p is the estimated average load for the period p .

\overline{Q}_p is the mean flow for the period.

\overline{W}_c is the mean daily loading for the days on which concentrations were determined.

\overline{Q}_c is the mean daily flow for the days on which concentrations were determined.

n is the number of days when concentrations were measured.

Also,

$$S_{QW} = [1/(n-1)] \left[\left(\sum_{i=1}^n Q_{ci} \cdot W_{ci} \right) - n \cdot \overline{Q}_c \cdot \overline{W}_c \right] \tag{6.4}$$

and

$$S_Q^2 = [1/(n-1)] \left[\left(\sum_{i=1}^n Q_{ci}^2 \right) - n \cdot \overline{Q}_c^2 \right] \tag{6.5}$$

Where: Q_{ci} are the individually measured flow values.

W_{ci} is the daily loading for each day on which the concentration was measured.

Dolan et al., (1981) found this estimator is best suited where there is extensive flow data but concentration data are sparse.

Some sources depend on a number of factors that may influence both flow and concentration. For example, the flow from urban runoff is usually highly intermittent resulting from variable precipitation, so at times there is no load being discharged, therefore, several input loads can be estimated through:

1. Equivalent annual (or other interval) loading rates.
2. Average load discharge per flow event.
3. Distribution of load within a flow event.

For any given problem, reductions in pollution sources may be required to relieve existing water quality violations. The choice of reducing point and non-point sources depends on the feasibility and economics of existing engineering controls and on the relative magnitudes of the sources. Early identification of major sources allows concentration of available resources on the most significant problems.

To estimate the water quality we need to describe how the discharge of pollution sources interacts with rivers. In the rest of this section the sources of pollutants adjacent to the drainage network are identified. In the next chapter we show how to construct the mass balance equation for various reaches of the river.

A water balance model is a representation of the mass balance of water within a particular control volume. It is a physical statement of the law of conservation of mass which states that matter cannot be created or destroyed. As a result, the rate of change of storage of water within the control volume is equal to the difference between its rates of inflow and outflow across the control surface. One may distinguish in constructing a spatial hydrologic model between the surface defining the outer boundary of the study region, and the surface defining the boundary of the spatial units within that region (for example, cells of a DEM). A spatially distributed hydrological model applies the law of conservation of mass to describe the mass balance within each spatial unit, and to this must be coupled a momentum equation (such as Darcy's law for groundwater flow) which defines how quickly water can move between units. Different sizes and shapes of spatial units are needed to deal with the different phases of the hydrologic cycle.

The basic assumption, for determining the load functions for point and non-point pollution sources, is that the river is homogeneous in terms of water quality variables across the river (laterally) and with depth (vertically). This assumption is illustrated in Figure 6.2.

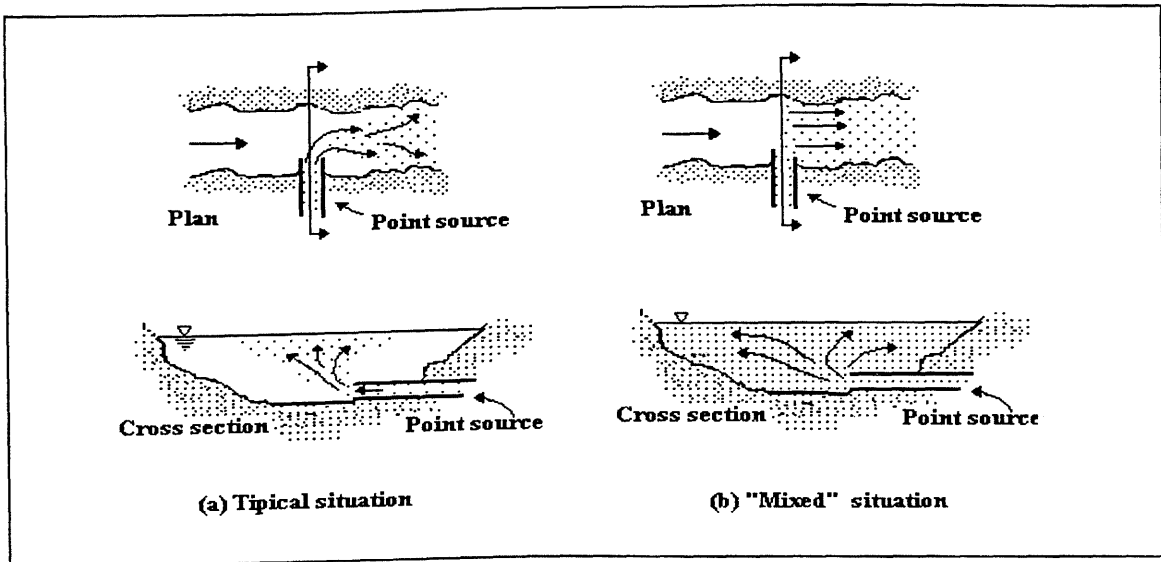


Figure 6.2 : Assumptions for point sources: (a) Typical situation and (b) "Mixed" situation.

6.2.1 - Load function for point sources

Point sources are considered as those sources that enter the river from a fixed discharge point such as an effluent pipe or tributary system. Following Figure 6.2 the second assumption to be made is that there is no mixing of one reach with another due to dispersion or velocity gradients. It is also assumed that the magnitude of the pollutants input and flows are temporally invariant (referred to a steady state condition). Finally, the substance that enters into the river is conserved, that is, there are no losses due to chemical reactions or biological degradation.

According to Pinder and Jones, (1969) if the substance is conservative, there is no change in total load between tributaries or effluent pipes. The concentration changes only at the entrance of new sources of pollutants with associated changes in flow. The upstream conditions of flow and concentration are often known or can be measured, and some information is available on the effluent conditions. Interest then centers on estimating the concentration of the pollutant in the river after mixing of the effluent with the upstream concentration. Figure 6.3 illustrates this case (Point and conservative sources).

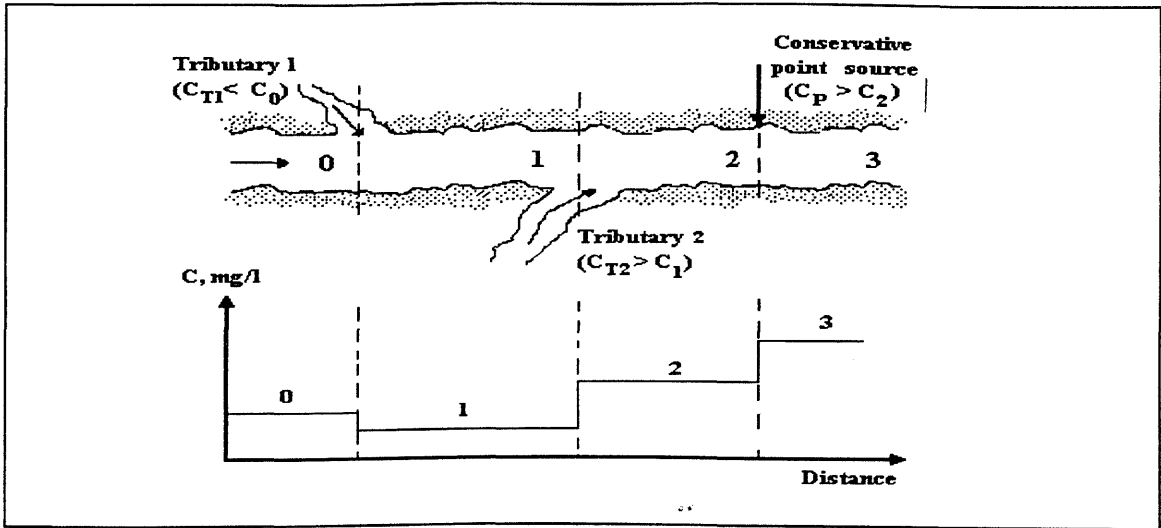


Figure 6.3 : Scheme of a conservative substance.

The scheme shown in Figure 6.3 indicates the mass balance through:

Mass rate of substance upstream + mass rate added in this reach = mass rate of substance downstream

The mass balance for reaches 0 and 1 of Figure 6.3 is given by:

$$Q_0 \cdot c_0 + Q_{T1} \cdot c_{T1} = Q_1 \cdot c_1 \tag{6.6}$$

A similar balance can also be made for the flows, that is:

$$Q_0 + Q_{T1} = Q_1 \tag{6.7}$$

Equation 6.6 is frequently solved for the downstream concentration c_1 :

$$c_1 = \frac{Q_0 \times c_0 + Q_{T1} \times c_{T1}}{Q_1} \tag{6.8}$$

The concentration remains at c_1 until the next point source where Equation 6.8 is again applied. In this way, the complete downstream profile can be generated. If, however, it is known (or suspected) that the substance is non conservative, in other words, the substance decays with time

due perhaps to chemical reactions, bacteriological degradation or radioactive decay, an additional consideration must be included. A useful assumption is that the substance decays according to a first-order reaction, that is, the rate of loss of the substance is proportional to the concentration at any time. Following O'Connor (1967), the mass balance equation, at steady state, is a first-order linear differential equation:

$$\frac{1}{A} \times \frac{d(Q.c)}{dx} = -K.c \tag{6.9}$$

Where: K is the decay rate [T^{-1}] of the substance.

A is the cross-sectional area [L^2].

The boundary condition is

$$c = c_0 \quad \text{at} \quad x = 0 \tag{6.9a}$$

If the derivative is expanded and an assumption is made that there is no change of flow between inputs ($dQ/dx = 0$), then:

$$\left(\frac{Q}{A}\right) \frac{dc}{dx} = -K.c \tag{6.9b}$$

Assuming a uniform cross-sectional area ($dA/dx = 0$), gives:

$$U \cdot \frac{dc}{dx} = -K.c \tag{6.10}$$

Where U is the flow velocity.

The solution to Equation 6.10 with boundary condition 6.9a is:

$$c = c_0 \cdot e^{\left(\frac{-K.x}{U}\right)} \tag{6.11}$$

Figure 6.4 shows a non conservative pollutant decaying at a rate K .

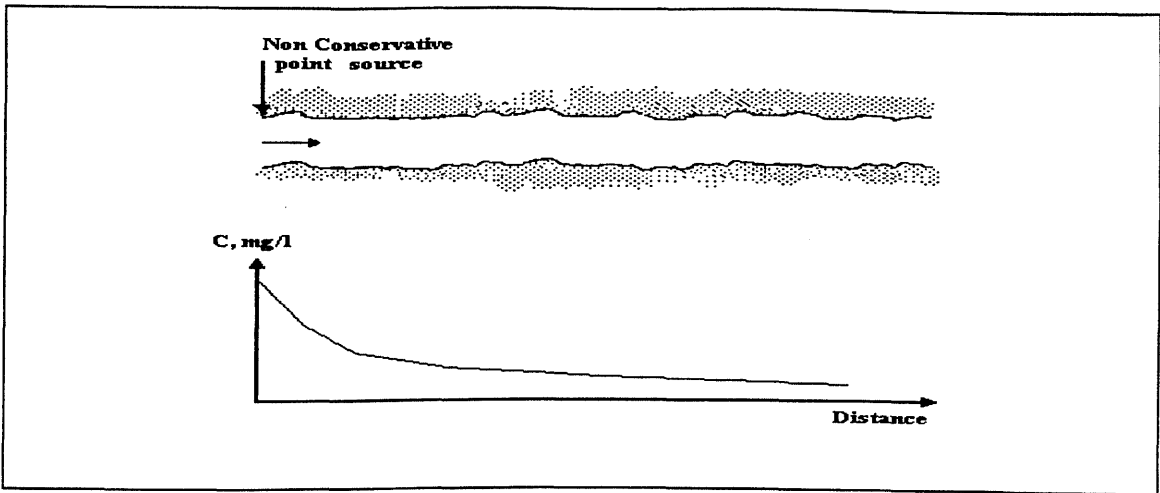


Figure 6.4 : Scheme of a non-conservative substance...

To link point sources (municipal sewage outfalls and industrial effluents) directly to a drainage network there is a need to:

1. Give the location of the point source adjacent to the drainage network.
2. Produce a load using Equation 6.1.
3. Assign point source loads to weight values.
4. Incorporate this location and load information as an attribute of a grid in the GIS.

Figures 6.5 and 6.6 illustrate the way in which point sources are represented adjacent to the drainage network in a grid.

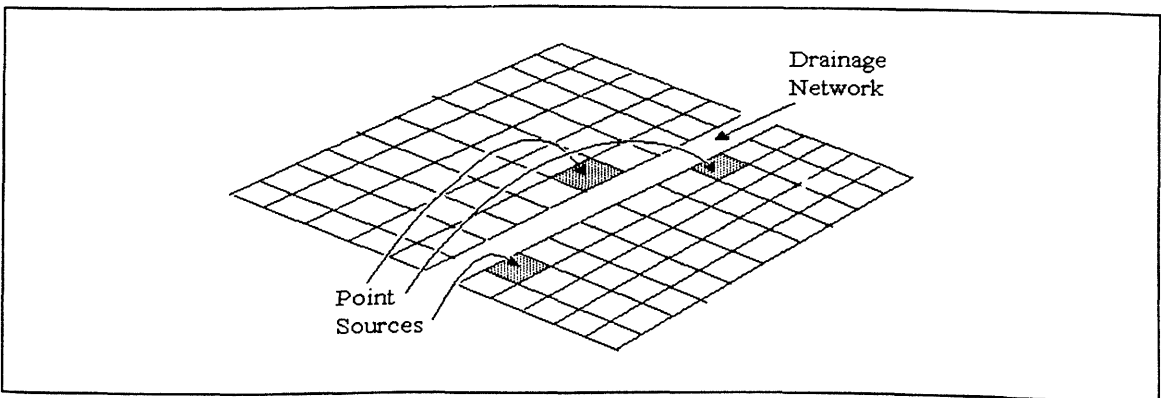


Figure 6.5 : Point sources around drainage network.

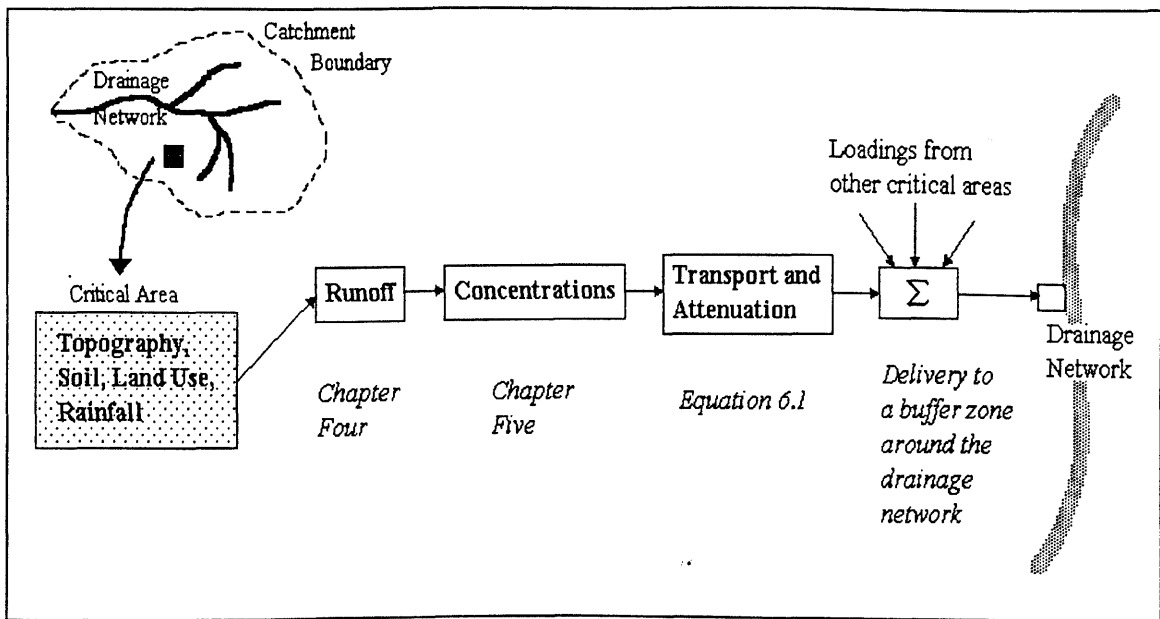


Figure 6.7 : Loading functions for estimation of non-point source pollution entering a drainage network.

To define the strength of non-point pollutants, information is needed on the delivery of pollutants between the critical areas (as presented in Chapter Five) and the receiving drainage network. Many factors and processes contribute to the delivery of pollutant and sediment to the drainage network. The delivery processes (or factors) can be divided into those occurring during overland flow or those occurring during the channel flow phase of pollutant transport. There are six major overland flow factors that affect the attenuation (Novotny, 1980):

1. *Rainfall impact* detaches soil particles and keeps them in suspension for the duration of the rainfall. When the energy from rainfall terminates or is reduced, the excess particles in suspension are redeposited.
2. *Overland flow energy* detaches soil particles from small rills and, together with some interrill contribution, the particles remain in suspension so long as overland flow persists.
3. *Vegetation* slows down flow and filters out particles during shallow-flow conditions.
4. *Infiltration* filters out the particles from the overland flow.
5. *Small depressions and ponding* allow particles to be deposited due reduction of velocity.
6. *Change of the slope of overland flow* due to concavity of the drainage area often flattens the slope near the drainage channel and steepens the slope uphill. The sediment and pollutant transport capacity of overland flow changes according to slope.

Flow and transport capacity of pollutants in the channel will be considered next chapter. There is, also, a *quality* dimension to the delivery problem (Walling, 1983). When rainwater reaches the surface of the soil, some pollutants are desorbed and go into solution; others remain absorbed and move with soil particles. In soils, most pollutants are adsorbed by clay and organic matter because of the high surface area, leading to the formation of strong adsorption bonds. The pollutants contained in runoff sediments are presented in higher concentrations than in the parent soil. This difference is termed the enrichment ratio (*ER*) (Walling, 1983), defined as:

$$ER = \frac{C_r}{C_s} \quad (6.12)$$

where: C_r : pollutant concentration of the runoff per gram of sediment.

C_s : pollutant concentration of the parent soil per gram.

The enrichment concept can be applied to clay, organic matter, and all pollutants adsorbed by soil particles. These include phosphates, ammonium, and many pesticides. It is inappropriate to apply enrichment ratios to pollutants that are mobile in soils, such as nitrates or soluble pesticides. Because of these complexities, the transport of pollutants from their source to a drainage network and their categorisation into mobile (dissolved in soil water) and immobile (adsorbed by soil) categories is one of the least understood aspects of non-point source pollution (Reinelt et al., 1988).

In a GIS framework, the catchment is manipulated so that each piece of land is represented by a single DEM cell, and these cells are flow ordered (see aspect in Chapter 3) so that the 'from' node is upstream and the 'to' node is downstream. Therefore, three pollutant variables can be associated with each cell: "*From Flow*", "*To Flow*", and "*Cell Flow*". From Flow is that cell pollutant load at the 'from' node; To Flow is the corresponding load at the 'to' node; and Cell Flow is that load generated inside the cell.

The components of the proposed loading function approach are shown in Figure 6.8. A catchment is divided into square cells, each of which is homogeneous with respect to soil, land use, topography and rainfall characteristics. Each source of non-point pollution is considered to be an independent contributor to the total catchment export of pollutants. The pollutant loads from a critical source area i,j are given by:

$$L = \sum_i \sum_j CA_{i,j} T \quad (6.13)$$

Where: L - Load of pollutant in a river buffer area representing all the pollution processes in the upslope cells.

$CA_{i,j}$ - Dissolved and solid-phase (see EDI concept in Chapter Five) load of a pollutant in a cell i,j as function of runoff and land use (See Chapter Five about critical areas).

T - Transport factor which indicates the fractions of pollutants that move from one cell to the next (assumed constant for a catchment).

Figure 6.7 illustrate the delivery of pollutants between the critical areas and a buffer zone around the drainage network. This buffer zone does not exist in reality; it is a concept, to represent the distributed pollutant loads along the river. In other words, it is artifact component of the model. The complexities of the delivery problem are represented by the transport factor T , in Equation 6.13. Here, I assume that the transport factor T for a pollutant in Equation 6.13 must be based on the movement of runoff from critical areas to the drainage network following preferential flow paths and stopping the transport process in a buffer zone adjacent to the drainage network as illustrated in Figure 6.8. If the pollutants are considered to be conservative, then all of them reach the drainage network, and the transport factor in Equation 6.13 is $T=1$. However, when decay is assumed the transport factor is $T<1$.

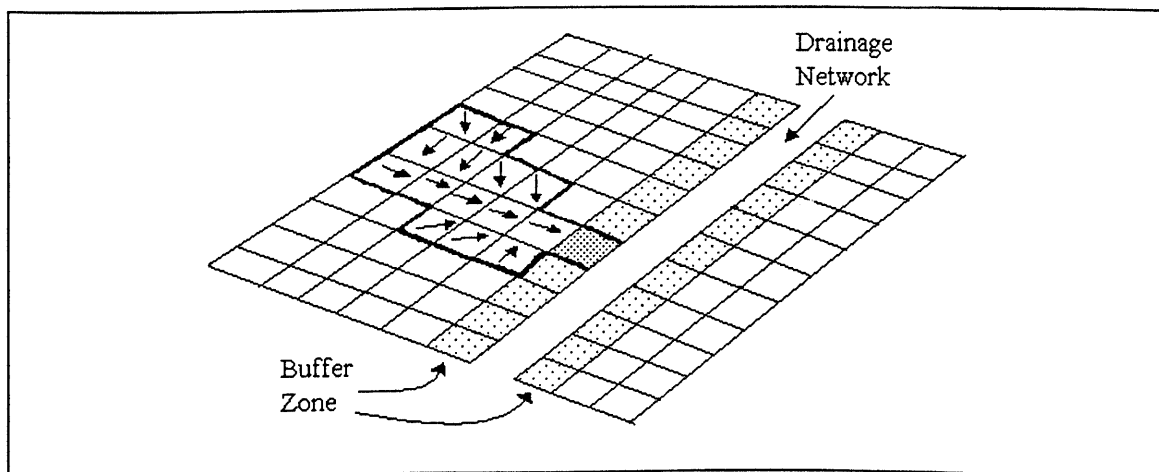


Figure 6.8 : Buffer zones around drainage network.

The spatial model presented above is based on flow vectors derived from the slope and aspect of the terrain (as presented in Chapter 3). The buffer zone is defined as all cells adjacent to the drainage network system. Using this representation of pollution-flow vector processes, all upstream cells are assigned to the cells in the buffer zone through the use of Equation 6.13 (The source code to implement this approach is given in the Appendix). All GIS have the ability to create a buffer zone around linear features such a drainage network (Operation SPAN on page 90 -Burrough, 1986 as an example). Figure 6.9 illustrates this operation for the drainage network shown in examples in Chapter 3.

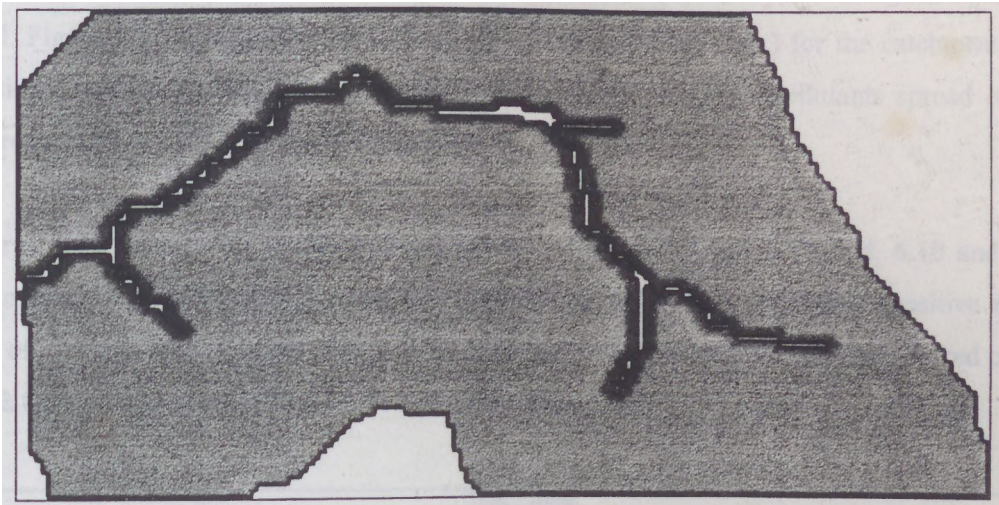


Figure 6.9 : Buffer zone around drainage network.

6.3 - Evaluation in Sinos catchment

In practice, the load model for multiple sources of pollutants consists of the two grids shown in Figures 6.5 and 6.8. It is straight forward to integrate these grids in any raster-based GIS and to implement further manipulation with grid overlays, such as water quality inside the drainage network (see next chapter).

Most river water quality models require approximate pollutant loadings as basic input data. These data can be summarised in two ways: (a) as point loads and (b) as non-point loads. For non-point loads the data set contains the intensities and spatial distributions of the loads. The intensities are represented by an average loading rate (concentration of pollutant - see Tables 5.2,

5.3 and 5.4) multiplied by a runoff index (Chapter Four) that is derived from the land use, soil type, upstream catchment area, slope and rainfall.

Figure 6.10 indicates the routing of pollutants over the terrain to the river buffer area using the conditions of Figure 5.9 (see Chapter Five). Figure 6.11 indicates the load of non-point pollution for nitrogen without runoff, i.e when the overland flow value is set to 1.

Figure 6.10 results in a reasonable prediction of the potential transport of non-point pollutants based on catchment parameters, including land use, soil, slope, upstream catchment area and rainfall. Figure 6.11 predicts the same thing with constant runoff (unit) for the catchment. Not surprisingly, the total change between these figures indicates that the pollutants spread over a wide area when runoff is included in the prediction.

The large differences in the spatial patterns between Figures 5.9 and 5.10, and, 6.10 and 6.11 indicate that the models (critical areas and transport of pollutants) are highly sensitive to the values of overland flow (Chapter Four). Both cases have more areas with high values (red colour in these figures) with the runoff solution than without.

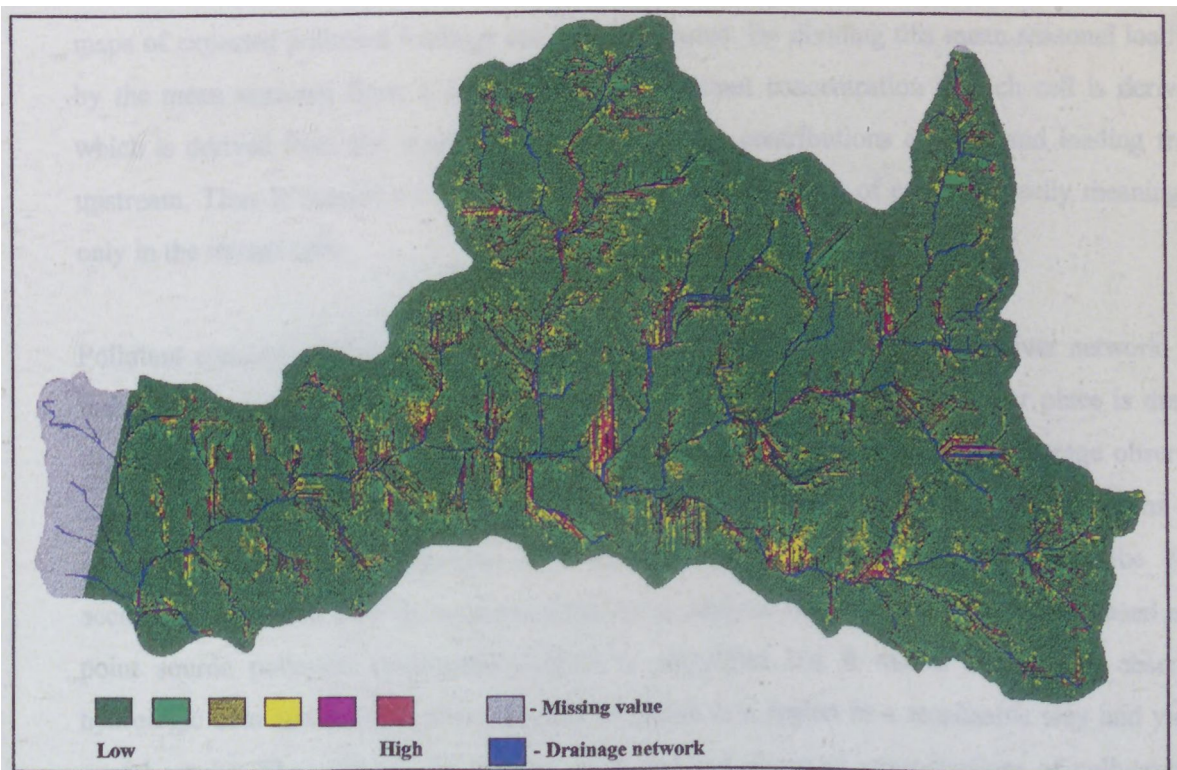


Figure 6.10 : Load of non-point pollutant (nitrogen), using runoff prediction.

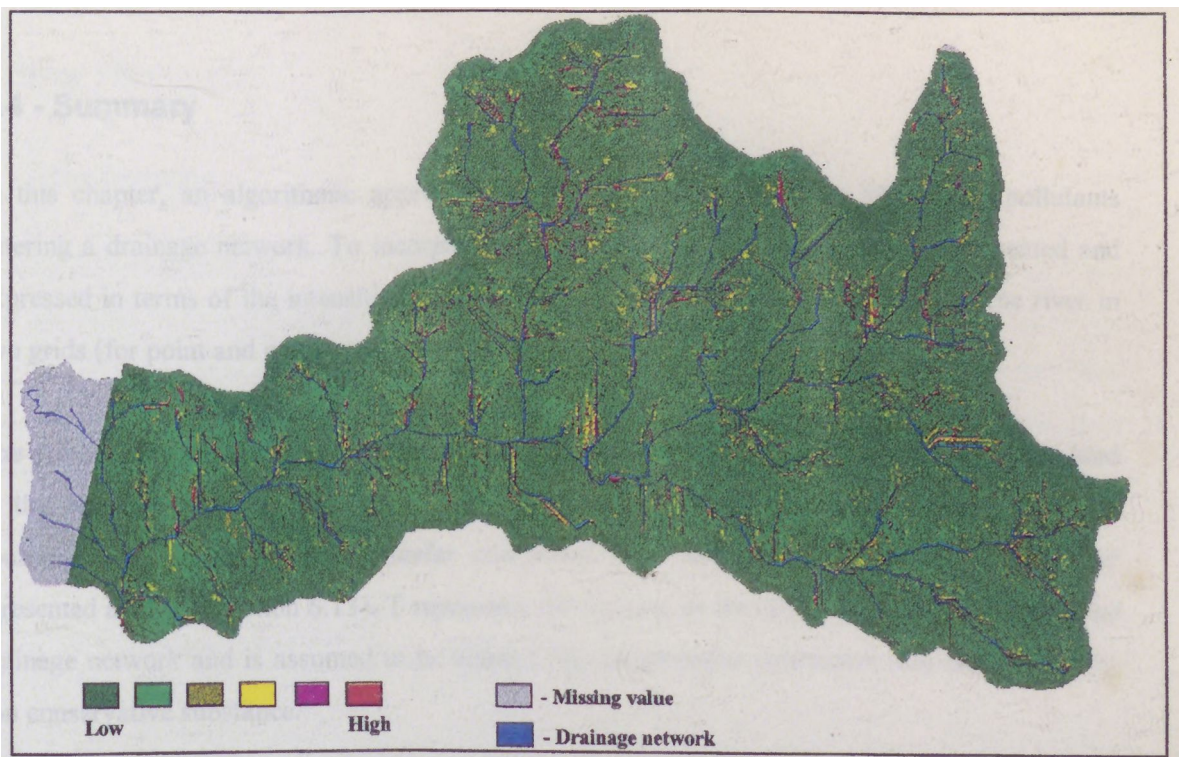


Figure 6.11 : Load of non-point pollutant (nitrogen), without runoff prediction.

Computing the weighted flow accumulation of this loading onto downstream cells until the buffer zone around the drainage network gives the mean seasonal pollutant loading in each cell. Useful maps of expected pollutant loadings can thus be created. By dividing this mean seasonal loading by the mean seasonal flow, a grid of expected pollutant concentration in each cell is derived, which is derived from the weighted average of all the contributions of flow and loading from upstream. Thus is created an expected concentration map, which of course is really meaningful only in the stream cells.

Pollutant concentration is normally sampled at a number of locations in the river network. By making the assumption that the concentration sampled each time at a particular place is drawn from the same water (i.e. that the data are statistically stationary in time), an average observed concentration can be computed for each sample point. The observed average concentrations can be compared with the expected mean seasonal concentrations computed from the flow accumulation model. Like the mean seasonal flow analysis (Chapter Four), this grid-based non-point source pollution assessment method is simplified but it makes use of the observed hydrologic data and the GIS data normally available in a region in a reasonable way and yields useful results. The comparisons between predicted and observed concentrations of pollutants in the Sinos river are all done in Chapter Eight.

6.4 - Summary

In this chapter, an algorithmic approach has been presented to isolate sources of pollutants entering a drainage network. To incorporate these sources, a river buffer zone was created and expressed in terms of the intensities and spatial distribution of the loads adjacent to the river in two grids (for point and non-point sources).

The present river buffer zone model has been developed to allow the transfer of loads from land to the drainage network. The model uses distinct data that differentiate point and non-point sources, and also an internal transfer coefficient from the non-point sources to the river (presented as T in Equation 6.13). T represents the fraction of the non-point sources reaching the drainage network and is assumed to be about 1 for conservative substances and less than 1 for non conservative substance.

This buffer zone approach has important implications for assessing potential water quality as proximal cells to the drainage network appear to be most influential to water quality, modifications resulting in an impact to downstream water quality. In this way, the use of GIS in combination with environmental information provides an excellent means of identifying the major sources of pollutants in a drainage network allowing application of available resources on the most significant pollutant inputs.

7. River processes

7.1 - Introduction

Having described the nature of the substances that can be considered as pollutants (Chapter Five) and the routes by which they may enter in the drainage network (Chapter Six), it now is necessary to examine the various processes that affect water quality in rivers. In this chapter it is described how the pollutant loads entering a river result in a concentration of the pollutant at any given point along a river network. Figure 7.1 shows the principal components of such a methodology.

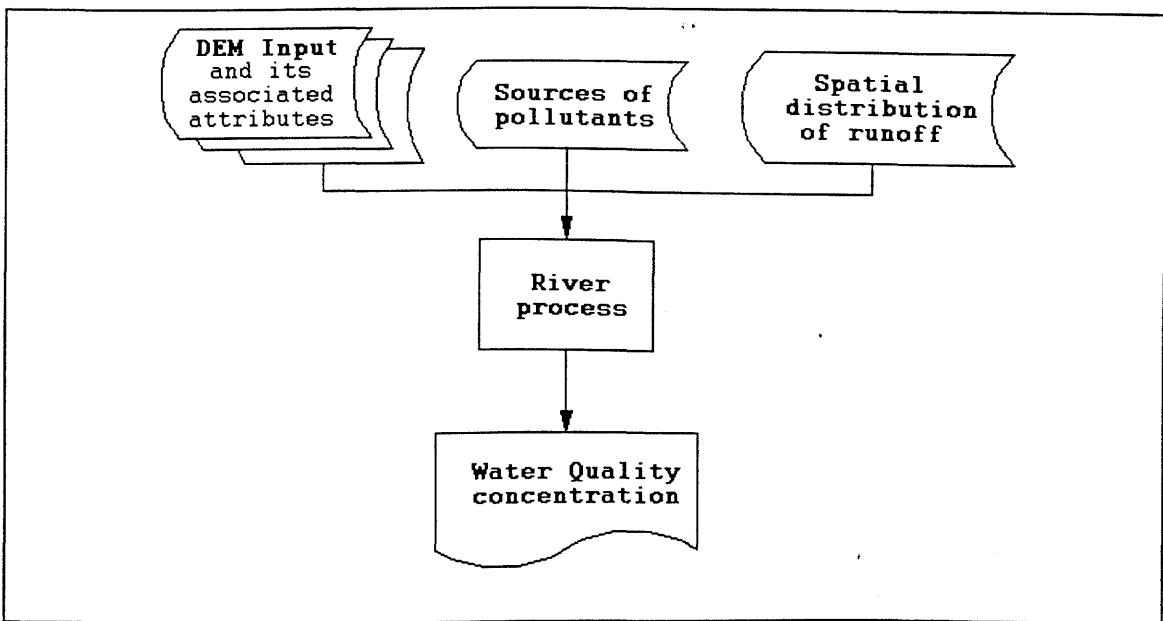


Figure 7.1 : Flow diagram illustrating the operations of river processes.

The water quality model, used here, applies a mass balance approach to calculate spatial profiles of total phosphorus, nitrogen and BOD. The model can also accommodate other pollutants. It is interactive and flexible, and permits the user to alter the location and magnitude of point and non-point loads to the drainage network (This is illustrated for Sinos catchment in Chapter Eight).

The water quality model, used in this thesis, is a steady-state mass balance model, which considers point and non-point sources distributed along of the drainage network (concept of *buffer zone*, in Chapter Six), in calculating the steady state, average pollutant concentration for each of the mixed model cells oriented along the major axis of the drainage network.

The water quality model applied in this thesis was designed for analysis the data for drainage network geometry (Topological table in Chapter Three), mass transport, net losses between cells and loads of pollutants (point and non-point sources). To evaluate water quality response in the drainage network, the user simply selects a land management scenario, reflecting the point and non-point sources of pollutants. The water quality model structure and its linkage to the pollutant loading model is achieved by the use of *buffer zone* concept (Chapter Six).

The differences in water quality projected for different scenarios highlight the insights offered by this coupled model framework. Graphical spatial output is emphasised here for its communication value.

7.2 - Characteristics of river systems

In addition to being a major source of water supply, rivers are also used as a principal means for disposal of sewage. In order to manage a river system and maintain adequate water quality it is essential to understand the mechanisms governing pollution within the river.

Pollutants discharged into rivers whether from point or non-point sources are subject to numerous processes. These processes can be considered from a physical, chemical, and biological perspective. For example Figure 7.2 indicates the effects of a pollutant source on a river and the changes occurring downstream.

Any pollutant present in flowing water moves with the current. The transport involved is called advective transport and its direction coincides with that of the current. This movement in rivers is achieved primarily under the effect of gravity. However, additional effects can also be exerted in large rivers such as, the forces in the curves of a river section and by wind.

The flow in the river can be obtained by several methods (Linsley et al., 1982). One direct method, where a measurement of river velocity U and cross-sectional area A at a specific location gives the flow Q as:

$$Q = U \cdot A \tag{7.1}$$

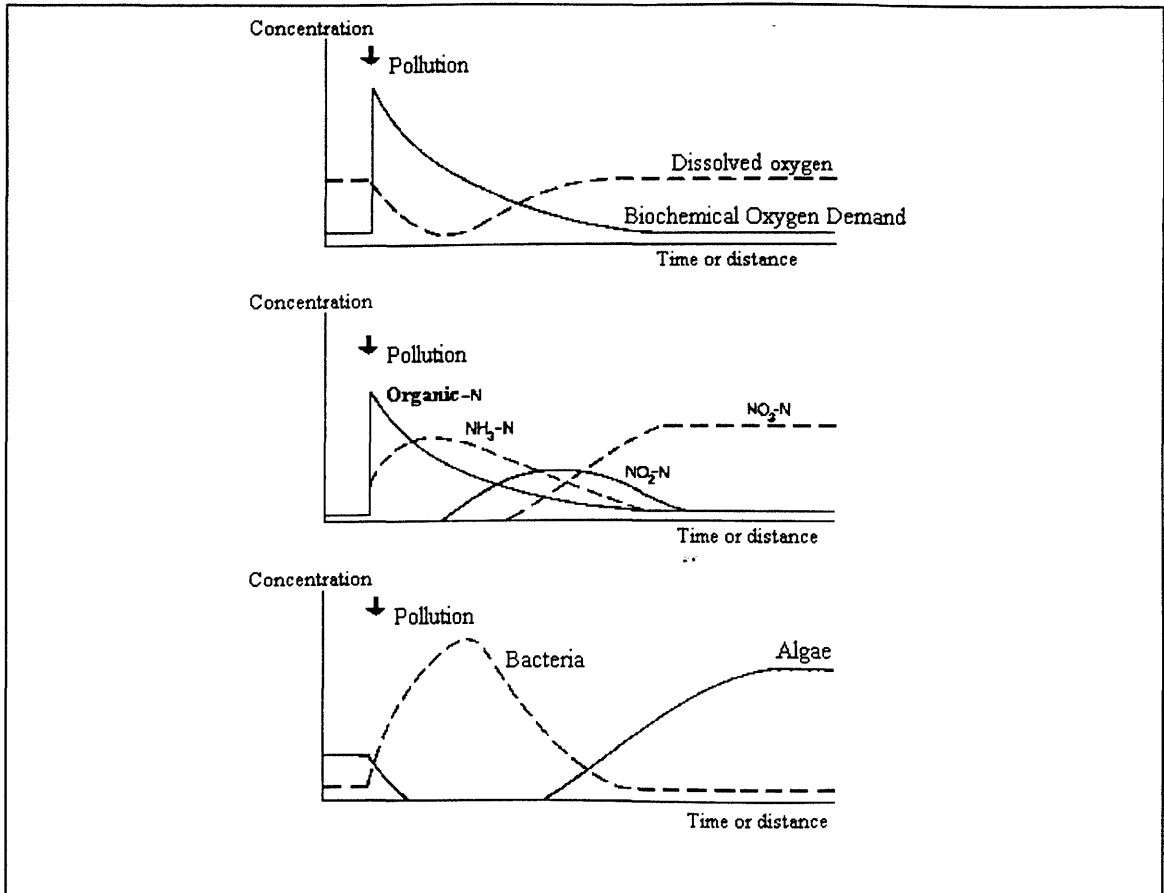


Figure 7.2 - Changes in river water quality.

Source: Unesco/WHO, (1978)

An extra direct method is the use of gauging stations and stage-discharge relationships. In Brazil the Departamento Nacional de Aguas e Energia Eletrica - DNAEE (*National department of water and electric energy*) has established a large number of flow gauging stations throughout the country. At each station a control section or dam is used to measure river stage (height) which is correlated to the flow past the section.

There have also been attempts to estimate river flows empirically from meteorological data, climate and catchment characteristics. Thomas and Benson (1970) carried out a statistical analysis of the relationship between river flow and catchment characteristics. One of the results from this study is:

$$\bar{Q} = a.(DA)^h.(P - 40)^{b_2} \quad (7.2)$$

Where: Q is the annual average flow.

DA is the drainage area.

P is the mean annual precipitation.

a , b_1 and b_2 - empirical coefficients.

In practice, the distribution of water velocity along the river increases with the slope of the river, however this distribution in a river cross-section shows great diversity and, in general, the following conditions apply:

- Velocity is smaller near the bottom, where the roughness of the river bed is the greatest.
- Velocity increases from the bottom towards the middle of the river and towards the surface, being at its maximum near the water surface or on the surface itself.

Of course, the flow (and velocity) varies seasonally. Usually minimum flows are the main concern in water quality studies as those give minimum dilution. An adequate description of low flow, and its consequences, require specification of three properties: magnitude, frequency or return period and duration. Generally, for most project work, the minimum average 7-day flow expected to occur once every 10 yr. is suggested as a project flow. The designation of this flow is given by $Q_{7,10}$.

So, the principal physical characteristics of rivers that are of interest include:

1. Geometry: width, depth.
2. River slope, bed roughness.
3. Velocity.
4. Flow.

With the above properties of the river system defined, it is possible to account the discharge of pollutants into rivers. Such pollutants may include discharges from waste treatment plants, industrial plants, combined sewer overflows, or from agricultural and urban runoff. Pollutants discharged into rivers whether from point or non-point sources are subject to the processes of dispersion (Welty et al., 1984).

The spreading of a pollutant due to the motion of the *molecules* at the interface with the receiving fluid is termed molecular diffusion. This spreading was expressed for the first time in quantitative terms by Fick in 1855 (Welty et al., 1984), who made an analogy between this process and the process of transfer of heat by conduction, to express the amount of substance diffusing through

unit area of a section. According to Fick , the rate of diffusing substance through a unit area of section is proportional to the concentration gradient measured normal to the section, that is:

$$F_i = -D \cdot \frac{\partial C}{\partial x} \quad (7.3)$$

Where: F_i is the amount of pollutant diffusing [L^2/T].

C is the concentration of the diffusing pollutant.

x is the distance measured normal to the section.

D is the diffusion coefficient.

The minus sign is due to the fact that the transfer of pollutants takes place in a direction along the decreasing concentration of the diffusing pollutant. Molecular diffusion process plays a significant role in laminar flows to spread pollutants (Spencer, 1980); however its effects are negligible in comparison to the turbulent diffusion process (described below). So, because in almost all natural rivers the flow is turbulent, the molecular diffusion process is not a dominant process in considering the spreading of pollutants.

The spreading of a pollutant due to the motion of the *fluid particles* in a turbulent flow is termed turbulent diffusion. Fluid particle means the volume of fluid which is so small that, within the framework of the theory of continuum, it can be identified with a point which is displaced together with the surrounding fluid (Spicio, 1967). Similarly to the motion of the molecules, the amount of pollutants diffusing per unit of area of a section per unit of time due to turbulent diffusion (F_i) is expressed in terms of a turbulent diffusion coefficient (ε) and the concentration gradient, that is:

$$F_i = -\varepsilon \frac{\partial C}{\partial x} \quad (7.4)$$

Spreading of a pollutant due to turbulent diffusion is much more rapid than that due to molecular diffusion. In other words, the numerical values of ε are greater than those of D .

An example is runoff from agricultural areas. Following McQuivey and Keefer, (1974) given a constant distributed source and given a river with constant parameters (flow, area, depth) over a given length, the mass balance equation at steady state is:

$$U \cdot \frac{dc}{dx} + K \cdot c = S_D \quad (7.5)$$

Where: S_D is a distributed source [$M.L^{-3}.T^{-1}$].

K is the decay rate [T^{-1}] of the substance.

U is the flow velocity.

Figure 7.3 shows a non-point input load w [$M.L^{-1}.T^{-1}$]. Solution of Equation 7.5, with a boundary condition of $c=0$ at $x=0$, is:

$$c = \frac{S_D}{K} \left(1 - e^{-Kx/U} \right) \quad (7.6)$$

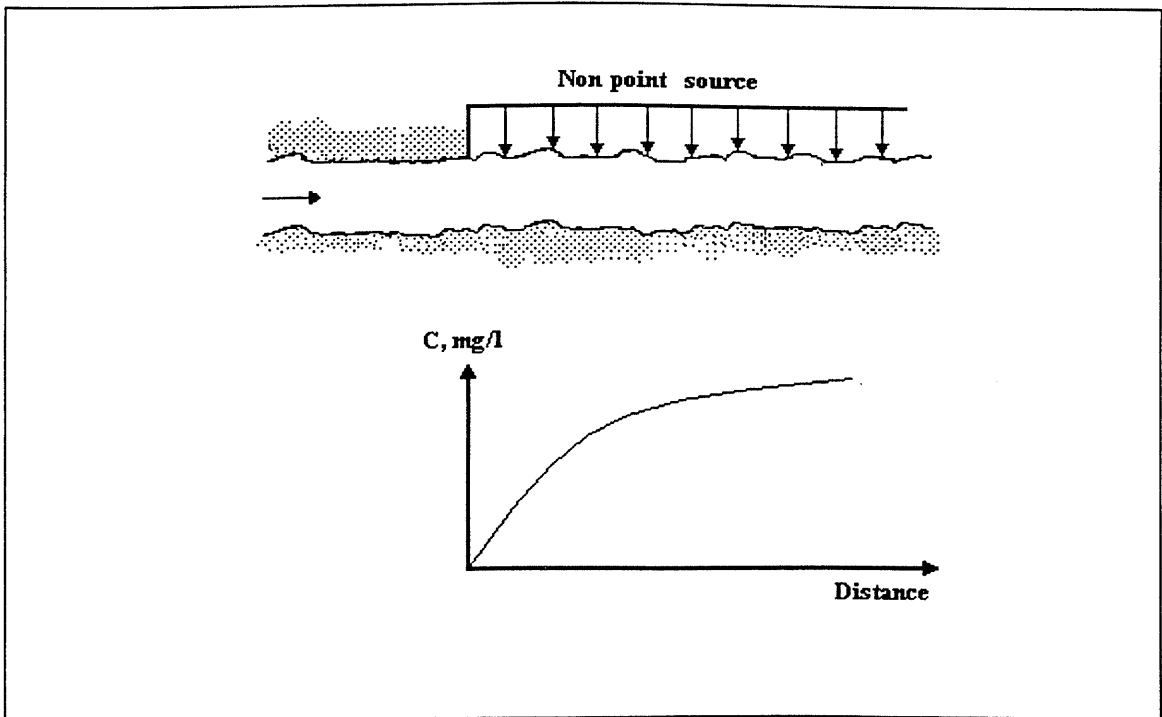


Figure 7.3 : Input of non-point pollution as a distributed source.

For such linear systems, the value of concentration due to multiple sources (point and non-point source) are the linear summation of the individual sources plus the upstream boundary condition.

As an example, for a river with constant flow and velocity subjected to a point source W at $x=0$ and an infinitely long non-point source w originating at $x=0$, the upstream boundary concentration is assumed to be zero, and the water quality response is the sum of the differential equations which govern the concentration c along a river x :

$$c = c_0 \times e^{\left(\frac{-Kx}{U}\right)} + \frac{S_D}{K} \left(1 - e^{-\frac{Kx}{U}}\right) \quad (7.7)$$

Where $c_0 = W/Q$. Also the decay rates for point and non-point sources are assumed equal in the river, that is $K(\text{point source}) = K(\text{non-point source}) = K$.

7.3 - Development of a square-grid transport model

7.3.1 - Mixing cell model

The physical process of mass transport and dispersion in a natural river is quite complex. Any mathematical description of natural systems requires simplifications and abstractions. The approach taken in this thesis is a mixing cell model of the phenomenon of longitudinal distribution of pollutant concentrations.

All the information concerning the loads of pollutants is included in two grids:

1. Point sources (as illustrated in Figure 6.5).
2. Non-point sources (as illustrated in Figure 6.8).

A basic assumption of this model is that once the pollutant load has been input to the river, the concentration is considered a conservative property (even to non-conservative pollutants) though the possibility of seasonal activity, that is, a complete mixing occurs in each cell due to the seasonal scale of the process. So, the concentration of the effluent from a particular river cell is equal to the concentration within that cell.

The basic idea in describing the discharge of pollutants into a river is to write a mass balance equation for various reaches of the river. The balance of mass equation states that the rate of change of mass inside the control volume must equal the mass flux through the control surface, as shown by figure 7.4. So, continuity is expressed mathematically by:

$$\frac{\partial M}{\partial t} = V \cdot \frac{\partial c}{\partial t} = I - O \quad (7.8)$$

Where: $\frac{\partial M}{\partial t}$ is the rate of change mass storage.

$I-O$ is the net flux through control surface.

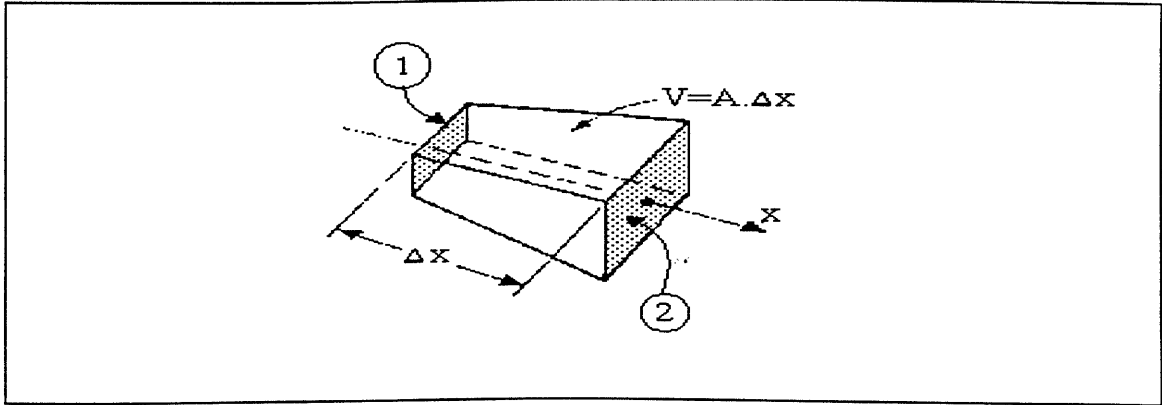


Figure 7.4 : Mass balance components.

For the purpose of derivation, we only consider the control volume represented in figure 7.4 based in one dimensional process. The transport of the pollutant by the current is account by:

$$\frac{\partial M}{\partial t} = Q_1 \cdot c_1 - Q_2 \cdot c_2 = Q \cdot c - (Q + \Delta Q)(c + \Delta c) \quad (7.9)$$

This approach features a mixing cell model of the phenomenon of longitudinal dispersion. Figure 7.5 indicates a steady uniform flow Q occurring in an open channel in which it is imagined that the river is composed of a series of cells. Initially, the concentration of some pollutant is zero in all cells $1, 2, \dots, n$, as the concentration of pollutant enters *cell 1* it suddenly changes from zero to C_1 , and thereafter remains at that value.

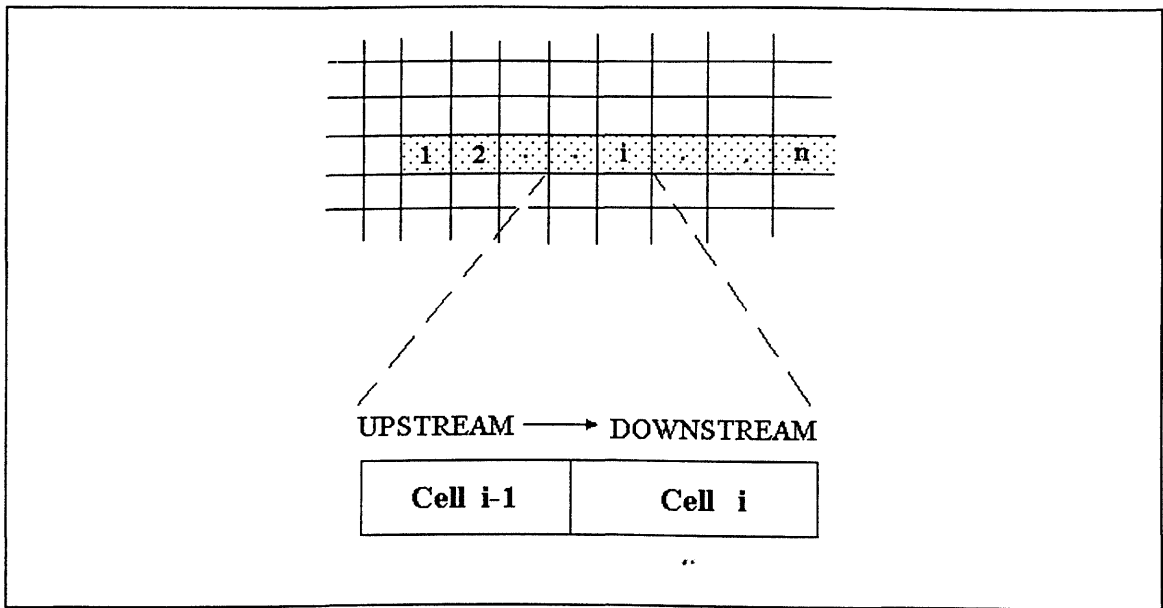


Figure 7.5 : Mixing cell model.

The basic equation is developed by applying the principle of conservation of mass. A mass balance is taken about a cell i (Figure 7.5) along the longitudinal axis of the channel. It is assumed that vertical and lateral uniformity exist. The pollutant enters the river from overland flow (non-point pollutant load) and point sources (groundwater pollution is not considered here). Consequently, in a given river, using the load data which differentiates between point and non-point source, the downstream concentration c_i is:

$$c_i = \frac{T \cdot (P + NP + c_{i-1} \cdot Q_{i-1})}{Q} \tag{7.10}$$

Where: c_{i-1} is the upstream concentration.

Q_{i-1} is the upstream flow.

P is the point source contribution.

NP is the non-point contribution.

T is the transport coefficient.

$$Q = Q_{i-1} + Q_p + Q_{NP} .$$

T reflects the transport of the pollutant loads once they have reached the drainage network. The physical significance of T is that during low flows one can expect values less than 1 due to

sedimentation and/or biological assimilation by organisms; to be about 1 on a yearly basis; and greater than 1 during periods of high flow (erosion, or re-suspension).

7.3.2 - Interface with drainage network topology

The modelling approach presented here makes a number of simplifications of the natural system. For instance flow routing in the channel must incorporate network topology, that is searched in the routing algorithm to define contributing river side cells and major tributary inputs to produce cumulative pollutant concentration downstream in the channel.

The drainage network is represented geometrically as a series of chained co-ordinate pairs, known as links or arcs, that are connected at points of intersection, termed junctions (see Chapter Three). Essentially, this network indicates the connections between and among links. In order to implement equation 7.10 for each link of a drainage network we use the topological table (illustrated in Table 3.1 and already explained in Chapter 3) and an algorithm for aggregating all upstream information, calculated from this table, derived from connected graph theory (Minieka, 1978).

Basically the algorithm works by recursively searching the network topology code TC for:

$$TC_i = 0 \text{ and } TC_{i-1} > 0 \quad (7.11)$$

If the link i satisfies Equation 7.11 the algorithm starts at the upstream junction co-ordinates applying the mixing cell model of Equation 7.10. Then the flow vector (aspect) and drainage network grids are scanned to identify the next river cell. The algorithm applies Equation 7.10 again in the next cell on the link i . Once the downstream junction co-ordinates are met, all cells in the link i have been identified and processed. Finally the link i is deleted from the topological table and:

$$TC_{i-1} = TC_{i-1} - 1 \quad (7.12)$$

If TC_{i-1} now satisfies equation 7.11, the process moves back through the recursion until some TC_{i-j} is found not satisfying equation 7.10 and the algorithm starts again.

As an example, Table 7.1 shows the above operations applied to the link number and topologic code presented in Table 3.1, describing the aggregation of information (loads of point and non-point sources) in each link through the drainage network. Each step shows which link must be processed in order to aggregate information to the downstream links, resulting in the sequence: 3, 5, 6, 4, 2, 7, 1.

Link Number	1	2	3	4	5	6	7
Topologic Code	2	2	0	2	0	0	0
	2	1	...	2	0	0	0
	2	1	...	1	...	0	0
	2	1	...	0	0
	2	0	0
	1	0
	0

Table 7.1 : Sequence of operations applying Equations 7.8 and 7.9.

Figure 7.6 shows the application of the mixing cell model for the drainage network. The program that implements the mixing model together with the use of topologic information (Equations 7.10, 7.11 and 7.12) is given in the Appendix.

In this approach, the drainage network is manipulated so that each stream is represented by a single link, and the links are flow ordered so that the 'from' node is upstream and the 'to node' is down stream (see Table 3.1 in Chapter 3). Each river link is enclosed within its associated buffer zone for point and non-point loads. Drainage network are delineated from each junction so at most a node can have two links flowing into it and one flowing out of it.

After finding the 'from node of a link (applying Equation 7.11) the next step is to that load (point and non-point) which comes into the link by drainage from the surrounding buffer zone. Pollutant concentration, within the link, is computed by applying equation 7.10 to the cell inside the stream, and it also include a component representing exchange of pollutant loads between the stream and the underlying *buffer zone*. One advantage of this algorithm is that network links can be divided

by the length of the stream and loads of pollutants added progressively to the discharge along the path of the stream.

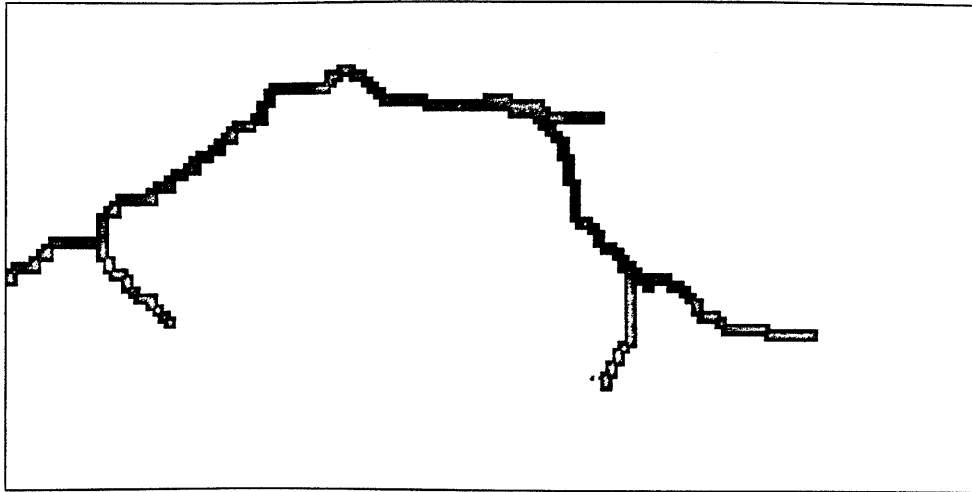


Figure 7.6 : Spatial distribution of pollutant concentration (lighter tones indicate greater values).

In such computations, there is a choice between sequencing the computations "*first in space and then in time*" or "*first in time and then in space*", in other words, doing all the computations for a given link through time and then moving to the next link, or doing the computations for all links for one time interval before moving to the next time interval.

In our case the main interest is regional hydrologic studies where the links do not influence one another the "*first in space then in time*" method works best. For more localised hydraulic analyses where water level in the river influences groundwater levels, the simultaneous nature of the interactions makes the "*first in time then in space*" method necessary. The nature of the process interactions governs the computational sequence. Full application of this approach for Sinos catchment data can be seen in Chapter Eight

7.4 - Conclusions

The modelling approach presented here is constructed using a very simple hypothesis concerning the origin (point and non-point sources) and the mode of transport (topological information) of pollutants. The model is proposed for entire catchments, taking into account both the causes

(intensity and spatial distribution of the sources - contributing land uses) and the consequences of pollution to surface waters.

Possible sources of error include errors in the spatial distribution of land uses in the flow generation and in the mass discharge calculation process. However, despite these present weaknesses the origin of a pollutant load, and the relative importance of each type of contributor, can be assessed, and the impact on water quality of changes in land use can be predicted.

In conclusion, although the above modelling approach is very simple, it should be emphasised that the generality of the mixing model combined with the topology of the river network makes it useful for any catchment with limited data availability.

8. Case study: Sinos catchment

8.1 - Introduction

This chapter demonstrates how the theory presented in the previous chapters can be applied to a relevant practical problem. The case study illustrates a real application of the system to planning decisions in the Sinos catchment, southern Brazil. The aim of this chapter is not so much to thoroughly describe the theory behind the case study or to analyse all aspects of the problem at hand, but to show how the GIS/modelling integration framework, proposed in this thesis, can be applied in practice. Thus the case study is used to show how to apply this framework and how meaningful conclusions can be drawn from it.

If a model is to be used, the user must have confidence in it. To some extent, this is a subjective procedure aimed at establishing that the assumptions made by the model about the real world are reasonable, and that the model reflects adequately the essential features and behaviour of the real world that are relevant to the objectives of the user. However, this confidence analysis, or validation of a complex distributed system, is not simply a comparison of model predictions and real world observations, given a permitted error bound. Decisions on the criteria for rejecting a model should always be made and one should consider that while a 30% error may be perfectly adequate for one user it might be totally unacceptable for another.

The validation of complex models causes several problems, which have been discussed by a number of authors (e.g. Loague and Freeze, 1985; Beven, 1989). Complex models do not always give results that are as correct as one would expect given their conceptual structure. One of the reasons for this is the need for model boundary conditions, for example, specifying initial soil moisture conditions and parameters, which vary both in time and space (Loague and Freeze, 1985). Beven (1989) discusses problems such as the spatial variability of hydrologic properties and precipitation processes, the balance between space and time lumping, model complexity and the complexity of the physics of erosion and transport process. Because of these problems, and based on comparisons of model performance, Loague and Freeze (1985) claimed that simple models can often perform as well as or better than more complex models, although complex models may give more insight into the physical processes and have larger predictive capabilities.

8.2 - Evaluation of system behaviour

The final stage in model evaluation should be to establish to what extent the model and the program implementation yields an accurate representation of reality. This evaluation can only be undertaken if there is comparable data available. Although some attempt has been made (along some previous Chapters) to determine how well the system predicts the various outcomes of the modelled processes, this cannot be achieved satisfactorily due to the lack of data.

In principle, the data used was obtained from maps and remotely sensed images that were stored in a GIS. The approach assumes that all data used are error free. Clearly this is not the case and we need to pay serious attention to the role of errors in GIS and how they accumulate when data are fed through models. This issue is considered further in the following chapter.

The purpose of this section is to present a summary of the results obtained during simulations, which provide answers to a range of management options. As the results obtained for these scenarios have not been validated they must be regarded as theoretical rather than operational, and serve to be illustrative of the potential of the approach only.

8.2.1 - General assessment

The critical areas for BOD is shown in Figure 8.1 (see Chapter Five). Figure 8.2 shows the nonpoint discharges for BOD in the drainage network, routing throughout the terrain (see Chapter Six). Figure 8.3 shows the intensities and spatial distributions of concentrations for BOD in the drainage network for non-point loads only (see Chapter Seven).

Problems arises when we have to compare point sources pollutant loads (flow and concentration usually expressed in $\text{m}^3.\text{s}^{-1}$ and $\text{mg}.\text{l}^{-1}$) with non-point loads (basically an index that reflects all the interactions over the terrain, explained in the preceding chapters). The only information available to estimate point loads in the Sinos catchment, are comparable to the data presented in Tables 2.4, 2.5 and 2.7. Therefore, the dimensionality of the loads (*point* - concentration and flow, *non-point* - index) is an important issue. Consequently, there is a need to obtain a practical and quick method to synthesise point loads so they can be compared with non-point loads. The solution adopted can be summarised in three steps:

- Perform a linear regression between the runoff index (y) (generated in Chapter Four) and available flow values (x) (Table 2.2). Procedure similar to what we did in Chapter Four. The results are shown in Table 8.1 and Figure 8.4.
- Translate the point sources concentration (Table 2.4 and Figure 2.14) into a set of GIS indices, in a similar manner to Chapter Five (see Table 5.2, for example).
- Obtain the point load ($\text{Point load}_{\text{index}} = Q_{\text{index}} \times c_{\text{index}}$).

	# 1	# 2	# 3	# 4	# 5	# 6	# 7	# 8	# 9	# 10
JAN	44.8	39.8	39.1	37.3	35.9	35.5	29.8	22.2	18.3	2.5
Flow index	14	14	13	13	14	13	13	13	12	10

$R^2 = 0.828$

$y = a.x + b$

Where : y - flow index

x - flow at river gages in Sinos' river. (Average values at summer season).

	<i>Coefficients</i>	<i>Standard Error</i>	<i>t Statistic</i>	<i>P-value</i>	<i>Lower 95%</i>	<i>Upper 95%</i>
a	0.085326	0.013737	6.211291	7.33E-06	0.053648	0.117004
b	10.29586	0.451078	22.825	9.73E-15	9.255675	11.33605

Table 8.1 : Results of a linear regression between the runoff indexes and flow values.

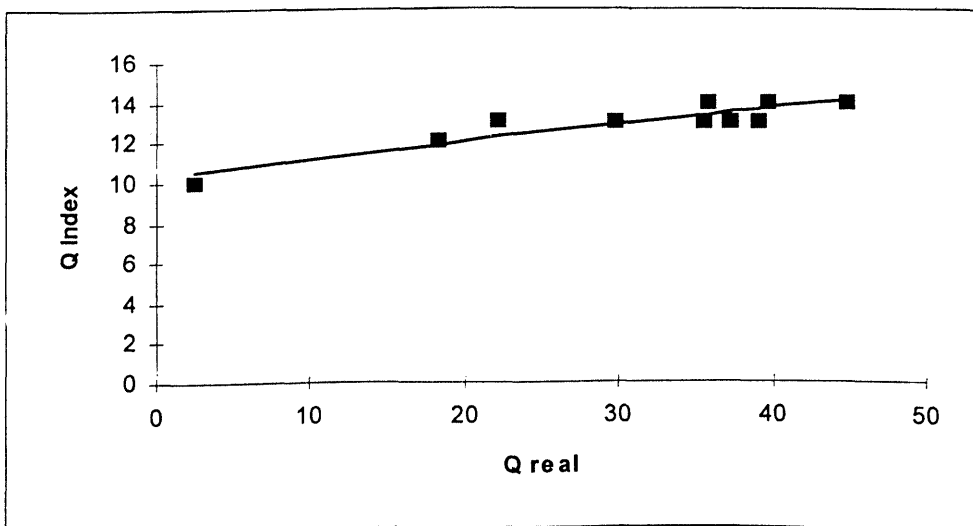


Figure 8.4 : Predicted and observed runoff indexes ($Q.\text{Index}=10.30+0.08*Q.\text{real}$).

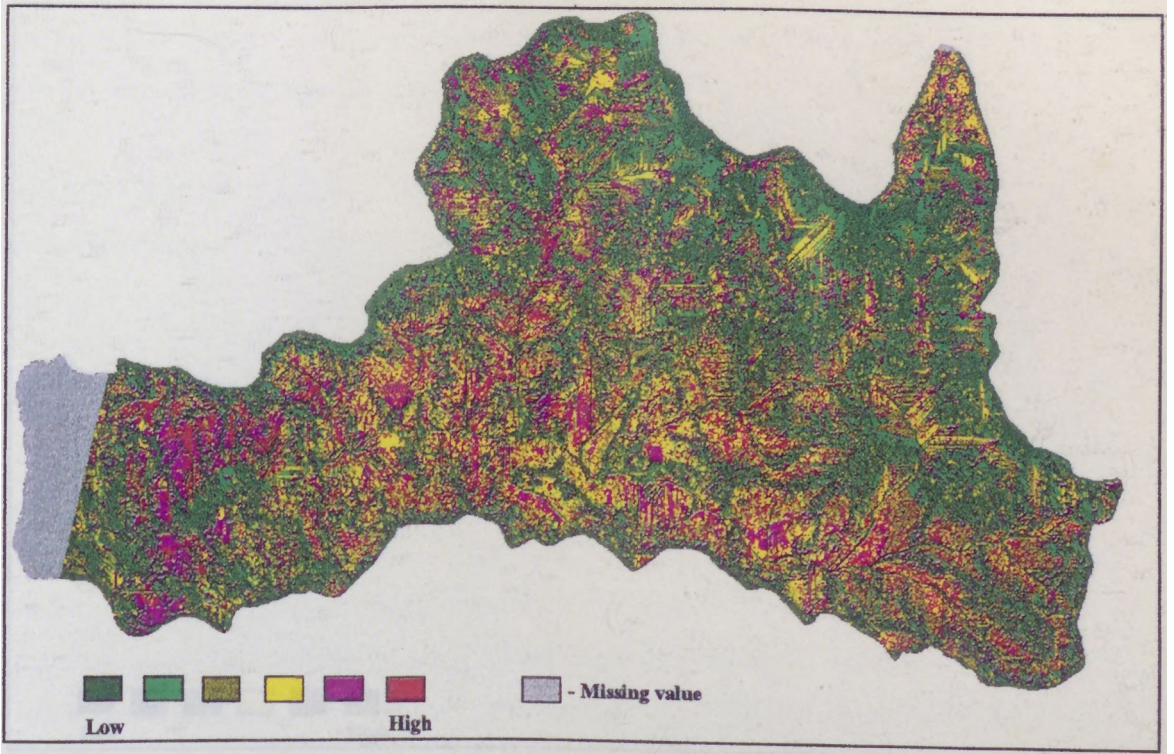


Figure 8.1 : BOD critical areas for Sinos catchment.

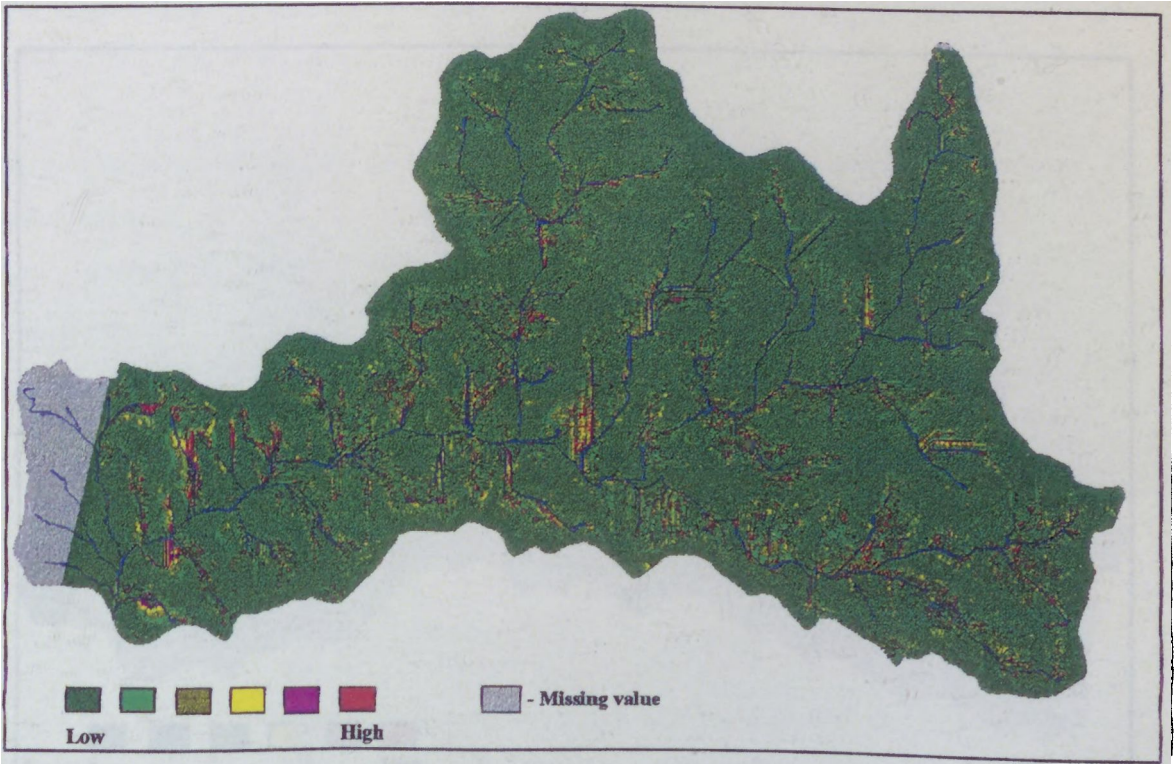


Figure 8.2 : Load of non-point pollutant (BOD).

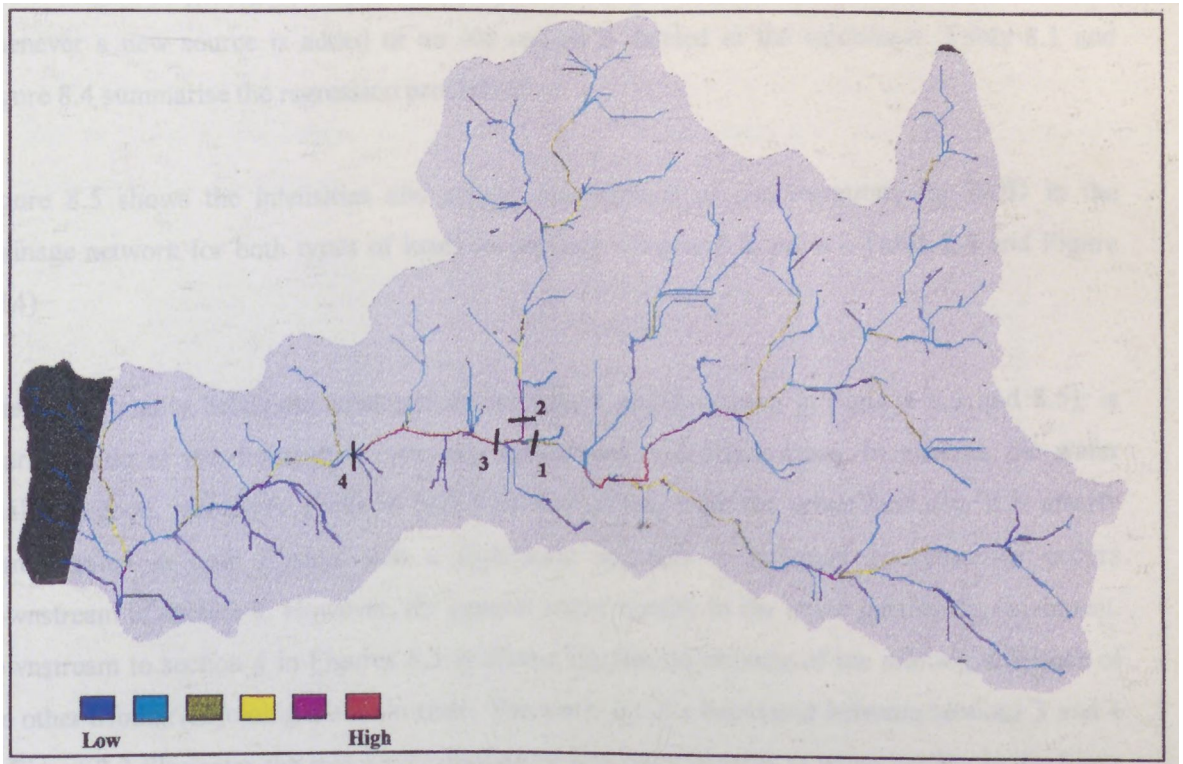


Figure 8.3 : Intensities and spatial distribution of BOD concentration considering only non-point loads.

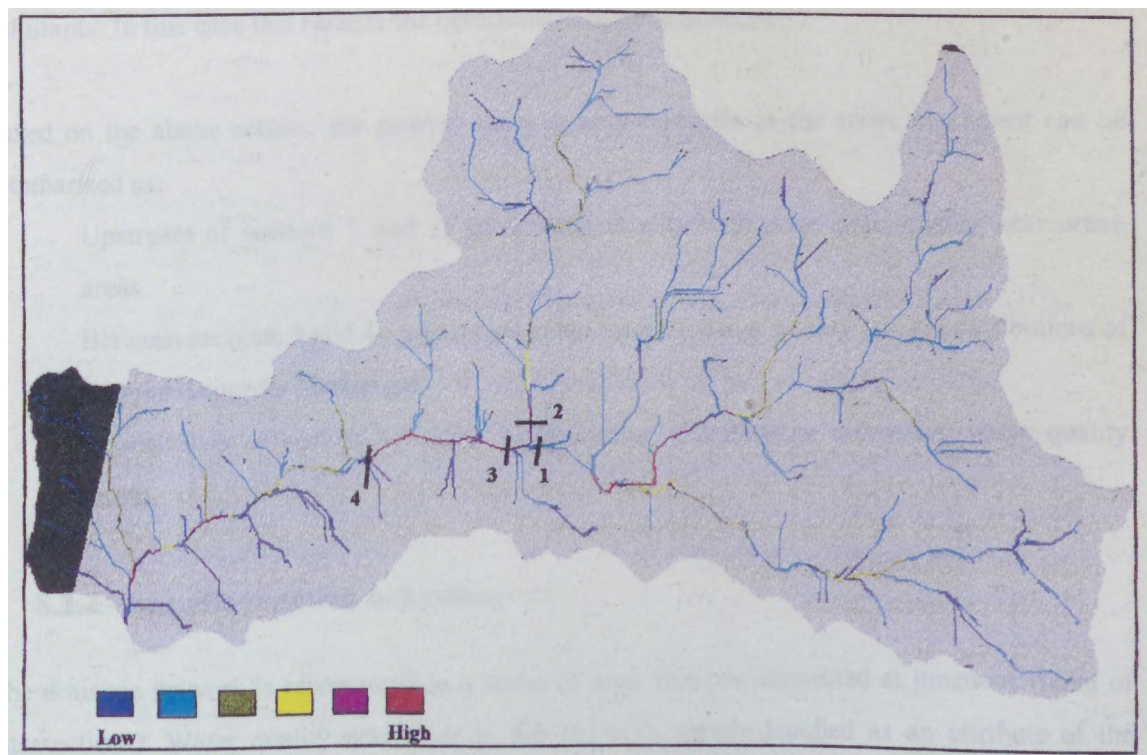


Figure 8.5 : Intensities and spatial distribution of BOD concentration for both types of loads.

While the above procedure is open to question on physical ground, it allows a quick update whenever a new source is added or an old source is deleted in the catchment. Table 8.1 and Figure 8.4 summarise the regression procedure.

Figure 8.5 shows the intensities and spatial distributions of concentrations for BOD in the drainage network for both types of loads (*non-point* - Figure 8.2, *point* - Table 2.4 and Figure 2.14)

The water quality behaviour upstream in sections 1 and 2 (shown in Figures 8.3 and 8.5), is characteristic of the drainage in forested, agricultural and urban areas. In general, the water quality is good, with some peaks of high values, resulting from the urban land use. It is clearly demonstrated in both Figures that a significant increase in pollutant concentration occurs downstream of section 3. However, the general water quality in the lower part of the catchment, downstream to section 4 in Figures 8.3 is almost unaffected because of the diluting influence of the other tributaries joining the main river. The water quality behaviour between sections 3 and 4 in Figure 8.3 illustrates the major contribution of non-point sources to water quality in the Sinos catchment, due mainly to agricultural activities. On the other hand, the worst water quality was noted downstream of section 4 in Figure 8.5, due a large increase in the concentration of pollutants. In this case this reflects the contribution of point sources.

Based on the above results, the general water quality response in the entire catchment can be summarised as:

- Upstream of sections 1 and 2: good water quality with some poor quality near urban areas.
- Between sections 3 and 4 : a decrease in the level of water quality due to contributions of non-point sources discharges.
- Downstream of section 4: Major point source contributions decreasing water quality levels.

8.2.2 - Specific junction behaviour

The drainage network is represented as a series of arcs, that are connected at junctions (point of intersections). Water quality behaviour in this thesis is mainly handled as an attribute of the drainage network. For this reason, the discussion of junction behaviour is presented here.

A steady state condition is assumed at the junction by using Equations 7.11 and 7.12 that implicitly apply the continuity equation (a mixing model, in this case) at the junction. However, Equations 7.11 and 7.12, that were initially used to analyse the topology of the network, are also used to transport the downstream concentration of the upstream links until the upstream section of the next link. This behaviour is illustrated in Figure 8.6.

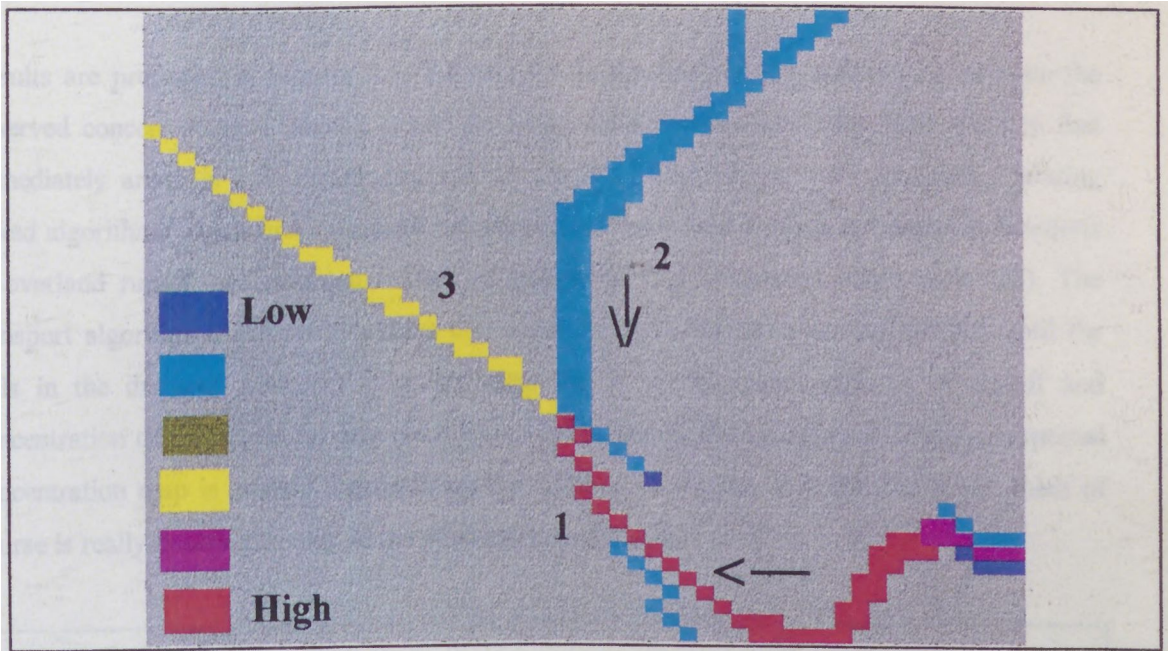


Figure 8.6 : Water quality behaviour at the junction.

Figure 8.6 indicates a portion of the drainage network with two links upstream (1 and 2) and one downstream (3). At the upstream boundary of link 3, Equation 7.10 is applied and in this case the concentration is reduced due to the dilution effect of the link 2, which shows a negligible concentration of the substance in question. In this way, the complete drainage network profile can easily be generated.

8.2.3 - Comparing observed and simulated pollutant concentrations

The evaluation of the system also involves a comparison of calculated and measured pollutant concentrations. This is achieved by the application of graphical and numerical comparisons. Similarly to what we did in Chapter Four, the pollutant concentration can be related to a index via an empirical equation as a regression equation.

Therefore we can use the distribution of the pollutant samples in Sinos catchment (Figure 2.20 and Table 2.7) and our potential of pollutants index map to determine this relationship (i.e., as a

regression model) and then create a spatial pollutant concentration map. We have data from 34 samples within Sinos catchment, as shown in Table 2.7. To find the values of concentration index we have to move a mouse to the same position of the samples in the drainage network and read the data value. Once we finished creating the pair of values file we can make the regression analysis.

Results are presented in Figures 8.7, 8.8 and 8.9 in the form of XY scatterplots between the observed concentrations (Table 2.7) and the simulated concentration index. The question that immediately arises is how meaningful are the results. These values were produced operating linked algorithms which first calculates key elements of over land budgets (*Production functions* of overland runoff, sediments and loads of pollutants that calculates within each cell). The transport algorithm (*Transfer functions* that move the pollutant from an isolated cell until the cells in the drainage network) then integrates the predicted spatial patterns of runoff and concentration of pollutants for any cell within a simulated drainage network. Thus an expected concentration map is created (representing the C.index of Figures 8.7, 8.8 and 8.9), which of course is really meaningful only in the drainage network cells.

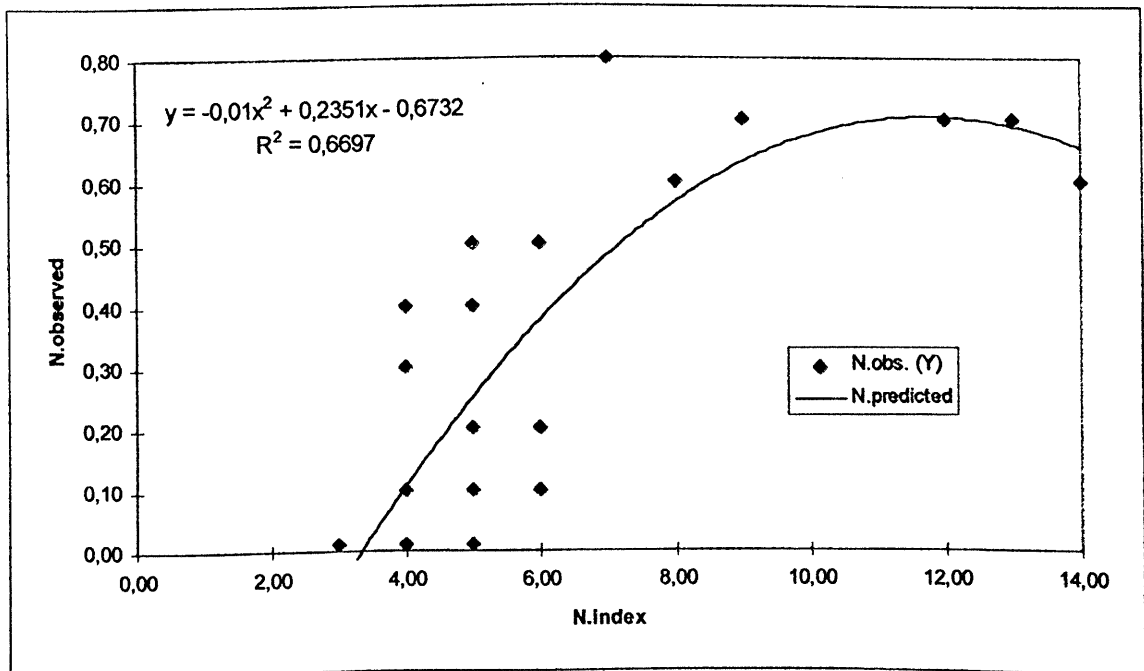


Figure 8.7 : Observed (N. obs.) and simulated (N. index) Nitrogen concentration for the Sinos catchment.

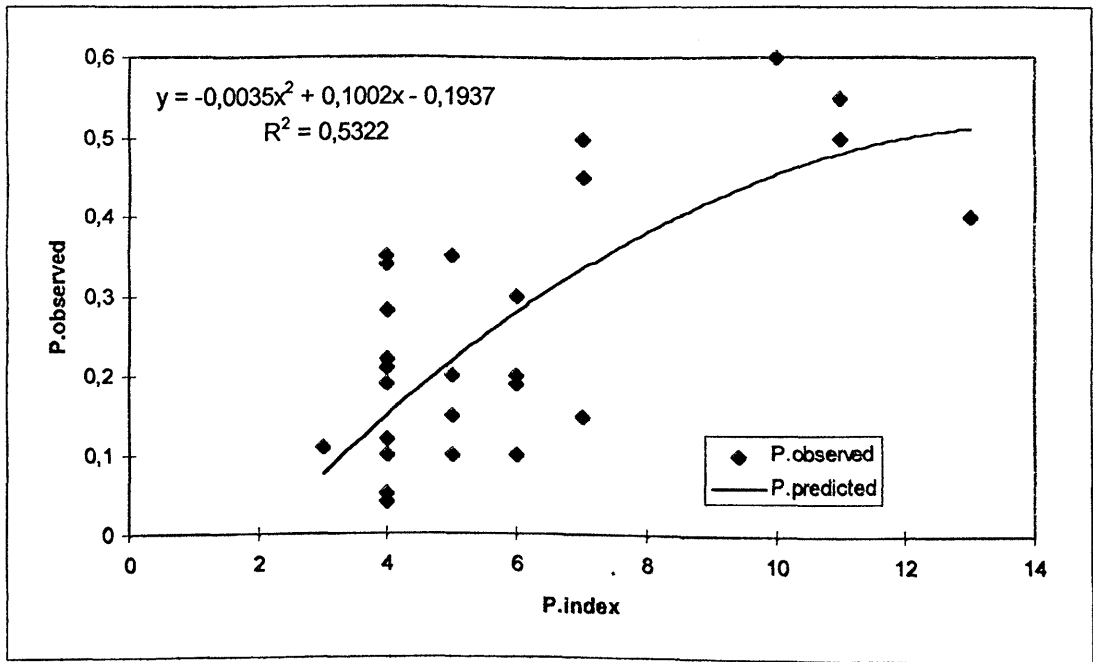


Figure 8.8 : Observed (P. obs.) and simulated (P. index) Phosphorus concentration for the Sinos catchment.

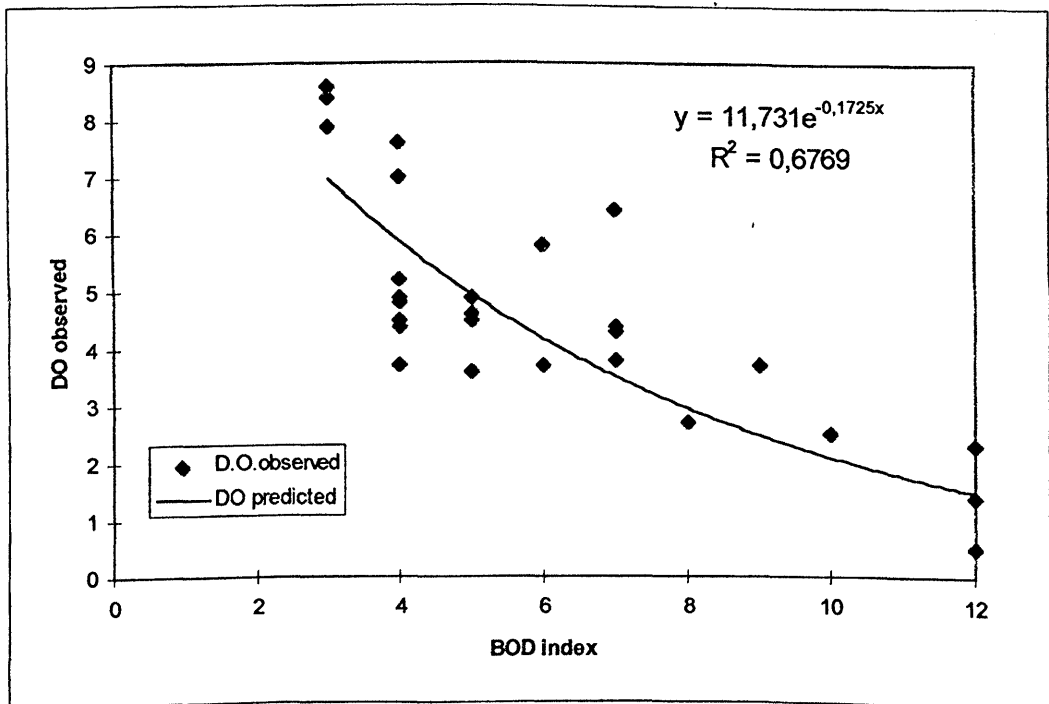


Figure 8.9 : Observed (DO. obs.) and simulated (BOD. index) concentration for the Sinos catchment.

Despite the differences between observed and simulated pollutant concentrations the incorporation of hydrological models with GIS introduced additional problems. To produce the preceding results, we had to aggregate the inputs and model parameters (each one with their own spatial variability), the scale being modelled and the representation of the hydrological process at this scale.

The algorithms in the distributed models used in this thesis are often based on an understanding of processes at the scale of laboratory or small catchments (from the order of hundreds of square metres - *laboratory scale*) where such characteristics as saturated hydraulic conductivity are well known. We are concerned here with the Sinos catchment (around 4000 km² - *management scale*). So, what happens to model structure and parameterization when element size increases from the order of *laboratory scale* to the *management scale* ?

In looking at the problem of scale in more detail, we can observe that to produce the pollutant concentration index (Figures 8.7, 88 and 8.9) Digital Elevation Model (DEM) of Sinos catchment are used to define element network (Flow vectors - see Chapter Three) and hydrological point data (e.g., precipitation, land use and soil characteristics based in DEM cell size) providing the input for the model simulations. The first thinking is that many of the scale related problem outlined above could be overcome simply by using a smaller cell size, since in most cases the spatial variation of topography is known at a much finer resolution than any hydrological data. Therefore, as the cell size is reduced, two possible scenarios are considered. In the first, the topography is assumed to be a useful surrogate for the dominant hydrological processes so a finer spatial resolution increases the information content. In the second case, hydrological processes are dominated by factors such as soil characteristics, geological structure or flow paths which are not related to topography. Thus, a finer spatial resolution does not increase the level of hydrological information.

Grayson et al., (1992) illustrated that it was possible to obtain similar fits to outflow hydrographs for different combinations of model parameters, but the distributed values of flow depth and velocity were vastly different. In his paper the parameters were “effective” in that they represented the input/output relationships, but the internal estimates of flow from the model were simply values that, at the scale of integration assumed by the model, provided satisfactory estimates of catchment outflow but were not true reflections of the catchment behaviour. This problem of different parameter combinations yielding similar output can be recognised in our case study. This points to the importance of analysing distributed model behaviour, rather than an

integrated value such as runoff or pollutant concentration, when assessing the performance of distributed model.

It is generally accepted that tools are needed to address the issues facing catchment managers but the preceding problems indicate that these should not be addressed by the combination of distributed hydrological models with GIS. The development of distributed models specifically designed to operate at the larger scale is an area of research which may yield “hydrologically defensible” results but in the mean time, alternative strategies are required.

There is a need for better data, hence better model forecast and in the desire for quantitative estimates (such as shown in Figures 8.7, 8.8 and 8.9), no matter how scientifically dubious, from models of the type discussed herein. In some cases, the framework used in this thesis can provide a qualitative understanding of distributed catchment response and the relative change in responding resulting from altered spatial characteristics (i.e., the patterns of catchment behaviour - see next section) but not quantitative estimates because of the problems already discussed. Patterns of catchment behaviour, however, can often be provided by much simpler methods than distributed parameter hydrological models. Traditionally, hydrological information has been provided in a quantitative form but as the type of information required becomes more complex it must be recognised that we rarely have models that can provide sound, quantitative estimates. We use the problem of pollutant dispersal by surface runoff on the Sinos catchment in southern Brazil as illustration of this approach. Nevertheless, given the lack of data at Sinos catchment as a whole and our current ability to represent this system, the approach provides a second-best alternative, because, for this example, the simple pattern approach is able to capture the basic behaviour of the process in question. Such approach may be undertaken within the GIS environment.

8.2.4 - Estimating the effects of spatial changes in land use

In this section scenarios of future cover crop in Sinos catchment will be evaluated. Consider the following hypothetical situation. The Environmentally Friendly Tannery Corporation presented a proposal to build a new industrial district in Igrejinha county (see Figure 1.4 to know where is Igrejinha). However, they proposed to build not only on their own lot but also on adjacent county owned conservation land. From the corporation standpoint, this was an excellent site for the industries because of its location at a major motorway with little competition and located in a county that has been growing in the last two decades (Table 1.3). But, the proposal was at odds

with efforts of the DMA - Departamento do Meio Ambiente (Department of Environment of Rio Grande do Sul) to maintain the land along the river, which includes the land parcel under corporation consideration, and to provide access for a river front park. A possible solution for these two parties was to allow development of the new industries while maintaining part of the land as a public park.

The modelling framework can be applied both in the evaluation of project impacts to select specific alternatives and in the planning process to minimise potential adverse impacts in future projects.

The system is used by evaluating the expected future condition of water quality 'with' the scenario of a new industrial district in Igrejinha county and 'without'. The level of pollutants is similar to those given in Table 2.4. The results for the 'without' and the 'with' scenarios are shown in Figures 8.10 and 8.11 for the BOD pollutant index.

The difference between the 'without' and the 'with' scenarios can be identified considering the drainage network upstream of section 2 until Igrejinha county. The negative change (increase of red areas in Figure 8.11) affects all the Igrejinha valley until the junction with Sinos river. These changes can be visualised if we display the percentage of difference between the 'with' and 'without' evaluations. The percentage change was calculated as:

$$\text{percent change} = \frac{\text{'with' - 'without'}}{\text{'without'}} \quad (8.1)$$

A summary of changes in Sinos catchment calculated by Equation 8.1 is shown in Figure 8.12.

Others scenarios that can be analysed with the proposed framework may also be stated in general terms in order to provide the flexibility needed to respond to future events whose details cannot be anticipated when the policies were developed. For example, the syntax of these statements can be given as:

The Rio Grande do Sul state government will provide a 50% subsidy to farmers to use all high-quality agricultural land in Sinos catchment.

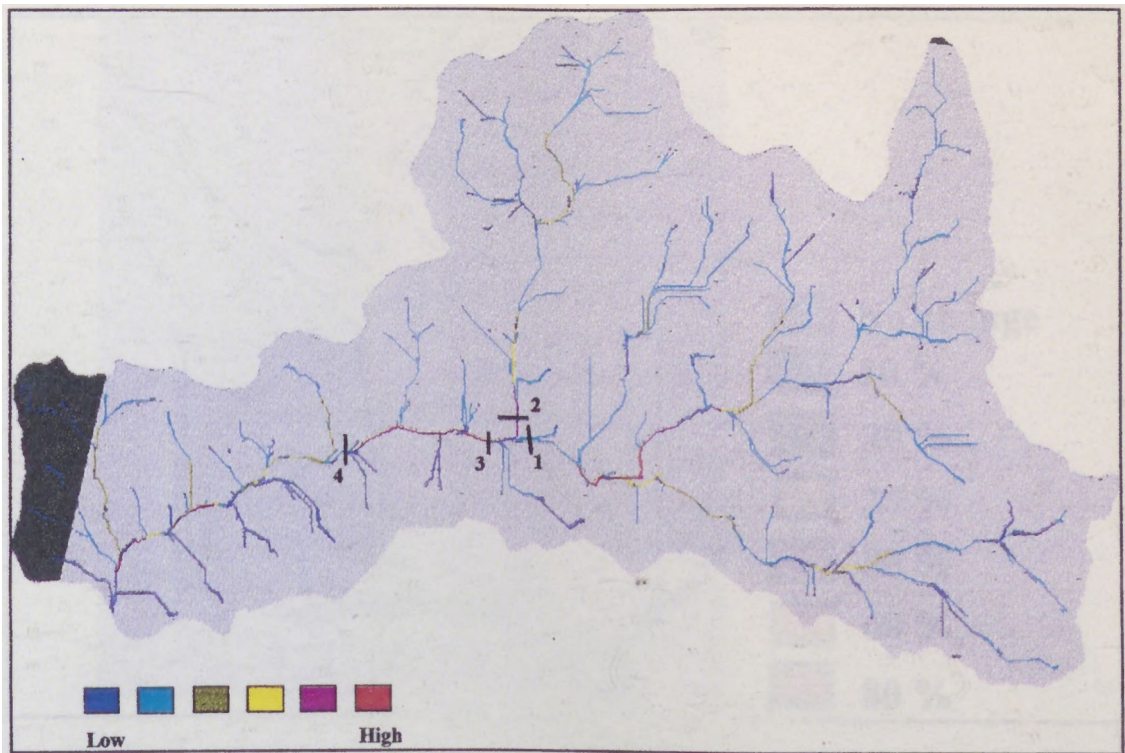


Figure 8.10 : Intensities and spatial distribution of BOD index considering both types of loads (point and non-point) and 'without' scenario.

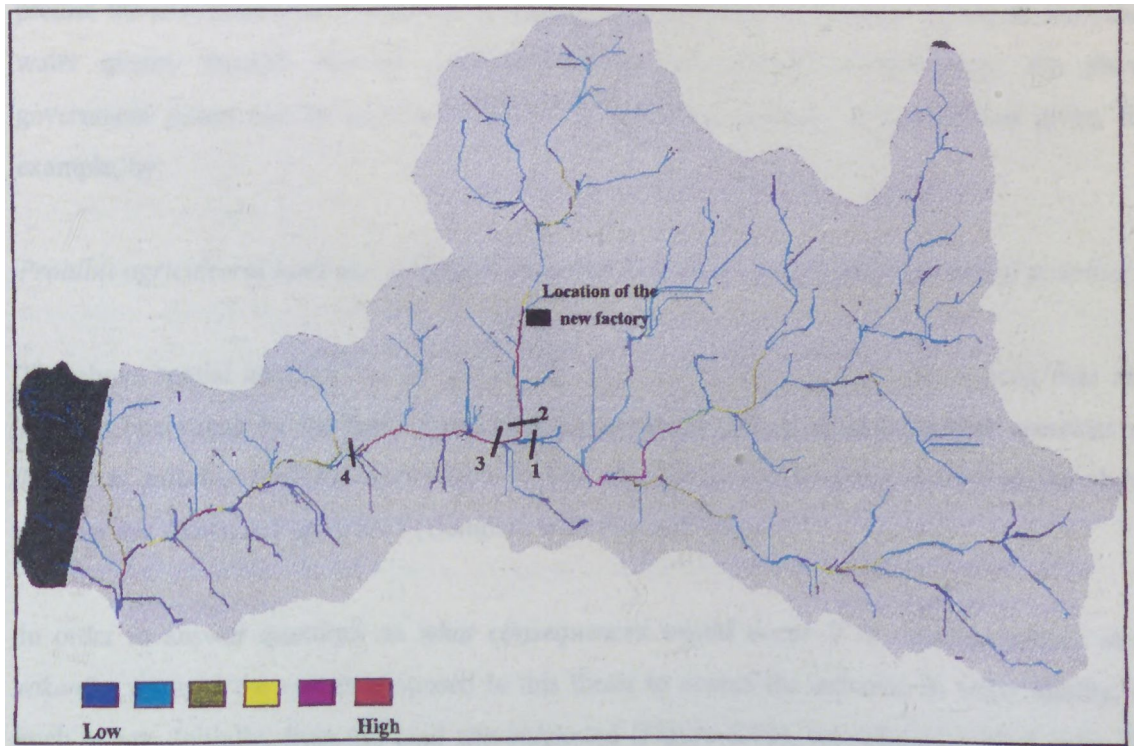


Figure 8.11 : Intensities and spatial distribution of BOD index considering both types of loads (point and non-point) and 'with' scenario.

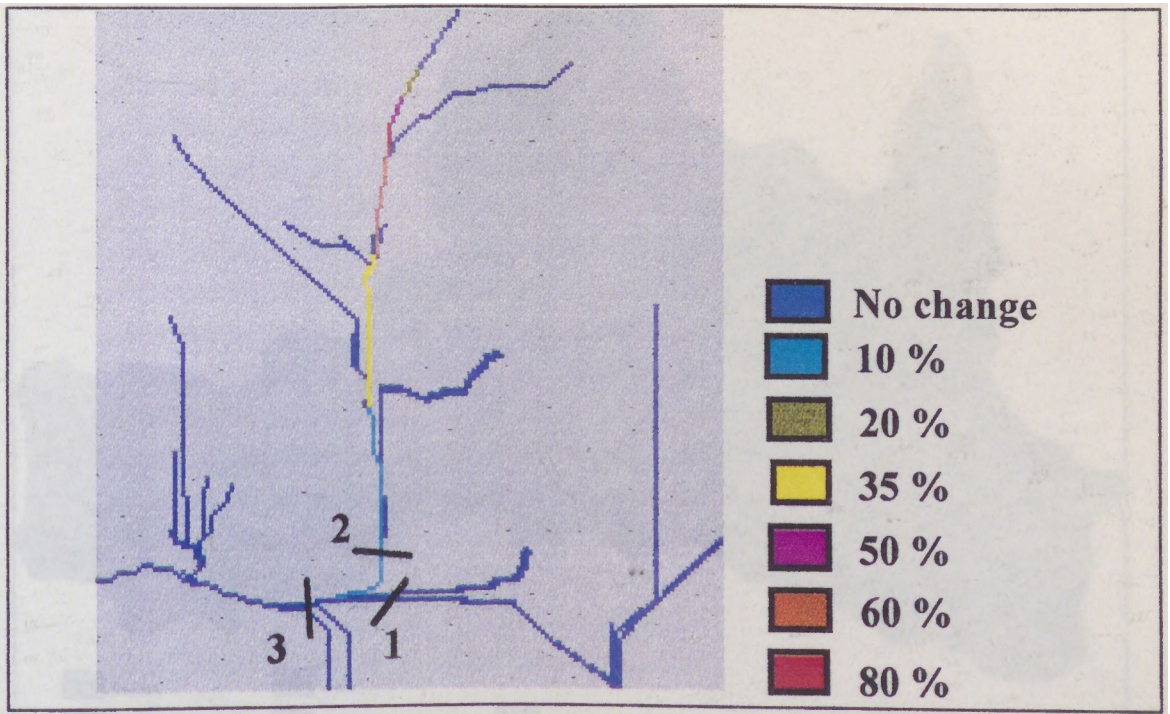


Figure 8.12 : Percentage of change in Igrejinha valley.

Now, we can more exactly state that the objective of the system proposed in this thesis is to predict the consequences of alternative explicit interpretations of policies aimed at analysing water quality through land-use and land-management controls. Consequently, the above government police can be represented as an agricultural suitability zoning scheme given, for example, by:

Prohibit agricultural land use if slope > 12% and soil type ≠ Moderately low runoff potential.

The above spatial analysis can be carried out with a GIS which create links among data and perform operations on the data. These spatial operations can be used to answer questions as *Where is suitable land for agriculture ?*. The changes in the land use, following the above criteria, are shown in Figure 8.13 (Compare with Figure 2.16).

In order to answer questions as *what consequences would occur if the zoning scheme were taken?*, we used the system proposed in this thesis to access the outcome in water quality, of such policy. Initially, from the land use suggested (Figure 8.13), we selected critical areas for non-point source pollution control, as shown in Figure 8.14.

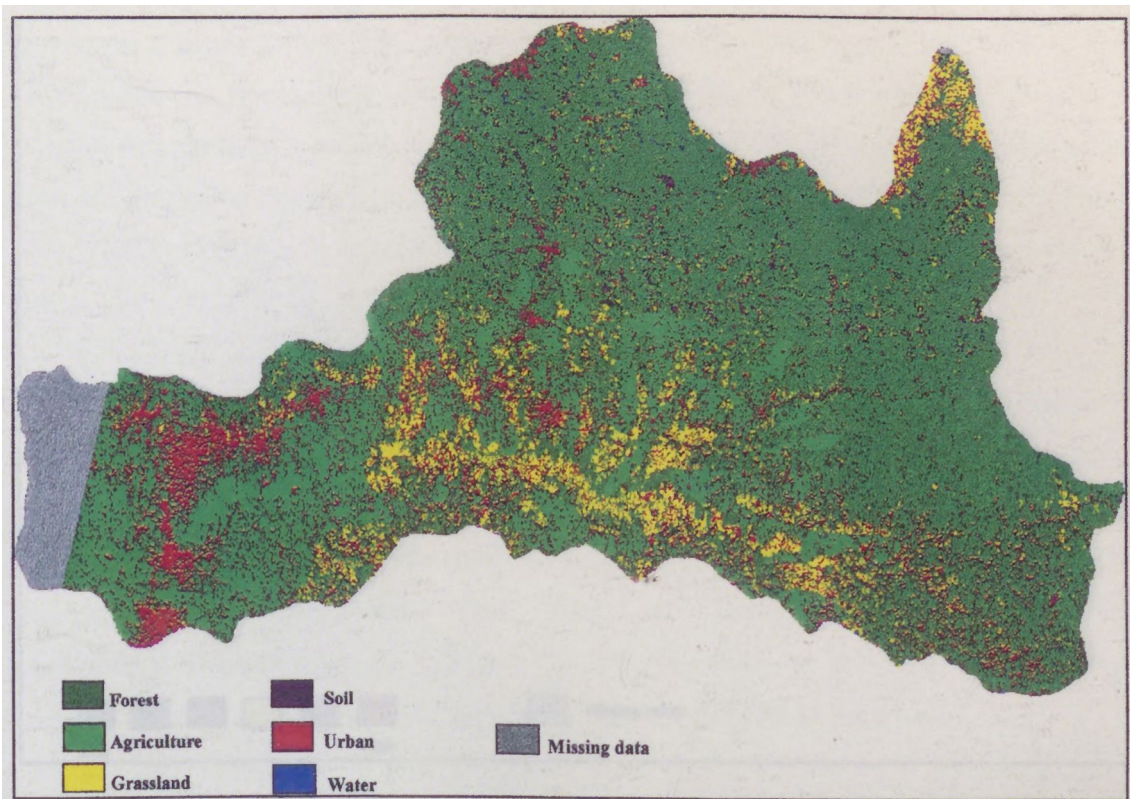


Figure 8.13 : Digital representation of land use data with changes proposed by government policies (agricultural suitability zoning scheme).

From Figure 8.14 it is possible to identify those areas or sources where the greatest improvement to reduce pollution can be obtained for the least investment in best management practices (BMPs). If the above result (Figure 8.14) is acceptable for the group in charge for the decisions (agriculture zoning scheme) we could suggest some methods, or practices (such as terraces, grass waterways, contour cropping, crop rotation, etc.) designed to prevent or reduce the pollution generated by intensive agriculture in Sinos catchment. If not, there is a need to re-evaluate or bargain within the decision makers new criteria for zoning scheme.

Another consequence of the agriculture zoning scheme is shown in Figure 8.15 where the expected future condition of nitrogen concentrations in the drainage network is presented. The system is used by evaluating the agriculture zoning scheme. In order to minimise potential adverse impacts in future projects, the results (Figure 8.14 and 8.15, for example) should be presented to the population to modify or accept the proposed project. It is presumed here that the population are concerned about the resulting hazards (Figures 8.14 and 8.15, for example), and thus pressure builds up on the government.

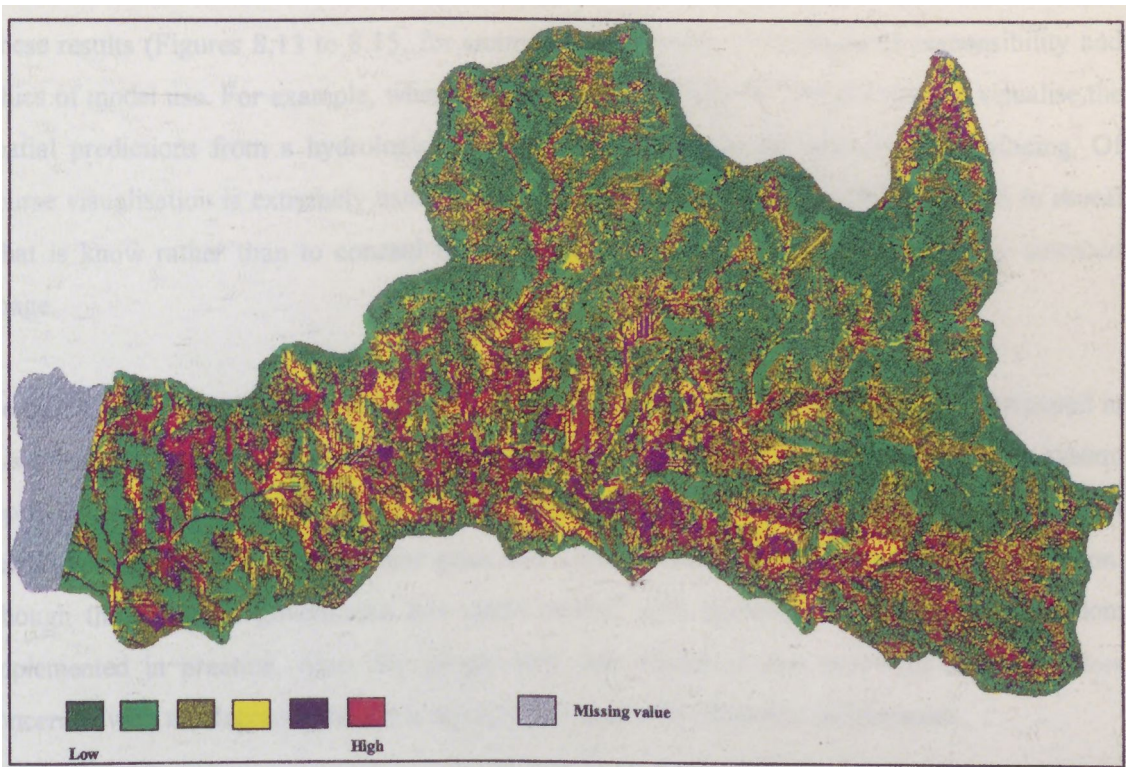


Figure 8.14 : Nitrogen critical areas for Sinos catchment adopting the agriculture zoning scheme as land use.

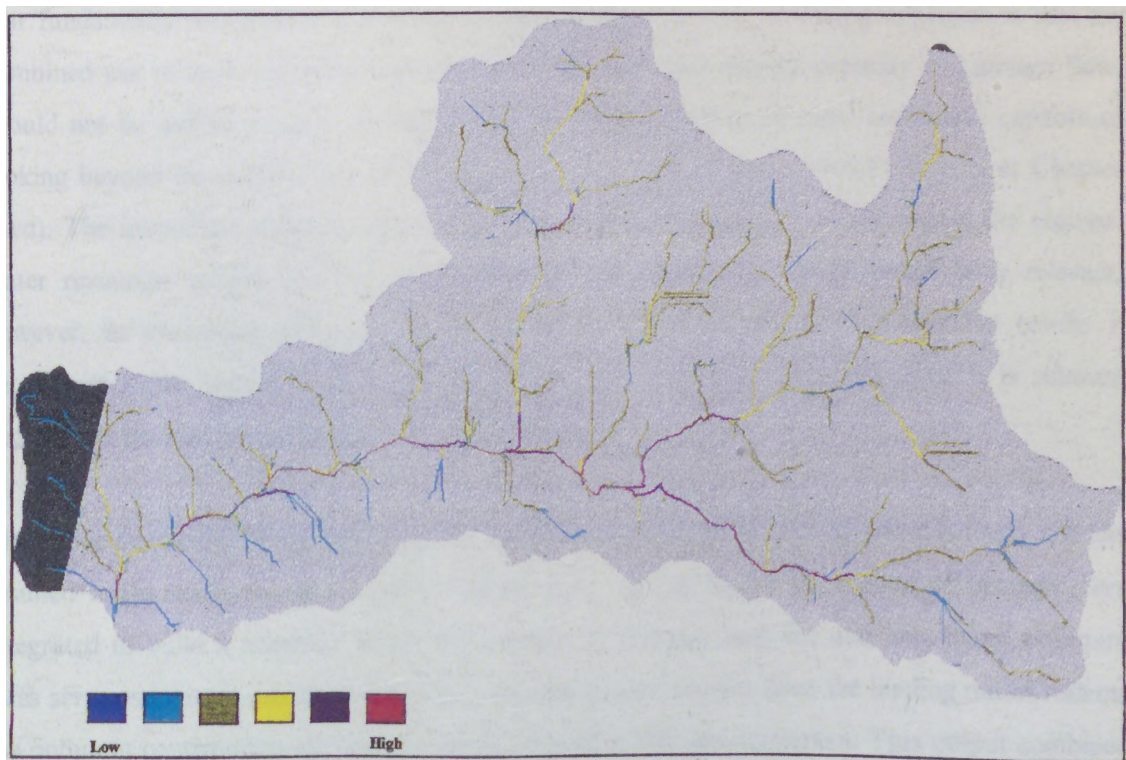


Figure 8.15 : Intensities and spatial distribution of nitrogen concentrations index adopting the agriculture zoning scheme scenario.

These results (Figures 8.13 to 8.15, for example) arise issues of professional responsibility and ethics of model use. For example, when the graphics capabilities of GIS are used to visualise the spatial predictions from a hydrological models, the results can be seductively convincing. Of course visualisation is extremely useful but we must ensure that this capability is used to reveal what is know rather than to conceal the assumptions and uncertainty underlying the coloured image.

Despite this additional danger of the GIS environment (nice colour maps) the system proposed in this thesis estimate the possible future land use in order to guide decision-makers. The system represents scenarios in a developing country like Brazil. The scenario, in this system, generates harmful pollutants. The pollution thus generated causes health hazards to the affected population. Though the Brazilian government has made several laws against pollution, they are seldom implemented in practice. Also, the people with low education and economic levels are less concerned with the degradation of the environment than with economic development.

A real-world macromodel is developed in this thesis to exhibit the comprehensive behaviour of the consequences of the unchecked use of point and non-point loads in a catchment water quality. Our fundamental motivation to develop a regional water quality modelling approach is that the combined use of such regional resources, both for waste assimilation capacity and stream flow, should not be judged socially desirable without the intervention of some institution capable of looking beyond the narrow interest of each individual activity (see COMITESINOS at Chapter Two). The immediate question that arises is how such an institution would model the regional water resources system and the links between that system and water users? It is relevant, however, in answering this question to consider how the institution achieves the results it determines to be 'best' by influencing the behaviour of the individual activities. It is relevant because the decision may affect the model structure.

The above discussion has been the one the main underlying concern throughout this thesis and has resulted in the methodology shown in Figure 8.16. In this figure the desires of managers are integrated to build a scenario. Once the scenario is defined, land use and area-based pollutant rates serve as input to a non-point source pollutant model. Output from the loading model reflects the pollutant contribution attribute to surface runoff within the catchment. This output combined with estimates of point source loadings serve as input to the water quality model of the river. Output from the water quality model may be compared with water quality objectives to determine if remedial action is required.

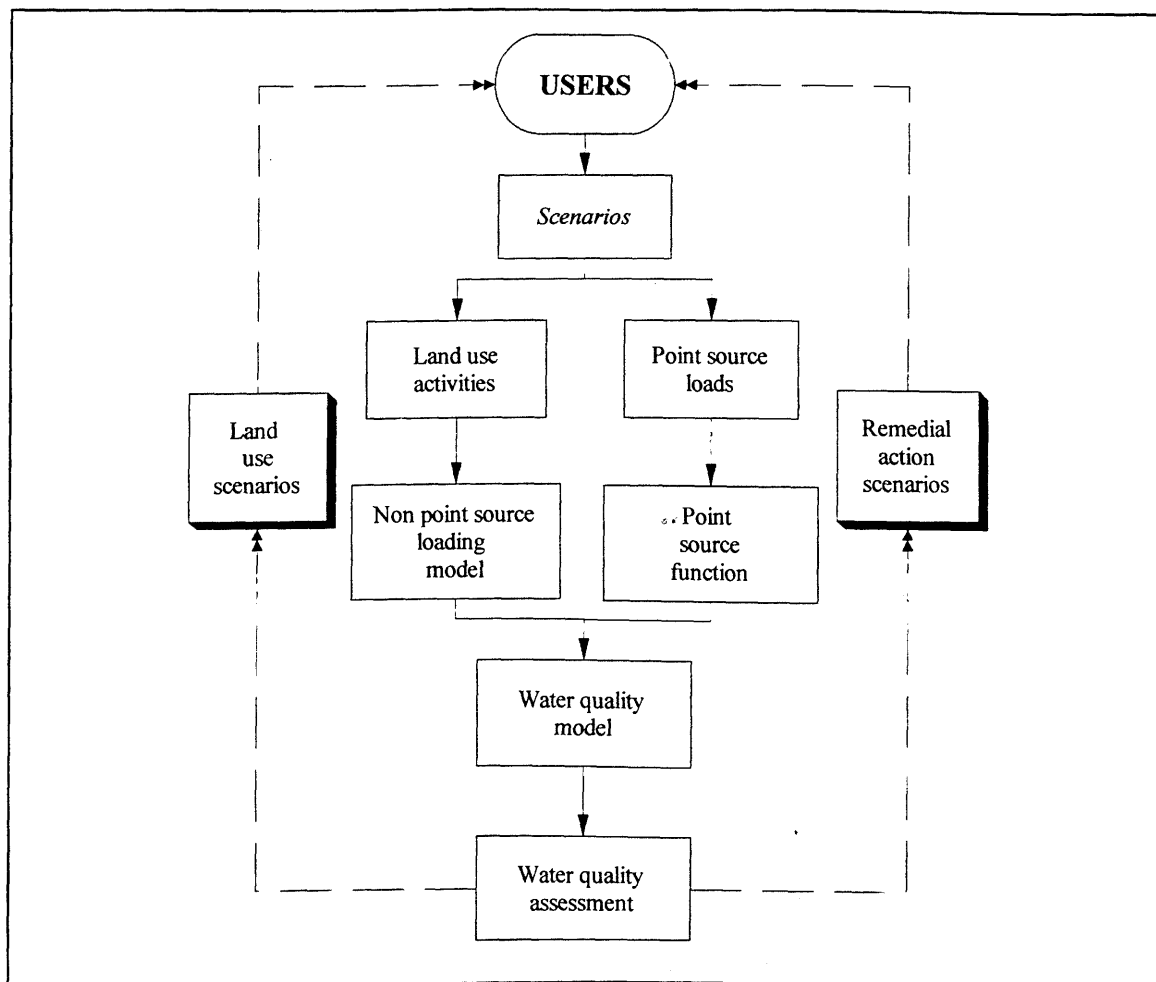


Figure 8.16 : System framework for evaluating different scenarios.

In this last section of the chapter regional modelling projects were conducted (Igrejinha scenarios and Agriculture zoning scheme - Figures 8.10 to 8.15) to emphasise many of the above points. However, the water quality modelling framework proposed allows the evaluation of a large number of different scenarios, such as expansion of agricultural or urban areas, control of land use distribution within the catchment, or municipal water demands (extraction).

8.3 - Conclusions

Throughout this chapter large quantities of data from different sources have been presented and analysed. The data bases are integrated within a GIS and graphical displays, provided by GIS, have facilitated the construction of models, assignment of attributes and allowed direct interactive inspection and visualisation of results of simulations.

Despite the conceptual attraction of linking distributed hydrological models with GIS a number of problems exist. These are due to the different scale between research catchments (*laboratory scale*) and management areas (Sinos catchment), the fundamental constraints of hydrological models and additional issues introduced by GIS. There is a perception that GIS can generate information via interpolation but this is only possible under certain specific circumstances. In addition, the sophisticated graphics features of GIS can be used to seduce the user into an unrealistic sense of model accuracy. We therefore conclude that the spatial output should not be used for quantitative predictive purposes. This is particularly true when the models are applied to large scale management areas like Sinos catchment where the actual description of hydrological processes are impaired by uncertainties. New uncertainties are added at every step from the data collection through the different steps of modelling procedures until the final water quality predictions.

Consequently, it is impossible to quantify how the various sources of error contribute to the differences between observed and simulated pollutant concentrations in Figures 8.7, 8.8 and 8.9. Implicit in the approach used here is that it can only yield rough approximations of the spatial distribution of pollutants in the Sinos catchment (or any other catchment).

Alternative approaches to management issues are needed. In the Brazilian context, where full data are scarce and funds for regular monitoring are unlikely to be sufficient for many years to come an alternative may be to shift from purely quantitative answers towards a greater reliance on simple spatial modelling combined with qualitative reasoning. This approach is consistent with the availability of data and with our ability to represent a large area like Sinos catchment.

A framework for water quality planning has been developed that incorporates very simple hypotheses concerning the origin (point and/or non-point sources), the causes (intensity and spatial distribution of the contributing land uses) and the consequences (enrichment of the surface waters), for an entire catchment. This approach has been applied for the Sinos catchment in Southern Brazil. The results from this case study have demonstrated that the modelling framework can be used successfully:

1. To extract problem-relevant information from sparse data.
2. To manage water quality in interactive controlled incremental steps.

One of the main problems in presenting the case study in this chapter was the difficulty of specifying what exactly should be evaluated, particularly given the limited data for verification. The strategy could not be based solely upon a series of empirical comparisons, but also upon the application of a broader series of suppositions, designed to test all phases of model construction.

I have used an implicit weighting system (high ... low) to analyse different scenarios. Displays of water quality responses to alternative management scenarios allow the users to judge the merits of changes in the catchment. In our opinion this weighting system is extremely useful as it enables relative comparisons to decide what is good or bad water quality, in the case of very limited available data. At the same time, the approach presented in this thesis must be used with caution, and common sense, because is too easy for such index approach to become a substitute for full acquisition of data (and use of better models) especially in the political environment of developing countries. Nevertheless, despite the weaknesses, the approach presented here seems well adapted to surface water quality problems and is especially relevant to developing countries like Brazil.

9.Environmental evaluation under uncertainty

9.1 - Uncertainties in water resources

In this chapter, several possible sources of error in complex physically based, distributed systems are identified and manipulated. The focus of this chapter is on demonstrating the use of a series of algorithms for manipulating uncertainty within components of the model and the results of applying these algorithms are presented for illustrative purpose only.

The planning of water resources requires information about a large quantity of physical, economic and social factors. Because it is not possible to measure the value of these factors everywhere, it is necessary to estimate information about fields using a finite collection of data (Kemp, 1993). Furthermore, all the models presented in this thesis are only an abstract description of the reality via mathematical representation. So, the forecast expressed by Equation 9.1 is affected by uncertainty in the relationship f , where f incorporates both data and models, and their results are only satisfactory when a certain level of quality is obtained. This can be expressed by:

$$\text{Quality}(\text{Forecasts}) = f(\text{quality}(\text{data}) , \text{quality}(\text{simulation model})) \quad (9.1)$$

Following Troutman (1985) uncertainties in hydrologic models result from:

1. The inherent variability in natural processes.
2. Model uncertainty.
3. Model input uncertainty.

There are many aspects of the problem of uncertainty and uncertainty propagation. In this thesis, I restrict myself to analyse how spatial variation of outputs can be related with spatial variability of models and input data.

Natural systems are inherently complex, and usually many of the governing principles of the system domain are unknown. Most physical laws are derived from measurements in laboratories or small scale field experiments. When applying the same laws to larger-scale systems there are problems of extrapolating these laws due to the spatial and temporal variability of system characteristics, which reduces the predictive ability of models. At the field scale, there is also a

high spatial variability associated with hydrologic properties. For instance, Vieira et al., (1981) suggested that spatial variability of soil hydrologic properties, such as saturated conductivity and the initial soil moisture content, is the most difficult problem to deal with for hydrologic modelling at the field scale. Wilson et. al., (1979) have also marked the influence of spatial variability of other input variables, such as rainfall, in model output. To incorporate these problems a probabilistic approach seems most appropriate. In particular, statistical representation of reality is used to model complex patterns of variation in cases where deterministic treatment is inefficient.

The spatial variation of a property is characterised by its probability distribution derived by sampling. Examples of this approach include the distribution of rainfall on the catchment, inflow into a reservoir, catchment infiltration characteristics and soil moisture conditions. De Roo et al., (1992) examined the effects of spatial variability of infiltration on the output of a distributed runoff and soil erosion model using Monte Carlo methods, assuming that the infiltration rate is selected from a probability distribution rather than a single quantity. Binley et al., (1989) used a stochastic approach in surface runoff analysis using the assumption that there is significant spatial correlation structure. Smith and Hebbert (1979) using a distributed catchment simulation model, demonstrated hydrograph bias due to deterministic spatial variability, based on random variation in surface soil properties. Basically, in all the above examples, random field theory was capable of representing the essential features of complex random processes in terms of a minimum number of physically meaningful parameters.

9.1.1 - Statistical representation of the real world

As discussed above, spatial variation of physical properties can be studied by means of statistical processes representing these variations in a field over the space considered. Following Vanmarcke (1988) a random field may be defined as the collection of all spatial distributions (realisations that are consistent with a set of statistical parameters identifying the field). Such a field may be written as $A_m(\mathbf{X})$; $m=1,2,\dots,n$ where m is a parameter identifying a given realisation, and \mathbf{X} is a point in two-dimensional space (or three), that is, $\mathbf{X}=(x,y)$. However to facilitate the notation, the parameter m is omitted and the field is written as $A(\mathbf{X})$.

The deterministic or trend component \bar{A} is defined as:

$$\bar{A}(X) = E[A(X)] \quad (9.2)$$

where $E[.]$ is the expected value operator, that is, the statistical average taken with respect to all realisations.

The fluctuation component ε of A is defined as:

$$\varepsilon(X) = A(X) - \bar{A}(X) \quad (9.3)$$

$\varepsilon(.)$ is described in terms of the following three statistical moments (Cressie, 1991):

$$E[\varepsilon(X)] = 0 \quad (9.4a)$$

$$E[\varepsilon^2(X)] = \sigma^2(X) \quad (9.4b)$$

$$E\{\varepsilon(X_1)\varepsilon(X_2)\} = R(X_1, X_2) \quad (9.4c)$$

where σ is the standard deviation and $R(X_1, X_2)$ is the auto covariance function. The field is statistically homogeneous if (Bras and Rodriguez-Iturbe, 1985):

$$\sigma^2(X) = \sigma^2 = \text{constant} \quad (9.5a)$$

$$R(X_1, X_2) = R(X_2 - X_1) = \sigma^2 \rho(X_2 - X_1) \quad (9.5b)$$

where $\rho(X_2 - X_1)$ is the auto correlation function.

The field is both homogeneous and isotropic if the auto correlation function depends only on the scalar distance r between the points X_1 and X_2 , but not on the orientation of the vector $X_2 - X_1$, that is (Bras and Rodriguez-Iturbe, 1985):

$$\rho(X_2 - X_1) = \rho(|X_2 - X_1|) = \rho(r) \quad (9.6)$$

$$\text{where : } r = \left[(x_2 - x_1)^2 + (y_2 - y_1)^2 \right]^{1/2}$$

The $\rho(r)$ measures the linear correlation between values of the field A at points separated by the distance r .

Within the above framework, it is assumed in this thesis, that a statistically homogeneous and isotropic field $A(\mathbf{X})$ (spatial attribute) is characterised by the (deterministic) mean $\bar{A}(X)$ and a zero-mean, auto correlated residual $\varepsilon(X)$ representing the fluctuations around the mean. So, a spatial attribute $A(\mathbf{X})$ may be written as:

$$A(X) = \bar{A}(X) + \varepsilon(X) \quad (9.7)$$

It is important to distinguish that the random behaviour of $A(\mathbf{X})$ refers only to the spatial variability of the attribute, and does not represent the uncertainty about it, such as errors of measurement (Delhomme, 1979).

In practice, multivariate extension of Equation 9.7 has to be considered. There are multiple attributes $A_i(X) = \bar{A}_i(X) + \varepsilon_i(X)$ and as a result there is a need to quantify the correlation between attributes. Journal and Huijbregts (1978) defines the correlation $\rho_{ij}(X_1, X_2)$ between spatial attributes $A_i(X_1)$ and $A_j(X_2)$ as:

$$\rho_{ij}(X_1, X_2) = \frac{R_{ij}(X_1, X_2)}{\sigma_i(X_1)\sigma_j(X_2)} \quad (9.8)$$

where $R_{ij}(X_1, X_2)$ is the covariance of $A_i(X_1)$ and $A_j(X_2)$. Following Journal and Huijbregts (1978) the matrix of covariance functions $R_{ij}(X_1, X_2)$ must be positive definite. Figure 9.1 illustrates the differences between the correlations 1: $\rho_{ij}(X_1, X_1)$, 2: $\rho_{ii}(X_1, X_2)$ and 3: $\rho_{ij}(X_1, X_2)$.

The differences between these correlations will become clear in Section 9.2, later in this chapter.

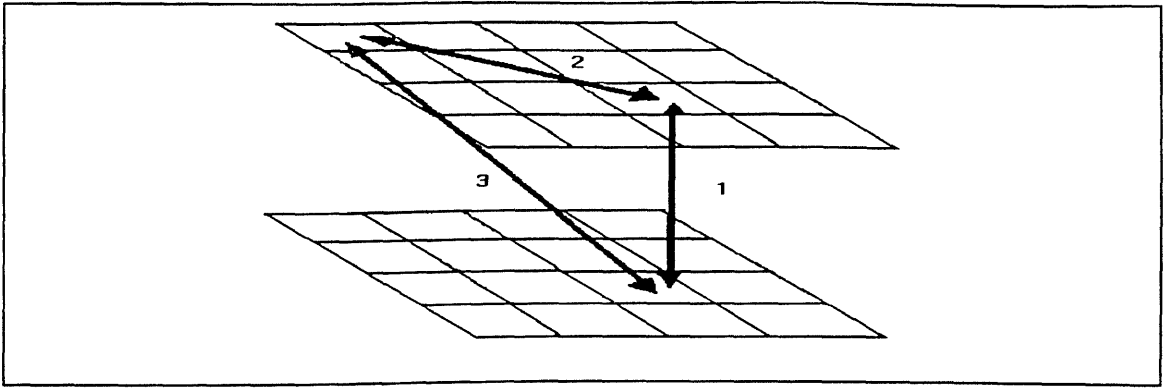


Figure 9.1 : Correlation for spatial attributes.

9.1.2 - Analysis of uncertainties

At this point it is assumed that a model of physical reality has been constructed, and the uncertainties of the inputs have been identified, following Equation 9.7. We show now how to propagate these uncertainties through the model to discover the uncertainties in the predicted output; and how to address the quality of the forecast indicated in Equation 9.1.

A model can be represented as a function f , with two uncertain attributes $A_1(X) - A_2(X)$ and one output y (Here we illustrate only with two inputs, but in general there is a vector with n uncertain inputs):

$$y = f(A_1, A_2) \tag{9.9}$$

Figure 9.2 illustrates the above function where the inputs are represented by the two horizontal dimensions, and the output is represented by the vertical dimension. Because it is assumed that the spatial attributes are represented by probabilistic distributions, the task of uncertainty propagation is to obtain the probability distribution over the predicted output.

A variety of procedures are available to treat the effects of uncertainties. These various approaches can be divided into two main groups:

1. Full distribution analyses.
2. First and second moment analysis.

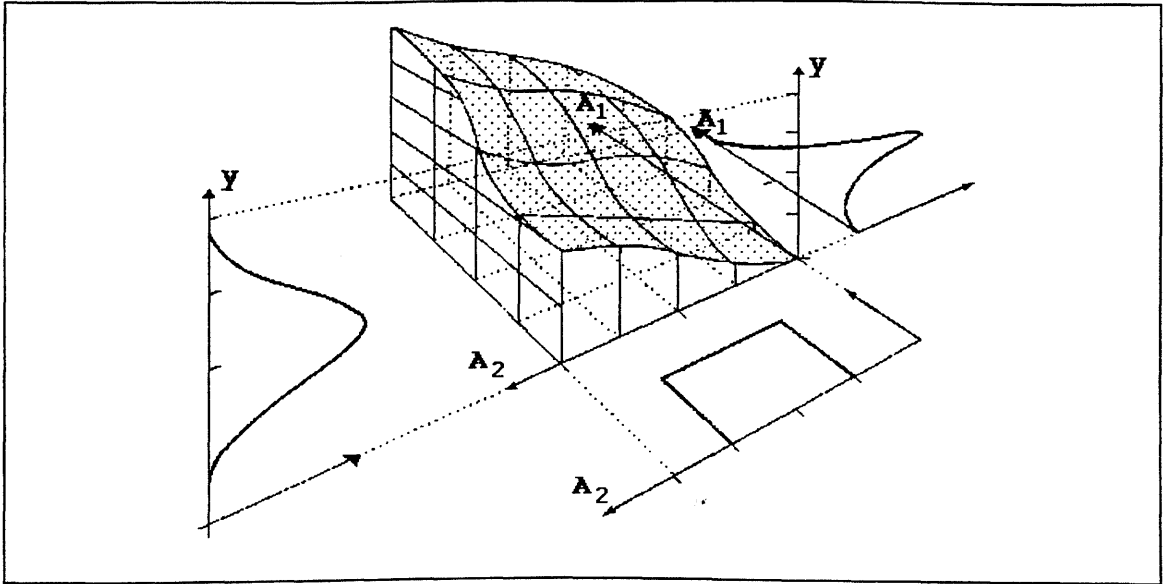


Figure 9.2 : Response surface for output (y) as a function of two inputs (A_1 and A_2).

The first method uses a complete specification of the probabilistic properties of all inputs in a system and attempts to specify the probability distribution of the resulting output. There are two main full distribution techniques:

- 1.1 Derived distribution.
- 1.2 Monte Carlo simulation.

The derived distribution approach is an analytical method for deriving the probability distribution of a random function given the distribution of its component variables (Benjamin and Cornell, 1970). This analysis becomes complicated unless applied to simple systems with simple probabilistic properties.

The idea of the Monte Carlo method is to repeatedly generate input values $A_i(X)$ that are sampled from their probability distribution, resulting in a random sample output, from which the parameters of the output distribution can be estimated (Lewis and Orav, 1989). This procedure will become clear with the examples in Section 9.2, later in this chapter.

First and second moment analysis allow an estimate to be made of the mean and variance of the output of the system y , based on the moments of the various inputs $A_i(X)$ (Benjamin and Cornell, 1970). If the dependent variable is given by:

$$y = f(A_1, A_2, \dots, A_n) \tag{9.10}$$

The expansion around the mean output using a Taylor series expansion (James, 1992) is:

$$y - \bar{y} = \sum_{i=1}^n (A_i - \bar{A}_i) \left[\frac{\partial y}{\partial A_i} \right] + \frac{1}{2} \sum_{i=1}^n \sum_{j=1}^n (A_i - \bar{A}_i)(A_j - \bar{A}_j) \left[\frac{\partial^2 y}{\partial A_i \partial A_j} \right] + \dots \text{rest term} \tag{9.11}$$

The first order analysis uses only the first right-hand term of the above expansion and the variables are normally distributed, so the expected value and variance of y is given by (Benjamin and Cornel, 1970):

$$E(y) = \bar{y} = f(\bar{A}_1, \bar{A}_2, \dots, \bar{A}_n) \tag{9.12a}$$

$$E[(y - E[y])^2] = \sigma^2 = \sum_{i=1}^n \sum_{j=1}^n \text{Covar}[A_i, A_j] \left[\frac{\partial y}{\partial A_i} \right] \left[\frac{\partial y}{\partial A_j} \right] \tag{9.12b}$$

It is normal to separate the variance terms, $\text{Var}[A_i] = \text{Covar}[A_i, A_i]$, from the covariance terms in Equation 9.12b, giving:

$$E[(y - E[y])^2] = \sigma^2 = \sum_{i=1}^n \text{var}[A_i] \left[\frac{\partial y}{\partial A_i} \right]^2 + 2 \sum_{i=1}^n \sum_{j=i+1}^n \text{Covar}[A_i, A_j] \left[\frac{\partial y}{\partial A_i} \right] \left[\frac{\partial y}{\partial A_j} \right] \tag{9.13}$$

If it is assumed that the inputs are independent, that is the second term on the right side of Equation 9.13 containing the covariances are zero, results (with two uncertain attributes $A_1(X)$ and $A_2(X)$), as an example):

$$E[(y - E[y])^2] = \sigma^2 = \text{var}[A_1] \left[\frac{\partial y}{\partial A_1} \right]^2 + \text{var}[A_2] \left[\frac{\partial y}{\partial A_2} \right]^2 \tag{9.14}$$

which states that (similarly to Equation 9.1) :

$$\left\{ \begin{array}{l} \text{Quality of} \\ \text{output } y \end{array} \right\} = \left\{ \begin{array}{l} \text{Quality of} \\ \text{input } A_1 \end{array} \right\} \cdot \left\{ \begin{array}{l} \text{Quality of} \\ \text{model with} \\ \text{respect to the} \\ \text{input } A_1 \end{array} \right\} + \left\{ \begin{array}{l} \text{Quality of} \\ \text{input } A_2 \end{array} \right\} \cdot \left\{ \begin{array}{l} \text{Quality of} \\ \text{model with} \\ \text{respect to the} \\ \text{input } A_2 \end{array} \right\}$$

Figure 9.3 illustrates the quality of the model with respect to the inputs $A_i(X)$ (derivative terms of the right-hand side of the Equation 9.14) as the slopes of two tangents, along the two vertical planes parallel to each of the horizontal axes.

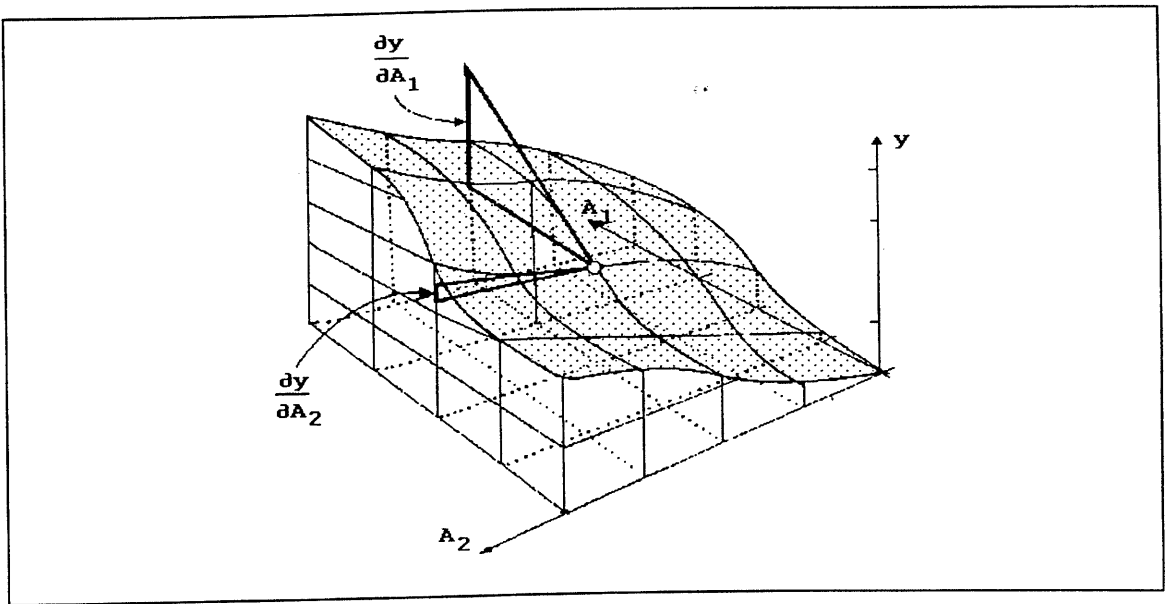


Figure 9.3 : Slopes of the output y as a measure of models' quality

9.1.3 -Discussions

Environmental models need to be improved in many ways. However, not only the theoretical structure or the physical basis needs more attention, but also the data problem should receive more attention.

Many scientists concentrate on the development of the theoretical structure of models and try to fill gaps in our understanding of these processes, which is in itself very important work. However the error in the data may have a much large effect on the simulation results obtained with the model. Furthermore, ignoring errors in data may lead to the erroneous conclusion that the theoretical structure of models is not correct. Consequently, it is pointless to develop models

requiring numerous variables that vary both in space and time, such that it is impossible to run or validate the model at all.

In the preceding sections, we have reviewed the concepts of uncertainty analysis. Once the errors in a measured attribute (A_1 or A_2) are generated, it is reasonable to consider how these errors should be combined to obtain the overall uncertainty in the output y . The techniques used in this chapter should be used to provide a more realistic presentation of the results by producing probability distributions rather than those single quantities. In the following sections we show how to apply the above theory and how meaningful conclusions can be drawn from it.

9.2 - Implementation of uncertainty analysis for environmental distributed models

This section demonstrates how the theory presented above can be applied to relevant practical problems. Three case studies are considered. The aim of this section is not so much to entirely describe the theory behind the three case studies or to analyse all aspects of the problems at hand, but to show how error propagation theory can be applied in practice.

9.2.1 - DEM evaluation under uncertainty

The slope and aspect (see Chapter 3) are abstract descriptions of the terrain system synthesised from available data and information. These abstractions are mathematical descriptions of the system only and provide no more than an approximate realisation of the terrain system. Beyond this there are various sources of uncertainty associated with the DEM such as interpolation errors, digitising error, errors in the contour map. The total uncertainty is highly complex and the techniques proposed in this chapter do not attempt to quantify this total variation, instead they attempt to preserve the spatial statistical properties of the uncertainties.

The analysis is carried out using first order analysis, even though that calculates slope and aspect involve operations that are not continuously differentiable at every place. The objective here is to only trace the mechanics of error propagation. Recalling Equation 9.7, it is assumed that a DEM, at a given spatial coordinate x , denoted by el , is a realisation of a stochastic function $El(x)$ given by:

$$El(x) = m(x) + \varepsilon(x) \quad (9.15)$$

where $m(x)$ is a deterministic prior mean (Figure 3.6) and $\varepsilon(x)$ is a zero-mean stochastic function (Figure 3.7) and is assumed normally distributed. In practice, is know only one realisation of $El(x)$ and the ergodic hypothesis must be used. Following Equation 9.14, the first problem is the determination of the derivatives. For the spatial positions,

$Z_{i-1,j-1}$	$Z_{i-1,j}$	$Z_{i-1,j+1}$
$Z_{i,j-1}$	$Z_{i,j}$	$Z_{i,j+1}$
$Z_{i+1,j-1}$	$Z_{i+1,j}$	$Z_{i+1,j+1}$

and the same concepts applied for the determination of slope (Equation 3.11), one derivative is:

$$\frac{dSLOPE}{dZ_{i+1,j}} = \frac{dSLOPE}{d(\Delta h)} \cdot \frac{d(\Delta h)}{d(\Delta y)} \cdot \frac{d(\Delta y)}{d(\Delta y_2)} \cdot \frac{d(\Delta y_2)}{dZ_{i+1,j}}$$

giving:

$$\frac{dSLOPE}{dZ_{i+1,j}} = \frac{1}{1+(\Delta h)^2} \cdot \frac{2\Delta y}{2\Delta h} \cdot \frac{1}{3\delta} \cdot (-1) \tag{9.16}$$

Equation 9.16 is one of the derivatives of the equation

$$\sigma_{SLOPE}^2 = \dots + \left(\frac{dSLOPE}{dZ_{i+1,j}} \right)^2 \cdot \sigma_{Z_{i+1,j}}^2 + \dots \tag{9.17}$$

that account for the spatial variability of the slope calculated by Equation 3.11. Equation 9.16 is the spatial error of the model and $\sigma_{Z_{i+1,j}}^2$ is the spatial quality of the DEM given by the error map value (Figure 3.7) on position $i+1,j$.

In practice, we implemented Equation 9.17 using a GRASS function *r.mapcalc* (Shapiro and Westervelt, 1992). The function *r.mapcalc* combines maps and images in expressions with arithmetic and logical operators and mathematical functions to produce new maps and images. The general format of the data is *map[r,c]* where *r* is the row and *c* is the column. As an example

correspond to the files given by Figures 3.6 and 3.7. The gridsize in my example is 25 m and *tmp1*,..., *tmp4* are temporary variables used to capture intermediate results for use in the later part of the expression.

```

error = eval (dx = ((dem.img[1,1]-dem.img[-1,1]) + \
                  (dem.img[1,0]-dem.img[-1,0]) + \
                  (dem.img[1,-1]-dem.img[-1,-1]))/75.0, \
            dy = ((dem.img[-1,1]-dem.img[-1,-1]) + \
                  (dem.img[0,1]-dem.img[0,-1]) + \
                  (dem.img[1,1]-dem.img[1,-1]))/75.0, \
            dh = sqrt((dx*dx)+(dy*dy)), \
            slope = round(atan(dh)), \
            . \
            . \
            tmp1 = 2.0*dh, \
            tmp2 = (1.0+sqr(dh)), \
            tmp3 = 2.0*dy*(-1.0/75.0), \
            tmp4 = ((tmp3/tmp1)/tmp2)*err.img[0,-1], \
            . \
            . \
            round(sqrt(.....+sqr(tmp4)+.....)), \
            )

```

GRASS

Because the slope and aspect are obtained from cells around position *i,j* they involve some spatial interaction. In this case the spatial correlation is needed between cell *i,j* and all the others within the window. The correlation term of Equation 9.8 can be approximated using an exponential correlation function (Figure 9.4):

$$\rho(Z, Z') = p.e^{\left(\frac{-|Z-Z'|}{a}\right)} \quad \text{for } Z \neq Z' \tag{9.18}$$

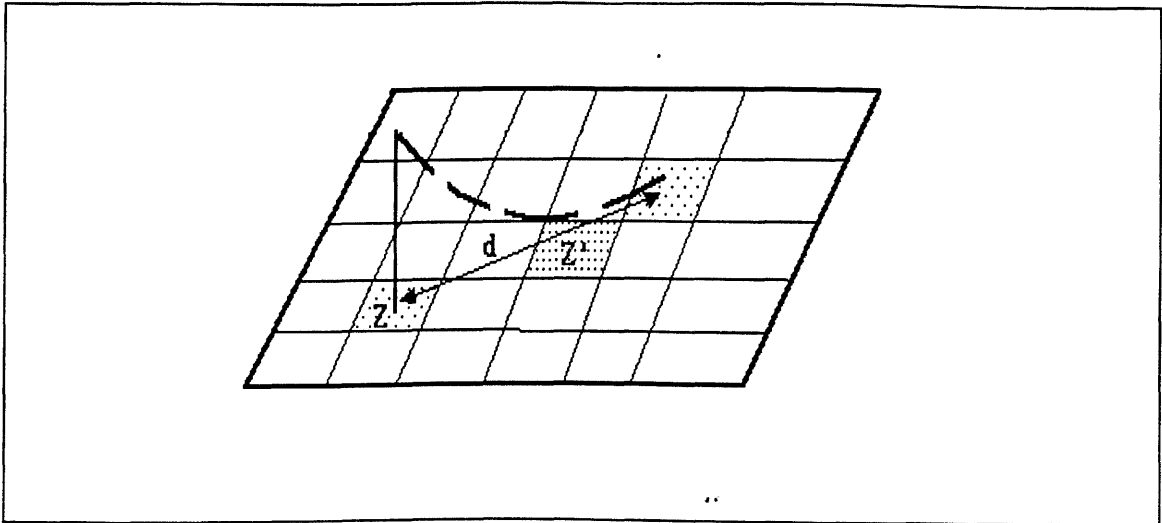


Figure 9.4 : Spatial autocorrelation.

The correlation (Equation 9.18) is between Z and Z' . Beyond d the auto correlation is assumed to be zero. In practice, the distance between Z and Z' is defined in terms of grid cells. The analysis is carried out using Equation 9.17 (with correlation terms) for three values of parameter p that are $p=0$, $p=0.5$ and $p=1.0$ (Figures 9.5a, b and c). These Figures show that when the errors in elevation are more correlated smaller errors occur in the prediction of slope. This can be observed when 'high error' areas (black areas on these Figures) decrease with the increase of the level of auto correlation. The same result are reported by Heuvelink et al., (1990) and Goodchild et al., (1992).

9.2.2 - Uncertainty assessment of runoff production

Equation 4.6 provides a single outcome runoff estimation (that is, it is a deterministic rainfall-runoff model) and does not represent any uncertainty in the prediction. In order to estimate this uncertainty I assume that the model output is a stochastic process, that is the prediction of runoff generates not a single outcome, but a distribution of possible outcomes. Hydrological catchment models, such as the distributed models used here, include operations where the result at some location may depend on input values at locations in the study area that are remote from the location of interest.

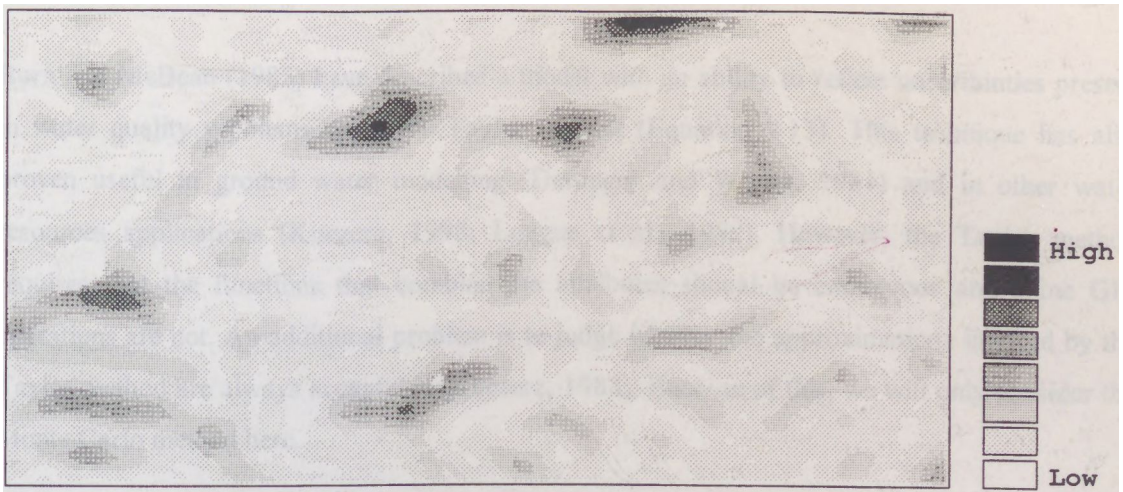


Figure 9.5a : Uncertainties of DEM slope with $p=0$

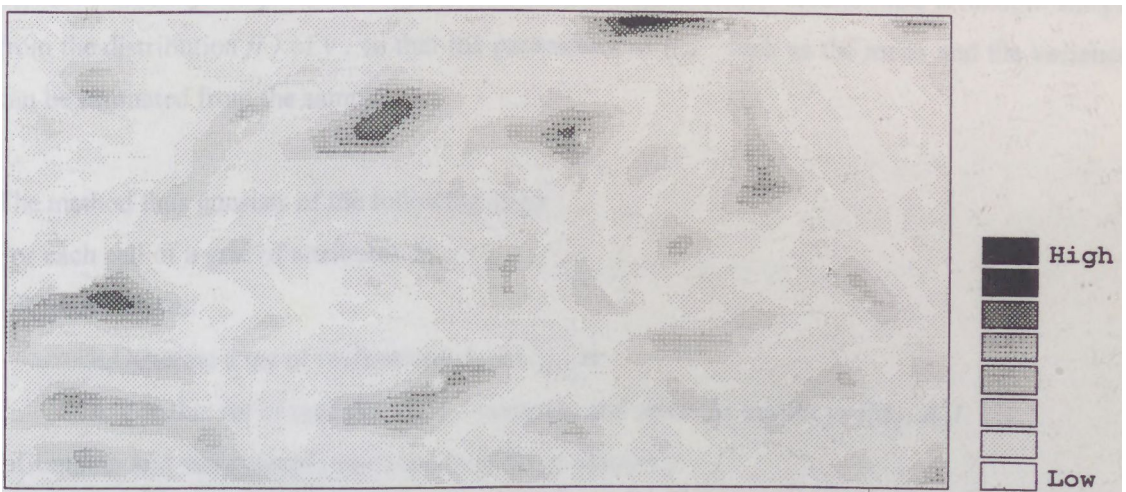


Figure 9.5b : Uncertainties of DEM slope with $p=0.5$

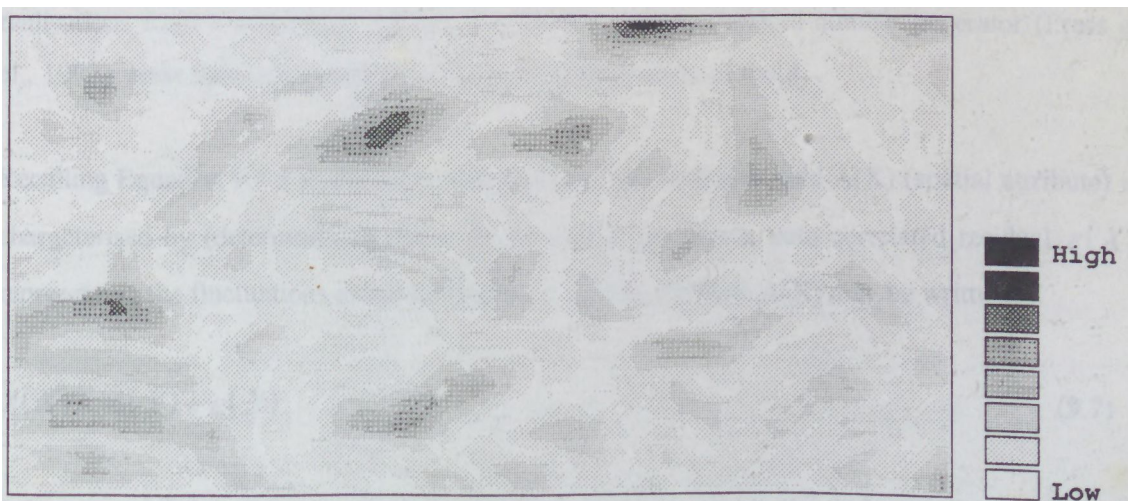


Figure 9.5c : Uncertainties of DEM slope with $p=1.0$

Burn and McBean (1985) have described a model with an ability to reflect uncertainties present in water quality problems using the Taylor method (Equation 9.13). This technique has also proven useful in ground water modelling (Dettinger and Wilson, 1981) and in other water resources applications (Kuczera, 1998; Loague et al., 1989). However, the Taylor method requires that the functions that combine the attributes should be continuous and some GIS operations are not. An additional problem is to judge whether the approximations invoked by the Taylor method are always acceptable (Kuczera, 1988). Because of this, we will only consider the Monte Carlo method here.

The idea of this method is to compute the result of Equation 9.9 repeatedly, with input values A_i that are randomly sampled from their joint distribution. The model results form a random sample from the distribution $f(\cdot)$ of y , so that the parameters of $f(\cdot)$, such as the mean and the variance, can be estimated from the sample.

The method thus consists of the following steps :

For each cell of a grid of attributes do :

1. Repeat n times:

a. Generate a set of realisations $A_i, i=1, \dots, m$

b. For this set of realisations A_i , compute and store the output $y=f(A_1, A_2)$

2. Compute and store sample statistics from the n outputs y .

A random sample from the m inputs A_i can be obtained by first generating independent realisations from a univariate uniform distribution, using a random number generator (Press et al., 1992). Next these are transformed from the distributions of the A_i .

Recalling Equation 9.7 a statistically homogeneous and isotropic field $A(\mathbf{X})$ (spatial attribute) is characterised by (deterministic) mean $\bar{A}(X)$ and a zero-mean, auto correlated residual $\varepsilon(X)$ representing the fluctuations around mean. So, a spatial attribute $A(\mathbf{X})$ may be written as:

$$A(X) = \bar{A}(X) + \varepsilon(X) \quad (9.7)$$

Now $A(\mathbf{X})$ represent the true unknown output of Equation 4.6 and $\bar{A}(X)$ a single deterministic runoff estimation from Equation 4.11. In order to predict a distribution of outcomes from

Equation 4.11 I write $A(\mathbf{X})$ as a sum of independent underlying random fields where each one of these can be simulated separately, using Monte Carlo methods.

The initial problem is to transform the error term of the above equation into a zero-mean, auto correlated residual $\varepsilon(X)$. In such situations the correlation structure of $\varepsilon(X)$ is implicitly known. An efficient manner to generate random fields, keeping the correlation structure, is that defined by spatial auto regressive models (Griffith, 1988; Cressie, 1991).

In linear regression analysis, the objective is to explain the variance of a dependent variable y by a linear combination of observed explanatory variables, X giving:

$$y = X\beta + \varepsilon \quad (9.19)$$

A special case of a regression model is where the explanatory variable consists of a spatial lag. That is, the dependent variable is regressed on a spatial lag of itself, named as spatial *auto* regression (Griffith, 1988; Cressie, 1991) and can be expressed as:

$$y = \rho W y + \varepsilon \quad (9.20)$$

where: ρ is a spatial autoregressive coefficient.

W is a spatial weight matrix reflecting the topology of the data set.

The estimate for ρ can be considered as an indication of spatial auto correlation. When ρ is zero, the variable has no spatial dependence. The maximum value of ρ is 0.25 to ensure stationarity (Cliff and Ord, 1981).

Usually the random field is approximated as a regular grid, with different constant y values at each of the cells shown in Figure 9.6 (Cliff and Ord, 1981). The modelling region contains m rows, n columns, and $p=m.n$ cells. Basically W determines those locations surrounding a given data point that would be considered to influence the observation at that data point.

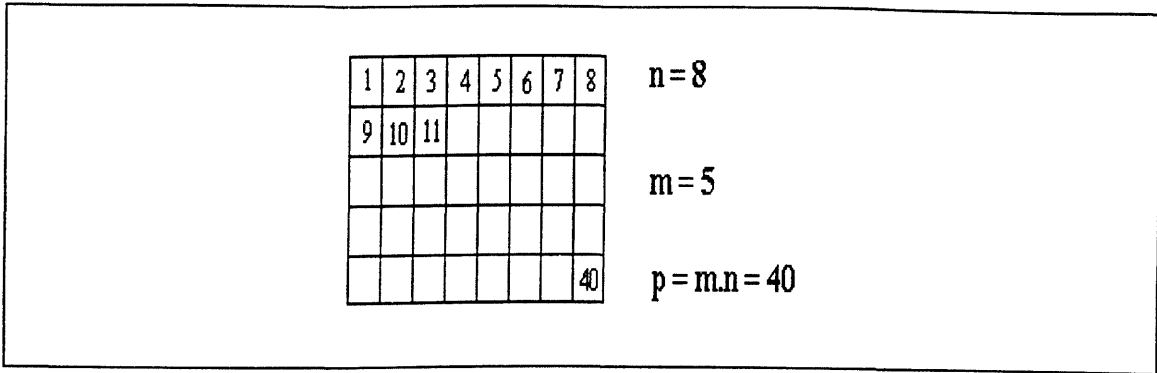


Figure 9.6 : The discretization scheme.

The elements w_{ij} of matrix W can be generated by the relation (Goodchild, 1980):

$$w_{ij} \begin{cases} 0 & \text{if } i \text{ and } j \text{ are not neighbours, or when } i = j \\ 1 & \text{if } i \text{ is neighbour of } j \end{cases} \tag{9.21}$$

Figure 9.7b shows a binary weight matrix, following the above model, for the rook criterion (four directions, row and column sequence) applied to the 16 observations in the 4x4 square grid (Figure 9.7a) The neighborhood set for each location is expressed by W with dimension equals to p where each row and matching column corresponds to an observation pair.

Following the above approach the zero-mean, auto correlated residual ε of Equation 9.7 can be expressed as :

$$\varepsilon = \lambda W \varepsilon + \zeta \tag{9.22}$$

where: λ is an autoregressive parameter (similarly to ρ), $0 \leq \lambda < 0.25$.

ζ is a zero-mean and uncorrelated residual with fixed variance.

So, the spatial autoregressive error can be rewritten as:

$$\varepsilon = (I - \lambda W)^{-1} \zeta \tag{9.23}$$

A	B	C	D
E	F	G	H
I	J	K	L
M	N	O	P

(a)

	A	B	C	D	E	F	G	H	I	J	K	L	M	N	O	P
A	0	1	0	0	1	0	0	0	0	0	0	0	0	0	0	0
B	1	0	1	0	0	1	0	0	0	0	0	0	0	0	0	0
C	0	1	0	1	0	0	1	0	0	0	0	0	0	0	0	0
D	0	0	1	0	0	0	0	1	0	0	0	0	0	0	0	0
E	1	0	0	0	0	1	0	0	1	0	0	0	0	0	0	0
F	0	1	0	0	1	0	1	0	0	1	0	0	0	0	0	0
G	0	0	1	0	0	1	0	1	0	0	1	0	0	0	0	0
H	0	0	0	1	0	0	1	0	0	0	0	1	0	0	0	0
I	0	0	0	0	1	0	0	0	0	1	0	0	1	0	0	0
J	0	0	0	0	0	1	0	0	1	0	1	0	0	1	0	0
K	0	0	0	0	0	0	1	0	0	1	0	1	0	0	1	0
L	0	0	0	0	0	0	0	1	0	0	1	0	0	0	0	1
M	0	0	0	0	0	0	0	0	1	0	0	0	0	1	0	0
N	0	0	0	0	0	0	0	0	0	1	0	0	1	0	1	0
O	0	0	0	0	0	0	0	0	0	0	1	0	0	1	0	1
P	0	0	0	0	0	0	0	0	0	0	0	1	0	0	1	0

(b)

Figure 9.7 : (a) observed data.
(b) Spatial weight matrix

Equation 9.23 aggregates a system of simultaneous linear equations that can be solved to find ε . The only problem is that Equation 9.23 requires the inversion of a $p \times p$ matrix (p =rows x columns), that is for a 100x50 grid requires inversion of a 5000x5000 matrix. Despite its conceptual simplicity, this method presents difficult computational problems. Heuvelink (1992) has proposed a iterative method which can be implemented for any matrix W , based on relaxation methods for boundary value problems. This method is only possible by exploiting the simplicity of W and reducing the inversion to the use of the following rules.

1. Generate a realisation of $\zeta_{i,j}$ (Using Monte Carlo procedures). (9.24a)
2. Take initial $\varepsilon_{i,j}^n = \zeta_{i,j}$. (9.24b)
3. Calculate $\varepsilon_{i,j}^{n+1} = \lambda(\varepsilon_{i+1,j}^n + \varepsilon_{i-1,j}^n + \varepsilon_{i,j+1}^n + \varepsilon_{i,j-1}^n) + \zeta_{i,j}$. (9.24c)
4. If $\varepsilon_{i,j}^{n+1} - \varepsilon_{i,j}^n < \delta$ then finish, else increment n and repeat 3 (δ is a value that guarantee that the iteration has converged). (9.24d)

The above method is in fact a classical method to solve systems of linear equations called Jacobi's method (James, 1992). Figures 9.8a-e show intermediate iterations from a completely uncorrelated random field (Figure 9.8a) to a correlated random field (Figure 9.8e) with the autoregressive parameter $\lambda = 0.245$ and a chosen critical value for the iteration $\delta = 0.001$.

The variogram (Webster & Oliver, 1990) is a common method of quantifying the spatial dependence structure of a variable. Figures 9.8f-j shows an increasing distance within which spatial dependence occurs. Figure 9.8j suggests that statistical independence can best be maintained by distances of 20 m or more apart.

Table 9.1 presents the results for different values of λ . The simulations were executed on a Sun 3/80 workstation. The accompanying example realisations are given in Figure 9.9a-j where an increase of spatial correlation with an increase of λ can be noted. The results show that the convergence of the method is sensitive to the value of λ . Examining Table 9.1, it appears that the number of iterations and computing time doubles with the increase of correlation parameter λ .

Figure #	λ	Number of iterations	Computing time (sec.)
9.9a	0	0	0
9.9b	0.10	3	1
9.9c	0.15	6	2
9.9d	0.20	13	3
9.9e	0.24	56	8
9.9f	0.245	101	13
9.9g	0.248	200	26
9.9h	0.249	330	41
9.9i	0.2495	502	58
9.9j	0.2499	890	108

Table 9.1 - Numerical results for a simulation of a 100x50 grid with $\delta = 0.001$.

The above simulation procedure allows construction of a spatially autocorrelated error map. Using Equation 9.7 we intend to write $A(\mathbf{X})$ as a sum of independent error maps and the calculate the variability of $A(\mathbf{X})$. This variability will be the uncertainty of runoff prediction.

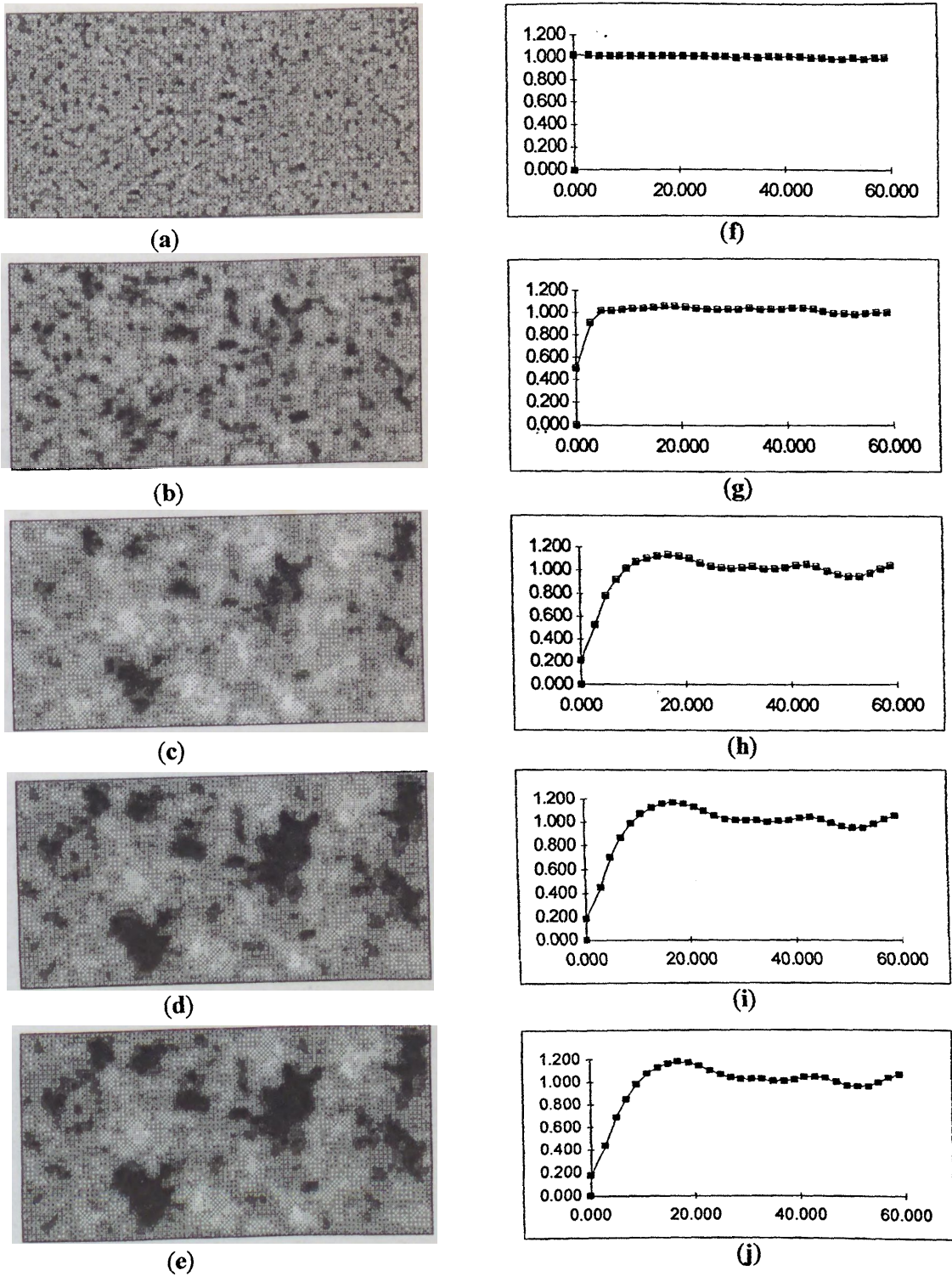


Figure 9.8 - Intermediate levels for iterative simulation of a 100x50grid with $\lambda=0.245$ and $\delta=0.001$: (a) initial random field, (b) after 2 iterations, (c) after 20 iterations, (d) after 50 iterations, and (e) last result after 101 iterations. From (f) to (j) are shown the computed variogram for the respective random fields.

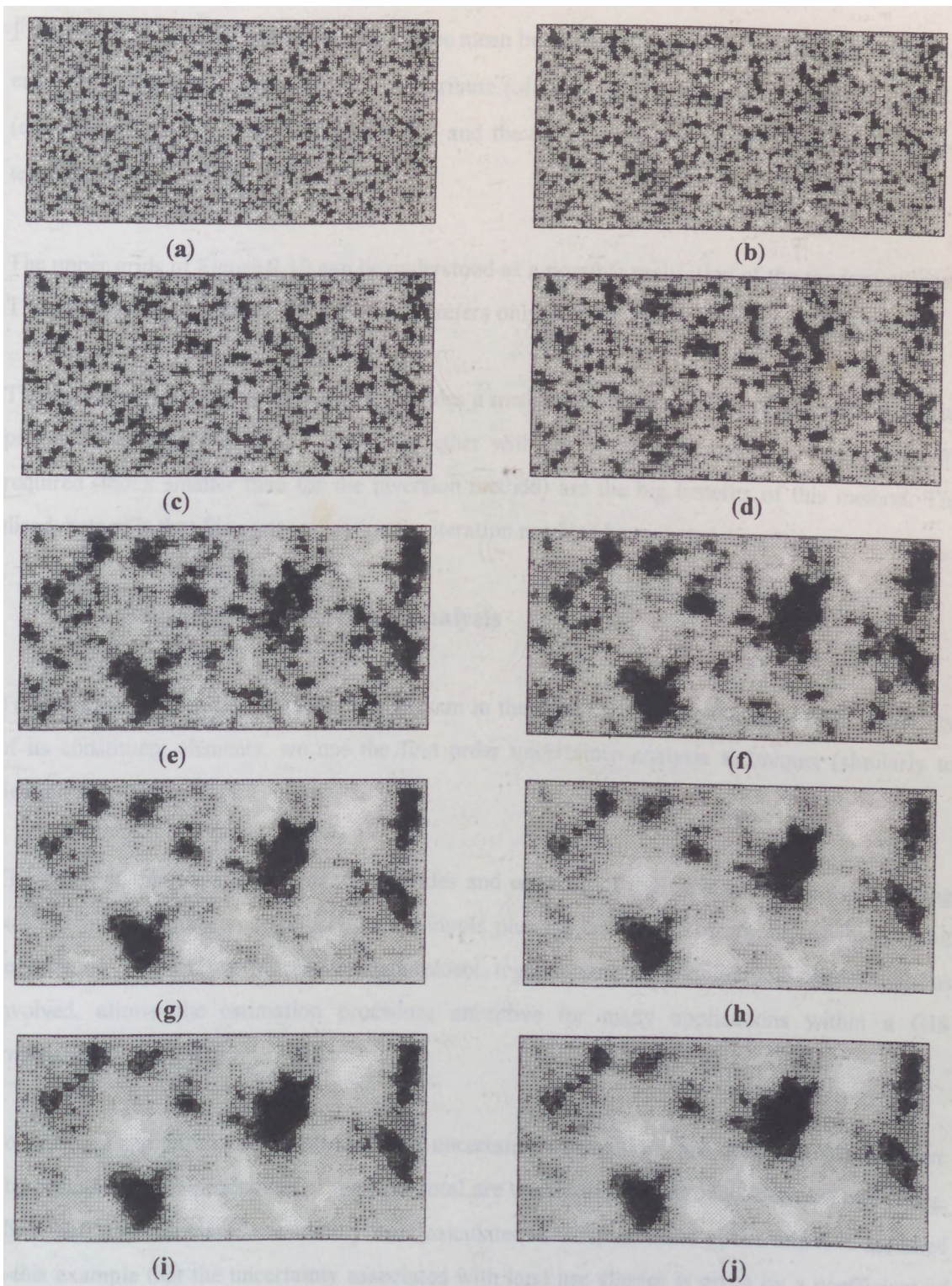


Figure 9.9 - Examples for different values of the spatial dependence parameter λ with critical value for iteration $\delta = 0.001$ in a 100×50 grid : (a) $\lambda = 0$, (b) $\lambda = 0.10$, (c) $\lambda = 0.15$, (d) $\lambda = 0.20$, (e) $\lambda = 0.24$, (f) $\lambda = 0.245$, (g) $\lambda = 0.248$, (h) $\lambda = 0.249$, (i) $\lambda = 0.2495$ and (j) $\lambda = 0.2499$.

Figure 9.10 shows two examples of the same mean but different degrees of spatial auto correlated error map. The upper grids are the true attribute ($A(X)$). The middle grid is the trend ($\bar{A}(X)$) (deterministic) component of Equation 9.7 and the lower grids are the auto correlated random term ($\varepsilon(X)$).

The upper grids of Figure 9.10 can be understood as a possible realisation of the random process. The stochasticity present in the upper grids refers only to the spatial variability of the attributes.

The iterative method described above provides a method for the simulation of almost any spatial process. The simplicity of the method together with the computing time and storage capacity required (much smaller than for the inversion method) are the big benefits of this method. The disadvantage is that for each realisation the iteration needs to be repeated many times.

9.2.3 - Critical area uncertainty analysis

To determine the degree of randomness present in the critical area approach due to the variability of its constituent elements, we use the first order uncertainty analysis technique, (similarly to Section 9.2.1).

The utility of this technique is that it provides an estimate of the variance of the output using only the mean and variance of each of the inputs plus the covariance of any inputs that exhibit dependence. This limited information requirement, together with the simplicity of the calculations involved, allows the estimation procedure to be attractive for many applications within a GIS framework.

To illustrate the approach the critical area uncertainty calculations are described for nitrogen. The critical area for production of nitrogen-total are the result of the product between two terms. The runoff and associated uncertainty were calculated in Chapter 4 and above and it is assumed in this example that the uncertainty associated with land use classes is given by a coefficient of variation of 25 per cent. In a real case, the land use uncertainty may be determined by a probability image in which each pixel represents a spectral distance from the pixel to center of cluster's class. The mean or trend component is given by Equation 5.10:

$$P_N = Q \cdot L_N \tag{5.10}$$

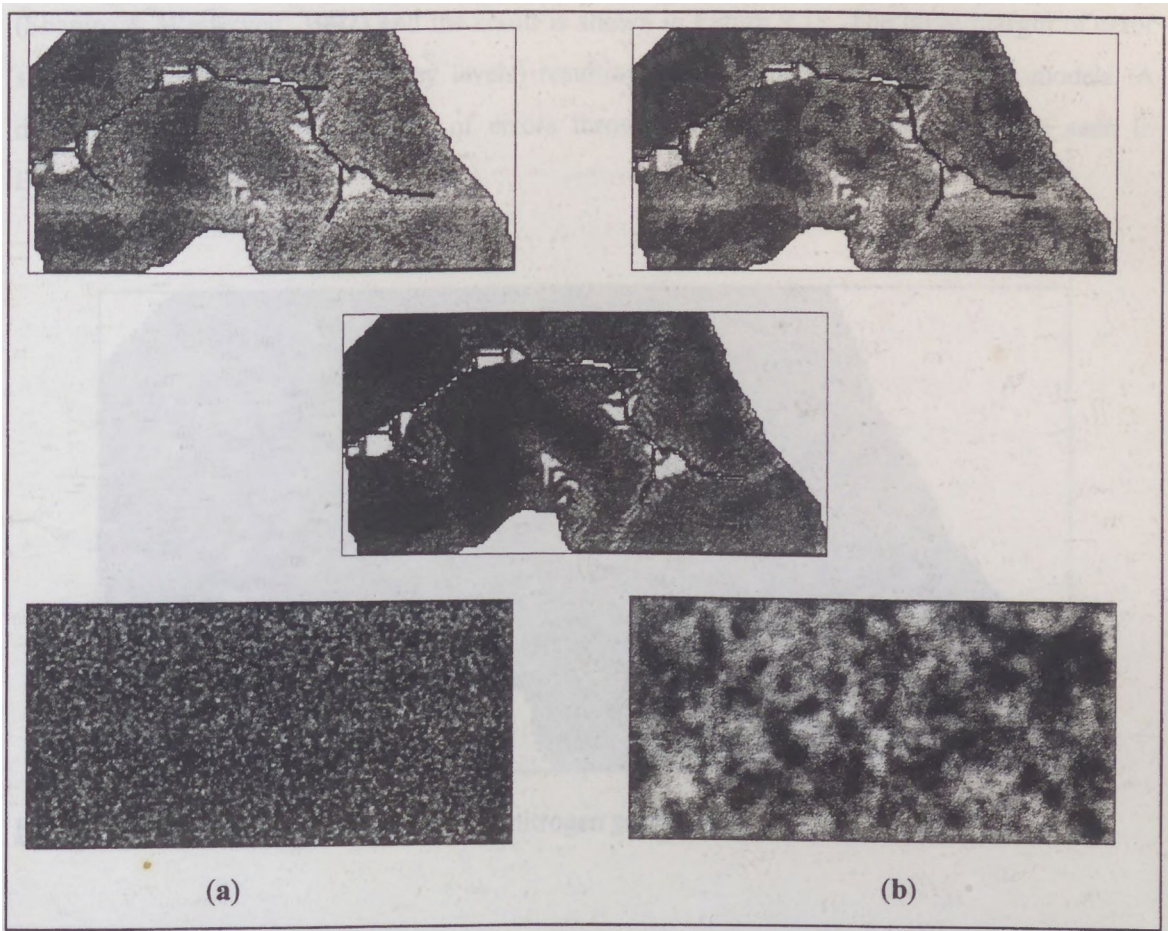


Figure 9.10 - Examples of generation of attributes $(A(X))$ that satisfy Equation 9.7: (a) Uncorrelated random field , (b) correlated random field. Bottom grids are the term $(\varepsilon(X))$. Middle grid is the term $(\bar{A}(X))$ calculated by Equation 4.6. The upper grids are the true attribute $(A(X))$.

and the quality of this prediction following Equation 9.14 (without any correlation structure) is given by:

$$\sigma_{P_N}^2 = \left(\frac{\partial P_N}{\partial Q}\right)^2 \cdot \sigma_Q^2 + \left(\frac{\partial P_N}{\partial L_N}\right)^2 \cdot \sigma_{L_N}^2 \tag{9.25}$$

So, determining the derivatives gives:

$$\sigma_{P_N} = \sqrt{(L_N \cdot \sigma_Q)^2 + (Q \cdot (0.25 \cdot L_N))^2} \tag{9.26}$$

Similarly to Section 9.2.1, we implemented Equation 9.26 using a GRASS's function *r.mapcalc* (Shapiro & Westervelt, 1992) and the result is shown in Figure 9.11. The large margin of error shown in Figure 9.11 (lighter grey levels) resulting from the use of multiplicative models. A discussion about the propagation of errors through arithmetical operations can be seen in Burrough, (1986).

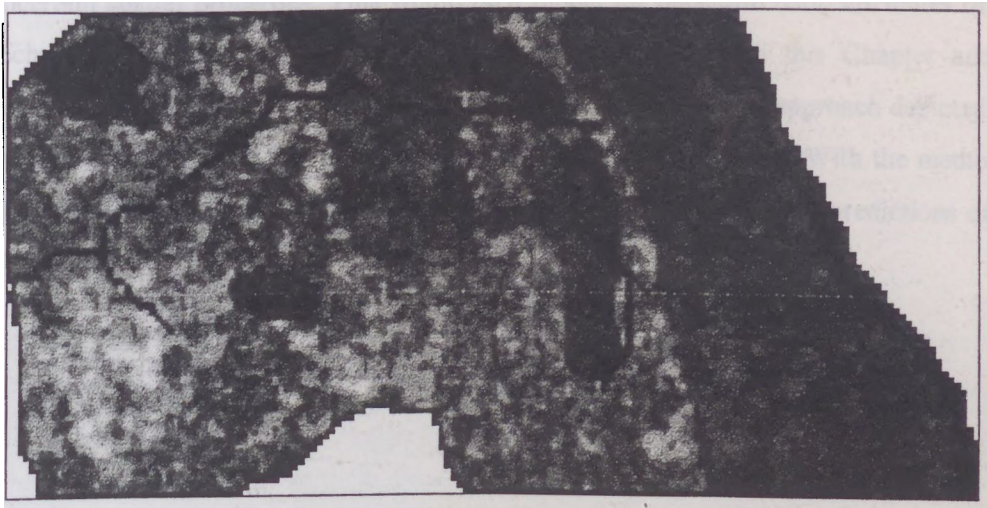


Figure 9.11 - Uncertainty of results for nitrogen prediction.

9.3 - Conclusions

Throughout this thesis we have discussed many sources of error that affect the result of distributed environmental models. There can be errors in the theoretical structure of the model, errors in the mathematical solution methods in the model, calibration errors, and errors in the data. Knowledge of these errors in physically based models is important to be able to make a correct judgement of a model.

A stochastic approach was formulated to represent error in qualitative spatial attributes. The rationale behind the choice of a stochastic model was that because of uncertainty, the best one can do is to represent the value of a spatial attribute at any given location by a distribution of possible values, and not by a single deterministic value.

The stochastic formulation presented here contains many parameters, such as the mean (representing the trend or bias) and the standard deviation (representing random error). These

parameters are functions defined on a geographical domain. The spatial dimension of the problems also requires that a full characterisation of the error model must include spatial autocorrelation. When multiple attributes are considered, spatial crosscorrelation must be defined as well.

The spatial water quality model presented in this thesis is 'unconcerned' of the fact that it operates with uncertain spatial data. A better solution would be if the model were to deal directly with uncertain spatial properties. This would be a model for uncertain data, attributes of which are stochastic rather than deterministic. The approach illustrated in this Chapter adapt the database structure to the specific properties of stochastic attributes. The approach depicted in this thesis works well in practice but it has its limitations (see Chapter eight). With the methodology presented in this chapter maps of predictions and standard deviations of the predictions can then be made.

10. Summary and conclusions

10.1 - Review of major points

In the introduction, Chapter one, the primary objective of this thesis was identified. It was simply, an attempt to analyse the relationship between loads of pollutants and water quality for actual and projected conditions in large areas, using a distributed water quality modelling approach , within a GIS framework.

The methodology presented here, proposed a model for water quality prediction under Brazilian conditions of limited data availability, aggregating both point and non point sources impacts originating from both urbanised and agricultural land uses. The approach has taken advantage of the visual communication potential of GIS to facilitate use at all levels of the modelling process. The modelling approach presented here is not intended to replace the use of more complex models in water quality analyses. Rather, the approach is seen as complementary to these models in that it provides a means of screening a multitude of actions and water quality management options to identify a select set of alternatives to be further examined. Further examination of a more specific set can then be done with more complex, data intensive modelling algorithms.

In this thesis, we presented what we felt a reasonable framework for conducting water quality studies and applied to Sinos catchment in southern Brazil.

Initially, the system uses land use and area-based pollutant loading rates as input to a non point source pollutant loading model. Output from the loading model reflects the pollutant contribution attributable to surface runoff within the catchment. This output, when combined with estimates of point source loadings, serves as input to a water quality model of the river network. Output from the water quality model may be compared with water quality objectives or standards to determine if remedial action is required. For example, if some load reduction is needed, the model framework permits the manager to quickly evaluate available alternatives, such as implementation of agricultural or urban runoff controls. In this manner, each remedial action can be readily screened to determine its effectiveness in achieving the specified objectives. As model inputs are manipulated to reflect implementation of a particular management plan, the model output can be instantly observed and the feasibility of the plan can be evaluated.

All of the models apply a mass balance approach to calculate spatial distribution of pollutants, which considers sources of pollutants (point and non point) for mixed models oriented along the flow paths. The delivery of pollutants to downstream locations occurs in two phases:

1. Slope-to-river processes where overland flow operates, and
2. Within-river processes where liquid-phase processes operates

The link between these two phases occurs in a river 'buffer' zone where point and non point source are stored.

The slope-to-river process can also be divided in three phases:

- 1.a Production of runoff.
- 1.b Production of pollutants-
- 1.c Transport of pollutants.

Within--river processes are divided into two levels:

- 2.a Aggregation of sources of pollutants
- 2.b The river process

The above division and sub-division provided a functional structure to this thesis and have confirmed to be useful as an aid in the analysis of environmental changes for water quality in Sinos catchment projects. It must, however, be used with caution and common sense, and should not become a mechanical tool to perform evaluations.

The general conclusions of this thesis, specially through the analysis of the case study, are outlined in the following statements:

1. Despite its limitations, the approach has been successfully applied to a case study in Sinos catchment.
2. It introduces the error assessment as an integral part of the evaluation process.
3. It provides useful information to water quality manages, without great cost and effort.
4. It presents results in realistic terms, under the circumstances.
5. It is readily adapted to improvements and modifications.
6. It is applicable to multi-objective projects in large catchments with different categories of land use and pollutant sources.

10.2 - Concluding remarks

During the development of this thesis a number of issues have arisen and been considered.

The assumptions underlying physically based hydrologic models such as those used in this thesis are extensive and operate at all levels of the model from the overall model structure to the constituent algorithms. The use of these assumptions presupposes that the physical processes can be represented in a deterministic way, that the overall catchment response can be represented by the combined action of the constituent process representations, and that the spatial variability of a catchment can be represented by distributed values of the model parameter at the scale which the model has been used. Therefore, there is a difference in scale between model cell size, the scale at which the algorithms were derived and the scale at which the parameters are measured. Although the algorithm approach works well, the concept of the integration that occurs in Sinos catchment is not well represented by the formulations in process-based, distributed hydrological models, and so the physical basis of the original algorithms may be lost.

A pertinent example from the Sinos catchment is the generation of runoff (Chapter Four). The complex heterogeneity of soils, land use, topography and their interaction with meteorological inputs that vary with space and time, results in fluxes of water in Sinos river whose scale properties are unknown. The complexity of Sinos catchment is integrated and attenuated in the field, and the challenge is to describe enough of the complexity to develop models that perform a similar integration on model parameters without the need for explicit representation of the underlying complexity. In Sinos catchment, the variation in simulated flow (Chapter Four) characteristics due to parameter choice is so great that argument over the complexity of the flow equations is futile. In large scales (around 4000 km² in Sinos catchment) there is no “physical basis” for the representation of surface flow. Therefore, there is no “physical basis” to estimated flow characteristics, nor to any subsequent estimates of pollutants loads and concentrations derived from those characteristics.

One implication is that there is little point in developing a highly detailed physical model that attempts to simulate the complex relationships between land use (point and non point sources) and water quality, if there are large uncertainties in the input data.

Geographical information systems were used for storing , manipulating and visualising spatially distributed catchment data. Such technique (also remote sensing) offer possibilities for providing

some of the information required for model development and testing but are, in themselves, not an answer.

In fact the development of concepts specifically designed to operate at larger scale is an active area of hydrological research but in the meantime alternative strategies are required. For management purposes, simpler models in which data requirements are low, assumptions are clearly stated and results are generally qualitative may be a more realistic approach and more in balance with the available level of knowledge. This approach was used in this thesis, providing a qualitative understanding of distributed catchment response and the relative change in response resulting from altered spatial characteristics but not quantitative estimates because of the problems already discussed.

The GIS-based water quality index model used in Sinos catchment provides an approach for other regions to consider for initial catchment screening. This screening does not produce precise values of pollutant generation or transport. It does indicate a relative comparison of pollution potential severity. We developed the modelling framework simultaneously with the GIS database compilation. The model relies in commonly used “physical basis” relationships providing a valid framework that can be modified for future use. It considers some pollutant generation and transport processes. The rationale underlying these approaches is that landscapes develop in response to hydrologic processes active in the landscape. If the variability of landscape characteristics, measured by a landscape attributes like $\ln(A/\tan \beta)$ (Chapter Four) and pollutant load index (Chapter Five), can be captured, then the variability of many hydrologic processes and pollutants characteristics can also be captured. The framework presented here based on simple assumptions about catchment response can provide qualitative information about catchment behaviour with very little field data. In order to accept these simple results I require to myself an end to desire for a quantitative answer, no matter how inaccurate and our level of knowledge is insufficient to provide a reliable, meaningful, absolute answer.

Because describing and understanding the variability of Sinos catchment (land use and water quality relationships) is difficult, resulting in a poorly modelled system, the error variability, which is superimposed on the system, can make it even more difficult to describe and understand. In Chapter 9, attention was draw to this particular weakness of the system, and the uncertainty analysis was used to compute how the various error sources combine to yield the error in the final output. One important point to be stressed, is that the applicability of this approach is limited to the case where functions are constant and deterministic. In other words, although all variables can

be considered as random variables, the functions that link those variables were assumed unchangeable. The procedure developed here seems applicable to many practical situations.

The disaggregation of the water quality problem was made until the point where common elements could be identified such as land use and runoff effects on water quality. However, other information may also be included, if its inclusion is deemed useful. However, this would increase the number of variables (and consequently model processes) and so increase substantially the computer time for simulation and the efforts for the mathematical calculations.

The main motivation for this thesis originated from meetings at COMITESINOS (See Chapter One) where one of the main problems are water quality in Sinos catchment. The hydrologic response of the catchment could not be represented by the available models, so estimates of pollutants movement overland were impossible. The modelling approach created in this thesis was developed as tool for understanding the catchment response. We conclude that our ability to model hydrologic response in a distributed, deterministic and precise way is poor. The algorithms used here, while appearing conceptually sophisticated (like the routing scheme in Chapter Seven), are based on assumptions that are often invalid or questionable, or that are crude representations of the reality and generally derived at a scale different from that to which they are applied, and the field data that are insufficient to estimate spatial variability of parameter or even to fully validate the model. Therefore, the results of this thesis are enabling us to ask more questions, many of which are fundamental to our understanding of the natural systems that are subjected of our models.

10.3 - Research issues for the near future

The approach developed in this thesis is largely a basic framework. In the longer term we believe that this water quality methodology will be generalised beyond the particular requirements of the Sinos catchment, despite its weakness. Integrated catchment management is now become accepted as being central to the better management of Brazil's water resources, and we see the framework proposed here as being an important resource for this management, since it links land use and management activities to water quality within a policy framework.

Some of the problems concerning the links between land use, water quality and management activities have merely been touched upon in the course of this research; others have been

completely ignored. Of course, a better understanding of all system components (if data is available to explain this 'understanding') is required for general improvement of the model. Therefore, the following research approaches are suggested to further extend and refine the application of the proposed approach:

1. The hydrological fluxes act in the heterogeneity of land use, soils, topography and meteorological inputs, all of which have different length scales. How should these parameters be linked across different scales ?
2. The relationship between delivery ratio, pollutant distribution in soil, surface runoff and sediment, and enrichment ratio should be established.
3. There is a need to generalise the system further and use it to analyse other water resources, i.e., geologic data should be included, in order to make assessments of groundwater pollution potential component.
4. The data units should be standardised and recorded. For example, a land use classification appropriate for water quality predictions or a water quality index for summarising the results should be used. Also, better information on uncertainty associated with the data should be requested.
5. Another problem ignored in this thesis is temporal variation. Evidently, many attributes vary in time as well in space, and so a model for spatio-temporal data should also include temporal variability.
6. The issue of error is another requirement. The premise that the parameters of the uncertainty model are correctly specified is commented on Chapter 9. However, it is doubtful whether this assumption is always acceptable in practice. This is an important problem because error propagation analysis will only yield sensible results if the input data and model errors have realistic values. More investigations in uncertainty analysis are needed.
7. The approach used in this research handle the spatial variation of the environment. A more fundamental problem is to decide which model of spatial variation to use for the representation of spatial data. We must make sure that the right model is used with the right data. For instance, there is attributes that vary gradually in space and others with abrupt changing properties. There should be more clarity on these issues of modelling spatial variation
8. The spatial model described in this thesis can be employed with both deterministic and statistical modes of water quality modelling. Distance-weighted predictor variables (i.e. point and non-point loads) could be employed in regression analysis to predict water quality in the drainage network when decay rates and pollutant loads are unknown. In using regression with this spatial model, both deterministic (the dependent or independent variables may contain distance and slope effects) and statistical modes of modelling are combined.

9. Regional water quality assessment methods such as the one describe here can be used for the design of optimum sampling networks because all possible pollution sources can be captured in the domain. Prediction zones that yield the greatest uncertainty would suggest the need for increased sampling densities.

In summary, the aim of this thesis has been to develop a water quality model, suitable for Brazilian conditions, which is useful as an aid in the determination on environmental changes for water resource development projects. It must, however, be used with caution and common sense, and should not become a mechanical tool.

Bibliography

- ABBOTT, M.B.; BATHURST, J.C.; CUNGE, J.A.; O'CONNELL, P.E. and RASMUSSEN, J. (1986) An introduction to the European Hydrological System - Systeme Hydrologique Europeen, 'SHE', 2: Structure of a physically-based distributed modelling system. Journal of Hydrology. **87**: 61-77.
- AGRAR-UND HYDROTECHNIK GmbH, Essem (1969) Rio dos Sinos: planejamento hidrologico. Essen. 4v em 7.
- AHUJA, L.R.; SHARPLEY, A.N. and LEHMAN, O.R. (1982) Effect of soil slope and rainfall characteristics on phosphorus in runoff. Journal of Environmental Quality. **11**: 9-13.
- AHUJA, L.R.; SHARPLEY, A.N.; YAMAMOTO, M. and MENZEL, R.G. (1981) The depth of rainfall-runoff-soil interaction as determined by ^{32}P . Water Resources Research. **17**: 969-974.
- AMOROCHO, J. and BRANDSTETTER, A. (1971) Determination of nonlinear functional response functions in rainfall-runoff processes. Water Resources Research. **7**: 1087-1101.
- ARNOLD, J.G.; WILLIAMS, J.R.; NICKS, A.D.; and SAMMONS, N.B. (1990) **SWRRB**: A basin scale simulation model for soil and water resources management. Dalas: Texas A&M University Press. 189p.
- BAND, L.E. (1986) Topographic partition of watersheds with digital elevation models. Water Resources Research. **22**: 15-24.
- BAND, L.E. (1989) Spatial aggregation of complex terrain. Geographical Analysis. **21**: 279-293.
- BEARD, L and CHANG, S. (1979) Urbanization impact of streamflow. Journal of the Hydraulics Division, American Society of Civil Engineers. **105**: 647-660.
- BEASLEY, D.B.; HUGGINS, L.F. and MONKE, E.J. (1980) ANSWERS: A model for watershed planning. Transactions of the American Society of Agricultural Engineers. **23**: 938-944.

- BENETTI, A.D. (1987) **Tratamento físico-químico de águas residuárias domésticas e industriais combinadas entre si**. Porto Alegre; UFRGS - Curso de Pós-Graduação em Engenharia Civil. 256p. Dissertação (mestrado).
- BENJAMIN, J.R. and CORNEL, C.A. (1970) **Probability, Statistics, and Decision for Civil Engineers**. New York: McGraw-Hill. 648p.
- BENNETT, R.J. and CHORLEY, R.J. (1978) **Environmental systems**. London: Methuen. 624p.
- BERRY, J. and SAILOR, J. (1987) Use of geographic information system for storm runoff prediction for small urban watersheds. Environmental Management. **11**: 21-27.
- BEVEN, K.J. (1989) Changing ideas in hydrology - the case of physically-based models. Journal of Hydrology. **105**: 157-172.
- BEVEN, K.J. and KIRKBY, M.J. (1979) A physically-based variable contributing area model of basin hydrology. Hydrological Sciences Bulletin. **24**: 43-69.
- BINLEY, A.; ELGY, J. and BEVEN, K. (1989) A physically based model of heterogeneous hillslopes: 2. Runoff production. Water Resources Research. **25**: 1219-1226.
- BRAS, R.L. and RODRIGUEZ-ITURBE, I. (1985) **Random functions and hydrology**. Reading: Addison- Wesley. 559p.
- BROWNE, F.X. and GRIZZARD, T.J. (1979) Water pollution: nonpoint sources. Journal. Water Pollution Control Federation. **51**: 1418-1444.
- BURKE, R. (1983) Velocity equation for water quality modeling in Georgia. Water Resources Bulletin. **19**: 271-276.
- BURN, D.H. and McBEAN, E.A. (1985) Optimization modeling of water quality in an uncertain environment. Water Resources Research. **21**: 934-940.
- BURROUGH, P.A. (1986) **Principles of geographical information systems for land resources assessment**. Oxford: Claredon. 194p.
- BURROUGH, P.A. (1992) Development of intelligent geographical information systems. International Journal Geographical Information Systems. **6**: 1-11.

- CASTILLO, J.E. (1991) A discrete variational grid generation method, SIAM Journal on Scientific and Statistical Computing. **12**: 454-468.
- CHENG, C. and HANSEN, V.E. (1966) Theory and characteristics of overland flow. Transactions of the American Society of Agricultural Engineers. **9**: 20-25.
- CHOW, V.T.; MAIDMENT, D.R. and MAYS, L.W. (1988) **Applied hydrology**. New York: McGraw-Hill. 572p.
- CLARKE, R.T. (1973) A review of some mathematical models used in hydrology, with observations on their calibration and use. Journal of Hydrology. **19**: 1-20.
- CLIFF, A.D. and ORD, J.K. (1981) **Spatial processes: Models and Applications**. London: Pion. 248p.
- CLUIS, D.A.; COUILLARD, D. and POTVIN, L. (1979) A square grid transport model relating land use exports to nutrient loads in rivers. Water Resources Research. **15**: 630-636.
- COHEN, P.; ALLEY, W.M. and WILBER, W.G. (1988) National water quality assessment: future directions of the U.S. Geological Survey. Water Resources Bulletin. **24**: 1147-1151.
- COLLINS, S.H. and MOON, G.C. (1981) Algorithms for dense digital terrain models. Photogrammetric Engineering and Remote Sensing. **47**:71-76.
- CONSELHO NACIONAL DO MEIO AMBIENTE - CONAMA (1992) Resoluções do CONAMA: 1984/91. 4. ed. rev. aum. Brasília: IBAMA. 245P.
- COOK, H.F. (1991) Nitrate protection zones: Targeting and land use over an aquifer. Land Use Policy. **8**: 16-28.
- COX, W.E. (1988) Water and Development: A complex relationship. Journal of Water Resources Planning and Management. **114**: 91-98.
- CRESSIE, N. (1991) **Statistics for spatial data**. New York: JohnWiley. 900p.
- CUSHMAN, J.H. (1984) Fourier representation of multiphase averaging theory. Advances in Water Resources. **7**: 126-131.

- DAGAN, G. (1986) Statistical theory of groundwater flow and transport: Pore to laboratory, laboratory to formation, and formation to regional scale. Water Resources Research. **22**: 120-134.
- DAVIS, D.W. (1978) Comprehensive flood plain studies using spatial data management techniques. Water Resources Bulletin. **14**: 587-604.
- DECOURSEY, D.G. (1985) Mathematical models for nonpoint water pollution control. Journal of Soil and Water Conservation. **40**: 408-413.
- DELHOMME, J.P. (1979) Spatial variability and uncertainty in groundwater flow parameters: a geostatistical approach. Water Resources Research. **15**: 269-280.
- DE LUCA, S., coord. (1987) **A problemática dos resíduos líquidos industriais na bacia do rio dos Sinos**. Porto Alegre, IPH/UFRGS. 2 v.
- De ROO, A.P.J.; HAZELHOFF, L. and BURROUGH, P.A. (1989) Soil erosion modelling using 'ANSWERS' and Geographical Information Systems. Earth Surface Processes and Landforms. **14**: 517-532.
- De ROO, A.P.J.; HAZELHOFF, L. and HEUVELINK, B.M. (1992) Estimating the effects of spatial variability of infiltration on the output of a distributed runoff and soil erosion model using Monte Carlo methods. Hydrological Processes. **6**: 127-143.
- DETTINGER, M.D. and WILSON, J.L. (1981) First order analysis of uncertainty in numerical models of groundwater flow. Part I. Mathematical development. Water Resources Research. **17**: 149-161.
- DEUTSCH, C.V. and JOURNEL, A.G. (1992) **GSLIB geostatistical software Library**. Oxford: Oxford University Press. 316p.
- DJOKIC, D. and MAIDMENT, D.R. (1991) Terrain analysis for urban stormwater modelling. Hydrological Processes. **5**:115-124.
- DMAE (1985) **Bacia hidrografica do rio Jacuí: diagnóstico hidrossanitário**. Porto Alegre. 30p. (DMAE publicação n. 44).
- DMAE and CESB (1981) **Qualidade sanitária do rio dos Sinos**. Porto Alegre. v. 2. (DMAE. publicação n. 33).

- DNPA (1973) **Levantamento de reconhecimento dos solos do estado do Rio Grande do Sul**. Recife. 431p. (Boletim Técnico n. 30).
- DOLAN, D.M.; YUI, A.K. and GEIST, R.D. (1981) Evaluation of river load estimation methods for total phosphorus. Journal of Great Lakes Research. **7**: 207-214.
- DUBRULE, O. (1984) Comparing splines and kriging. Computers and Geosciences. **10**:327-338.
- DUDA, A.M. (1982) Municipal point source and agricultural nonpoint source contributions to coastal eutrophication. Water Resources Bulletin. **18**: 397-407.
- DUNNE, T.; MOORE, T.R.; and TAYLOR, C.M. (1975) Recognition and prediction of runoff-producing zones in humid regions. Hydrological Sciences Bulletin. **20**: 305-327.
- EAGLESON, P.S. (1970) **Dynamic Hydrology**. New York: McGraw-Hill. 462 p.
- EISEMAN, P.R. (1985) Grid generation for fluid mechanics computations. Annual Review of Fluid Mechanics. **17**: 487-522.
- EVANS, B.M. and MYERS, W.L. (1990) A GIS-based approach to evaluating regional groundwater pollution potential with DRASTIC. Journal of Soil and Water Conservation. **45**: 242-245.
- EVANS, I.S. (1980) An integrated system of terrain analysis and slope mapping. Zeitschrift fur Geomorphologie: Supplementband. **36**:274-295.
- FAIRFIELD, J. and LEYMARIE, P. (1991) Drainage networks from grid digital elevation models. Water Resources Research. **27**: 709-717.
- FALKENMARK, M. (1990) Environmental management and the role of the hydrologist. Nature and Resources. **26**: 14-23.
- FEDRA, K. (1986) Decision making in water resources planning. In: Unesco Symposium on Decision Making in Water Resources Planning. Oslo: p.161-174.
- FEDRA, K. (1993) Models, GIS and expert systems: integrated water resources models. In: KOVAR, K.;NACHTNEBEL, H.P., ed. Application of Geographic Information Systems in hydrology and water resources management. IAHS. p.297-308. (International Association of Hydrological Sciences. Publication n. 211).

- FERREIRA, V. (1986) **Influência da nitrificação no coeficiente de desoxigenação "k₁" do rio dos Sinos**. Porto Alegre; UFRGS - Curso de Pós-Graduação em Engenharia Civil. 139p. Dissertação (mestrado).
- FISCHER, H.B.; LIST, E.J.; KOH, R.C.Y.; IMBERGER, J. and BROOKS, N.H. (1979) **Mixing in inland and coastal waters**. New York: Academic Press. 483p.
- FLACKE, W.; AUERSWALD, K. and NEUFANG, L. (1990) Combining a modified Universal Soil Loss Equation with a digital terrain model for computing high resolution maps of soil loss resulting from rain wash. Catena. **17**: 383-397.
- FOSTER, G.R. (1982) Modeling the erosion process. In: HAAN, C.; JOHNSON, H.; BRAKENSIEK, D., ed. Hydrologic modeling of small watersheds. Saint Joseph: American Society of Agricultural Engineers. p.297-380. (ASAE Monograph n. 5).
- FRANCHINI, M. and PACCIANI M. (1991) Comparative analysis of several conceptual rainfall-runoff models. Journal of Hydrology. **122**: 161-219.
- FREEMAN, G.T. (1991) Calculating catchment area with divergent flow based on a regular grid. Computers and Geosciences. **17**: 413-422.
- FREITAS, A. et al., (1981) Pesquisa E: qualidade das águas dos formadores do rio Guaíba. In: BORDAS, M., (coord) Uso e conservação dos recursos hídricos do Rio Grande do Sul. segunda etapa: relatório final. Porto Alegre, IPH/UFRGS, v. 5, cap. 7.
- GANDOY-BERNASCONI, W. and PALACIOS-VELEZ, O. (1990) Automatic cascade numbering of unit elements in distributed hydrological models. Journal of Hydrology. **112**:375-393.
- GOODCHILD, M.F. (1992) Geographical data modelling. Computers and Geosciences. **18**: 401-408.
- GOODCHILD, M.F.; GUOQING, S. and SHIREN, Y. (1992) Development and test of an error model for categorical data. International Journal Geographical Information Systems. **6**:87-104.

- GRAYMAN, W.M.; MALES, R.M.; GATES, W.E. and HADDER, A.W. (1975) Land-based modeling system for water quality management studies. Journal of the Hydraulics Division, American Society of Civil Engineers. **101**: 567-580.
- GRAYSON, R.B.; MOORE, I.D.; and McMAHON, T.A. (1992) Physically based hydrologic modeling. 1. A terrain-based model for investigative purposes. Water Resources Research. **28**: 2639-2658.
- GREENLEE, D.D. (1987) Raster and vector processing for scanned linework. Photogrammetric Engineering and Remote Sensing. **53**:1383-1387.
- GREGORY, K.J. and WALLING, D.E. (1968) The variation of drainage density within a catchment. Bulletin. International Association of Scientific Hydrology. **13**:61-68.
- GRIFFITH, D.A. (1988) **Advanced Spatial Statistics**. Dordrecht: Kluwer. 287p.
- GUPTA, S.K. and SOLOMON, S.I. (1977) Distributed numerical model for estimating runoff and sediment of ungaged rivers. Water Resources Research. **13**: 613-636.
- HAITH, D.A. (1976) Land use and water quality in New York rivers. Journal of the Environmental Engineering Division, American Society of Civil Engineers. **102**: 1-15.
- HAITH, D.A. and TUBBS, L.J. (1981) Watershed loading functions for nonpoint sources. Journal of the Environmental Engineering Division, American Society of Civil Engineers. **107**: 121-137.
- HARMS, L.L.; DORNBUSH, J.N. and ANDRESEN, J.R. (1974) Physical and chemical quality of agricultural land runoff. Journal. Water Pollution Control Federation. **46**: 2460-2470.
- HAZZANIZADEH, M. and GRAY, W.G. (1979) General averaging equations for multi-phase systems: 1.Averaging procedure. Advances Water Resources. **2**: 131-144.
- HELMER, R. (1987) Socio-economic development levels and adequate regulatory policy for water quality management. Water Science Technology. **19**: 257-272.
- HEUVELINK, G.B.M. (1992) An iterative method for multidimensional simulation with nearest neighbour models. In: DOWD, P.A., and ROYER, J.J., ed., CODATA: 2nd Conference on Geomathematics and Geostatistics. Nancy: Sciences de la Terre. p.51-57. (Informatique et Geologique n. 31).

- HEUVELINK, G.B.M.; BURROUGH, P.A. and LEENAERS, H. (1990) Error propagation in spatial modelling with GIS. In: HARTS, J. et al., ed., EGIS'90: proceedings. Utrecht. EGIS Foundation. p.453-462.
- HOLLAND, M.M.; RAST, W. and RYDING, S.O. (1990) Water quality management. Nature and Resources. **26**: 3-13.
- HOLTAN, H.N.; ENGLAND, C.B. and SHANHOLTZ, V.O. (1967) Concepts in hydrologic soil grouping. Transactions of the American Society of Agricultural Engineers. **10**: 407-410.
- HOPKINS, L. (1984) Evaluation of methods for exploring ill-defined problems. Environment and Planning B. **11**: 339-348.
- HORNBERGER, G.H.; BEVEN, K.J.; COSBY, B.J. and SAPPINGTON, D.E. (1985) Shenandoah watershed study: calibration of a topography-based, variable contributing area hydrological model to a small forested catchment. Water Resources Research. **21**: 1841-1850.
- HORTON, R.E. (1945) Erosional development of streams and their drainage basins; hydrophysical approach to quantitative morphology. Bulletin of the Geological Society of America. **56**:275-370.
- HUTCHINSON, M.F. (1989) A new procedure for gridding elevation and stream line data with automatic removal of spurious pits. Journal of Hydrology. **106**:211-232.
- IBGE-(1990) Estimativa da populacao residente em 01 de julho de 1990. Rio de Janeiro, IBGE (Instituto Brasileiro de Geografia e Estatistica). 387p.
- ITACONSULT - LATINOCONSULT BRASILEIRA (1974) **Estudo hidro-sanitário do rio dos Sinos**. Roma. 5v.
- JAGER, H.I.; SALE, M.J. and SCHMOYER, R.L. (1990) Cokriging to assess regional stream quality in the Southern Blue Ridge Province. Water Resources Research. **26**: 1401-1412.
- JAMES, G. (1992) **Modern Engineering mathematics**. Wokingham: Addison-Wesley. 897p.
- JARVIS, R.S. (1977) Drainage network analysis. Progress in Physical Geography. **1**:271-295.

- JENSON, S.K. and DOMINGUES, J.O. (1988) Extracting topographic structure from digital elevation data for geographic information system analysis. Photogrammetric Engineering and Remote Sensing. **54**:1593-1600.
- JOHANSON, R.C. and KITTLE, J.L. (1983) Design, programming and maintenance of HSPF. Journal of Technical Topics in Civil Engineering. **109**: 41-57.
- JOHNSON, L.E. (1986) Water resources management decision support systems. Journal of Water Resources Planning and Management. **112**: 308-325.
- JOHNSTON, C.A.; DETENBECK, N.E.; BONDE, J.P. and NIEMI, G.J. (1988) Geographic information system for cumulative impact assessment. Photogrammetric Engineering and Remote Sensing. **54**: 1609-1615.
- JONES, N.L.; WRIGHT, S.G. and MAIDMENT, D.R. (1990) Watershed delineation with triangle-based terrain modes. Journal of Hydraulic Engineering. **116**:1232-1251.
- JOURNEL, A.G. and HUIJBREGTS, C.H.J. (1978) **Mining Geostatistics**. London: Academic Press. 376p.
- JULIEN, B.; FENVES, S.J. and SMALL, M.J. (1992) An environmental impact identification system. Journal of Environmental Management. **36**: 167-184.
- KELLY, R.E.; McCONNELL, P.R.H. and MILDENGERGER, S.J. (1977) The Gestalt photomapping system. Photogrammetric Engineering and Remote Sensing. **43**: 1407-1417.
- KEMP, K.K. (1993) Environmental modelling and GIS: dealing with spatial continuity. In: KOVAR, K.;NACHTNEBEL, H.P., ed. Application of Geographic Information Systems in hydrology and water resources management. IAHS. p.107-115. (International Association of Hydrological Sciences. Publication n. 211).
- KIRKBY, M.J.; LOCKWOOD, J.; THORNES, J.B.; WOODWARD, I.; BAIRD, A.; McMAHON, M.; MITCHELL, P. and SHEEHY, J. (1992) **MEDALUS Project Report**: Development of a physically based simulation model for vegetation growth, hydrology and soil degradation. London: Interim report. 19 p.

- KNISEL, W.G. (1980) **CREAMS: A field-scale model for chemicals, Runoff and erosion from Agricultural Management Systems**. Tucson: U.S. Department of Agriculture. 643p. (Conservation Research Report n. 26).
- KOVAR, K. and NACHTNEBEL, H.P. ed. (1993) **Application of Geographic Information System in Hydrology and Water Resources Management**. Wallingford: IAHS. 693 p. (International Association of Hydrological Sciences. Publication n.211).
- KUCZERA, G. (1988) On the validity of first-order prediction limits for conceptual hydrologic models. Journal of Hydrology. **103**: 229-247.
- LEBERL, F.W. and OLSON, W. (1982) Raster scanning for operational digitizing of graphical data. Photogrammetric Engineering and Remote Sensing. **48**:615-627.
- LEWIS, P.A.W. and ORAV, E.J. (1989) **Simulation methodology for statisticians, operation analysts and engineers**. Pacific Grove: Wadsworth and Brooks/Cole. v.1.
- LINSLEY, R.K.; KOHLER, M.A. and PAULHUS, L.H. (1982) **Hydrology for engineers**. 3rd. ed., New York: McGraw-Hill. 415p.
- LOAGUE, K. and FREEZE, R. (1985) A comparison of rainfall-runoff modeling techniques on small upland catchments. Water Resources Research. **21**: 229-248.
- LOAGUE, K.; YOST, R.S.; GREEN, R.E.; and LIANG, T.C. (1989) Uncertainty in pesticide leaching assessment in Hawaii. Journal of Contaminant Hydrology. **4**: 139-161.
- LOEHR, R.C. (1974) Characteristics and comparative magnitude of non point sources. Journal. Water Pollution Control Federation. **46**: 1849-1872.
- LOUCKS, D.P; KINDLER, J. and FEDRA, K. (1985) Interactive water resources modeling and model use: an overview. Water Resources Research. **21**: 95-102.
- LUNA CAICEDO, N. and SIMÕES LOPES, M. (1976) **Modelo reduzido do rio dos Sinos, proteção contra inundações: relatório final preliminar**. Porto Alegre, IPH/UFRGS. 25p.
- McELROY, A.D.; CHIU, S.Y.; NEBGEN, J.W.; ALETI, A. and BENNETT, F.W. (1976) Loading functions for assessment of nonpoint sources. Washington: U.S. Environmental Protection Agency. (EPA/600/2-76/150).

- McQUIVEY, R.S. and KEEFER, T.N. (1974) Simple method for predicting dispersion in streams. Journal of the Environmental Engineering Division, American Society of Civil Engineers. **100**: 997-1011.
- MAIDMENT, D.R. (1993) Environmental modeling within GIS. In: International Conference/Workshop on Integrating Geographic Information Systems and Environmental Modeling. 2., 1993, Breckenridge: NCGIA.
- MARK, D.M. (1975) Computer analysis of topography: a comparison of terrain storage methods. Geografiska Annaler. **57A**:179-188.
- MARK, D.M. (1984) Automated detection of drainage networks from digital elevation models. Cartographica. **21**:168-178.
- MARSALEK, J. (1989) Modelling agricultural runoff: overview. In: HADLEY, R.F.; ONGLEY, E.D., ed. Sediment and the environment. Wallingford: IAHS. p.201-209. (International Association of Hydrological Sciences. Publication n.184).
- MASS, R.P.; SMOLEN, M.D. and DRESSING, S.A. (1985) Selecting critical areas for nonpoint-source pollution control. Journal of Soil and Water Conservation. **40**: 68-71.
- MEADOWS, M.E.; WEETER, D.W. and GREEN, J.M. (1978) Assessing nonpoint water quality for small streams. Journal of the Environmental Engineering Division, American Society of Civil Engineers. **104**: 1119-1133.
- MEGAHAN, W.F. and KING, P.N.(1985) Identification of critical areas on forest lands for control of nonpoint sources of pollution. Environmental Management. **9**: 7-11.
- MENDES, C.A.B. (1990) **Uso das tecnicas de sensoriamento remoto na regio estuarina da laguna dos patos -RS**. Porto Alegre; UFRGS - Curso de Pós-Graduação em Engenharia Civil. 191p. Dissertação (mestrado).
- MEYER, S.P.; SALEM, T.H. and LABADIE, J.W. (1993) Geographic information systems in urban storm-water management. Journal of Water Resources Planning and Management. **119**: 206-228.
- MINIEKA, E. (1978) **Optimization algorithms for networks and graphs**. New York: Marcel Dekker. 389p.

- MOORE, I.D. (1988) A contour-based terrain analysis program for the environmental sciences (TAPES). EOS. Transactions American Geophysical Union. **69**:345.
- MOORE, I.D.; GALLANT, J.C.; GUERRA, L.; and KALMA, J.D. (1993) Modeling the spatial variability of hydrological processes using GIS. In: KOVAR, K.; NACHTNEBEL, H.P., ed. Application of Geographic Information Systems in hydrology and water resources management. IAHS. p.161-169. (International Association of Hydrological Sciences. Publication n. 211).
- MOORE, I.D. and GRAYSON, R.B. (1989) Hydrologic and digital terrain modelling using vector elevation data. EOS. Transactions American Geophysical Union. **70**:1091.
- MOORE, I.D. and GRAYSON, R.B. (1991) Terrain-based catchment partitioning and runoff prediction using vector elevation data. Water Resources Research. **27**:1177-1191.
- MOORE, I.D.; GRAYSON, R.B. and LADSON, A.R. (1991) Digital terrain modelling: A review of hydrological, geomorphological, and biological applications. Hydrological Processes. **5**:3-30.
- MORETTI, L. (1979) Estudo da qualidade das águas do rio dos Sinos e sua capacidade autoperflocadora. Porto Alegre, IPH/UFRGS. Apresentado no 9º Congresso Brasileiro de Engenharia Sanitaria, Manaus, 1977.
- MORETTI, L. (1980) **Análise de autodepuração em cursos de água: aplicação ao rio dos Sinos**. Porto Alegre; UFRGS - Curso de Pós-Graduação em Engenharia Civil. 131p. Dissertação (mestrado).
- NASH, J. and SUTCLIFFE, J. (1970) River flow forecasting through conceptual models: part 1 - A discussion of principles. Journal of Hydrology. **10**: 282-290.
- NOVOTNY, V. (1980) Delivery of suspended sediment and pollutants from non point sources during overland flow. Water Resources Bulletin. **16**: 1057-1065.
- O'CONNOR, D.J. (1967) The temporal and spatial distribution of dissolved oxygen in streams. Water Resources Research. **3**: 65-79.
- O'LOUGHLIN, E.M. (1981) Saturation regions in catchments and their relationships to soil and topographic properties. Journal of Hydrology. **53**: 229-246.

- ORDNANCE SURVEY (1994) Digital Map Data - Catalogue 1994. Southampton. 27p.
- PARKER, H. (1988) Unique qualities of a geographic information system: A commentary. Photogrammetric Engineering and Remote Sensing. **54**: 1547-1549.
- PEDERSEN, J.T.; PETERS, J.C. and HELWEY, O. (1980) Hydrographs by single linear reservoir model. Journal of the Hydraulics Division, American Society of Civil Engineers. **106**: 837-851.
- PENTLAND, R.L. and CUTHBERT, D.R. (1971) Operational hydrology for ungaged streams by the grid square technique. Water Resources Research. **7**: 283-291.
- PINDER, G.F. and JONES, J.F. (1969) Determination of the ground-water component of peak discharge from the chemistry of total runoff. Water Resources Research. **5**: 438-445.
- PRESS, W.H.; TEUKOLSKY, S.A.; VETTERLING, W.T. and FLANNERY, B.P. (1992) **Numerical recipes in C: the art of scientific computing**. 2nd ed. Cambridge: Cambridge University Press. 994 p.
- QUINN, O.; BEVEN, K.; CHEVALLIER, P. and PLANCHON, O. (1991) The prediction of hillslope flow paths for distributed hydrological modelling using digital terrain models. Hydrological Processes. **5**:59-79.
- RAGAN, R.M. and JACKSON, T.J. (1980) Runoff synthesis using Landsat and the SCS Model. Journal of the Hydraulics Division, American Society of Civil Engineers. **106**: 667-678.
- RAWLS, W.J.; BRAKENSIEK, D.L. and SAXTON, K.E. (1982) Estimation of soil properties. Transactions of the American Society of Agricultural Engineers. **25**: 1316-1320.
- REINELT, L.E.; HORNER, R.R. and MAR, B.W. (1988) Nonpoint source pollution monitoring program design. Journal of Water Resources Planning and Management. **114**: 335-352.
- REZENDE, B. et al., (1977) **Modelo reduzido do rio dos Sinos** : proteção contra inundações. SINOS II, relatório final preliminar. Porto Alegre, IPH/UFRGS. 23 p.
- RICHARDS, J.A. (1986) **Remote sensing digital image analysis**. New York: Springer-Verlag. 315p.
- RIPLEY, B.D. (1981) **Spatial Statistics**. New York. John Wiley. 252 p.

- RISSO, A. (1993) **Obtenção e manipulação de parâmetros da MUSLE através de técnicas de geoprocessamento**. Porto Alegre; UFRGS - Curso de Pós-Graduação em Engenharia Civil. 166p. Dissertação (mestrado).
- ROBINOVE, C.J. (1982) Computation with Physical Values from Landsat digital data. Photogrammetric Engineering and Remote Sensing. **48**: 781-784.
- ROSENBERG, D.U. (1975) **Methods for the numerical solution of partial differential equations**. New York: American Elsevier. 128 p.
- ROSS, B.B.; CONTRACTOR, D.N. and SHANHOLTZ, V.O. (1977) Finite element simulation of overland and channel flow. Transactions of the American Society of Agricultural Engineers. **20**: 705-712.
- ROSS, M.A. and TARA, P.D. (1993) Integrated hydrologic modeling with geographic information systems. Journal of Water Resources Planning and Management. **119**: 129-140.
- ROUQUETTE, F.M.; MATOCHA, J.E. and DUBLE, R.L. (1973) Recycling and recovery of nitrogen, phosphorus and potassium by coastal bermudagrass: II. under grazing conditions with two stocking rates. Journal of Environmental Quality. **2**: 125-129.
- SCHILLING, W. and FUCHS, L. (1986) Errors in stormwater modeling - A quantitative assessment. Journal of the Hydraulics Division, American Society of Civil Engineers. **112**: 111-123.
- SHAPIRO, M. and WESTERVELT, J. (1992) R.MAPCALC: an algebra for GIS and Image processing. Champaign: U.S.Army Construction Engineering Research Laboratory. 22p.
- SHARPLEY, A.N. (1985) Depth of surface soil-runoff interaction as affected by rainfall, soil slope, and management. Soil Science Society of American Journal. **49**: 1010-1015.
- SHIKLOMANOV, I.A. (1990) Global Water Resources. Nature and Resources. **26**: 34-43.
- SHREVE, R.L. (1966) Statistical law of stream numbers. Journal of Geology. **74**:17-37.
- SHREVE, R.L. (1974) Variation of mainstream length with basin area in river networks. Water Resources Research. **10**:1167-1177.

- SIDLE, R.C. and SHARPLEY, N. (1991) Cumulative effects of land management on soil and water resources: an overview. Journal of Environmental Quality. **20**: 1-3.
- SIEVERS, D.M.; LENTZ, G.L. and BEASLEY, R.P. (1970) Movement of agricultural fertilizers and organic insecticide in surface runoff. Transactions of the American Society of Agricultural Engineers. **13**: 323-325.
- SILVEIRA, A. (1986) **Modelo hidrodinâmico bidimensional com aplicação ao rio Guaíba**. Porto Alegre; UFRGS - Curso de Pós-Graduação em Engenharia Civil. 237p. Dissertação (mestrado).
- SILVEIRA, R. (1980a) **Estudos hidrológicos no delta do rio Jacuí (RS) visando ao programa de operação dos modelos analógicos e matemático de simulação hidráulica**. Porto Alegre. IPH/UFRGS. 34 p.
- SILVEIRA, R. (1980b) **Sinopse sobre as condições hidrológicas e hidráulicas do rio dos Sinos (RS)**. Porto Alegre. IPH/UFRGS. 10 p.
- SIMÕES LOPES, M. and ALMEIDA, L. (1978a) **Modelo reduzido do rio dos Sinos : proteção contra inundações**. SINOS II, anexo ao relatório final. Porto Alegre, IPH/UFRGS. 15 p.
- SIMÕES LOPES, M. and REZENDE, B. (1978b) **Proteção contra inundações no rio dos Sinos**, modelos de conjunto e detalhe; relatório final. Porto Alegre, IPH/UFRGS. 2 v.
- SINGH, V.P. (1975) Hybrid formulation of kinematic wave models of watershed runoff. Journal of Hydrology. **27**: 33-50.
- SIVERTUN, A.; REINELT, L.E. and CASTENSSON, R. (1988) A GIS method to aid in non-point source critical area analysis. International Journal Geographical Information Systems. **2**: 365-378.
- SKIDMORE, A. (1989) A comparison of techniques for calculating gradient and aspect from gridded elevation model. International Journal Geographical Information Systems. **3**:323-334.
- SMART, J.S. (1968) Statistical properties of stream length. Water Resources Research. **4**:1001-1014.

- SMART, J.S. (1970) Use of topologic information in processing data for channel networks. Water Resources Research. **6**:932-936.
- SMITH, R.E. and HEBBERT, R.H.B (1979) A Monte Carlo analysis of the hydrologic effects of spatial variability of infiltration. Water Resources Research. **15**: 419-429.
- SOBRAL, M.M.; HIPEL, K.W. and FARQUHAR, G.J. (1981) A multicriteria model for solid waste management. Journal of Environmental Management. **12**: 97-110.
- SOLOMON, S.I.; DENOUEVILLIEZ, J.P.; CHART, E.J.; WOOLLEY, J.A. and CADOU, C. (1968) The use of a square grid system for computer estimation of precipitation, temperature and runoff. Water Resources Research. **4**: 919-929.
- SPENCER, A.J.M. (1980) **Continuum mechanics**. London: Longman. 183 p.
- SPICIO, L.A. (1967) **Principles of continua with applications**. New York: John Wiley. 268 p.
- STOCKING, M. (1981) A working model for the estimation of soil loss suitable for underdeveloped areas. Norwich: University of East Anglia, 54 p. (Development Studies, Occasional paper n.15).
- STUMM, W. (1986) Water, an endangered ecosystem. Ambio. **15**: 201-207.
- THOMAS, D.M. and BENSON, M.A. (1970) Generalization of streamflow characteristics from drainage-basin characteristics. Geological Survey Water Supply Paper, Washington, n.1975.
- TOMLIN, C.D. (1990) **Geographic information system and cartographic modeling**. Englewood-Cliffs: Prentice Hall. 249p.
- TROUTMAN, B.M. (1985) Errors and parameter estimation in precipitation-runoff modelling: 1. Theory. Water Resources Research. **21**: 1195-1213.
- TUCCI, C. and MORETTI, L. (1982) Steady and nonsteady flow models for simulation of water quality in river. In: PERRY, R., ed. Effects of waste disposal on groundwater and surface water. London: IAHS. p.235-244. (International Association of Hydrological Sciences. Publication n.139)

- UNESCO/WHO (1978) Water quality surveys. Paris: 54p. (Studies and reports in hydrology n.23).
- U.S.GEOLOGICAL SURVEY (1987) Digital Elevation Models. Reston: 38 p. (Data User's Guide. n.5).
- U.S. SOIL CONSERVATION SERVICE (1986) Urban hydrology for small watersheds. Washington: U.S. Department of Agriculture. (Technical Release n.55).
- VANMARCKE, E. (1988) **Random fields**. Analysis and Synthesis. Cambridge: MIT Press. 297p.
- VIEIRA, S.R.; NIELSEN D.R.; and BIGGAR, J.W. (1981) Spatial variability of field measured infiltration rate. Soil Science Society of American Journal. **45**: 1040-1048.
- VIEIRA, V. (1970) **Estudo da relação benefício-custo das obras de proteção contra enchentes de perímetros urbanos, no Vale do Rio dos Sinos**. Porto Alegre; UFRGS - Curso de Pós-Graduação em Engenharia Civil. 43p. Dissertação (mestrado).
- WALESH, S.G.; KAWATSKI, L.A. and CLAVETTE, P.J. (1977) Land data management system for resource planning. Journal of the Water Resources Planning and Management Division, American Society of Civil Engineers. **103**: 177-192.
- WALKER, J.F.; PICKARD, S.A. and SONZOGNI, W.C. (1989) Spreadshet watershed modeling for nonpoint-source pollution management in a Wisconsin basin. Water Resources Bulletin. **25**: 139-147.
- WALLACE, D.A. and DAQUE, R.R. (1973) Modeling of land runoff effects on dissolved oxygen. Journal. Water Pollution Control Federation **45**: 1795-1806.
- WALLING, D.E. (1983) The sediment delivery problem. Journal of Hydrology. **65**: 209-237.
- WALSH, S.J. (1985) Geographic information system for natural resource management. Journal of Soil and Water Conservation. **40**: 202-205.
- WANIELISTA, M.P.; YOUSEF, Y.A and McLELLON, W.M. (1977) Nonpoint source effects on water quality. Journal. Water Pollution Control Federation. **49**: 441-451.

- WEBSTER, R. and OLIVER, M.A. (1990) **Statistical methods in soil and land resource survey**. Oxford: Oxford Press. 316p.
- WELTY, J.R.; WICKS, C.E and WILSON, R.E. (1984) **Fundamentals of momentum, heat and mass transfer**. New York: John Wiley. 803 p.
- WHIPPLE, W.; BERGER, B.B.; GATES, C.D.; RAGAN, R.M. and RANDAL, C.W. (1978) Characterization of urban runoff. Water Resources Research. **14**: 370-372.
- WHITE, I.D.; MOTTERSHEAD, D.N. and HARRISON, S.J. (1992) **Environmental systems: An introductory text**. London: Chapman and Hall. 616 p.
- WILLIAMS, J.R. and BERNDT, H.D. (1977) Sediment Yield Prediction Based on Watershed Hydrology. Transactions of the American Society of Agricultural Engineers. **20**: 1100-1104.
- WILLIAMS, J.R.; JONES, C.A. and DYKE, P.T. (1984) A modeling approach to determining the relationship between erosion and soil productivity. Transactions of the American Society of Agricultural Engineers. **27**: 129-144.
- WILSON, C.B.; VALDES, J.B. and RODRIGUEZ-ITURBE, I. (1979) On the influence of the spatial distribution of rainfall on storm runoff. Water Resources Research. **15**: 321-328.
- WISCHMEIER, W.H. and SMITH, D.D. (1958) Rainfall energy and its relationship to soil loss. Transactions of American Geophysical Union. **39**: 285-291.
- WISCHMEIER, W.H. and SMITH, D.D. (1978) Predicting rainfall erosion losses - a guide to conservation planning. Washington. Department of Agriculture. 287p (Agriculture Handbook n.537).
- WOOD, E.F.; SIVAPALAN, M.; BEVEN, K. and BAND, L. (1988) Effects of spatial variability and scale with implications to hydrologic modeling. Journal of Hydrology. **102**: 29-47.
- WOOLHISER, D.A. and LIGGETT, J.A. (1967) Unsteady, one-dimensional flow over a plane-the rising hydrograph. Water Resources Research. **3**: 753-771.
- WORLD HEALTH ORGANIZATION - WHO (1988) Assessment of freshwater quality. Geneva. 80p.

- YANG, C.T. (1971) Potential energy and stream morphology. Water Resources Research. 7:311-322.
- YOUNG, R.A.; ONSTAD, C.A.; BOSCH, D.D. and ANDERSON, W.P. (1989) AGNPS: A nonpoint-source pollution model for evaluating agricultural watersheds. Journal of Soil and Water Conservation. 44: 168-173.
- ZEID, M.A. and BISWAS, A.K. (1990) Impacts of agriculture on water quality. Water International. 15: 160-167.
- ZEVENBERGEN, L.W. and THORNE, C.R. (1987) Quantitative analysis of land surface topography. Earth Surface Processes and Landforms. 12:47-56.
- ZNOTINAS, N.M. and HIPEL, K.W. (1979) Comparison of alternative engineering designs. Water Resources Bulletin. 15: 44-59.

During the course of this research many programs were written, certainly too many for all to be included in this thesis. Some programs have been chosen to illustrate the broad structure of the programming involved in the research:

Page	Program
230	Header file with used data structures
231	Header file with utility routines
234	Program to treat depressions in the Digital Elevation Mode (DEM).
237	Program to determine upstream catchment areas and drainage network
241	Program to evaluate the drainage network composition
247	Program to generate the spatial distribution of runoff
261	Program to define link number configuration
268	Program to route the pollutants over the terrain
272	Program to evaluate the transport of pollutants within the drainage network
279	Program for solving equation $X[k+1]=\text{roo} * W * X[k] + e$
284	Program for generating random number of Gauss distribution
286	Program for returns a normally distributed deviate with zero mean and unit variance
287	Program to returns a uniform random deviate between 0.0 and 1.0
290	Program for calculating cumulative distribution function (normal)

```
/* -----  
/*   Header file with data structures used  
/*   CABM                               1993  
/* ----- */  
  
#include <stdio.h>  
#include <math.h>  
  
#define MAXROW 700  
#define MAXCOL 1100  
#define MAXLABEL 20  
struct POINT {  
    float x;  
    float y;  
};  
struct GRID_I {  
    char grid_descriptor[MAXLABEL];  
    long nrows;  
    long ncols;  
    struct POINT corners[4];  
    int **zi;  
} gridi;  
  
struct GRID_F {  
    float **zf;  
} gridf;
```

```

/* -----
/*   Header file with utility routines
/*   Most of the routines listed below are described in Press et al., (1992)
/* -----*/
#include <stdio.h>
#include <stddef.h>
#include <stdlib.h>
#define NR_END 1
#define FREE_ARG char*

nerror(error_text)
char error_text[];
/* ----- standard error handler */
{
    fprintf(stderr, "\nRun-time error...\n");
    fprintf(stderr, "%s\n", error_text);
    fprintf(stderr, "...now exiting to system...\n\n");
    exit(1);
}

int **imatrix(nrl, nrh, ncl, nch)
long nrl, nrh, ncl, nch;
/* ----- Allocate a int matrix with subscript range m[nrl..nrh][ncl..nch] */
{
    long i, nrow=nrh-nrl+1, ncol=nch-ncl+1;
    int **m;

    /* Allocate pointers to rows */
    m=(int **) malloc((size_t)((nrow+NR_END)*sizeof(int*)));
    if (!m) nerror("allocation failure 1 in matrix()");
    m += NR_END;
    m -= nrl;

```

```

/* Allocate rows and set pointers to them */
m[nrl]=(int *)
    malloc((size_t)((nrow*ncol+NR_END)*sizeof(int)));
if (!m[nrl]) nerror("allocation failure 2 in matrix()");
m[nrl] += NR_END;
m[nrl] -= ncl;

for (i=nrl+1;i<=nrh;i++) m[i]=m[i-1]+ncol;

/* Return pointer to array of pointers to rows */
return m;
}

float **matrix(nrl, nrh, ncl, nch)
long nrl,nrh,ncl,nch;
/* _____ Allocate a int matrix with subscript range m[nrl..nrh][ncl..nch] */
{
    long i, nrow=nrh-nrl+1,ncol=nch-ncl+1;
    float **m;

    /* Allocate pointers to rows */
    m=(float **) malloc((size_t)((nrow+NR_END)*sizeof(float*)));
    if (!m) nerror("allocation failure 1 in matrix()");
    m += NR_END;
    m -= nrl;

    /* Allocate rows and set pointers to them */
    m[nrl]=(float *) malloc((size_t)((nrow*ncol+NR_END)*sizeof(float)));
    if (!m[nrl]) nerror("allocation failure 2 in matrix()");
    m[nrl] += NR_END;
    m[nrl] -= ncl;

    for (i=nrl+1;i<=nrh;i++) m[i]=m[i-1]+ncol;

    /* Return pointer to array of pointers to rows */
}

```

```
        return m;
    }

void free_matrix(m, nrl, nrh, ncl, nch)
float **m;
long nrl,nrh,ncl,nch;
/* _____ Free a float matrix allocated by matrix() */
{
    free((FREE_ARG) (m[nrl]+ncl-NR_END));
    free((FREE_ARG) (m+nrl-NR_END));
}

free_imatrix(m, nrl, nrh, ncl, nch)
int **m;
long nrl,nrh,ncl,nch;
/* _____ Free an int matrix allocated by imatrix() */
{
    free((FREE_ARG) (m[nrl]+ncl-NR_END));
    free((FREE_ARG) (m+nrl-NR_END));
}
```



```
/* -----  
/*    Program to fill depressions  
/*    CABM                1993  
/* ----- */  
  
#include <stdio.h>  
#include <strings.h>  
#include "t_util.h"  
#include "t_obj.h"  
  
/* ----- Main program */  
main(argc, argv)  
int argc;  
char *argv[];  
{  
    float N, C, S;  
    char NameHeadIMG[14], NameFileIMG[14], NameHeadSMT[14], NameFileSMT[14];  
    FILE *ElevIMG, *ElevSMT, *HeadIMG, *HeadSMT;  
    int x, y, i, j, sum;  
    float min, ElevF;  
    short int ElevFi;  
    char AreaName[9], suav[9];  
    char texto[21][256];  
  
/* ----- Input section */  
    printf("\nType the name of the file please\n\n--> : ");  
    gets(AreaName);  
    strcpy(suav, AreaName);  
    suav[3] = '\0';  
    sprintf(NameFileIMG, "%s.img", AreaName);  
    sprintf(NameHeadIMG, "%s.hed", AreaName);  
    sprintf(NameFileSMT, "%s_sm1a.img", suav);  
    sprintf(NameHeadSMT, "%s_sm1a.hed", suav);  
    if ((HeadIMG=fopen(NameHeadIMG,"r"))==NULL) perror("Can't open input file");  
    if ((HeadSMT=fopen(NameHeadSMT,"w"))==NULL) perror("Can't open output file");
```

```

for (i = 1; i <= 21; i++) {
    fgets(texto[i - 1], 256, HeadIMG);
    texto[1][14]='r'; texto[1][15]='e'; texto[1][16]='a'; texto[1][17]='l';texto[1][18]='\n';
    texto[1][19]='\0';
    fprintf(HeadSMT, "%s", texto[i - 1]);
}
fclose(HeadIMG);
fclose(HeadSMT);
for (i=14,j=0; i<=strlen(texto[3]);i++) {
    texto[3][j] = texto[3][i];
    j++;
}
texto[3][j] = '\0';
sscanf(texto[3], "%d", &gridi.ncols);
for (i=14,j=0; i<=strlen(texto[4]);i++) {
    texto[4][j] = texto[4][i];
    j++;
}
texto[4][j] = '\0';
sscanf(texto[4], "%d", &gridi.nrows);
gridi.zi=imatrix(1,gridi.nrows,1,gridi.ncols);
gridf.zf=matrix(1,gridi.nrows,1,gridi.ncols);
if ((ElevIMG=fopen(NameFileIMG,"r+b"))==NULL) perror("Can't open input file");
for (i = 1; i <= gridi.nrows; i++) {
    for (j = 1; j <= gridi.ncols; j++) {
        fread(&ElevFi, sizeof(short int), 1, ElevIMG);
        gridi.zi[i][j] = ElevFi;
        gridf.zf[i][j] = gridi.zi[i][j];
    }
}
fclose(ElevIMG);
/* _____ Loop over grid */
do {
    sum = 0;
    for (i = 2; i < gridi.nrows-1; i++) {

```

```

for (j = 2; j < gridi.ncols-1; j++) {
  if (gridf.zf[i][j] != 0.0) {
    min = gridf.zf[i][j] * 10.0;
    for (x = -1; x <= 1; x++) {
      for (y = -1; y <= 1; y++) {
        if ((x != 0) && (y != 0)) {
          if (gridf.zf[x + i][y + j] < min) { /*Value lower than lowest neighbour elevation*/
            min = gridf.zf[x + i][y + j];
          }
        }
      }
    }
    sum++;
  }
}
} while (sum > 0);

/* _____ Output section */
if ((ElevSMT=fopen(NameFileSMT,"w+b"))==NULL) perror("Can't write output file");
for (i = 1; i <= gridi.nrows; i++) {
  for (j = 1; j <= gridi.ncols; j++) {
    ElevF = gridf.zf[i][j];
    fwrite(&ElevF, sizeof(float), 1, ElevSMT);
  }
}
fclose(ElevSMT);
free_imatrix(gridi.zi,1,gridi.nrows,1,gridi.ncols);
free_matrix(gridf.zf,1,gridi.nrows,1,gridi.ncols);
exit(0);
}

```

```

/* -----
/*   Program to calculate the upstream catchment areas
/*   and/or the the drainage network
/*   CABM                1993
/* ----- */
#include <stdio.h>
#include <strings.h>
#include "t_util.h"
#include "t_obj.h"
/* ----- Main program */
main(argc, argv)
int argc;
char *argv[];
{
    long ax[129], ay[129];
    char NameFileASP[14], NameHeadASP[14], NameFileACM[14], NameHeadACM[14];
    FILE *FileASP, *FileACM, *HeadASP, *HeadACM, *Posicao;
    int km, kn, m, n;
    unsigned char ElevFi;
    long posi, posj, i, j, min;
    double max;
    float ElevF;
    char AreaName[9], suav[9];
    char texto[21][256];

/* ----- Input section */
    printf("\nType the name of the file please\n\n--> : ");
    gets(AreaName);
    strcpy(suav,AreaName);
    suav[3] = '\0';
    sprintf(NameFileASP, "%s_aspl.img", suav);
    sprintf(NameHeadASP, "%s_aspl.hed", suav);
    sprintf(NameFileACM, "%s_acml.img", suav);

```

```

sprintf(NameHeadACM, "%s_acml.hed", suav);
if ((HeadASP=fopen(NameHeadASP,"r"))==NULL) perror("Can't open input file");
if ((HeadACM=fopen(NameHeadACM,"w"))==NULL) perror("Can't open output file");
for (i = 1; i <= 21; i++) {
    fgets(texto[i - 1], 256, HeadASP);
    fprintf(HeadACM, "%s", texto[i - 1]);
}
fclose(HeadACM);
fclose(HeadASP);
for (i=14,j=0; i<=strlen(texto[3]);i++) {
    texto[3][j] = texto[3][i];
    j++;
}
texto[3][j] = '\0';
sscanf(texto[3], "%d", &gridi.ncols);
for (i=14,j=0; i<=strlen(texto[4]);i++) {
    texto[4][j] = texto[4][i];
    j++;
}
texto[4][j] = '\0';
sscanf(texto[4], "%d", &gridi.nrows);
for (i = 1; i <= 129; i++) {
    ax[i] = 0; ay[i] = 0;
}
ax[4] = 1; ax[8] = 1; ax[16] = 1; ax[1] = -1; ax[128] = -1; ax[64] = -1;
ay[1] = 1; ay[2] = 1; ay[4] = 1; ay[16] = -1; ay[32] = -1; ay[64] = -1;
max = 0.0; min = 0;
gridi.zi=imatrix(1,gridi.nrows,1,gridi.ncols);
gridf.zf=matrix(1,gridi.nrows,1,gridi.ncols);
if ((FileASP=fopen(NameFileASP,"r+b"))==NULL) perror("Can't open input file");
for (i = 1; i <= gridi.nrows; i++) {
    for (j = 1; j <= gridi.ncols; j++) {
        fread(&ElevFi, sizeof(char), 1, FileASP);
        gridi.zi[i][j] = ElevFi;
        gridf.zf[i][j] = 0.0;
    }
}

```

```

    }
}
fclose(FileASP);

/* _____ Main section */
for (i = 2; i < gridi.nrows-1; i++) {
    for (j = 2; j < gridi.ncols-1; j++) {
        if ((gridi.zi[i][j] > 0) && (gridi.zi[i][j] <= 128)) {
            m = i; n = j;
            do {
                km = m + ax[gridi.zi[m][n]];
                kn = n + ay[gridi.zi[m][n]];
                m = km; n = kn;
                gridf.zf[m][n] += 0.01;
                if (max < gridf.zf[m][n]) {
                    max = gridf.zf[m][n];
                    posi = m - 1; posj = n - 1;
                }
                if ((m<=1) || (m>=gridi.nrows) || (n<=1) || (n>=gridi.ncols)) break;
            } while ((m>1) || (m<gridi.nrows) || (n>1) || (n<gridi.ncols) ||
                (gridi.zi[m][n] != 0) || (gridi.zi[m][n] != 130));
        }
    }
}
if ((Posicao=fopen("position","w"))==NULL) nerror("Can't open output file");
fprintf(Posicao, "%i\t%i", posi,posj);
fclose(Posicao);
if ((FileACM=fopen(NameFileACM,"w+b"))==NULL) nerror("Can't write output file");
for (i = 1; i <= gridi.nrows; i++) {
    for (j = 1; j <= gridi.ncols; j++) {
        if (gridf.zf[i][j] >= 3.5) { /* Threshold value = 3.5, in this case */
            ElevFi = 1;
            fwrite(&ElevFi, sizeof(char), 1, FileACM);
        } else {
            ElevFi = 5;

```

```
        fwrite(&ElevFi, sizeof(char), 1, FileACM);
    }
}
fclose(FileACM);
free_imatrix(gridi.zi,1,gridi.nrows,1,gridi.ncols);
free_matrix(gridf.zf,1,gridi.nrows,1,gridi.ncols);
exit(0);
}
```

```

/* -----
/*   Program to evaluate the drainage network
/*   throughout the topological relationships
/*   CABM                               1993
/* ----- */
#include <stdio.h>
#include <strings.h>
#include "t_util.h"
#include "t_obj.h"
typedef char string256[256];
/* ----- Main program */
main (argc, argv)
    int argc;
    char *argv[];
{
    string256 posi, posj;
    char NameFileEST[14], NameHeadEST[14], NameFileASP[14], NameFileTOP[14];
    FILE *FileEST, *FileTOP, *HeadEST, *FileASP, *Posicao, *Tabela;
    long ax[129], ay[129];
    unsigned char ElevF;
    unsigned short int ElevFi;
    int x, y, i, j, m, n, km, kn, flag, flog, stx, sty, numero;
    long link, code, tox, toy, fromx, fromy;
    int **z1, **z2, **z3, pix[18], dir[18], asp[19], npix, cpix;
    char AreaName[9], suav[9];
    char texto[21][256];
    static short AS1[3][3] = {4, 8, 16,
                               2, 0, 32,
                               1, 128, 64};

/* ----- Input section */
    printf ("\nType the name of the file please\n\n--> : ");
    gets (AreaName);

```



```

strcpy (suav, AreaName);
suav[3] = '\0';
sprintf (NameFileASP, "%s_asp1.img", suav);
sprintf (NameHeadEST, "%s_est.hed", suav);
sprintf (NameFileEST, "%s_est.img", suav);
sprintf (NameFileTOP, "%s_dos4.img", suav);
if ((HeadEST = fopen (NameHeadEST, "r")) == NULL) perror ("Can't open input file");
for (i = 1; i <= 21; i++) {
    fgets (texto[i - 1], 256, HeadEST);
}
fclose (HeadEST);
for (i = 14, j = 0; i <= strlen (texto[3]); i++) {
    texto[3][j] = texto[3][i];
    j++;
}
texto[3][j] = '\0';
sscanf (texto[3], "%d", &gridi.ncols);
for (i = 14, j = 0; i <= strlen (texto[4]); i++) {
    texto[4][j] = texto[4][i];
    j++;
}
texto[4][j] = '\0';
sscanf (texto[4], "%d", &gridi.nrows);
if ((Posicao = fopen ("position", "r")) == NULL) perror ("Can't open input file");
fgets (posi, 256, Posicao);
fclose (Posicao);
sscanf (posi, "%d\t%d", &stx, &sty);
++stx;
++sty;
z1 = imatrix (1, gridi.nrows, 1, gridi.ncols);
z2 = imatrix (1, gridi.nrows, 1, gridi.ncols);
z3 = imatrix (1, gridi.nrows, 1, gridi.ncols);
if ((FileTOP = fopen (NameFileTOP, "r+b")) == NULL) perror ("Can't open input file");
if ((FileASP = fopen (NameFileASP, "r+b")) == NULL) perror ("Can't open input file");
if ((FileEST = fopen (NameFileEST, "r+b")) == NULL) perror ("Can't open input file");

```

```

for (i = 1; i <= gridi.nrows; i++) {
    for (j = 1; j <= gridi.ncols; j++) {
        fread (&ElevFi, sizeof (unsigned short int), 1, FileTOP);
        z1[i][j] = ElevFi;
        fread (&ElevF, sizeof (char), 1, FileASP);
        z2[i][j] = ElevF;
        fread (&ElevF, sizeof (char), 1, FileEST);
        z3[i][j] = ElevF;
    }
}
fclose (FileTOP);
fclose (FileASP);
fclose (FileEST);
for (i = 1; i <= 129; i++) {
    ax[i] = 0;
    ay[i] = 0;
}
ax[4] = 1; ax[8] = 1; ax[16] = 1; ax[1] = -1; ax[128] = -1; ax[64] = -1;
ay[1] = 1; ay[2] = 1; ay[4] = 1; ay[16] = -1; ay[32] = -1; ay[64] = -1;
link = z1[stx][sty];
code = z3[stx][sty];
tox = stx;
toy = sty;
/* _____ Main Section */
for (x = -1; x <= 1; x++) /* _____ Start pixel*/
{
    for (y = -1; y <= 1; y++)
    {
        if ((x == 0) && (y == 0)) continue;
        if ((AS1[x + 1][y + 1] == z2[x + stx][y + sty]) && (z1[x + stx][y + sty] == 1)) {
            m = x + stx;
            n = y + sty;
        }
    }
}
}

```

```

flag = 1;          /* _____ Scan the drainage network */
do
{
fim:if ((m == stx) && (n == sty))
    {
        flag = 0;
        break;
    }
cpix = 0; /* _____ Number of contributions pixels */
for (x = -1; x <= 1; x++) {
    for (y = -1; y <= 1; y++) {
        if ((AS1[x + 1][y + 1] == z2[x + m][y + n]) && (z1[x + m][y + n] >= z1[m][n]))
            cpix++;
    }
}
if (cpix == 0)
{
    /* _____ Starting Zero-order network - downstream */
    fromx = m;
    fromy = n;
    if ((Tabela = fopen ("table", "a+")) == NULL) nerror ("Can't open input file");
    fprintf ( Tabela, "%i\t%i\t%i\t%i\t%i\t%i\n", link, code, fromx, fromy, tox, toy);
    fclose (Tabela);
    flog = 0;
    do
    {
        km = m + ax[z2[m][n]];
        kn = n + ay[z2[m][n]];
        m = km;
        n = kn;
        if ((m == stx) && (n == sty)) {
            flag = 0;
            flog = 1;
            break;
        }
        for (x = -1; x <= 1; x++) {

```

```

    for (y = -1; y <= 1; y++) {
        if ((AS1[x+1][y+1] == z2[x+m][y+n]) && (z1[x+m][y+n] > link)) {
            flog = 1;
            m = m + x;
            n = n + y;
            link = z1[m][n];
            code = z3[m][n];
            tox = m;
            toy = n;
            goto fim;
        }
    }
} while (flog != 1);
}
else if (cpix == 1)
{ /* _____ Marking upstream pixels */
    for (x = -1; x <= 1; x++) {
        for (y = -1; y <= 1; y++) {
            if ((AS1[x+1][y+1] == z2[x+m][y+n]) && (z1[x + m][y + n] == z1[m][n]))
            {
                m = m + x;
                n = n + y;
                goto fim;
            }
        }
    }
}
else
{ /* _____ Network junctions */
    numero = z1[m][n] + 1;
    for (x = -1; x <= 1; x++) {
        for (y = -1; y <= 1; y++) {
            if ((AS1[x+1][y+1] == z2[x+m][y+n]) && (z1[x+m][y+n] == numero)) {
                fromx = m;

```

```
    fromy = n;
    if ((Tabela=fopen ("table","a+")) == NULL) perror ("Can't open input file");
    fprintf(Tabela,"%i\t%i\t%i\t%i\t%i\t%i\n", link,code,fromx, fromy, tox, toy);
    fclose (Tabela);
    m = x + m;
    n = y + n;
    link = z1[m][n];
    code = z3[m][n];
    tox = m;
    toy = n;
    goto fim;
}
}
}
} while (flag != 0);
free_matrix (z1, 1, gridi.nrows, 1, gridi.ncols);
free_matrix (z2, 1, gridi.nrows, 1, gridi.ncols);
free_matrix (z3, 1, gridi.nrows, 1, gridi.ncols);
exit (0);
}
```

Program And_model;

{ _____ Implementation of equation 4.6 using the multiple downslope algorithm }

Uses Dos,Crt;

label 50,10;

Var AreaName,suav,b : string;
 DataFileIMG,DataFileHED : string;
 DataFileSMT,DataSootHED : string;
 FileSTO,FileWTS,FilePRE : string;
 FiWTS : File of integer;
 FiSTO,FiPRE : File of shortint;
 ElevIMG,ElevSMT,ElevACM : File of single;
 conta,dx,iter,wts1 : integer;
 i,j,k,nr,nc,natb : integer;
 nrout,nslp : integer;
 stol,prel : shortint;
 texto : array [1..21] of string;
 FileHED,FileSMT : text;
 P : pointer;
 dx2,dx1,sum,sumtb,c : single;
 route,tanb : array [1..9] of single;
 ElevFi,Elev1,Elev2 : single;
 atb1,a1,a2 : single;

{ _____ MarkTime }

procedure MarkTime(Message : string);

var Hour, Minute, second, Hundredth : word;

```

begin
  GetTime(Hour,Minute,second,hundredth);
  write(Hour:5); Write(Minute:5); write(second:5);
  write(Hundredth:5); write(' ');writeln(Message)
End;

{_____ MAIN PROGRAM }

```

```

Begin
  Mark(P);
  ClrScr;
  write('Give me the file"s name  :');
  read(AreaName); readln;
  suav := copy(Areaname,1,3);
  DataFileIMG := suav + '_SMT.IMG';
  DataFileHED := suav + '_SMT.HED';
  DataFileSMT := suav + '_LNA.IMG';
  DataSootHED := suav + '_LNA.HED';
  FileSTO := suav + '_STO.IMG';
  FileWTS := suav + '_WTS.IMG';
  FilePRE := suav + '_PRE.IMG';
  assign(FileHED,DataFileHED);
  assign(FileSMT,DataSootHED);
  reset(FileHED);
  rewrite(FileSMT);
  for i := 1 to 21 do begin
    readln(FileHED, texto[i]);
    writeln(FileSMT, texto[i]);
  end;
  close(fileHED);
  close(fileSMT);
  delete(texto[4],1,14);
  val(texto[4],nc,conta);
  delete(texto[5],1,14);
  val(texto[5],nr,conta);

```

```
b := copy(texto[14],15,2);
val(b,dx,conta);
writeln( nr,' ', nc,' ',dx);
readln;
natb := 0;
assign(FiWTS,FileWTS);
reset(FiWTS);
assign(ElevSMT,DatafileSMT);
rewrite(ElevSMT);
assign(ElevACM,'Acumulo');
rewrite(ElevACM);
For i := 0 to nr-1 do begin
  For j := 0 to nc-1 do begin
    seek(FiWTS,(nc*i)+j);
    read(FiWTS,wts1);
    if (wts1 > 1) then begin
      ElevFi := -10;
      seek(ElevSMT,(nc*i)+j);
      write(ElevSMT,ElevFi);
      ElevFi := (dx*dx);
      seek(ElevACM,(nc*i)+j);
      write(ElevACM,ElevFi);
    end;
    if (wts1 <= 1) then begin
      ElevFi := 1;
      seek(ElevSMT,(nc*i)+j);
      seek(ElevACM,(nc*i)+j);
      write(ElevSMT,ElevFi);
      write(ElevACM,ElevFi);
      natb := natb + 1;
    end;
  end;
end;
close(ElevSMT);
close(ElevACM);
```



```
close(FiWTS);
dx2 := 1/(1.414*dx);
dx1 := 1/dx;
iter := 0;
MarkTime('Inicio');
50: iter := iter + 1;
assign(FiWTS,FileWTS);
reset(FiWTS);
assign(FiPRE,FilePRE);
reset(FiPRE);
assign(FiSTO,FileSTO);
reset(FiSTO);
assign(ElevIMG,DataFileIMG);
reset(ElevIMG);
assign(ElevSMT,DataFileSMT);
reset(ElevSMT);
assign(ElevACM,'Acumulo');
reset(ElevACM);
for i := 0 to nr-1 do begin
  for j := 0 to nc-1 do begin
    seek(FiWTS,(nc*i)+j);
    read(FiWTS,wts1);
    if (wts1 > 1) then begin
      seek(ElevSMT,(nc*i)+j);
      read(ElevSMT,atb1);
      if (atb1 > -9) then begin goto 10 end;
      if (i-1 >= 0) then begin
        if (j-1 >= 0) then begin
          seek(ElevIMG,(nc*(i-1)+j-1));
          read(ElevIMG,Elev1);
          seek(ElevIMG,(nc*i)+j);
          read(ElevIMG,Elev2);
          seek(ElevSMT,(nc*(i-1)+j-1));
          read(ElevSMT,atb1);
          if (Elev1 > Elev2) and (atb1 < 0) then begin goto 10 end;
```

```
end;
seek(ElevIMG,(nc*(i-1)+j));
read(ElevIMG,Elev1);
seek(ElevIMG,(nc*i)+j);
read(ElevIMG,Elev2);
seek(ElevSMT,(nc*(i-1)+j));
read(ElevSMT,atb1);
if (Elev1 > Elev2) and (atb1 < 0) then begin goto 10 end;
if (j+1 <= nc-1) then begin
  seek(ElevIMG,(nc*(i-1)+j+1));
  read(ElevIMG,Elev1);
  seek(ElevIMG,(nc*i)+j);
  read(ElevIMG,Elev2);
  seek(ElevSMT,(nc*(i-1)+j+1));
  read(ElevSMT,atb1);
  if (Elev1 > Elev2) and (atb1 < 0) then begin goto 10 end;
end;
end;
if (j-1 >= 0) then begin
  seek(ElevIMG,(nc*i)+j-1);
  read(ElevIMG,Elev1);
  seek(ElevIMG,(nc*i)+j);
  read(ElevIMG,Elev2);
  seek(ElevSMT,(nc*i)+j-1);
  read(ElevSMT,atb1);
  if (Elev1 > Elev2) and (atb1 < 0) then begin goto 10 end;
end;
if (j+1 <= nc-1) then begin
  seek(ElevIMG,(nc*i)+j+1);
  read(ElevIMG,Elev1);
  seek(ElevIMG,(nc*i)+j);
  read(ElevIMG,Elev2);
  seek(ElevSMT,(nc*i)+j+1);
  read(ElevSMT,atb1);
  if (Elev1 > Elev2) and (atb1 < 0) then begin goto 10 end;
```

```

end;
if (i+1 <= nr-1) then begin
  if (j-1 >= 0) then begin
    seek(ElevIMG,(nc*(i+1)+j-1));
    read(ElevIMG,Elev1);
    seek(ElevIMG,(nc*i)+j);
    read(ElevIMG,Elev2);
    seek(ElevSMT,(nc*(i+1)+j-1));
    read(ElevSMT,atb1);
    if (Elev1 > Elev2) and (atb1 < 0) then begin goto 10 end;
  end;
  seek(ElevIMG,(nc*(i+1)+j));
  read(ElevIMG,Elev1);
  seek(ElevIMG,(nc*i)+j);
  read(ElevIMG,Elev2);
  seek(ElevSMT,(nc*(i+1)+j));
  read(ElevSMT,atb1);
  if (Elev1 > Elev2) and (atb1 < 0) then begin goto 10 end;
  if (j+1 <= nc-1) then begin
    seek(ElevIMG,(nc*(i+1)+j+1));
    read(ElevIMG,Elev1);
    seek(ElevIMG,(nc*i)+j);
    read(ElevIMG,Elev2);
    seek(ElevSMT,(nc*(i+1)+j+1));
    read(ElevSMT,atb1);
    if (Elev1 > Elev2) and (atb1 < 0) then begin goto 10 end;
  end;
end;
sum := 0;
for k := 1 to 9 do begin route[k] := 0 end;
nrout := 0;
if (i-1 >= 0) then begin
  if (j-1 >= 0) then begin
    seek(ElevIMG,(nc*(i-1)+j-1));
    read(ElevIMG,Elev1);

```

```
seek(ElevIMG,(nc*i)+j);
read(ElevIMG,Elev2);
if (Elev1 < Elev2) then begin
  tanb[1] := (Elev2 - Elev1)*dx2;
  route[1] := 0.354*dx*tanb[1];
  sum := sum + route[1];
  nrout := nrout + 1;
end;
end;
seek(ElevIMG,(nc*(i-1)+j));
read(ElevIMG,Elev1);
seek(ElevIMG,(nc*i)+j);
read(ElevIMG,Elev2);
if (Elev1 < Elev2) then begin
  tanb[2] := (Elev2 - Elev1)*dx1;
  route[2] := 0.5*dx*tanb[2];
  sum := sum + route[2];
  nrout := nrout + 1;
end;
if (j+1 <= nc-1) then begin
  seek(ElevIMG,(nc*(i-1)+j+1));
  read(ElevIMG,Elev1);
  seek(ElevIMG,(nc*i)+j);
  read(ElevIMG,Elev2);
  if (Elev1 < Elev2) then begin
    tanb[3] := (Elev2 - Elev1)*dx2;
    route[3] := 0.354*dx*tanb[3];
    sum := sum + route[3];
    nrout := nrout + 1;
  end;
end;
end;
if (j-1 >= 0) then begin
  seek(ElevIMG,(nc*i)+j-1);
  read(ElevIMG,Elev1);
```

```
seek(ElevIMG,(nc*i)+j);
read(ElevIMG,Elev2);
if (Elev1 < Elev2) then begin
  tanb[4] := (Elev2 - Elev1)*dx1;
  route[4] := 0.5*dx*tanb[4];
  sum := sum + route[4];
  nrout := nrout + 1;
end;
end;
if (j+1 <= nc-1) then begin
  seek(ElevIMG,(nc*i)+j+1);
  read(ElevIMG,Elev1);
  seek(ElevIMG,(nc*i)+j);
  read(ElevIMG,Elev2);
  if (Elev1 < Elev2) then begin
    tanb[6] := (Elev2 - Elev1)*dx1;
    route[6] := 0.5*dx*tanb[6];
    sum := sum + route[6];
    nrout := nrout + 1;
  end;
end;
if (i+1 <= nr-1) then begin
  if (j-1 >= 0) then begin
    seek(ElevIMG,(nc*(i+1)+j-1));
    read(ElevIMG,Elev1);
    seek(ElevIMG,(nc*i)+j);
    read(ElevIMG,Elev2);
    if (Elev1 < Elev2) then begin
      tanb[7] := (Elev2 - Elev1)*dx2;
      route[7] := 0.354*dx*tanb[7];
      sum := sum + route[7];
      nrout := nrout + 1;
    end;
  end;
  seek(ElevIMG,(nc*(i+1)+j));
```

```

read(ElevIMG,Elev1);
seek(ElevIMG,(nc*i)+j);
read(ElevIMG,Elev2);
if (Elev1 < Elev2) then begin
  tanb[8] := (Elev2 - Elev1)*dx1;
  route[8] := 0.5*dx*tanb[8];
  sum := sum + route[8];
  nrout := nrout + 1;
end;
if (j+1 <= nc-1) then begin
  seek(ElevIMG,(nc*(i+1)+j+1));
  read(ElevIMG,Elev1);
  seek(ElevIMG,(nc*i)+j);
  read(ElevIMG,Elev2);
  if (Elev1 < Elev2) then begin
    tanb[9] := (Elev2 - Elev1)*dx2;
    route[9] := 0.354*dx*tanb[9];
    sum := sum + route[9];
    nrout := nrout + 1;
  end;
end;
end;
if (nrout = 0) then begin
  sumtb := 0;
  nslp := 0;
  if (i-1 >= 0) then begin
    if (j-1 >= 0) then begin
      seek(ElevIMG,(nc*(i-1)+j-1));
      read(ElevIMG,Elev1);
      seek(ElevIMG,(nc*i)+j);
      read(ElevIMG,Elev2);
      sumtb := sumtb + (Elev1 - Elev2)*dx2;
      nslp := nslp + 1;
    end;
  end;
  seek(ElevIMG,(nc*(i-1)+j));

```

```
read(ElevIMG,Elev1);
seek(ElevIMG,(nc*i)+j);
read(ElevIMG,Elev2);
sumtb := sumtb + (Elev1 - Elev2)*dx1;
nslp := nslp + 1;
if (j+1 <= nc-1) then begin
  seek(ElevIMG,(nc*(i-1)+j+1));
  read(ElevIMG,Elev1);
  seek(ElevIMG,(nc*i)+j);
  read(ElevIMG,Elev2);
  sumtb := sumtb + (Elev1 - Elev2)*dx2;
  nslp := nslp + 1;
end;
end;
if (j-1 >= 0) then begin
  seek(ElevIMG,(nc*i)+j-1);
  read(ElevIMG,Elev1);
  seek(ElevIMG,(nc*i)+j);
  read(ElevIMG,Elev2);
  sumtb := sumtb + (Elev1 - Elev2)*dx1;
  nslp := nslp + 1;
end;
if (j+1 <= nc-1) then begin
  seek(ElevIMG,(nc*i)+j+1);
  read(ElevIMG,Elev1);
  seek(ElevIMG,(nc*i)+j);
  read(ElevIMG,Elev2);
  sumtb := sumtb + (Elev1 - Elev2)*dx1;
  nslp := nslp + 1;
end;
if (i+1 <= nr-1) then begin
  if (j-1 >= 0) then begin
    seek(ElevIMG,(nc*(i+1)+j-1));
    read(ElevIMG,Elev1);
    seek(ElevIMG,(nc*i)+j);
```

```

    read(ElevIMG,Elev2);
    sumtb := sumtb + (Elev1 - Elev2)*dx2;
    nslp := nslp + 1;
end;
seek(ElevIMG,(nc*(i+1)+j));
read(ElevIMG,Elev1);
seek(ElevIMG,(nc*i)+j);
read(ElevIMG,Elev2);
sumtb := sumtb + (Elev1 - Elev2)*dx1;
nslp := nslp + 1;
if (j+1 <= nc-1) then begin
    seek(ElevIMG,(nc*(i+1)+j+1));
    read(ElevIMG,Elev1);
    seek(ElevIMG,(nc*i)+j);
    read(ElevIMG,Elev2);
    sumtb := sumtb + (Elev1 - Elev2)*dx2;
    nslp := nslp + 1;
end;
end;
sumtb := sumtb/nslp;
if (sumtb > 0.000001) then begin
    seek(FiSTO,(nc*i)+j);
    read(FiSTO,sto1);
    seek(FiPRE,(nc*i)+j);
    read(FiPRE,pre1);
    seek(ElevACM,(nc*i)+j);
    read(ElevACM,a1);
    a2 := sto1/10;
    atb1 := (a1*pre1/10) / (2*dx*sumtb*a2);
    atb1 := ln(atb1);
    seek(ElevSMT,(nc*i)+j);
    write(ElevSMT,atb1);
end
else begin
    atb1 := 9999;

```



```
    seek(ElevSMT,(nc*i)+j);
    write(ElevSMT,atb1);
end;
natb := natb + 1;
goto 10;
end;
seek(FiSTO,(nc*i)+j);
read(FiSTO,sto1);
seek(FiPRE,(nc*i)+j);
read(FiPRE,pre1);
seek(ElevACM,(nc*i)+j);
read(ElevACM,a1);
a2 := sto1 / 10;
c := (a1*pre1/10) / (sum*a2);
atb1 := ln(c);
seek(ElevSMT,(nc*i)+j);
write(ElevSMT,atb1);
natb := natb + 1;
if (i-1 >= 0) then begin
  if (j-1 >= 0) then begin
    seek(ElevACM,(nc*(i-1)+j-1));
    read(ElevACM,a1);
    a2 := a1 + c*route[1];
    seek(ElevACM,(nc*(i-1)+j-1));
    write(ElevACM,a2);
  end;
  seek(ElevACM,(nc*(i-1)+j));
  read(ElevACM,a1);
  a2 := a1 + c*route[2];
  seek(ElevACM,(nc*(i-1)+j));
  write(ElevACM,a2);
  if (j+1 <= nc-1) then begin
    seek(ElevACM,(nc*(i-1)+j+1));
    read(ElevACM,a1);
    a2 := a1 + c*route[3];
```

```
    seek(ElevACM,(nc*(i-1)+j+1));
    write(ElevACM,a2);
end;
end;
if (j-1 >= 0) then begin
    seek(ElevACM,(nc*i)+j-1);
    read(ElevACM,a1);
    a2 := a1 + c*route[4];
    seek(ElevACM,(nc*i)+j-1);
    write(ElevACM,a2);
end;
if (j+1 <= nc-1) then begin
    seek(ElevACM,(nc*i)+j+1);
    read(ElevACM,a1);
    a2 := a1 + c*route[6];
    seek(ElevACM,(nc*i)+j+1);
    write(ElevACM,a2);
end;
if (i+1 <= nr-1) then begin
    if (j-1 >= 0) then begin
        seek(ElevACM,(nc*(i+1)+j-1));
        read(ElevACM,a1);
        a2 := a1 + c*route[7];
        seek(ElevACM,(nc*(i+1)+j-1));
        write(ElevACM,a2);
    end;
    seek(ElevACM,(nc*(i+1)+j));
    read(ElevACM,a1);
    a2 := a1 + c*route[8];
    seek(ElevACM,(nc*(i+1)+j));
    write(ElevACM,a2);
    if (j+1 <= nc-1) then begin
        seek(ElevACM,(nc*(i+1)+j+1));
        read(ElevACM,a1);
        a2 := a1 + c*route[8];
```

```
    seek(ElevACM,(nc*(i+1)+j+1));
    write(ElevACM,a2);
    end;
    end;
    end;
10: end;
    end;
    gotoXY(1,3);
    writeln ( 'interacao : ', iter);
    writeln;
    Close(ElevSMT);
    Close(elevACM);
    Close(ElevIMG);
    Close(FiSTO);
    Close(FiPRE);
    Close(fiWTS);
    if (natb < nr*nc) then begin goto 50 end;
    MarkTime('Fim');
    Erase(elevACM);
    Release(P);
End.
```

```

/* -----
/*   Program to calculate the topologic
/*   definition of the drainage network
/*   CABM                               1993
/* ----- */

#include <stdio.h>
#include <strings.h>
#include "t_util.h"
#include "t_obj.h"
typedef char string256[256];
/* ----- Main program */
main(argc, argv)
int argc;
char *argv[];
{
string256 posi, posj;
char NameHeadEST[14], NameFileRIO[14], NameHeadTOP[14];
char NameFileASP[14], NameFileTOP[14];
FILE *FileEST, *FileTOP, *HeadEST, *HeadTOP, *FileRIO, *FileASP, *Posicao;
long ax[129], ay[129];
int x, y, i, j, m, n, km, kn, flag, flog, stx, sty, start, ElevF;
unsigned char ElevFi;
int **z1, **z2, **z3, pix[18], dir[18], asp[19], npix, cpix, cpix0, number_rio;
char AreaName[9], suav[9];
char texto[21][256];
short static POS[3][3]={ 9, 2, 3,
                        8, 1, 4,
                        7, 6, 5 };
static short AS1[3][3]= { 4, 8, 16,
                        2, 0, 32,
                        1, 128, 64 };
static short ASP[3][3]= { 64, 128, 1,

```

```

32, 0, 2,
16, 8, 4 };

```

```

/* _____ Input section */
printf("\nType the name of the file please\n\n--> : ");
gets(AreaName);
strcpy(suav,AreaName);
suav[3] = '\0';
sprintf(NameFileASP, "%s_aspc.img", suav);
sprintf(NameFileRIO, "%s_acml.img", suav);
sprintf(NameHeadEST, "%s_est.hed", suav);
sprintf(NameHeadTOP, "%s_tpl.hed", suav);
sprintf(NameFileTOP, "%s_tpl.img", suav);
if ((HeadEST=fopen(NameHeadEST,"r"))==NULL) perror("Can't open input file");
if ((HeadTOP=fopen(NameHeadTOP,"w"))==NULL) perror("Can't open output file");
for (i = 1; i <= 21; i++) {
    fgets(texto[i - 1], 256, HeadEST);
    fprintf(HeadTOP, "%s", texto[i - 1]);
}
fclose(HeadTOP);
fclose(HeadEST);
for (i=14,j=0; i<=strlen(texto[3]);i++) {
    texto[3][j] = texto[3][i];
    j++;
}
texto[3][j] = '\0';
sscanf(texto[3], "%d", &gridi.ncols);
for (i=14,j=0; i<=strlen(texto[4]);i++) {
    texto[4][j] = texto[4][i];
    j++;
}
texto[4][j] = '\0';
sscanf(texto[4], "%d", &gridi.nrows);
if ((Posicao=fopen("position","r"))==NULL) perror("Can't open input file");
fgets(posi,256,Posicao);

```

```

fclose(Posicao);
sscanf(posi, "%d\t%d", &stx, &sty);
++stx; ++sty;
z1=imatrix(1,gridi.nrows,1,gridi.ncols);
z2=imatrix(1,gridi.nrows,1,gridi.ncols);
z3=imatrix(1,gridi.nrows,1,gridi.ncols);
if ((FileRIO=fopen(NameFileRIO,"r+b"))==NULL) perror("Can't open input file");
if ((FileASP=fopen(NameFileASP,"r+b"))==NULL) perror("Can't open input file");
for (i = 1; i <= gridi.nrows; i++) {
    for (j = 1; j <= gridi.ncols; j++) {
        fread(&ElevFi, sizeof(char), 1, FileRIO);
        z1[i][j] = ElevFi;
        if (z1[i][j]==1) {
            z3[i][j] = ElevFi;
        } else {
            z3[i][j] = 0;
        }
        fread(&ElevFi, sizeof(char), 1, FileASP);
        z2[i][j] = ElevFi;
    }
}
fclose(FileRIO);
fclose(FileASP);
for (i = 1; i <= 129; i++) {
    ax[i] = 0; ay[i] = 0;
}
ax[4] = 1; ax[8] = 1; ax[16] = 1; ax[1] = -1; ax[128] = -1; ax[64] = -1;
ay[1] = 1; ay[2] = 1; ay[4] = 1; ay[16] = -1; ay[32] = -1; ay[64] = -1;

/* _____ Main section */
number_rio = 2; /* _____ Initial pixel */
z3[stx][sty] = number_rio;
for (x=-1; x<=1; x++) {
    for (y=-1; y<=1; y++) {
        if ((x==0) && (y==0)) continue;

```

```

if ((AS1[x+1][y+1]==z2[x+stx][y+sty]) && (z1[x+stx][y+sty]==1)) {
    m = x + stx ;
    n = y + sty;
}
}
}
z3[m][n] = number_rio;
flag = 1; /* _____ Scan the drainage network */
do {
fim: printf("%d\t%d\t%d\n",m,n, number_rio);
    if ((m==stx) && (n==sty)) {
        flag=0;
        break;
    }
    cpix=0 ; /* _____ Number of contributions pixels */
    for (x=-1; x<=1; x++) {
        for (y=-1; y<=1; y++) {
            if ((AS1[x+1][y+1]==z2[x+m][y+n]) && (z3[x+m][y+n]==1)) cpix++;
        }
    }
    if (cpix==0) { /* _____ Starting Zero-order network - downstream */
        flog = 0;
        do {
            km = m + ax[z2[m][n]];
            kn = n + ay[z2[m][n]];
            m = km; n = kn;
            if ((m==stx) && (n==sty)) {
                flag=0;
                flog=1;
                break;
            }
        }
        cpix0=0 ;
        for (x=-1; x<=1; x++) {
            for (y=-1; y<=1; y++) {
                if ((AS1[x+1][y+1]==z2[x+m][y+n]) && (z1[x+m][y+n]>0)) cpix0++;
            }
        }
    }
}

```

```

    }
}
if (cpix0 > 1) {
    cpix0=0;
    for (x=-1; x<=1; x++) {
        for (y=-1; y<=1; y++) {
            if ((AS1[x+1][y+1]==z2[x+m][y+n]) && (z3[x+m][y+n]==1)) {
                cpix0++;
                m = m + x;
                n = n + y;
                goto comecol;
            }
        }
    }
comecol: if (cpix0 > 0) {
    flog=1;
    number_rio++;
    z3[m][n] = number_rio;
    goto fim;
}
} while (flog != 1);
} else if (cpix==1) { /* _____ Marking upstream pixels */
for (x=-1; x<=1; x++) {
    for (y=-1; y<=1; y++) {
        if ((AS1[x+1][y+1]==z2[x+m][y+n]) && (z3[x+m][y+n]==1)) {
            m = m + x;
            n = n + y;
            z3[m][n] = number_rio;
            goto fim;
        }
    }
}
} else { /* _____ Network junctions */
for (x=-1; x<=1; x++) {

```



```

for (y=-1; y<=1; y++) {
    dir[POS[x+1][y+1]]=z2[x+m][y+n];
    pix[POS[x+1][y+1]]=z3[x+m][y+n];
    asp[POS[x+1][y+1]]=AS1[x+1][y+1];
}
}
for (x=2; x<=9; x++) {
    dir[x+8] = dir[x];
    pix[x+8] = pix[x];
    asp[x+8] = asp[x];
}
for (x=2; x<=9; x++) {
    if (pix[x]==number_rio) {
        start= x;
        break;
    }
}
for (x=start; x<=18; x++) {
    if (dir[x]==asp[x]) {
        start=asp[x];
        break;
    }
}
for (x=-1; x<=1; x++) {
    for (y=-1; y<=1; y++) {
        if ((AS1[x+1][y+1]==z2[x+m][y+n]) && (z3[x+m][y+1]==1)) {
            m = x + m ;
            n = y + n;
            number_rio++;
            z3[m][n] = number_rio;
            goto fim;
        }
    }
}
}
}

```

```
    } while (flag!=0);
/* _____ Output section */
if ((FileTOP=fopen(NameFileTOP,"w+b"))==NULL) nerror("Can't write output file");
for (i = 1; i <= gridi.nrows; i++) {
    for (j = 1; j <= gridi.ncols; j++) {
        ElevF = z3[i][j];
        if (ElevF > 0) ElevF--;
        fwrite(&ElevF, sizeof(short), 1, FileTOP);
    }
}
fclose(FileTOP);
free_imatix(z1,1,gridi.nrows,1,gridi.ncols);
free_imatix(z2,1,gridi.nrows,1,gridi.ncols);
free_imatix(z3,1,gridi.nrows,1,gridi.ncols);
exit(0);
}
```

```

/* -----
/*   Program to route the loads over the terrain
/*   CABM                               1993
/* ----- */
#include <stdio.h>
#include <strings.h>
#include "t_util.h"
#include "t_obj.h"
#define T 0.9 /* Coeffiecient of transport */

/* ----- Main program */
main(argc, argv)
int argc;
char *argv[];
{
    long ax[129], ay[129];
    char NameFileASP[14], NameHeadASP[14], NameFilePAR[14];
    char NameFileLOD[14], NameHeadLOD[14];
    FILE *FileASP, *FileLOD, *FilePAR, *HeadASP, *HeadLOD;
    int ElevFi, km, kn, m, n, **z1, **z2, min;
    long i, j;
    double max;
    float **z3;
    char AreaName[8], suav[8];
    char texto[21][256];

/* ----- Input section */
    printf("\nType the name of the file please\n\n--> : ");
    gets(AreaName);
    strcpy(suav, AreaName);
    suav[3] = '\0';
    sprintf(NameFileASP, "%s_asp.img", suav);
    sprintf(NameHeadASP, "%s_asp.hed", suav);

```

```

sprintf(NameFilePAR, "%s.img", AreaName);
sprintf(NameFileLOD, "%sl.img", AreaName);
sprintf(NameHeadLOD, "%sl.hed", AreaName);
if ((HeadASP=fopen(NameHeadASP,"r"))==NULL) perror("Can't open input file");
if ((HeadLOD=fopen(NameHeadLOD,"w"))==NULL) perror("Can't open output file");
for (i = 1; i <= 21; i++) {
    fgets(texto[i - 1], 256, HeadASP);
    fprintf(HeadLOD, "%s", texto[i - 1]);
}
fclose(HeadLOD);
fclose(HeadASP);
for (i=14,j=0; i<=strlen(texto[3]);i++) {
    texto[3][j] = texto[3][i];
    j++;
}
texto[3][j] = '\0';
sscanf(texto[3], "%d", &gridi.ncols);
for (i=14,j=0; i<=strlen(texto[4]);i++) {
    texto[4][j] = texto[4][i];
    j++;
}
texto[4][j] = '\0';
sscanf(texto[4], "%d", &gridi.nrows);
for (i = 1; i <= 129; i++) {
    ax[i] = 0; ay[i] = 0;
}
ax[4] = 1; ax[8] = 1; ax[16] = 1; ax[1] = -1; ax[128] = -1; ax[64] = -1;
ay[1] = 1; ay[2] = 1; ay[4] = 1; ay[16] = -1; ay[32] = -1; ay[64] = -1;
z1=imatrix(1,gridi.nrows,1,gridi.ncols);
z2=imatrix(1,gridi.nrows,1,gridi.ncols);
z3=matrix(1,gridi.nrows,1,gridi.ncols);
if ((FileASP=fopen(NameFileASP,"r+b"))==NULL) perror("Can't open input file");
if ((FilePAR=fopen(NameFilePAR,"r+b"))==NULL) perror("Can't open input file");
for (i = 1; i <= gridi.nrows; i++) {
    for (j = 1; j <= gridi.ncols; j++) {

```

```

fread(&ElevFi, sizeof(short), 1, FileASP);
z1[i][j] = ElevFi;
fread(&ElevFi, sizeof(short), 1, FilePAR);
z2[i][j] = ElevFi;
z3[i][j] = 0.0;
}
}
fclose(FileASP);
fclose(FilePAR);

/* _____ Main section */
max = 0.0; min=1000;
for (i = 2; i < gridi.nrows-1; i++) {
  for (j = 2; j < gridi.ncols-1; j++) {
    m = i; n = j;
    do {
      if (z2[m][n]==1) {
        z3[m][n]=0;
        break;
      } else {
        km = m + ax[z1[m][n]];
        kn = n + ay[z1[m][n]];
        z3[km][kn]= z3[km][kn] + T*z2[m][n];
        m = km; n = kn;
      }
      if (max < z3[m][n]) max = z3[m][n];
      if (min > z3[m][n]) min = z3[m][n];
      if ((m<=1) || (m>=gridi.nrows) || (n<=1) || (n>=gridi.ncols)) break;
    } while ((m>1) || (m<gridi.nrows) || (n>1) || (n<gridi.ncols));
  }
}

/* _____ Output section */
if ((FileLOD=fopen(NameFileLOD,"w+b"))==NULL) perror("Can't write output file");
for (i = 1; i <= gridi.nrows; i++) {

```

```
for (j = 1; j <= gridi.ncols; j++) {
    if (z2[i][j]==1) {
        ElevFi=0;
    } else {
        ElevFi = (short) (4+(9*((z3[i][j]-min)/(max-min))));
    }
    fwrite(&ElevFi, sizeof(short), 1, FileLOD);
}
}
fclose(FileLOD);
free_imatrix(z1,1,gridi.nrows,1,gridi.ncols);
free_imatrix(z2,1,gridi.nrows,1,gridi.ncols);
free_matrix(z3,1,gridi.nrows,1,gridi.ncols);
exit(0);
}
```

```
/* -----
/*   Calculates the concentration of pollutant in
/*   river network
/*   CABM                               1993
/* ----- */

#include <stdio.h>
#include "t_util.h"
#include "t_obj.h"
#define NU_LINKS 1000
#define T 1

/* ----- Main program */
main(argc, argv)
int argc;
char *argv[];
{
    struct reach {
        int link;
        int code;
        int fx;
        int fy;
        int tx;
        int ty;
    } r[NU_LINKS], temp;
    char line[256], AreaName[8], suav[8], texto[21][256];
    FILE *Tabela;
    int nl, c, i, j, **z2, **z4;
    float **z1, **z3, soma;
    char NameFilePOL[14], NameHeadPOL[14], NameFileCRO[14], NameFilePON[14];
    char NameFileASP[14], NameFileLOD[14], NameHeadLOD[14];
    FILE *FilePOL, *HeadPOL, *FileCRO, *FileASP, *FileLOD, *HeadLOD, *FilePON;
    long ax[129], ay[129], m, n, km, kn;
```

```

int x, y, stx, sty, ElevFi;
static short ASI[3][3]= { 4, 8, 16,
                          2, 0, 32,
                          1, 128, 64 };

/* _____ Input section */
printf("\nType the name of the file please\n\n--> : ");
gets(AreaName);
strcpy(suav,AreaName);
suav[3] = '\0';
sprintf(NameFileASP, "%s_asp.img", suav);
sprintf(NameFileCRO, "%s_cro.img", suav);
sprintf(NameFilePON, "%sp.img", AreaName);
sprintf(NameFileLOD, "%sl.img", AreaName);
sprintf(NameHeadLOD, "%sl.hed", AreaName);
sprintf(NameHeadPOL, "%sr.hed", AreaName);
sprintf(NameFilePOL, "%sr.img", AreaName);
if ((HeadLOD=fopen(NameHeadLOD,"r"))==NULL) perror("Can't open input file");
if ((HeadPOL=fopen(NameHeadPOL,"w"))==NULL) perror("Can't open output file");
for (i = 1; i <= 21; i++) {
    fgets(texto[i - 1], 256, HeadLOD);
    fprintf(HeadPOL, "%s", texto[i - 1]);
}
fclose(HeadLOD);
fclose(HeadPOL);
for (i=14,j=0; i<=strlen(texto[3]);i++) {
    texto[3][j] = texto[3][i];
    j++;
}
texto[3][j] = '\0';
sscanf(texto[3], "%d", &gridi.ncols);
for (i=14,j=0; i<=strlen(texto[4]);i++) {
    texto[4][j] = texto[4][i];
    j++;
}

```



```

texto[4][j] = '\0';
sscanf(texto[4], "%d", &gridi.nrows);
nl =0;
if ((Tabela=fopen("table","r"))==NULL) nerror("Can't open input file");
while((c = fgetc(Tabela)) != EOF) {
    if (c == '\n') ++nl;
}
fclose(Tabela);
if ((Tabela=fopen("table","r"))==NULL) nerror("Can't open input file");
for (i=1; i<=nl; i++) {c = fscanf(Tabela, "%d\t%d\t%d\t%d\t%d\t%d\n",
    &r[i].link, &r[i].code,&r[i].fx, &r[i].fy, &r[i].tx,&r[i].ty);
}
fclose(Tabela);
z1=matrix(1,gridi.nrows,1,gridi.ncols);
z2=imatrix(1,gridi.nrows,1,gridi.ncols);
z3=matrix(1,gridi.nrows,1,gridi.ncols);
z4=imatrix(1,gridi.nrows,1,gridi.ncols);
if ((FileCRO=fopen(NameFileCRO,"r+b"))==NULL) nerror("Can't open input file");
if ((FileASP=fopen(NameFileASP,"r+b"))==NULL) nerror("Can't open input file");
if ((FileLOD=fopen(NameFileLOD,"r+b"))==NULL) nerror("Can't open input file");
if ((FilePON=fopen(NameFilePON,"r+b"))==NULL) nerror("Can't open input file");
for (i = 1; i <= gridi.nrows; i++) {
    for (j = 1; j <= gridi.ncols; j++) {
        fread(&ElevFi, sizeof(short), 1, FileCRO);
        z1[i][j] = ElevFi;
        fread(&ElevFi, sizeof(short), 1, FileASP);
        z2[i][j] = ElevFi;
        fread(&ElevFi, sizeof(short), 1, FileLOD);
        z3[i][j] = ElevFi;
        fread(&ElevFi, sizeof(short), 1, FilePON);
        z4[i][j] = ElevFi;
    }
}
fclose(FileCRO);
fclose(FileASP);

```

```

fclose(FileLOD);
fclose(FilePON);
for (i = 1; i <= 129; i++) {
    ax[i] = 0; ay[i] = 0;
}
ax[4] = 1; ax[8] = 1; ax[16] = 1; ax[1] = -1; ax[128] = -1; ax[64] = -1;
ay[1] = 1; ay[2] = 1; ay[4] = 1; ay[16] = -1; ay[32] = -1; ay[64] = -1;

/* _____ Main section */
do {
    for (i=1; i<=nl; i++) {
        if (r[i].code == 0) {
            for (j=i-1 ; j>=1; j--) {
                if (r[j].code > 0) {
                    temp.link = r[i].link;
                    temp.code = r[i].code;
                    temp.fx = r[i].fx;
                    temp.fy = r[i].fy;
                    temp.tx = r[i].tx;
                    temp.ty = r[i].ty;
                    if (z1[temp.fx][temp.fy] == 3) {
                        soma = 0.0;
                        for (x=-1; x<=1; x++) { /* _____ Upstream junction */
                            for (y=-1; y<=1; y++) {
                                if ((x==0) && (y==0)) continue;
                                if (AS1[x+1][y+1]==z2[x+temp.fx][y+temp.fy]) {
                                    soma += T*z3[x+temp.fx][y+temp.fy]; /* ___ Non-point load */
                                    if (z4[x+temp.fx][y+temp.fy] > 1)
                                        soma += z4[x+temp.fx][y+temp.fy]; /* ___ Point load */
                                }
                            }
                        }
                    }
                    z3[temp.fx][temp.fy] = soma;
                    z1[temp.fx][temp.fy] = soma;
                    m = temp.fx; n = temp.fy;

```

```

do { /* _____ Scanning the link */
    km = m + ax[z2[m][n]];
    kn = n + ay[z2[m][n]];
    m = km; n = kn;
    if (z1[m][n] == 3) {
        soma = 0.0;
        for (x=-1; x<=1; x++) {
            for (y=-1; y<=1; y++) {
                if ((x==0) && (y==0)) continue;
                if (AS1[x+1][y+1]==z2[x+m][y+n]) {
                    soma += T*z3[x+m][y+n];
                    if (z4[x+m][y+n] > 1) soma += z4[x+m][y+n];
                }
            }
        }
        z3[m][n]=soma;
        z1[m][n]=soma;
    }
    if ((m==temp.tx) && (n==temp.ty)) break;
} while (z1[temp.tx][temp.ty]==3);
}
break;
}
}
r[(r[j].link)].code--;
if (r[i].code == 0) r[i].code = (-1);
break;
}
}
} while (r[1].code != 0);
soma = 0.0;
for (x=-1; x<=1; x++) { /* _____ Starting last link */
    for (y=-1; y<=1; y++) {
        if ((x==0) && (y==0)) continue;
        if (AS1[x+1][y+1]==z2[x+r[1].fx][y+r[1].fy]) {

```

```

        soma += T*z3[x+r[1].fx][y+r[1].fy];
        if (z4[x+r[1].fx][y+r[1].fy] > 1) soma += z4[x+r[1].fx][y+r[1].fy];
    }
}
}
z3[r[1].fx][r[1].fy] = soma;
z1[r[1].fx][r[1].fy] = soma;
m = r[1].fx; n = r[1].fy;
do { /* _____ Last link */
    km = m + ax[z2[m][n]];
    kn = n + ay[z2[m][n]];
    m = km; n = kn;
    if (z1[m][n] == 3) {
        soma = 0.0;
        for (x=-1; x<=1; x++) {
            for (y=-1; y<=1; y++) {
                if ((x==0) && (y==0)) continue;
                if (AS1[x+1][y+1]==z2[x+m][y+n]) {
                    soma += T*z3[x+m][y+n];
                    if (z4[x+m][y+n] > 1) soma += z4[x+m][y+n];
                }
            }
        }
        z3[m][n]=soma;
        z1[m][n]=soma;
    }
    if ((m==r[1].tx) && (n==r[1].ty)) break;
} while ((m!=r[1].tx) && (n!=r[1].ty));
z1[r[1].tx][r[1].ty] =soma;

/* _____ Output section */
if ((FilePOL=fopen(NameFilePOL,"w+b"))==NULL) nerror("Can't write output file");
for (i = 1; i <= gridi.nrows; i++) {
    for (j = 1; j <= gridi.ncols; j++) {
        ElevFi = (short) z1[i][j];
    }
}

```

```
    fwrite(&ElevFi, sizeof(short), 1, FilePOL);  
  }  
}  
fclose(FilePOL);  
free_matrix(z1,1,gridi.nrows,1,gridi.ncols);  
free_imatrix(z2,1,gridi.nrows,1,gridi.ncols);  
free_matrix(z3,1,gridi.nrows,1,gridi.ncols);  
free_imatrix(z4,1,gridi.nrows,1,gridi.ncols);  
exit(0);  
}
```

```

/* -----
/*   program for solving equation  $X[k+1] = \text{roo} * W * X[k] + e$ 
/*       norm is gaussian Cumulative Distribution Function
/*       gout is a random number matrix generated by gauss.c
/*   CABM                                     1994
/* ----- */

#include          <stdio.h>
#include          <math.h>
#define row      80    /* 1000 600 */
#define col      160   /* 1000 600 */
#define rpt      0     /* for reducing edging effect 244 44 */
#define eps      0.001

/* ----- Main program */
main (argc, argv)
    int argc;
    char*argv[];
{ char  input1[20], input2[20], output[20];
  FILE  *ifp1, *ifp2, *ofp, *fopen();
  doublenorm[1000],min,max,a[row][col],b[row][col],c[row][col];
  doublemean, std, size, e[row][col], delta=0.2, roo;
  inti,j,k,n,x,y,A[(row-2*rpt)*(col-2*rpt)],B[1000];

  if(argc<4) { printf("\nUsage: need output file\n"); exit(1); }
    strcpy(input1, argv[1]);
  if((ifp1=fopen(input1, "r"))==NULL) printf("\nCan't open norm");
    strcpy(input2, argv[2]);
  if((ifp2=fopen(input2, "r"))==NULL) printf("\nCan't open gout");
    strcpy(output, argv[3]);
  if((ofp=fopen(output, "w"))==NULL) printf("\nCan't open output file");

/* ----- read in norm and roo */

```

```

printf("%s", "Enter roo --> : ");
scanf("%lf",&roo);
for(i=0; i<1000; i++) {
    fread(&norm[i], sizeof(double), 1, ifp1);
}
for(i=0; i<1000; i++) B[i] = 0;
size = (double) (row-rpt*2)*(col-rpt*2);
/* _____ read in gout */
for(i=0; i<row-1; i++)
    for(j=0; j<col; j++) { fread(&e[i][j], sizeof(double), 1, ifp2); }
for(i=0; i<row; i++) {
    for(j=0; j<col-1; j++) { a[i][j]=e[i][j]; b[i][j]=e[i][j]; }
}
system("date");
/* _____ main iteration */
for(k=0; k<1000 ; k++) {
    printf("Iteration = %d\n", k);
    for(i=1; i<row-1; i++) {
        for(j=1; j<col-1; j++) {
            b[i][j]=roo*(a[i-1][j]+a[i+1][j])+roo*(a[i][j-1]+a[i][j+1])+e[i][j];
        }
    }
    for(i=1; i<row-1; i++) {
        for(j=1; j<col-1; j++) {
            a[i][j]=roo*(b[i-1][j]+b[i+1][j])+roo*(b[i][j-1]+b[i][j+1])+e[i][j];
            c[i][j] = a[i][j]-b[i][j];
        }
    }
    y=0;
    for(i=1; i<row-1; i++) {
        for(j=1; j<col-1; j++) { if(fabs(c[i][j])>eps) y++; }
    }
    /* printf("y = %d\n\n", y); */
    if (y==0) break;
} /* _____ iteration end */

```

```

printf("Iteration = %d\n", k);
system("date");
getchar();

/* change subscripts to desired dimension and conversion to */
/* integers for finding maximum-minimum using quicksort */

for(i=rpt; i<row-rpt; i++)
    for(j=rpt; j<col-rpt; j++) {
        c[i-rpt][j-rpt] = a[i][j];
        A[(col-2*rpt)*(i-rpt)+j-rpt]=(int) 1000000.0*a[i][j];
    }
k=(row-2*rpt)*(col-2*rpt);
quicksort(A, k); /* sort for finding maximum and minimum */
min=(double) A[0]/1000000;
max=(double) A[k-1]/1000000;
size = (double) (row-rpt*2)*(col-rpt*2);

/* transform variable to the interval of -5.0 to +5.0 */
for(i=0; i<row-rpt*2; i++)
    for(j=0; j<col-rpt*2; j++)
        c[i][j] = 9.99999*(c[i][j]-min)/(max-min) - 4.999995;
mean = 0.0; std = 0.0;
for(i=0; i<row-rpt*2; i++)
    for(j=0; j<col-rpt*2; j++) mean=mean+c[i][j]/size;
for(i=0; i<row-rpt*2; i++)
    for(j=0; j<col-rpt*2; j++)
        std = std + (c[i][j]-mean)*(c[i][j]-mean);
std = sqrt(std/size);
printf("\nmean= %lf std = %lf", mean, std);

/* transform c that mean=0.0 and std=1.0 */
for(i=0; i<row-rpt*2; i++)
    for(j=0; j<col-rpt*2; j++)
        c[i][j] = (c[i][j]-mean)/std;

```



```

/* _____ Store results */
    for(i=0; i<row; i++)
        for(j=0; j<col; j++) { fprintf(ofp, "%3.5f\n",    c[i][j]); }
}
quicksort (a, n)
int a[], n;
{
    int    k, pivot;
    if (find_pivot(a,n,&pivot) !=0)
        {
            k = partition (a, n, pivot);
            quicksort(a, k);
            quicksort(a+k, n-k);
        }
}
find_pivot (a, n, pivot_ptr)
int    a[], n, *pivot_ptr;
{
    int    i;
    for (i = 1; i<n; ++i)
        if (a[0] != a[i]) {
            *pivot_ptr = (a[0] > a[i]) ? a[0] : a[i];
            return (1);
        }
    return (0);
}

int partition (a, n, pivot)
int    a[], pivot;
{
    int    i=0, j=n-1, k, l, temp;
    while(i<=j) {
        while (a[i]<pivot) { ++i; }
        while (a[j]>=pivot) --j;
        if (i<j) {
            k = i++;    l = j--;
            temp = a[k];    a[k] = a[l];    a[l] = temp;
        }
    }
}

```

```
    }  
  }  
  return(i);  
}
```

```

/* -----
/*    program for generating random number of Gauss distribution
/*    with mean = 0.0 and standard deviation od 1.0
/*    gaussin: row*col - number of data generated 600*600 = 360000
/*    CABM                                1994
/* ----- */

#include          <stdio.h>
#include          <math.h>          ..
#define interval 200

/* ----- Main program */
main (argc, argv)
int argc;
char*argv[];

{   char   input[20], output1[20],output2[20];
    FILE   *ifp, *ofp1, *ofp2, *fopen();
    double *a, mean, std, min, max, delta;
    long   idum=(-13);
    float   gasdev();
    int     i,j,k, number, num[interval], total, *A;

    if(argc<2) {
        printf("\nUsage: need output file");
        exit(1);
    }
    strcpy(output1, argv[1]);
    strcpy(output2, argv[2]);
    strcpy(input, argv[3]);
    if((ofp1=fopen(output1, "w"))==NULL) printf("\nCan't open output file");
    if((ofp2=fopen(output2, "w"))==NULL) printf("\nCan't open output file");
    if((ifp =fopen( input, "r"))==NULL) printf("\nCan't open output file");

```

```
printf("number of random data generated ? ");
fscanf(ifp, "%d",&number);
printf("\n%d\n", number); getchar();
A=(int *) calloc(number, sizeof(int));
a=(double *) calloc(number, sizeof(double));

for(i=0; i<interval; i++) num[i] = 0;
for(i=0; i<number; i++) a[i] = gasdev(&idum);

for(i=0; i<number; i++) A[i] = (int) 1000000*a[i];
for(i=0; i<number; i++) {
    ..
    /* if(i%8==0) fprintf(ofp1,"\n"); */
    fwrite( &a[i], sizeof(double), 1, ofp1);
    /* fprintf(ofp1,"%+1.4f\n",a[i]); */
}
quicksort(A, number);

fprintf(ofp2,"\nmin=%2.4f ",(double) A[0]/1000000);
fprintf(ofp2,"\nmax=%2.4f ",(double) A[number-1]/1000000);
for(i=0; i<number; i++) mean= mean+a[i]/((double) number);
for(i=0; i<number; i++) std = std + (a[i]-mean)*(a[i]-mean);
fprintf(ofp2,"\nmean=%2.4f std=%2.4f ",mean, sqrt(std/((double) number)));
}
```

```
/* -----  
/*      Program for returns a normally distributed deviate with zero  
/*      mean and unit variance.  
/*      Source : Press et al., (1992) pag 289  
/* ----- */  
  
float gasdev(idum)  
long *idum;  
{  
    float ran3();  
    static int iset=0;  
    static float gset;  
    float fac,rsq,v1,v2;  
  
    if (iset == 0) {  
        do {  
            v1 = 2.0*ran3(idum) - 1.0;  
            v2 = 2.0*ran3(idum) - 1.0;  
            rsq = v1*v1 + v2*v2;  
        } while (rsq >= 1.0 || rsq == 0);  
        fac=sqrt(-2.0*log(rsq)/rsq);  
        gset=v1*fac;  
        iset=1;  
        return v2*fac;  
    } else {  
        iset=0;  
        return gset;  
    }  
}
```

```
/* -----  
/*      Program to returns a uniform random deviate between 0.0 and 1.0  
/*      Source : Press et al., (1992) pag 283  
/* -----  
  
#define MBIG 1000000000  
#define MSEED 161803398  
#define MZ 0  
#define FAC (1.0/MBIG)  
  
float ran3(idum)  
long *idum;  
{  
    static int inext, inextp;  
    static long ma[56];  
    static int iff=0;  
    long mj, mk;  
    int i, ii, k;  
  
    if (*idum < 0 || iff == 0) {  
        iff=1;  
        mj=MSEED-(*idum < 0 ? -*idum : *idum);  
        mj %= MBIG;  
        ma[55]=mj;  
        mk=1;  
        for (i=1;i<=54;i++) {  
            ii=(21*i) % 55;  
            ma[ii]=mk;  
            mk=mj-mk;  
            if (mk < MZ) mk += MBIG;  
            mj=ma[ii];  
        }  
        for (k=1;k<=4;k++)
```

```

        for (i=1; i<=55; i++) {
            ma[i] -= ma[1+(i+30) % 55];
            if (ma[i] <MZ) ma[i] += MBIG;
        }
        inext=0;
        inextp=31;
        *idum=1;
    }
    if (++inext == 56) inext=1;
    if (++inextp ==56) inextp=1;
    mj=ma[inext]-ma[inextp];
    if (mj < MZ) mj += MBIG;
    ma[inext]=mj;
    return mj*FAC;
}

#undef MBIG
#undef MSEED
#undef MZ
#undef FAC

/*=====*/
quicksort (a, n)
int    a[], n;
{ int    k, pivot;
  if(find_pivot(a,n,&pivot) !=0)
      { k=partition(a,n,pivot); quicksort(a,k); quicksort(a+k,n-k); }
}
/*=====*/

find_pivot (a, n, pivot_ptr)
int    n, a[], *pivot_ptr;
{ int    i;
  for(i=1; i<n; ++i)
      if (a[0] != a[i])
          { *pivot_ptr=(a[0]>a[i]) ? a[0] : a[i]; return (1); } return (0);
}

```

```
}
/*=====*/
int partition (a, n, pivot)
int    a[], pivot;
{    int    i=0, j=n-1, k, l, temp;
    while(i<=j)
        { while (a[i]<pivot) ++i;
          while (a[j]>=pivot) --j;
          if (i<j) { k = i++;    l = j--;
                   temp = a[k]; a[k] = a[l];    a[l] = temp;
                 }
        }
    } return(i);
}
```



```
/* -----  
/*   program for calculating cumulative distribution function (normal)  
/*   CABM                               1994  
/* ----- */  
  
#include <stdio.h>  
#include <math.h>  
#define PI 3.1415926535897936  
main()  
{  
    long i, j, k, dsl, n;  
    double p[300], t, b, c, d, sqr;  
    FILE *f1;  
  
    sqr = 1/sqrt(2.0*PI);  
    c = 0.0;  
    j = 0;  
    f1 = fopen("norm.dat", "w+b");  
    for(i=0; i<10000000; i++) {  
        t = ((double) (i-5000000))/1000000.0;  
        b = sqr*exp(-t*t/2.0);  
        c = c+b;  
        if (i%10000==0) {  
            d = c/1000000.0;  
            fwrite( &d, sizeof(double), 1, f1);  
        }  
    }  
    fclose(f1);  
}
```